# Genes involved in meiotic recombination in *Petunia hybrida* and *Arabidopsis thaliana*

Veena G. Hedatale

Front Cover : Petunia and Arabidopsis flower (Petunia photographed by Anneke Rijpkema)
Back Cover : A defective tetrad of the *xrs4* mutant

ISBN number: 978-90-9025670-2
Printed by: Ipskamp Drukkers

# Genes involved in meiotic recombination in *Petunia hybrida* and *Arabidopsis thaliana*

een wetenschappelijke proeve op het gebied van de
Natuurwetenschappen, Wiskunde en Informatica

**Proefschrift**

ter verkrijging van de graad van doctor
aan de Radboud Universiteit Nijmegen
op gezag van de rector magnificus Prof. Mr. S.C.C.J. Kortmann,
volgens besluit van het College van Decanen
in het openbaar te verdedigen op dinsdag 21 december 2010
om 15.30 precies

door

Veena Hedatale
geboren op 3 Juni 1972
te Bangalore (India)

Promotor:
Prof. dr. A.G.M. Gerats

Copromotors:
Dr J.L. Peters
Prof. dr. J. de Jong (Wageningen Universiteit)

Manuscriptcommissie:
Prof. dr. C. Mariani
Prof. dr. P. Hooykaas (Leiden University)
Dr. M. Grélon (Institut Jean-Pierre Bourgin, INRA Centre de Versailles)

# Contents

# Chapter 1

General Introduction

**Introduction**

In eukaryotes, DNA is the carrier of the genetic information needed for development and maintenance of cells. Genetic material is organized into DNA-protein complexes called chromatin within the chromosomes of the nucleus and organelles like mitochondria and plastids (in plants). During cell division DNA protein complexes condense and are visible under the microscope as chromosomes. A unique set of all chromosomes together is called a genome. Although well organized and protected against damage, DNA molecules are vulnerable to double strand breaks (DSBs). These breaks are introduced in a controlled manner during meiosis but can occur due to environmental factors such as ionizing radiation, mutagenic chemicals or active transposable elements. Broken DNA molecules can be repaired by homologous recombination (HR) or by non-homologous end joining (NHEJ). In diploid eukaryotes such exchanges take place between homologous chromosome segments and in meiosis, they are confined to the non-sister chromatids of the homologous chromosomes from father and mother. HR occurs prior to the formation of gametes, during the prophase of the first meiotic division. Albeit very rarely, it also occurs in the nuclei of mitotic tissues, where it presumably drives the faithful repair of broken parts of the genome and ensures a balanced distribution of the homologs amongst the emerging daughter cells.

During meiosis, DSB repair may lead to crossover (CO) recombination between the non-sister chromatids of a homologous chromosome pair whereas during mitosis such a repair occurs only between sister-chromatids and usually remains undetected, as sister chromatids are molecularly identical. Mitotic DSBs repair rarely occur between homologs, which may lead to loss of heterozygosity and/or gross chromosomal rearrangements. HR events can only occur upon a DSB. While in mitotic cells DSBs are due to random damage, they seem to be induced enzymatically during meiosis, which partly explains the much higher incidence of HR during meiosis.

Meiosis is a specialized form of cell division that occurs in all sexually reproducing eukaryotes and consists of a single round of DNA replication followed by two successive cell divisions (meiosis-I and -II), thus creating four haploid cells from a single diploid cell. Important aspects of meiosis that distinguish it from mitosis include 1) the formation of a proteinaceous structure, the synaptonemal complex, in which the homologous chromosomes align, enabling the precise exchange of segments of chromosomes during homologous recombination, 2) the separation of the nonsister centromere pairs leading to the disjoin of homologs during meiosis-I and 3) subsequently the separation of sister centromeres during meiosis-II without an intervening S-phase or replication phase. Cnudde and Gerats (2005) provide a more extensive overview of the most important aspects of meiosis.

Since HR is important for maintaining the integrity of chromosomes in both meiotic and mitotic cells, one may expect a common set of proteins to operate in the repair mechanism of DSBs in both processes. This is true in particular for the DSB repair genes of the MRN complex, the RAD52 epistatic group and the mismatch repair (MMR) complex (Table 1.1). Another very important function of HR is to provide a mechanical means for proper disjunction of homologous chromosomes at the first meiotic division.

Functional similarities as well as sequence conservation in HR proteins are evident across a large range of species. While a majority of HR defective mutants are lethal in both fungi and animals, they are able to survive in plants as reduced and fully sterile mutants. Hence plants seem more appropriate to investigate their role in DNA repair and recombination. The focus of this chapter is on the recent advances in understanding plant HR through mitotic and meiotic studies. We will not discuss the occurrence or structure of protein complexes that participate in processes like synapsis and segregation; instead we will highlight mutant phenotypes of recombination-related genes in *Arabidopsis* and compare them to orthologs in (other) higher eukaryotes to see which complexes may have evolved differently.

**DSB repair in the context of the cell cycle**

An efficient mechanism to maintain the integrity of the genome is necessary in plants (and other eukaryotes) to eliminate deleterious DNA errors in somatic cells that otherwise would be passed on to differentiating sporogenic cells. The conditions in which repair pathways are engaged are not fully understood (Paques and Haber, 1999). In higher eukaryotes, somatic cells repair DSBs mainly via non-homologous end joining (NHEJ). NHEJ is an error prone repair process that rejoins ends of the break, independent of sequence homology. Sometimes repair is mediated by HR, depending on the availability of homologous templates, or by a combination of both processes competing for available DSBs (Puchta et al., 2005).

The preference of repair mechanisms probably depends on the phase of the cell cycle (Fig. 1.1). In the gap-1 part of the interphase (G1 phase), cells grow and prepare for DNA replication. Break-Induced-Replication (BIR) is active during the G1 phase in which a one-end DSB invades the homologous sequence and initiates DNA synthesis from the site of invasion to the end of the telomeres (reviewed by Krogh and Symington, 2004). DNA replication occurs in the synthesis phase (S phase).

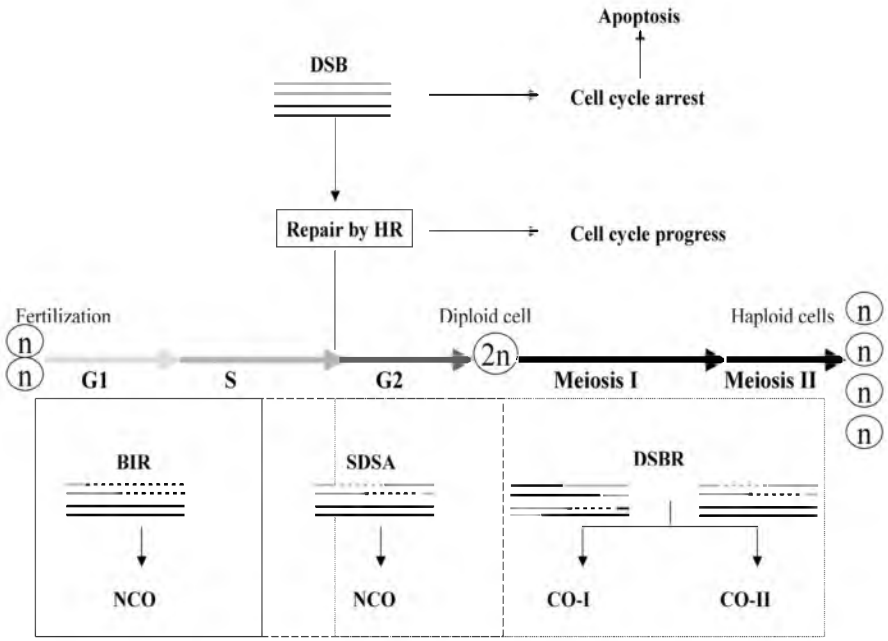


**Fig. 1.1: Pathways of homologous recombination active at different phases of the cell cycle.** Damaged chromosomes cause temporary arrest of the cell cycle until they are repaired. DSBs are predominantly repaired by Break Induced Replication in G1 phase, and early S phase, Synthesis Dependant Strand Annealing during the late S phase, G2 phase and during meiosis-I to generate Non Cross Overs. The Double Stranded Break Repair pathway is activated by programmed DSBs only during meiosis-I and results in Cross Overs sensitive to interference (CO-I) or those insensitive to interference (CO-II). Abbreviations: DSB- double stranded break, NCO- non-crossover, CO-crossover

During the late S-phase Synthesis Dependant Strand Annealing (SDSA) accomplishes DSB repair in the vertebrate cell cycle (Allers and Lichten, 2001). In SDSA, the invading strand uses the sequence of the homolog to synthesize the new strand resulting in a non-reciprocal exchange of (small fragments) of genetic material; this process is called gene conversion (GC). The HR-based pathway SDSA is active during the G2 phase. NHEJ is active throughout the cell cycle and competes for the available DSBs (Mao et al., 2008) but it is mostly preferred in G1 and early S-phase (Takata et al., 1998, Karathanasis & Wilson, 2002). In plants, cells arrest at the G1/S phase (Costsaftis et al., 2005) and meiosis starts after the G2 phase is completed (Fig. 1.1). The Double Strand Break Repair (DSBR) pathway acts predominantly during meiosis (Watrin and Peters, 2006) and relies on the availability of a homologous template in close proximity for repair.

**Meiotic HR**

HR is an obligate part of meiosis where it secures correct chromosome segregation and enhances genetic diversity by the exchange of parental alleles between homologs. Homologous recombination and synapsis are closely coordinated events in meiosis. Synapsis refers to the coaxial connection of homologs, along their entire length forming the synaptonemal complex (SC) (von Wettstein et al., 1984). The small spherical protein complexes associated with the SC complexes are called recombination nodules (RNs). A large number of randomly distributed small RNs are formed at early zygotene to mid pachytene (early nodules), but only a subset of these persist to become the larger and more spherical RNs at late pachytene (late nodules), which correspond to the sites of crossovers (CO) (for an overview, see Zickler and Kleckner, 1998, 1999).

The Szostak model (Szostak et al., 1983) is currently the most relevant DSBR model to describe the molecular processes of CO recombination in meiosis (Fig. 1.2). An alternative fate of DNA breaks is to be repaired by a non-double Holliday-Junction mechanism (ndHJ) via the SDSA pathway (Allers and Lichten, 2001), which always results in a non-crossover (NCO) (Hollingsworth and Brill et al., 2004; Terasawa et al., 2007). An NCO has a short conversion tract, which maintains the order and nature of linked alleles as present in the parental homologs, is the most recently described form of repair (Chromie and Smith, 2007). The pathway for formation of NCOs remains to be elucidated. New evidence from studies in mouse and yeast suggests that the decision to form a CO or a NCO probably occurs soon after DSB or D-loop formation (see below and Fig. 1.2) (Borner et al., 2004; Terasawa et al., 2007) and that NCOs form much earlier than CO (Allers and Lichten, 2001).

**The Double Strand Break Repair (DSBR) pathway**

In the DSBR pathway nicks in both DNA strands of one homolog result in a double stranded break (DSB) and initiate recombination (Fig. 1.2). The broken ends are resected by an exonuclease at the 5'-end to expose single stranded 3'-OH tails. Single end invasion (SEI), where one of the tails invades the homolog, locates its equivalent sequence and forms a displacement loop (D-loop). The invading strand primes DNA synthesis and further extends the D-loop that then becomes stabilized by subsequent branch migration via DNA synthesis, until it reaches the other end of the single stranded break in what is known as second end capture. Further DNA synthesis and ligation of the ends results in two four-way junction intermediates called double Holliday junctions (dHJs). Cleavage involving strands from both parental chromosomes results in crossovers (CO) while cleavage involving two similar strands results in non-crossovers (NCO). Thus, depending on the orientation of cleavage of strands at dHJs, CO or NCO results.

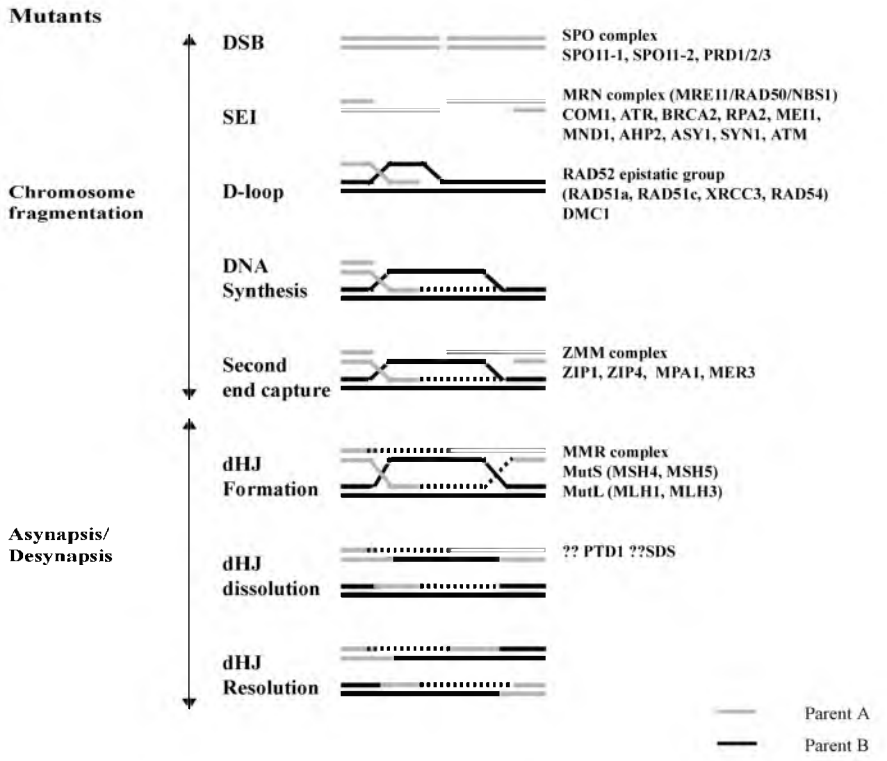


**Fig 1.2: The Double stranded Break Repair pathway model.** Common mutant phenotypes observed due to disruption of specific steps of meiotic homologous recombination and the major Arabidopsis genes identified so far. Abbreviations used in the figure **DSB**: double stranded break, **SEI**: single end invasion, **dHJ**: double Holliday Junction

Occurrence of one CO often influences the occurrence of a second, neighboring CO in a distance-dependent manner; this phenomenon is referred to as interference. The COs arise *via* two pathways- one subject to interference (CO-I) (de Boer et al., 2007; Lhuissier et al., 2007) and the other insensitive to interference (CO-II). Condensins control CO frequency and numbers by regulating DSB distribution as shown in *C. elegans* (Mets and Meyer, 2009). Furthermore, Youds et al., (2010) show that RTEL-1 enforces interference by channelizing DSBs into NCO indicating a second level of CO regulation in meiosis.

Some of the protein complexes involved in homologous recombination in *Arabidopsis* are described below and their corresponding genes are listed in Table 1.1. Some of the genes play a role during both meiosis and mitosis. Others show interesting differences in mutant phenotypes when compared to their homologs in yeast and mammals. The meiotic HR process can be broadly

classified into DSB formation, DSB repair and Resolution of products: CO or NCO.

**Table 1.1:** Major Arabidopsis HR genes and phenotype of the corresponding mutants in mitosis and meiosis

| Gene | *Gene ID | Mutant phenotype | | Reference |
|---|---|---|---|---|
| | | Mitosis | Meiosis | |
| **DSB formation** | | | | |
| AtSPO11-1 | At3g13170 | | no DSBs, synapsis failure with many univalents | Grelon et al., 2001 |
| AtSPO11-2 | At1g63990 | insensitive to UV light and MMS | severe sterility, univalents at meiotic metaphase-I | Stacey et al., 2006 |
| AtSPO11-3 | AT5g02820 | extreme dwarf phenotype associated with defects in endo-reduplication, insensitive to UV light and MMS | | Stacey et al., 2006 |
| AtPRD1 | AT4g14180 | - | synapsis failure associated with a total absence of chiasmata | De Muyt et al., 2007 |
| AtPRD2 | At5g57880 | - | synapsis failure and a total absence of chiasmata | De Muyt et al., 2009 |
| AtPRD3 | At1g01690 | - | synapsis failure and a total absence of chiasmata | De Muyt et al., 2009 |
| **Early recombination** | | | | |
| AtBRCA1 | At4g21070 | induced by ioninzing radiation; sensitive to mitomycin C | Fully fertile | Lafarge and Montané 2003; Reidt et al., 2006 |
| AtBRCA2 | At5g01630 | - | partial sterility; chromosome bridges and chromosome fragmentation | Siaud et al., 2004; |
| AtRPA2 | At2g24490 | hypersensitive to MMS | smaller than wild-type plants and flowered earlier, fertile | Elmayan et al., 2005 |
| AtAHP2 | At1g13330 | **n.d. | sterility, chromosome fragmentation, chromatin bridges and unbalanced segregation at anaphase I and anaphase II | Schommer et al., 2003 |

| Gene | *Gene ID | Mutant phenotype | | Reference |
|---|---|---|---|---|
| | | Mitosis | Meiosis | |
| AtSDS1 | AT1g14750 | n.d. | defective chromosome synapsis, segregation and bivalent formation at prophase-I | Azumi et al., 2002 |
| ATK | At4g21270 | n.d. | defective chromosome segregation and spindle organization | Chen et al., 2002 |
| AtMMD1/ DUET | AT1g66170 | n.d. | male-meiosis specific single division meiosis, chromosome fragmentation, cytoplasmic shrinkage | Reddy et al., 2003;Yang et al., 2003 |
| **Cell cycle check point** | | | | |
| AtATM | At3g48190 | sensitive to gamma-rays, MMS but not UV-B | residual fertility of 10%; chromosome fragmentation | Garcia et al., 2003; Culligan & Britt 2008 |
| AtATR | At5g40820 | hypersensitivity to hydroxyurea (HU), aphidicolin, and UV-B and mildly to gamma-irradiation | fertile | Culligan & Britt 2008 |
| AtRAD9 | At3g05480 | Sensitive to bleomycin and MMC, DSB repair defect, somatic hyper recombination | n.d. | Heitzberg et al., 2004 |
| AtRAD17 | At5g66130 | Sensitive to Bleomycin and MMC, DSB repair defect, somatic hyper recombination | n.d. | Heitzeberg et al., 2004 |
| **DSB Repair :MRN complex** | | | | |
| AtRAD50 | At2g31970 | hypersensitive to MMS, exhibit somatic hyper-recombination, hyper-Rec phenotype, defects in telomere maintenance | sterile, chromosome fragmentation | Gherbi et al., 2001; Gallego et al., 2001; Stevens et al., 2004 |
| AtMRE11 | AT5g54260 | Hypersensitivity to genotoxic stress, lengthened teolmeres; dicentric | sterile, chromosome fragmentation | Bundock and Hooykaas, 2002; Garcia et al., 2003; |

| Gene | *Gene ID | Mutant phenotype | | Reference |
|---|---|---|---|---|
| | | Mitosis | Meiosis | |
| | | chromosomes | | |
| AtNBS1 | At3g02680 | hypersensitive to MMS, MMC | single mutants are fertile; Double mutants of Atatm-/-/Atnbs-/- are completely infertile with incomplete chromosome pairing and synapsis in meiotic prophase, and extensive chromosome fragmentation in metaphase I and subsequent stages | Waterworth et al., 2007 |
| AtCOM1/ AtGR1 | At3g52115 | hypersensitive to MMC, gamma radiation | sterile, chromosome fragmentation | Deveaux et al., 2000; Uanschou et al., 2007 |
| | | **RAD52 epistatic group** | | |
| AtRAD51a | At5g20850 | Sensitive to mitomycin C, insensitive to bleomycin, gamma rays | Chromosome fragmentation together with the absence of normal chromosomal pairing and synapsis. | Bleuyard and White 2004; Li et al., 2004; Markmann-Mulisch et al., 2007 |
| AtRAD51b | At2g28560 | Moderately sensitive to gamma-ray and hypersensitive to cisplatin. | viable and fertile | Osakabe et al., 2005; Bleuyard and White 2004 |
| AtRAD51c | At2g45280 | increased sensitivity to gamma-irradiation and cisplatin; 2-fold reduction in HR | viable and sterile; extensive chromosome fragmentation | Abe et al., 2005; Osakabe et al., 2002; Bleuyard and White 2004 |
| AtRAD51d | AT1g07745 | | | |
| AtXRCC2 | AT5g64520 | moderately sensitive to gamma-ray and hypersensitive to cisplatin, mitomycin C | viable and fertile | Bleuyard and White 2004 |
| ATXRCC3 | AT5g57450 | hypersensitivity to cross-linking agents | chromosome fragmentation; Unresolved interhomolog interactions do not seem to prevent synapsis and bivalent formation | Osakabe et al., 2002; Bleuyard and White 2004 |
| AtDMC1 | At3g22880 | - | no chiasma formation resulting | Doutriaux et al., 1998 |

| Gene | *Gene ID | Mutant phenotype | | Reference |
|---|---|---|---|---|
| | | Mitosis | Meiosis | |
| | | | in univalents and missegregation | |
| AtRAD54 | At3g19210 | increased sensitivity to cisplatin, gamma radiation; reduced intrachromosomal and interchromosomal recombination | viable and fertile | Osakabe et al., 2006 |
| | | **Late recombination** | | |
| RECQL4A | AT1g10930 | somatic HR increased 7-fold; hypersensitive to UV and MMS but resistant to MMC | n.d. | Bagherieh-Najjar et al., 2005 |
| RECQL4B | At1g60930 | somatic HR reduced 3-fold; insensitive to MMS, cisplatin, bleomycin | n.d. | Hartung et al., 2007 |
| AtTOP3a | At5g63920 | Fragmented chromosomes; Frequency of somatic homologous recombination ~ 5 to 7 fold higher. more sensitive to DNA damaging agents MMS and cisplatin; hyper-recombination | abnormal pachytene chromosomes, severe chromosome fragmentation; anaphase defects | Hartung et al., 2009 |
| RMI1 | At5g63540 | | | Hartung et al., 2009 |
| AtPTD1 | At1g12790 | n.d. | defective CO formation in the interference-sensitive pathway | Wijeratne et al., 2006 |
| AtMUS81 | At4g30870 | sensitive to MMS, cisplatin, gamma radiation; reduced somatic recombination induced by genotoxic stress | CO reduced by 10% | Holger et al., 2006; Berkowitz et al., 2007 |
| AtSHOC1 | AT5g52290 | n.d. | reduction in the number of chiasmata, abnormal embryo sacs | Macaisne et al., 2008 |
| AtMPA1 | At1g63770 | - | desynapsis, frequency of crossovers was dramatically reduced | Sanchez-Moran et al., 2004 |
| | | **ZMM complex** | | |
| AtMER3 | At3g27730 | - | Residual fertility of | Mercier et al., |

| Gene | *Gene ID | Mutant phenotype | | Reference |
|---|---|---|---|---|
| | | Mitosis | Meiosis | |
| | | | 13%; synapsis defect, bivalent shortage | 2005 |
| AtZIP1a | At1g22260 | - | no synapsis, bivalent shortage, multivalents; chiasma frequency reduced by 20% | Higgins et al., 2005 |
| AtZIP1b | At1g22275 | - | no synapsis, bivalent shortage, multivalents; chiasma frequency reduced by 20% | Higgins et al., 2005 |
| AtZIP4 | At5g48390 | synapsis defect, bivalent shortage | | Chelysheva et al., 2007 |
| | | **MMR complex** | | |
| *MutS* | | | | |
| AtMSH2 | At3g18524 | mutants exhibit increased microsatellite (dinucleotide repeat) instability | mutants show 40% percent increase in crossover rates | Leonard et al., 2003 |
| AtMSH4 | At4g17380 | n.d. | chiasma frequency reduced by 72% | Higgins et al., 2004; Franklin et al., 2006 |
| AtMSH5 | AT3G20475 | n.d. | chiasma frequency reduced by 87% | Higgins et al., 2008 |
| *MutL* | | | | |
| AtMLH1 | AT4g09140 | reduced HR, increased homeologous recombination | reduced fertility, component of late RNs that form COs | Dion et al., 2007 |
| AtPMS1 | AT4g02460 | Increased microsatellite instability | unaltered in fertility | Alou et al., 2004 |
| AtMLH3 | AT4g35520 | n.d. | reduced fertility, reduced crossover, delayed prophase-I progression | Jackson et al., 2006 |
| *MutH* | - | - | - | - |

RN = Recombination Nodule
HR = Homologous Recombination
CO = Cross Over
*Gene ID = Gene identifier assigned by TAIR (http://www.arabidopsis.org/)
**n.d. = not determined

## I. DSB formation

The lesions involving DSBs cannot be repaired using the complementary strand as both strands are disrupted and repair of a broken strand requires the intact strand of a homologous chromosome as a template. Programmed DSBs initiate

homologous recombination during meiosis; SPO11 and its interacting proteins mediate them.

**I-1. The SPO complex**

A complex of at least 9-12 proteins mediates the initiation of DSBs in yeast meiotic HR but only five of these have homologs outside the fungal kingdom: *SPO11, MRE11, RAD50, XRS1* and *SKI8*. While there is only one *SPO11* gene known in mammals and yeast, *Arabidopsis* possesses three SPO11 homologs showing differentiated though still related functions. Single mutations in *SPO11-1* and *SPO11-2* genes lead to severe meiotic defects (Grelon et al., 2001, Stacey et al., 2006) while mutations in *SPO11-3* affect mitotic functions and exhibit sensitivity to DNA damage (Stacey et al., 2006). The SKI8 protein directly interacts with SPO11 in yeast (Arora *et al.* 2004), whereas the plant homolog of SKI8 is not required for meiosis (Jolivet et al. 2006). MRE11, RAD50 and NBS together known as the MRN complex in higher eukaryotes, plays a role in DSB repair rather than in DSB formation. AtPRD1, a functional homolog of MEI1 interacts with SPO11 in DSB formation (De Muyt et al., 2007). AtPRD2 (yeast MEI4 functional ortholog; Kumar et al., 2010) and AtPRD3 are also part of the meiotic recombination complex. Meiotic DSBs and DMC1 loading are abolished in *Atprd2* and *Atprd3* mutants (De Muyt et al., 2009). So far, it seems that SPO11 and PRD2/MEI4 are functionally conserved members of the complex in plants.

**II. DSB repair**

According to the Szostak model, 5' end resection occurs after DSB formation, creating 3'-OH tails and the MRN complex mediates this step. The *RAD52* epistatic group acts on SEI intermediates and forms the D-loop (see below for explanations).

A critical early step in DSB repair is the removal of SPO11 that is covalently linked after the break. This step is known to depend on RAD50, MRE11 and COM1/SAE2 from studies in yeast (Uanschou et al., 2007). Removal of the SPO11 protein occurs by nicking the DNA next to the cleavage site, thereby releasing the catalytic protein attached to a few nucleotides. In *Atcom1* mutants, chromosome fragmentation and failure of pairing is observed (Uanschou et al., 2007). This indicates that meiotic DSBs are produced, but downstream events such as DNA end processing or heteroduplex formation are impaired. *AtCOM1* acts downstream of *AtSPO11-1* and upstream of *AtDMC1* during meiosis. The selective sensitivity of vegetative cells of *Atcom1* mutants to mitomycin C (MMC) suggests that in somatic tissues, AtCOM1 is needed for the repair of interstrand DNA cross-links (Uanschou et al., 2007). BRCA2 has a role in recruiting RAD51 and eventually DMC1 onto the meiotic chromosomes (Sharan et al, 2003). The Arabidopsis *Atbrca2* knock-down mutant presents severe

chromosome fragmentation, univalents and disorganized chromosomes and therefore has a role in early meiotic recombination. BRCA2 possibly acts after DNA DSB break by SPO11 but before RAD51 and DMC1 in the repair of DSBs (Siuad et al., 2004).

Several lines of evidence suggest a role for BRCA1 in DSBR. BRCA1 interacts with several proteins that are intimately involved in this process, including RAD51 and the MRE11/RAD50/NBS-1 (MRN) complex (Cantor et al., 2001). In plants, *Atbrca1* mutants are sensitive to ionizing radiation and mitomycin C, but are fully fertile (Reidt et al., 2006). Hence its role in meiosis in plants is not obvious. In addition we know that CtIP, the mammalian COM1 homolog, interacts with BRCA1 for DNA damage checkpoint activation in G2 phase (Yu and Chen 2004; Greenberg et al., 2006). BRCA1 interacts with BACH1, a member of the DEAH helicase family. BACH1 binds directly to the BRCT repeats of BRCA1. Mutations in a key residue of BACH1, that is essential for catalytic function in other helicases, interfered with normal DSBR in a manner that was dependent upon its ability to interact with BRCA1 (Cantor et al., 2001).

**II-1. The MRN complex**

The well conserved multifunctional trimeric complex MRN/X (MRE11-RAD50-NBS/XRS1) plays a major role in DNA checkpoint, double-strand break repair, nucleolytic processing of DNA ends, meiosis, and telomere maintenance (Garcia et al. 2003). In mammals, the MRN complex participates in the clustering of DSB-containing chromosomal domains during G1 phase (Aten et al., 2004). The MRN complex is involved in DNA repair together with the SAE2 protein in single strand annealing (SSA) of meiotic and mitotic DSBs. Meiotic chromosomes of *mre11* mutants in general exhibit severe chromosome fragmentation as DSB repair is hampered. *Mre11* mutants in vertebrates are non-viable due to gross chromosome instability leading to cancer (Xiao and Weaver, 1997; Carney et al., 1998, Luo et al., 1999, Yamaguchi-Iwai et al., 1999). In Arabidopsis, *Atmre11* mutants are viable, exhibit growth defects and are infertile (Puizina et al., 2004). They are extremely sensitive to ionizing radiation (IR) and differ in this respect from the *Saccharomyces cerevisiae mre11* mutants that are only mildly sensitive to ionizing radiation (IR) (Llorente et al., 2004). *RAD50* mutants are embryo-lethal in vertebrates (Helleday, 2003) and hyper-recombinant in yeast (Lewis et al., 1999) but their ortholog in *Arabidopsis*, *Atrad50*, is surprisingly viable, though completely sterile. They exhibit mitotic hyper-recombination and are sensitive to DNA damaging agents. Meiosis is severely disturbed in the mutant as homologous chromosomes are unable to synapse at pachytene, resulting in extensive chromosome fragmentation. Plants seem to be more similar to mammals with preferences for NHEJ over HR for

somatic DNA repair and yet, they are similar to yeast mutants in their hyper-recombination phenotype. The role of the MRN complex in DNA repair and recombination is unique in plants and its interaction with COM1/SAE2, RAD51 and other signaling repair proteins seems crucial to evolution of DNA damage responses in plants (Uanschou et al., 2007, Bleuyard and White, 2004).

### II-2. The epistatic RAD52 group

Recombination-mediated DNA repair in eukaryotes also relies upon the epistatic RAD52 group of proteins including RAD51-59. Species like chicken, mouse, *Drosophila melanogaster*, *Caenorhabditis elegans*, and *Arabidopsis thaliana* predominantly prefer NHEJ, whereas *Sacharomyces cerevisiae* and *Physcomitrella patens* prefer to employ HR. In vertebrates, RAD51 is an essential protein for cell viability and its depletion leads to chromosomal fragmentation, cell cycle arrest and death (Sonoda et al., 1998) and in plants it is actively used in HR in slow evolving species like *P. patens* (Markmann-Mulisch et al., 2007). Other members like RAD52, RAD54 and RAD57 are involved in HR, but are not essential for cell viability. In yeast, RAD52 is the most important DSB repair protein as it participates in all DSB repair pathways. *Scrad52* class C mutants are incapable of any kind of DSB repair involving strand invasion or simple end annealing (Lettier et al., 2006). Biochemical studies indicate that RAD52 anneals to complementary single stranded DNA (ssDNA) and stimulates the RAD51 proteins to these sites (Sung et al., 2000). Intriguingly, no homologs of RAD52 have been found so far in the organisms *D. melanogaster*, *C. elegans* and *A. thaliana*. The apparent absence of RAD52 in *Arabidopsis* has been correlated with the low levels of HR in plants (Ray and Langer, 2002). Mutants of the epistatic RAD52 group are in general sensitive to IR and show recombination deficiency. *Atrad51* mutants are insensitive to bleomycin that induces DSB but sensitive to a cross-linking agent mitomycin C indicating a role for this gene in interstrand cross-linking (ICL) repair (Bleuyard and White, 2004). Only AtRad51 and AtXrcc3 proteins are required for HJ resolution and branch migration during meiosis and repair of meiotic DSBs (Bleuyard and White, 2004; Li et al., 2004). The other *RAD51* paralogs are speculated to have a role in branch migration-the DNA extension step of the repair process, which is common to all HR mechanisms (Bleuyard et al., 2005).

### III. Resolution of products: CO or NCO

After DNA repair synthesis, the joined molecules are held together by structures called double Holliday Junctions (dHJs), which function to facilitate strand exchange between non-sister chromatids. A majority of the COs (85-90%) in Arabidopsis is subject to interference *via* ZMM proteins (see III-1) CO-I pathway (Higgins et al., 2004, Mercier et al., 2005). The ZMM complex

participates during second end invasion that involve DNA synthesis and ligation of the broken ends and subsequently, the MMR complex stabilizes the double-Holliday Junction intermediates. Few COs that are insensitive to interference (10-15%) are processed via the CO-II pathway through MUS81 (Copenhaver et al., 2002) as confirmed by mutant analysis (see below).

**III-1. The ZMM complex**

The complex of ZIP1, ZIP2, ZIP3, ZIP4, MSH4, MSH5 and MER3 is commonly referred to as the ZMM proteins and are necessary for the correct progression from DSBs to stable SEI intermediates in yeast (Borner et al., 2004, Lynn et al., 2007). They have important roles in SC assembly and mediate CO-I formation. ZIP4/SPO22 functions with ZIP2 to promote polymerization of Zip1 along chromosomes (reviewed by Lynn et al., 2007). Mutations in AtZIP4 eliminate approximately 85% of crossovers and unlike the situation in yeast, they do not influence synapsis (Chelysheva et al., 2007). The two closely related Arabidopsis *ZIP1* genes (*AtZIP1a* and *AtZIP1b*) have limited structural similarity to its homologs in yeast. In the absence of AtZIP1, recombination is reduced by 20% with multiple non-homologous associations at metaphase-I (Osman et al., 2006). In addition to its role in transverse filament formation during synapsis, AtZIP1 is thought to prevent non-homologous recombination; it hardly influences recombination (Higgins et al., 2005). This is in sharp contrast to the dramatic reduction in CO reported for yeast and mouse *ZIP1* mutants (de Vries et al. 2005; Sym and Roeder, 1994). MER3 has a role in extending the DNA heteroduplex and it stabilizes molecules in the pathway leading to dHJ formation and, hence, crossovers (Nakagawa et al., 2001, Mazina et al., 2004). Mutation of *Atmer3* reduces CO frequency (Mercier et al., 2005) and its function is conserved between yeast and plants. *Msh4*, *Msh5* are discussed as part of the MMR complex (below); *ZIP2* and *ZIP3* remain to be identified in Arabidopsis.

**III-2. The MMR complex**

Much of what we know about the conserved post-replicative mismatch repair (MMR) complex comes from studies of its role in mitotic recombination and cancer research. MMR repair is bi-directional being specific to the newly synthesized DNA strand (reviewed by Li et al., 2008). MMR complexes contain the MutS, MutL and MutH proteins in prokaryotes; their roles are conserved in eukaryotes. However, they are more complex in higher eukaryotes with the existence of six *MutS* homologues and multiple *MutL* homologs, and have roles in both meiotic and mitotic mismatch repair. Plant MutS homologs include *AtMSH2*, *AtMSH3*, *AtMSH6*, *AtMSH4* and *AtMSH5*. Mutation of *AtMSH2* causes dinucleotide repeat instability and increases crossover rates by 40% (Leonard et al., 2003). Both *AtMSH4* and *AtMSH5* are involved in CO formation during

meiosis (Higgins et al., 2004; Franklin et al., 2006; Higgins et al., 2008). *MSH4* and *MSH5* are also expressed along with the DNA repair genes in the shoot apical meristem (SAM) under UV-B irradiation (Kimura et al., 2004) suggesting that recombination repair is active in proliferating cells. The MutL protein AtMLH1 interacts with AtPMS1 during mitosis and AtMLH3 during CO formation in meiotic HR (Jackson et al., 2006). It has a key role in both types of homologous recombination. While both male and female MLH1 and MLH3 knockout mice (Baker et al., 1996; Lipkin et al., 2002), and male PMS2 knockout mice (Baker et al., 1995) are completely sterile, Arabidopsis mutants show more subtle phenotypic alterations. *Atmlh1* shows a strong decrease in homologous recombination although the decrease in recombination due to homeology (introduced synthetically in an experiment) was less reduced compared to the wildtype. At*MLH1* is required for correcting recombination-related errors and prevents recombination between divergent sequences (Dion et al., 2007). *Atmlh3* mutants are viable although they are partially reduced in fertility with a concomitant decrease in CO formation during meiosis (Jackson et al., 2006).

### III-3. Mus81

The Mus81 endonuclease is involved in mitotic DNA damage repair and in the generation of interference-insensitive COs in meiotic recombination (de los Santos et al., 2003). Mus81 protein is highly conserved in eukaryotes and shares homology with the XPF/Rad1 family of proteins involved in DNA nucleotide excision repair. However its role is drastically different across eukaryotes. *mus81* $^{-/-}$ loss-of-function mutants show prominent sterility defects in fission yeast and to a lesser extent in budding yeast, while they are fertile in mammals and plants, implying that in yeast, meiotic recombination is greatly dependant on this gene. In Arabidopsis, *AtMUS81* seems to be required for repair by homologous recombination in somatic cells only under genotoxic stress. The *Atmus81*$^{-/-}$ mutant shows decreased homologous recombination under mutagenic treatments with chemicals like bleomycin, methyl methane sulfonate and mitomycin C (Hartung et al., 2006). A slight decrease in meiotic recombination frequency of only 10% within linked genetic intervals was observed for the *Atmus81*$^{-/-}$ mutant (Berchowitz et al., 2007) conforming to the hypothesis that AtMUS81 is required for a secondary subset of meiotic COs, insensitive to interference.

### III-4. Plant-specific genes in HR

In the last decade, a number of plant genes involved in the HR pathway have been identified based on the yeast homologs. Forward genetic screens have identified some meiotic genes that are so far unique to plants. A lack of significant sequence homology of DSB formation proteins AtPRD1 and AtPRD2 (De Muyt et al., 2009) outside the plant kingdom is an indication that this

complex has evolved divergently across kingdoms. AtSDS1 is a meiosis-specific cyclin that has limited sequence identity to known animal cyclins and has evolved differently in plants. *AtSDS*$^{-/-}$ mutants show synaptic and segregation defects that result in univalents, abnormal chromosome distribution and ultimately aneuploid cells (Azumi et al., 2002). Another gene *AtPTD1* is specific to CO interference sensitive pathway and is found only in plants. *AtPTD1*$^{-/-}$ is affected only in the late stages of CO formation showing reduced chiasmata formation. However, synapsis and late recombination nodule are normal in the mutant (Wijeratne et al., 2006).

**DNA damage check points**

Surveillance mechanisms or checkpoints coordinate formation and repair of DSBs during cell cycle progression. DNA damage and recombination checkpoints are activated to temporarily arrest the cell cycle and allow repair of damaged DNA. Failure to adequately repair the DNA damage leads to elimination of the defective cells by apoptosis (Norbury and Hikson, 2001) and hinders our understanding of the nature of the defect via mutant investigation. Plants, on the other hand, seem to lack a tight meiotic checkpoint - most mutants are viable with normal vegetative growth but show sterility defects. There is only a delay in progression to the next stage of meiosis. Hence most meiotic mutants in plants manage to complete meiosis in sharp contrast with the mouse mutants that arrest defective germline cells altogether. Protein kinases like Ataxia telangiectasia mutated (ATM) and Ataxia telangiectasia and RAD3 related (ATR) are involved in DNA damage detection in yeast, plants and humans. ATM is rapidly induced by DSBs in meiotic and mitotic HR (Table 1.1) and interacts with the MRN/X complex during repair (Lee and Paul, 2004). The ATM phosphorylation targets include DNA repair, cell cycle control, and apoptosis proteins (Garcia et al., 2003). ATM substrates include proteins involved in G1, intra-S-phase and G2/M checkpoints. Following DNA damage during meiosis, ATM phosphorylates the C-terminal domain of its targets like NBS1 and COM1. The ATR mediated signaling is induced mainly upon UV damage causing stalled replication forks with a slower kinetics of response to DSBs (Shecter et al., 2004). The action of ATR in DSB repair is ATM-dependant and involves ssDNA ends occurring at DSB sites (Zou et al., 2003). Mutants in the AtATM gene exhibit chromosome fragmentation, characteristic of defective early DSB repair (Garcia et al., 2003) while the disruption of AtATR1 alone does not seem to have an effect on meiosis (Culligan and Britt, 2008).

**Theoretical and practical aspects of altered HR**

Understanding the precise roles of genes involved in meiosis is imperative to our understanding of sexual reproduction, and thus of understanding the maintenance

of genetic diversity and of natural variation. Knowledge of the basic mechanisms of HR is fundamental to making advances in technologies employing targeted gene modifications for therapeutics (humans) and crop improvement. In plant breeding increased recombination rates at specific chromosome regions would allow higher genetic variation at target regions and hence quicker selection of (un)desired traits. Mutants with altered recombination rates may help to promote genetic exchanges with wild genotypes and polyploid cultivars that currently have crossing barriers. Mutants like *dyad* (Ravi et al., 2008) exhibit apomixis-like developmental phenomena and are desirous in F1 hybrid seed production to achieve little or no recombination. In the future, we can potentially fix favourable gene combinations in plant varieties by decreasing or nullifying meiotic recombination (ref inverse breeding).

Gene targeting (GT) is the precise and targeted repair, modification or replacement of an endogenous gene by homologous recombination. Gene targeting in plants is generally achieved at a frequency of only $10^{-4}$ to $10^{-6}$. Species with a good targeting efficiency of 10 in $10^5$ cells like moss (Schaefer and Zryd, 1997) and yeast predominantly employ HR. A number of approaches to increase the efficiency of targeted integration have been attempted. In an attempt to enhance HR, prominent yeast HR genes have been introduced into plants. Shaked et al., (2005) were able to achieve a 27-fold increase in GT efficiency of a reporter gene by constitutive overexpression of the chromatin-remodeling gene *ScRAD54* in *Arabidopsis*. Targeted DSB induction has been used to induce site-specific repair. Using a combination of repair construct with nptII gene and homologous sequences and the I-Sce-I nuclease construct was shown to increase the frequency of HR 10- to 100-fold (Puchta et al., 1996; Reiss et al., 2003). Homology-dependent GT with positive-negative selection has succeeded in achieving an efficiency of 2% per surviving callus in rice (Terada et al., 2007). Species with low levels of HR like Arabidopsis and mammals mostly employ NHEJ for DNA repair. Since the NHEJ mechanism is more error prone, it is useful for mutagenesis-based gene targeting in plants. Zinc finger nucleases (ZFN) with tailor-made sequence specificities have been employed to achieve site-specific mutagenesis (Lloyd et al., 2005). All these strategies need further optimization but have shown that it is in principle possible to improve gene-targeting efficiencies in plants. A better understanding of the mechanism of HR in plants will provide new tools to effectively alter HR for crop improvement and increase gene targeting efficiency in plants.

Identifying genes involved in microsporogenesis should include characterization of their respective promoter fragments that drive germline stage-specific expression. The lily LIM10 promoter was characterized to improve transposon tagging efficiency in rice. The activity of the transposon depends on a transposase for activation. The expression of the transposase under a constitutive

promoter (CaMV35S) is not desired in somatic cells or throughout development as it creates multiple transpositions and secondary mutations. Hence induction of the transposase only in the germline ensures regulated transposition and the transposon can be stably transmitted to the subsequent generations (Morita et al., 2003). The quest for a germline stage-specific promoter has started and a number of promoters have recently been tested for germline-specificity (Verweire et al., 2007). Amongst the promoters characterized from genes functioning at various stages of pollen development, *APETALA1* (Irish and Sussex, 1990) and *AtSUPERMAN* (Ito et al., 2003), *AtDMC1* (Klimyuk and Jones et al., 1997), *AtSDS1* (Azumi et al., 2002), *AML* (Kaur et al., 2006) are capable of driving expression during meiosis but are not meiosis-specific.

**Scope of my thesis**

The main theme of my thesis is to enhance our understanding of meiotic recombination with the focus on contributing to the development of novel strategies and approaches for plant reproduction.

The **second chapter** deals with the identification of genes involved in meiosis and recombination. The last decade of meiotic research has exploited sequence homology to characterize plant meiotic genes using mutant collections especially in *Arabidopsis* and maize. Meiotic genes seem to be surprisingly diverse across species with respect to conservation in sequence and function along with an expanding list of recombination - related genes with limited sequence similarity and previously unknown functions. The focus of our research was to conduct a search to identify novel plant-meiotic genes. We employed partial transcriptome profiling by cDNA AFLP in *Petunia hybrida* to track the expression of genes that were differentially expressed during the consecutive meiotic stages.

The **third chapter** describes the partial analysis of the genes we sourced from our expression profiling experiment described in the previous chapter. The focus was to identify *Arabidopsis* homologs of the sequenced *Petunia* partial transcripts. A reverse genetics strategy was then employed to screen mutant collections for mutants in 64 selected genes. We present the outcome of our screen with a better understanding of the challenges in unraveling the function of genes involved in plant meiotic processes.

In the **fourth chapter**, we test four mutants for altered meiotic recombination. Meiotic tester lines with linked fluorescent markers were developed to rapidly identify changes in recombination frequencies. These testers can be employed for meiotic recombination assays to screen for recombination-related genes.

The **fifth chapter** involves the characterization of the *xrs4* mutant that is affected in DNA-damage repair in mitosis and meiosis, using forward genetic approaches. Map-based cloning was performed to identify the underlying gene

and to understand the nature of the protein that is crucial to both meiosis and mitosis in plants. The mutant is defective in meiosis-II with chromosome segregation defects and found to have a pleiotropic effect on plant development.

The **sixth chapter** focuses on understanding the role of a mismatch repair gene *AtMLH3* in meiosis. We measured meiotic recombination in the mutant and characterized the promoter. This work has enhanced our understanding of the role of the gene in crossover formation. In addition we now have a meiosis-specific promoter that can be used to express genes specifically in germline cells.

Finally, the **seventh chapter** provides a comprehensive concluding discussion. It summarizes the work done in this thesis and presents a perspective on its importance for meiosis research. Meiotic mutants are useful tools in crop research particularly in the areas of developing breeding methods, and understanding evolution of polyploid species.

# Chapter 2

## Changes in gene expression during male meiosis in *Petunia hybrida*

Veena Hedatale[1], Filip Cnudde[1], Hans de Jong, Elisabeth S. Pierson, Daphne Y. Rainey, Marc Zabeau, Koen Weterings, Tom Gerats and Janny L. Peters.

[1] Authors have equally contributed to this work

*A Petunia flower with its anthers and pistils exposed*

*Published in Chromosome Research 2006, 14: 919-932.*

**Abstract**

We analyzed changes in gene expression during male meiosis in Petunia by combining the meiotic staging of pollen mother cells from a single anther with cDNA-AFLP transcript profiling of mRNA from the synchronously developing sister anthers. The transcript profiling experiments focused on the identification of genes with a modulated expression profile during meiosis, while premeiotic archesporial cells and postmeiotic microspores served as a reference. About 8000 transcript tags, estimated at 30% of the total transcriptome, were generated, of which around 6% exhibited a modulated gene expression pattern at meiosis. Cluster analysis revealed a transcriptional cascade that coincides with the initiation and progression through all stages of the two meiotic divisions. Fragments that exhibited high expression specifically during meiosis I were characterized further by sequencing; 90 out of the 293 sequenced fragments showed homology with known genes, belonging to a wide range of gene classes, including previously characterized meiotic genes. *In-situ* hybridization experiments were performed to determine the spatial expression pattern for five selected transcript tags. Its concurrence with cDNA-AFLP transcript profiles indicates that this is an excellent approach to study genes involved in specialized processes such as meiosis. Our data set provides the potential to unravel unique meiotic genes that are as yet elusive to reverse genetics approaches.

## 2.1 Introduction

Meiosis is a special type of cell division that produces haploid gametes from diploid parental cells and creates natural variation through crossovers and chromosome recombination. The chromosome number is halved during meiosis because a single round of DNA replication is followed by two consecutive rounds of chromosome segregation. Yeast, *Drosophila melanogaster*, mouse, *Arabidopsis thaliana* and *Caenorhabditis elegans* are well known attractive models for meiotic studies. Before the sixties, meiosis was mostly studied at the microscopic level using a range of plant and insect species (Pearson et al. 1997). Despite a long history of research in flowering plants, the molecular and functional analysis of meiotic genes was relatively underdeveloped until recently.

Nowadays investigations into plant meiosis begin to benefit from the immense amount of data generated by large-scale gene expression studies on meiosis in yeast. A genome-wide transcriptome analysis during meiosis in *S. cerevisiae* using DNA microarrays led to the identification of 1600 genes exhibiting a modulated expression at different stages of meiosis (Primig et al., 2000). These genes could be grouped into seven clusters, each with a unique expression pattern. Based on these expression data, Rabitsch et al. (2001) carried out a targeted mutagenesis program for a further characterisation of genes

required for meiosis. Comparison with a similar analysis in *S. pombe* revealed a strikingly small overlap of the meiotic transcriptomes (Mata et al., 2002). Microarrays have also been used to study gene expression profiles during mouse spermatogenesis, which may lead to the identification of genes with potential relevance to mammalian meiosis (Schultz et al., 2003, Yu et al., 2003). In a comparative study, Hwang et al. (2001) performed a bioinformatics-based search for homologues of meiosis-induced yeast genes in *C. elegans*, *D. melanogaster* and mammals, thus demonstrating that yeast sporulation and meiosis in higher eukaryotes were evolutionary highly conserved. However, intriguing differences do exist, reflecting that distinctive mechanisms govern progression of meiosis in each organism (Cnudde and Gerats, 2005).

In plants, a number of genes playing a role in meiosis have been identified based on a gene-by-gene approach, using both reverse and forward genetics. Several mutants, such as *Atrad51* and *Atdmc1* (Doutriaux et al., 1998), *Atrad50* (Gallego et al., 2001) and *Atmre11* (Bundock and Hooykaas, 2002) resulted from a reverse genetics strategy, based on sequence information of known meiotic genes in yeast. In the forward genetics approach, chemical and insertion mutants with sterility phenotypes have been screened followed by a detailed secondary screen to detect meiotic defects. Genes like the *AtSDS* (Azumi et al 2002), *ZmSGO1* (Hamant et al., 2005) and *ZmPHS1* (Pawlowski et al., 2005) in maize have been identified in this manner. Identification of specific types of meiotic genes remains a challenge due to limited sequence conservation between species, existence of closely related gene families and in some cases functional redundancy between gene family members (Sanchez-Moran et al., 2005). For instance, structural proteins involved in the formation of the synaptonemal complex (SC) have been elusive to detection based purely on primary sequence homology. Although functionally analogous, yeast and mammalian SC proteins exhibit no homology. The central element protein AtZIP1 was identified using a combination of primary sequence information and secondary structure prediction (Higgins et al., 2005).

Recently, alternative approaches have been developed to identify novel meiotic genes. Peptide mass-finger printing and matrix-assisted laser desorption ionization time of flight mass spectrometry have been successfully employed to analyze proteins expressed in meiocytes during prophase I of meiosis (Sanchez-Moran et al., 2005). A cDNA microarray comparing gene expression in rice seedlings, meiotic anthers and mature anthers, as well as gibberellic acid (GA3) or jasmonic acid (JA) treated suspension cells identified 2155 genes as preferentially expressed in anthers and 47 genes as differentially expressed in meiotic and mature anthers (Wang et al., 2005). Microarray analysis of gene expression is exhaustive but depends on the availability of sequence information. Gel-based transcript profiling systems like mRNA differential display (DDRT-

PCR) and cDNA-AFLP are powerful techniques because they allow identification of differentially expressed transcripts without any *a priori* knowledge of their sequence or function. Once identified, the transcripts of interest can be sequenced for further analysis. The reproducibility of cDNA-AFLP patterns allows great confidence in the acquired data and differences in the intensities of amplified products can be informative and may allow quantitative expression comparision at different meiotic time points (Breyne et al., 2003).

In this study, we employ cDNA-AFLP transcript profiling to identify genes in *Petunia hybrida* that are modulated in their expression during male meiosis. The advantage of *Petunia* is the size of the chromosomes that are large enough for a straightforward microscopic staging of meiotic samples. In addition, each anther contains approximately 10,000 relatively synchronously dividing meiocytes which is much more than seen in *Arabidopsis* anthers with an average of only 30 meiocytes in a locule (Armstrong et al., 2001). Sufficient mRNA can be obtained from three anthers derived from a single flower bud, allowing a reproducible gene expression analysis by cDNA-AFLP.

Among the 8,000 amplicons obtained we selected 475 candidate cDNA fragments displaying a modulated and/or meiosis-specific gene expression pattern. Fragments that exhibited a modulated expression were further analyzed by direct sequencing. Homologies with diverse classes of known meiosis genes were retrieved, confirming that our screening was effective. We identified five large clusters of co-expressed genes by hierarchical average linkage clustering and adaptive quality-based cluster analysis. Furthermore, we performed *in situ* hybridizations with five selected fragments as a probe to check the temporal gene expression patterns generated by cDNA-AFLP transcript profiling and to obtain additional spatial expression information.

## 2.2 Materials and Methods

### Plant material

*Petunia hybrida* var. Mitchell (W115) (Mitchell et al., 1980) plants were grown under greenhouse conditions of 21°C on average and 16h photoperiod. Immature flower buds of 2- 5 mm were dissected under a binocular using a small pair of forceps. The smallest anther of each flower bud was out of phase with the rest and therefore discarded. Of the remaining four anthers, one was fixed in a freshly prepared ethanol-acetic acid (3:1) mixture at room temperature for 12-18h for microscopic analysis. The remaining three anthers of a single flower bud were frozen in liquid nitrogen and then stored at –80°C until subsequent RNA isolation.

**Staining of enzyme-digested spread pollen mother cells**

The ethanol-acetic acid fixed anthers were washed in water, incubated in a mix of pectolytic enzymes for cell wall digestion, spread on a slide and stained with 4', 6-diamidino-2-phenylindole (DAPI) for staining the chromatin as described by Ross et al., (1996). The preparations were studied under a fluorescence microscope and meiotic cells were captured with a CoolSNAP CCD camera (Roper Scientific, USA). We used Photoshop for adapting resolution sharpening and cropping of the images.

**Total RNA isolation and cDNA synthesis**

For a total RNA sample of any meiotic stage we always used the three anthers of one flower bud; whereas for samples of premeiotic stages we used the anthers of two flower buds at the same stage. Using complete anthers implies that in addition to the meiocytes in the pollen sac, the samples contain other anther tissues such as the epidermis, the endothecium, the connective tissue and the tapetum. Anthers were homogenized in an MM300 bead laboratory mixer mill (Retsch GmbH and Co, Haan, Germany) for 40 sec at 20Hz. Immediately after homogenization RNeasy-buffer was added and total RNA was isolated using the RNeasy Kit according to the manufacturer's instructions (Qiagen, Hilden, Germany). Total RNA was treated with DNase (Promega, Madison, WI, USA) for 30 min at 37°C and purified by phenol-chloroform-extraction and ethanol precipitation. For the cDNA synthesis we used 3 µg of total RNA. First and second cDNA strands were synthesized according to standard protocols (Sambrook et al., 1989) and finally purified by phenol extraction and ethanol precipitation.

**cDNA-AFLP analysis**

Double-stranded cDNA was used for cDNA-AFLP-based transcript profiling procedure according to Breyne et al. (2003) with the *Bst*YI and *Mse*I restriction enzymes (New England Biolabs, Beverly, MA, USA). For preamplifications, an *Mse*I-primer without selective nucleotides was combined with a *Bst*YI-primer containing a T at the 3'-end. We used 5 µL of a 600 times diluted amplification mixture for final selective amplifications following Breyne et al. (2002). The *Bst*YI+T- and *Mse*I-primers with two selective nucleotides each were used for the cDNA-AFLP analysis and all 256 possible primer combinations were performed. The $^{33}$P-ATP-labeled fragments were separated on a 5% polyacrylamide gel. The dried gels were exposed to Kodak Biomax films and scanned in a Phospho-Imager (Molecular Dynamics, Sunnyvale, CA, USA) to cut out and quantify the bands of interest, respectively.

**Reamplification of AFLP fragments and direct sequencing**

Fragments corresponding to differentially expressed transcripts were excised from the dried polyacrylamide gel and suspended in 150 µL $H_2O$ for 3h at 20 °C. A 5 µL aliquot of the eluted DNA suspension was used for the reamplification reaction under the same PCR conditions and using the same primer combination as for selective amplification. Reamplified products were checked on a 1% agarose gel. Sequence information was obtained by direct sequencing of one strand using the selective *Bst*YI-primer as a sequencing primer. As a control, we checked whether the sequences corresponded to the excised fragments in size and selective nucleotides of the *Mse*I-primer. The whole procedure was repeated if quality of the sequenced fragment was insufficiently clear.

**Data analysis**

Transcript tags were compared to sequences in GenBank using BLASTX (Altschul et al., 1997and FASTX (Pearson et al., 1997) algorithms. Transcripts returning scores under the significance cutoff value of E=0.001 were compared with the database using the Smith-Waterman algorithm (Smith and Waterman, 1981).

**Quantitative measurements of the expression profiles and data analysis**

Gel images were quantitatively analyzed using the AFLP-QuantarPro image analysis software (Keygene, Wageningen, The Netherlands). All AFLP fragments were scored and individual band intensities were measured for quantification of the expression profile of each transcript. The raw data were corrected for differences in total lane intensities after which individual gene expression profiles were variance-normalised (Breyne et al., 2002). The Cluster and TreeView software (Eisen et al., 1998) was used for hierarchical, average linkage clustering, followed by a second, adaptive quality-based clustering (De Smet et al., 2002). The minimal number of tags in a cluster and the acquired probability of genes belonging to a cluster were set to 2 and 0.95, respectively.

**RNA *in situ* hybridization**

RNA *in situ* hybridization experiments were performed as described by Cox and Goldberg (1988) with minor modifications. The fresh selected flower buds were fixed overnight at 4°C in 0.25% (w/v) glutaraldehyde, 4% (w/v) formaldehyde in 0.01M phosphate buffer (pH 6.8), and subsequently dehydrated, cleared and embedded in paraffin. We hybridized the [$^{33}$P]-UTP-labeled RNA probes at a specific activity of 4 to 5 x $10^8$ dpm/µg onto the 10 µm sections. Sense and antisense RNA probes were synthesized using the cDNA-AFLP tags cloned into a pGEM-T vector. After hybridization and emulsion development, sections were studied under a bright field, differential interference contrast or dark field

microscope. The slides were also stained with DAPI and studied under the fluorescence microscope to establish the stage of meiosis.

**2.3 Results**

**Meiotic staging and synchrony within the anthers**

Developmental staging of *Petunia* flowers by Porceddu et al., (1999) was based on developmental landmarks linked with morphometric data. However, we found that bud and anther size at male meiosis vary considerably under different environmental conditions making it difficult to correlate meiotic stages based on size alone. We therefore identified the precise meiotic stage of each sample on the basis of DAPI-stained enzyme-digested pollen mother cells (Fig 2.1). Analyzing the microscopic slides containing the spread cells from a single anther we observed a high synchrony of meiotic development especially during the long prophase I stages. During the fast evolving meiosis II, often three subsequent meiotic stages like anaphase II, telophase II and tetrad could be observed in the same preparation.

The progression through meiosis occurred synchronously in four out of the five anthers of a flower bud, while in the smallest anther the meiotic stages had progressed further (data not shown). The special nature of the abaxial anther is not uncommon in the solanaceae family. While this anther is tiny compared to the other anthers in Petunia, it is completely aborted in its close relative Salpiglossis (Fries, 1911). Hence, the smallest anther of each flower bud was discarded from sampling.

For studying the expression profiles we selected meiotic samples containing pollen mother cells at premeiotic interphase, early prophase I (including leptotene and part of zygotene), synizesis (including part of zygotene and early pachytene), late pachytene up to metaphase I, dyad to telophase II and post-meiotic stages. The morphological criteria are based on meiotic prophase description for tomato (Moens, 1964) and Beta (de Jong and Oud, 1979) and include synizesis and diffuse diplotene. Leptotene and zygotene are not distinguishable in the strict sense as the onset and progress of chromosome pairing cannot be assessed reliably. Diagnostic substaging of early prophase can be made on the basis of heterochromatin patterns. Most plants with pericentromere heterochromatin display a variable number of chromocentres at interphase and very early meiotic prophase that aggregate during very early prophase to form ultimately the synizetic knot (De Jong and Oud, 1979). The changes in heterochromatin morphology and clustering of the chromocenters, along with pairing in the visible chromosome loops can be used to substage early prophase I events (Abirached-Darmency et al., 1991).

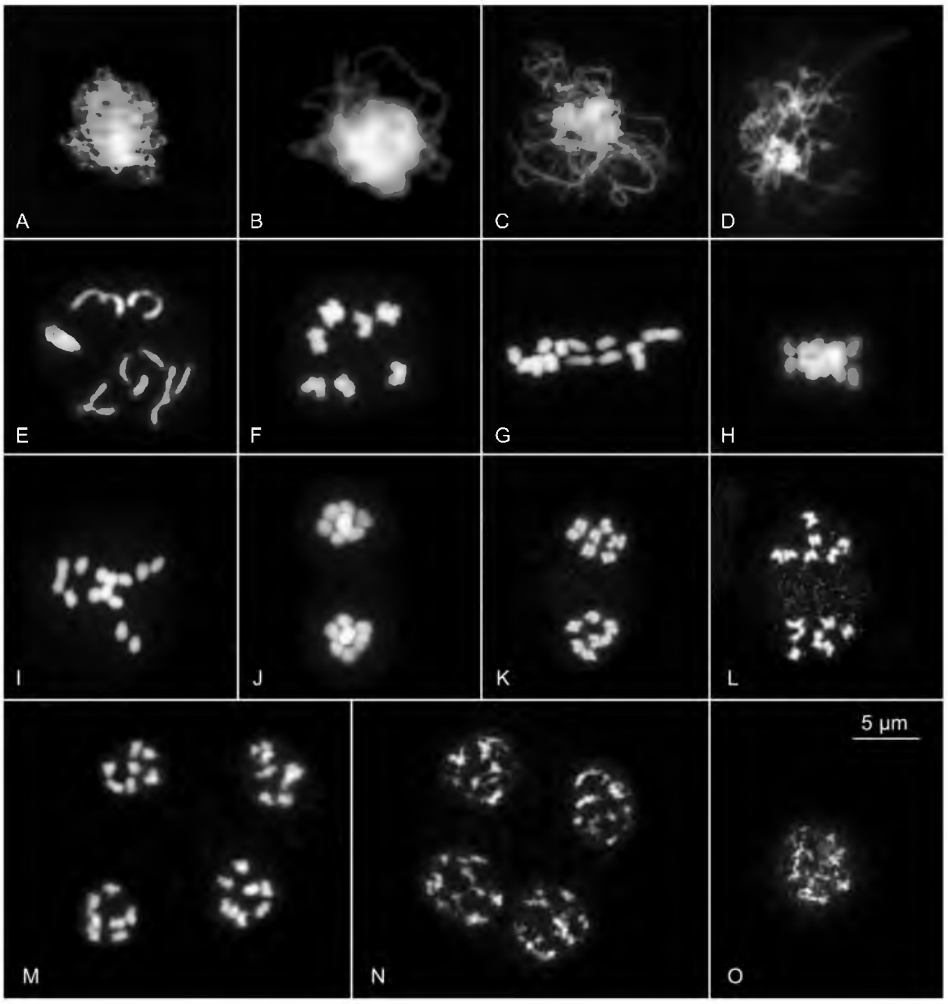


**Fig. 2.1**: Overview of meiotic stages as determined by DAPI-staining in microsprocytes of *Petunia hybrida*. A, B. very early meiotic prophase C. synizesis (including pachytene), D. early diplotene, E. late diplotene, F. early metaphase I, G. metaphase I, H. early anaphase I, I. anaphase I, J. telophase I, K. dyad stage, L. metaphase II, M. telophase II, N. tetrad, O. end of tetrad stage.

We focused on prophase I stages to investigate the meiosis-specific processes of chromosome pairing and recombination. The high level of synchrony of meiotic prophase I stages is an important advantage for gene expression analysis. The two premeiotic samples were prepared from anthers derived from two flower buds of 1.8 and 2.2 mm in size, respectively (stage 2 in Porceddu et al., 1999). Two postmeiotic samples were taken from anthers derived from single flower buds of 4.75 and 5 mm, respectively (stage 4 in Porceddu et al., 1999).

**cDNA-AFLP transcript profiling**

The cDNA-AFLP transcript profiling with the BstYI+T- and MseI-primers and two additional selective nucleotides generated 30-35 AFLP tags per primer combination, which is sufficient for quantitative analysis. While the majority of the signals were constitutive, cDNA fragments exhibiting a modulated expression pattern were well represented (Fig 2.2).

We regularly observed an abrupt transition of cDNA profiles between the zygotene and the pachytene sample, which seemed to necessitate a more refined meiotic staging. Therefore, we repeated our transcript profiling experiment on an extended set of 36 samples derived from partially overlapping, meiotic stages, with emphasis on the transition between synizesis and pachytene. The expression profiles were found to be consistent with the first experiment including the abrupt transition between the zygotene and pachytene stages (data not shown). The experiment with 256 primer combinations resulted in approximately 8,000 transcript tags.

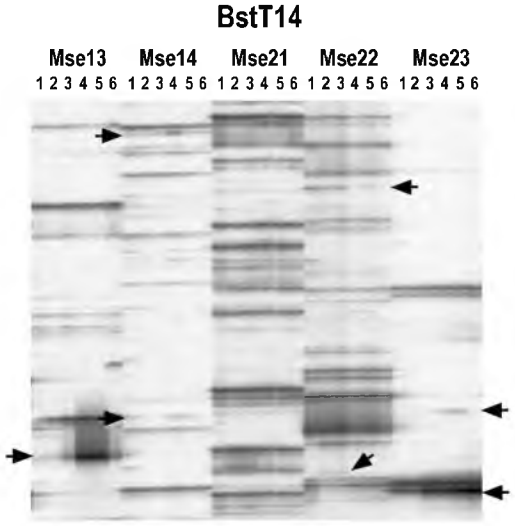


**Fig. 2.2** cDNA-AFLP transcript profiling during male meiosis, using BstT/Mse +2/+2 primer combinations. Expression levels are compared during 6 stages, which are determined by cytological analysis. Arrows indicate fragments with a modulated expression pattern during meiosis. 1 premeiotic, 2 very early meiotic prophase, 3 early synizesis, 4 pachytene-metaphase I, 5 dyad stage-telophase II, 6 postmeiotic.

Based on a comparative restriction site analysis (Breyne et al., 2003), we estimated that roughly 30% of the total *Petunia* transcriptome was covered. Six percent (475) of the transcript tags showed a visually modulated gene expression pattern during meiosis.

**Cluster analyses of the expression profiles**

We performed a cluster analysis on 7408 expression profiles. Approximately 500 expression profiles were not included because of insufficient quality for cluster analysis or because the corresponding PhosphoImager scans were not available. The threshold level chosen for identifying significant differences in signal intensity corresponded to a three-fold transcriptional change, which is a stringent condition to minimize false-positives. As a result, a set of 978 significantly modulated fragments was obtained, which included a significant number of the 475 gene fragments that were selected upon simple visual inspection.

In a first approach, we performed a hierarchical average linkage clustering according to Eisen et al., (1998). Hierarchical clustering is a pairwise average-linked algorithm that sorts through all the data to identify pairs of genes that behave most similarly and then progressively adds other genes to the initial pairs to form clusters of genes with a correlated expression profile. An overview of the resulting clusters of genes with similar expression profiles is presented in Figure 2.3. A transcriptional cascade can be observed that governs initiation and progression through the meiotic cell cycle. These successive waves of transcription reveal a high level of coordination and a precise temporal activation of meiotic genes, indicating a strict regulation at the transcriptional level.

Large clusters of co-regulated genes were expressed exclusively premeiotically or postmeiotically, while other clusters harboured meiosis-specific genes, which displayed high expression levels during early, middle or late meiosis (Fig. 2.3). The highest levels of gene induction were found in the cluster with postmeiotically expressed genes with up to a 60-fold increase in mRNA levels. In contrast, a majority of the premeiotically expressed genes is 20- to 30-fold down-regulated upon meiotic initiation. A second group of premeiotically expressed genes is less repressed and remains transcriptionally active during early prophase. We focused on genes modulated during meiosis. Most of the 475 transcript tags selected for further characterization belonged to the clusters with meiosis-specific gene expression patterns. Two major clusters harbor genes expressed in early prophase (up to synizesis) or later in meiosis (from pachytene to telophase II). A third, smaller cluster contains 'middle' genes reaching their peak expression level at the zygotene stage.

To confirm the results obtained by hierarchical average linkage clustering, the data set was subjected to a second clustering algorithm, called adaptive quality-based clustering (De Smet et al., 2002). The program defines separate groups of significantly co-expressed genes without the requirement to specify the number of clusters *a priori*. Expression profiles that do not fit in any cluster are rejected. The substantial discriminatory power of this method allows a further refinement in the classification of co-expressed genes, compared to hierarchical average linkage clustering. As a result, 11 clusters were obtained,

representing the expression profiles of 826 genes, which is 85% of the total data set (data not shown). Of these, five major clusters of co-expressed genes were generated (Fig. 2.4) namely, premeiotic (254), downregulated (50), early meiotic (66), late meiotic (100), and postmeiotic (244), which is 80% of the total data set. Overall, adaptive quality-based clustering confirmed the clustering tree of Figure 2.3. However, the substantial discriminatory power of the second method allows a further refinement in the classification of co-expressed genes, compared to hierarchical average linkage clustering.

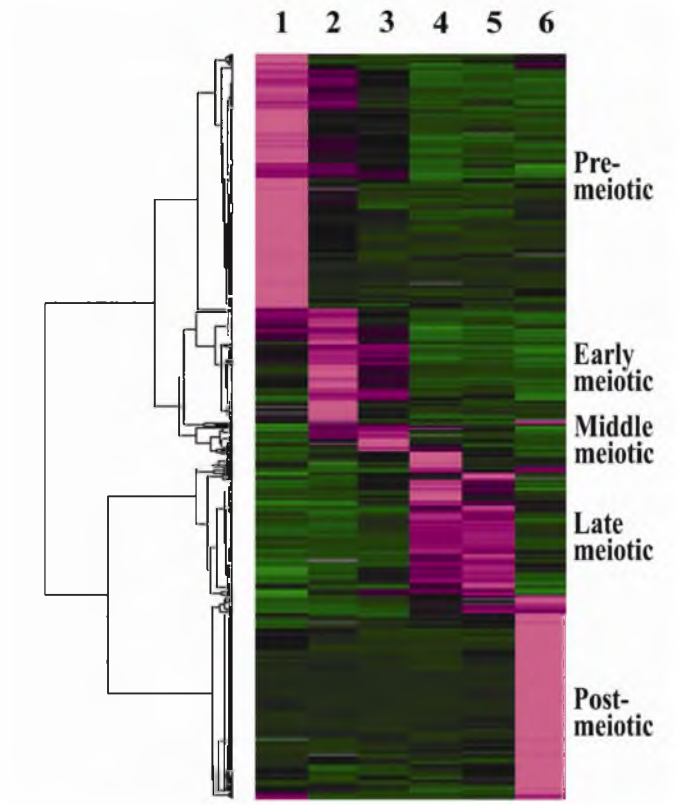


**Fig. 2.3** Hierarchical average linkage clustering of the expression patterns of 978 significantly modulated cDNA-AFLP fragments according to Eisen et al. (1998). The matching dendrogram shows five different clusters of co-expressed genes, with maximal expression level at different stages during meiosis. The color scale ranges from saturated red (highest expression) to saturated green (lowest expression). *1* premeiotic, *2* very early meiotic prophase, *3* early synizesis, *4* pachytene-metaphase I, *5* dyad stage-telophase II, *6* postmeiotic.

**Homology search for known genes**

Direct sequencing of 475 selected cDNA-AFLP fragments resulted in useful sequence information for 293 cDNA fragments (62%). The sequences obtained were compared to those present in the GenBank database using BLAST

(Altschul et al., 1997) and FASTA (Smith and Waterman, 1981) algorithms; 90 fragments (30%) showed significant homology (maximum E-value 0.001) to genes with known function, while another 25 tags (8%) matched with genes without an allocated function (ESTs or putative proteins). The remaining 178 fragments (62%) shared no homology with sequences in the database. These figures are comparable to earlier cDNA-AFLP analyses in *Petunia* (Cnudde et al., 2003) and tobacco (Breyne et al., 2003).

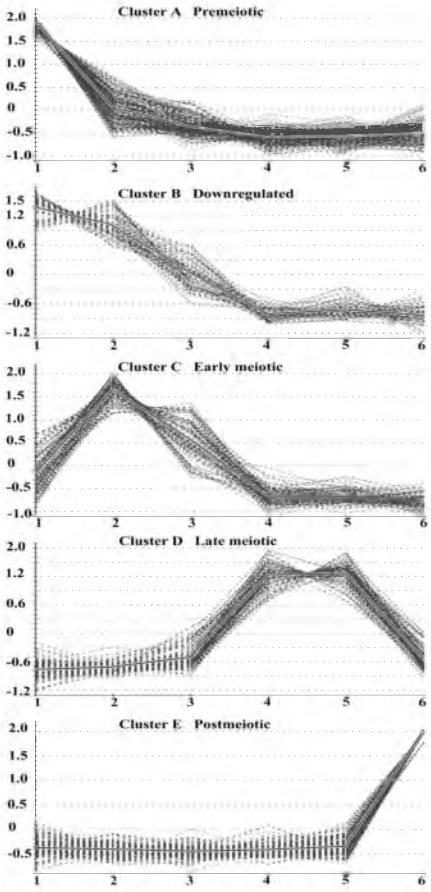


**Fig. 2.4** Adaptive quality-based clustering of the expression patterns of 978 significantly modulated cDNA-AFLP fragments according to De Smet et al. (2002). **A-E** Five major clusters harboring 87% of all expression patterns. **1-6** Sampled stages. *1* premeiotic, *2* very early meiotic prophase, *3* early synizesis, *4* pachytene-metaphase I, *5* dyad stage-telophase II, *6* postmeiotic

The consistent expression pattern seen for the multiple tags corresponding to the same gene served as a good internal control. The successfully sequenced transcript tags were annotated and classified according to their putative functions, based on literature searches. An overview is provided in Table 1, while the analyzed sequence tags (submitted to NCBI) are provided as supplementary data.

In general, the extent of homology between the *Arabidopsis* proteins characterized so far and their meiotic homologs in yeast and humans range from 20-45% identity and 40-60% similarity (Schwarzacher, 2003; Kerzendorfer et al.,

2006). Homologies with known meiotic genes from plants, yeast and mammals showed that our screening was in principle effective. We were able to retrieve cDNA tags homologous to *Arabidopsis* genes involved in meiosis-specific processes. In the early meiotic cluster, tags 12, 46 and 56 correspond to *AtDMC1*, involved in meiotic recombination (Doutriaux et al., 1998). In the down-regulated cluster, tags 265, 285 correspond to *AtASK2*/*AtASK1* with a role in meiosis, flower and embryo development (Yang et al., 1999; Yang and Ma, 2001) and tags 203, 204 correspond to *AtASY1* involved in synapsis (Ross et al., 1997; Caryl et al., 2000; Armstrong et al., 2002). Several links were found with mammalian testis development, for example protein kinases that are denoted as testis-specific in the database. Another striking homology was found with a RecA-gene of *Streptococcus* (tag 229), adding further proof to the high level of evolutionary conservation of meiotic recombination proteins. Some of the upregulated expression tags correspond to genes that are also characterized to be essential for male fertility, gametogenesis and embryo development (Table 2.1). These include homologs of tapetum differentiation gene *AtGPAT1* (tag 358), tomato meiotic serine proteinase *LeTMP* (tag 76) essential for microsporogenesis ((Riggs et al., 2001) and auxin response factor *AtARF4* (tag 393) as auxin is critical for anther/pollen grain development (Feng et al., 2006). The cell wall biosynthesis gene *AtTPS1* (tag 40), polyA- specific ribonuclease *AtPARN* (tag 245) are essential for embryogenesis, while the polyamine biosynthetic gene *AtADC1* (tag 99) is needed for seed development. However, our finding that their expression is upregulated in meiotic anthers is new. In addition, the roles of some of the genes known to be essential for meiotic processes in yeast and mammals are yet to be proven in *Arabidopsis*. These include tag 280, corresponding to the plant homolog of Damaged DNA Binding Protein 1 (DDB1), a protein originally identified because of its role in the human disease *xeroderma pigmentosa*. Tag 106 is a putative ubiquitin-conjugating enzyme. In mammals these enzymes are known to interact with recombination RAD51 protein and with proteins of the synaptonemal complex (Kovalenko et al., 1996). *Ubc9* interacts with the meiosis-specific *RecA* homolog, *Lim15/Dmc1* in the basidiomycete *Coprinus cinereus* (*CcLim15*), and mediates its sumoylation during meiosis (Koshiyama et al., 2006). Other tags of the ubiquitin family correspond to tags 15, 37, 66, 121, 333, 388, 445, 452 and the histone-2B family 223, 237, 246, 414, 019 and are expressed at higher levels during the early meiotic phase.

**Table 2.1** Functional classification of transcript tags with a significant level of homology (E-value < 0.001) using BLAST at NCBI.

| Function | No. of tags |
|---|---|
| DNA replication and modification | 7 |
| Proteolysis | 10 |
| Signal transduction | 7 |
| Cytoskeleton | 8 |
| DNA repair and recombination | 7 |
| Synapsis and sister chromatid cohesion | 2 |
| RNA processing | 4 |
| Protein synthesis | 7 |
| Hormone response | 1 |
| Metabolism | 33 |
| Transcription factors | 1 |
| Transport and secretion | 3 |
| Unknown function | 25 |

Transcript tags showing a significant homology in database searches were unequally distributed over the clusters described above. In particular, fragments expressed late during meiosis have a considerably smaller chance of finding a match in the BLAST database than early meiotic fragments. Of the 100 sequenced fragments belonging to cluster D (Fig. 2.4), only 8 showed a significant homology (8%), compared to 18 of the 66 sequenced cluster C fragments (27%) and 16 of the 50 sequenced cluster B fragments (32%).

**Expression analysis by RNA *in situ* hybridization**

To obtain spatial expression patterns and to confirm the cDNA-AFLP expression profiles, we examined the expression of five tags in reproductive tissues, using RNA *in situ* hybridization. Two transcript tags are homologs of characterized meiotic genes in *Arabidopsis*, namely, *DMC1* (tag 56) and *ASY1* (tag 203). *DMC1* was expressed during leptotene and zygotene, also showing high levels of meiocyte-specific expression (Fig. 2.5). However, while no premeiotic expression was visible in the cDNA-AFLP pattern, the *in situ* hybridizations showed a clear signal in the pollen mother cells before meiosis. For *ASY1*, the *in situ* data confirmed the cDNA-AFLP pattern (Fig. 2.6), showing high levels of *ASY1* expression in the early meiotic stages, localized in premeiocytes and leptotene microsporocytes. The timing of ASY1 expression corresponds to the initiation of synaptonemal complex formation that precedes the start of chromosome synapsis at zygotene.

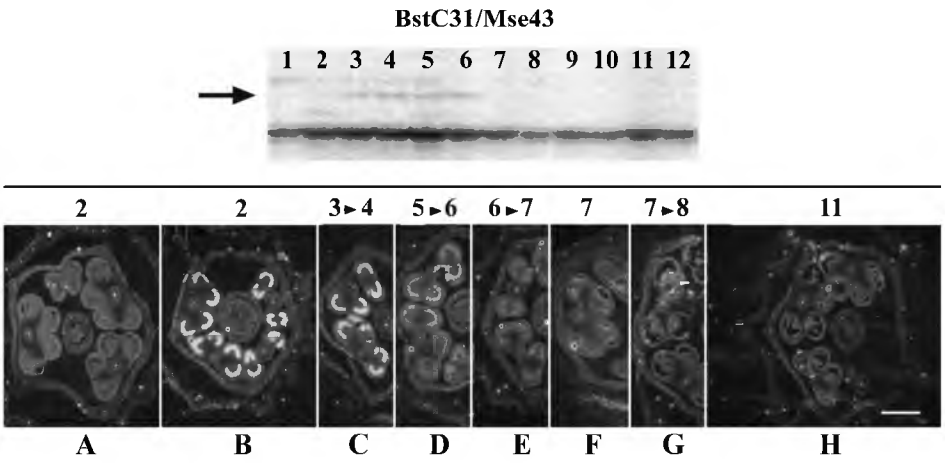


**Fig. 2.5** Expression analysis of *DMC1* homologue M56. **Upper panel** cDNA-AFLP expression pattern. *1,2* premeiotic, *3* very early meiotic prophase, *4* early meiotic prophase, *5* early synizesis, *6* synizesis, *7* pachytene, *8* metaphase I, *9* dyad stage, *10* telophase II, *11,12* postmeiotic. **Lower panel** *In situ* hybridization using [$^{33}$P]-UTP-labeled RNA probe on sections of *Petunia* buds, exposed for 35 days and examined using dark-field illumination. *A* Sense; *B-H* Antisense. *A, B* premeiotic, *C* very early meiotic prophase, *D* synizesis, *E* synizesis-pachytene, *F* pachytene, *G*, diplotene, *H*, tetrad. Bar = 0.5mm.

Furthermore, preliminary *in situ* data were obtained for fragments homologous to genes encoding a poly (A) ribonuclease (PARN) (tag 245), a checkpoint protein (BUB1) (tag 342) and a C3HC4 zinc finger protein (tag 407) (data not shown). *PARN* expression was detected before meiosis and in the leptotene and zygotene stages. *BUB1* transcripts accumulated in all cell types of the anther during early meiosis but from pachytene onwards, the signals could no longer be detected. The expression of the C3HC4 zinc finger gene appeared to be localized in the tapetum layer, rather than in the meiocytes. Further analysis will show whether this gene does exert its function in the tapetum itself or whether it has a non-autonomous function in meiocytes. In general, the *in situ* hybridization experiments confirmed the gene expression patterns for all selected genes, validating our cDNA-AFLP results, while adding spatial information.

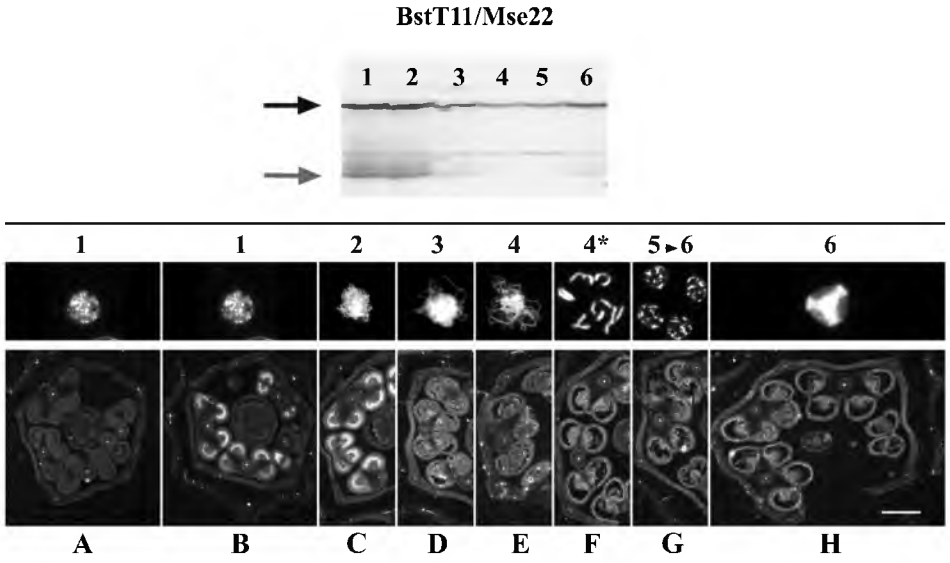


**Fig. 2.6** Expression analysis of *ASY1* homologue M203. **Upper panel** cDNA-AFLP expression pattern. **Middle panel** *1* premeiotic, *2* very early prophase, *3* synizesis, *4* pachytene → metaphase I, *4** diplotene, *5* dyad stage → telophase II, *6* postmeiotic. **Lower panel** *In situ* hybridization using [$^{33}$P]-UTP-labeled RNA probe on sections of *Petunia* flower buds, exposed for 35 days and examined using dark-field illumination. *A* Sense, B-H Antisense. *A,B* premeiotic; *C* very early prophase; *D* synizesis; *E* pachytene; *F* diplotene; *G* tetrad; *H* pollen

## 2.4 Discussion

We employed cDNA-AFLP transcript profiling for the identification of genes that are modulated in their expression during male meiosis in *Petunia hybrida*. Cluster analyses on our data set identified five large clusters of co-expressed genes, representing 83% of all selected gene tags. A transcriptional cascade is thus observed that governs initiation and progression through the meiotic cell cycle, as has been demonstrated in a temporal analysis of the meiotic transcriptome in yeast (Chu et al., 1998; Primig et al., 2000; Mata et al., 2002). These successive waves of transcription reveal a high level of coordination and a precise temporal activation of meiotic genes. As genes with related functions tend to be expressed in similar patterns, cluster analysis may provide a first clue for the functional characterization of yet unknown co-expressed genes. A strict co-regulation of genes with a transcript profile that specifically correlates with the biological function within a phase of the cell cycle has been demonstrated in plants (Breyne et al., 2002) and gene expression profiling data have been successfully used to infer gene functions in yeast meiosis (Toth et al., 2000). Accordingly, we may find support for the proposed functions of several isolated fragments with varying levels of homology, based on their temporal association with meiotic genes of known function.

The 254 premeiotically expressed genes in our study are strongly repressed upon entry into meiosis. Fragments belonging to this class have not been characterized further by sequencing. Another 50 Petunia cDNA-AFLP fragments were more gradually down-regulated, showing a gradual decrease in transcript levels up to the end of the zygotene stage. Many of the transcript tags with this expression pattern putatively have roles in ubiquitin-mediated proteolysis, RNA processing and protein biosynthesis. Homologies were found to genes involved in DNA replication, synapsis of homologous chromosomes (ASY1), SCF complex subunit (SKP1/ASK1) and spindle assembly (BUB3), indicating the preparation of the meiotic cell for the recruitment of a specialized set of proteins upon commitment to meiosis. Sixty-six fragments showed a pattern of expression characterized by an early induction at leptotene, followed by a decrease in transcript levels at zygotene. Characterized genes with this transient induction pattern encode proteins, involved in meiotic recombination (DMC1), DNA modification, checkpoint control and membrane transport. This cluster is comparable to the 'early gene clusters' distinguished in budding yeast (Chu et al. 1998, Primig et al., 2000) and fission yeast (Mata et al., 2002).

A fourth cluster of 100 fragments followed a pattern of expression characterized by a late induction at pachytene and sustained expression during the meiotic divisions. Compared to the clusters discussed above, fewer homologs were found to genes expressed in the late meiotic phase, which is of a short duration (Armstrong & Jones, 2003), indicating that their corresponding sequences are yet underrepresented in databases. Sequenced transcript tags showed homology to genes encoding DNA repair proteins that may be involved in Holliday junction resolution and mismatch repair. Further, homologies are found with proteases, signal transduction proteins (kinases, phosphatases) and those required for proper chromosome segregation such as the structural maintenance of chromosomes (SMC) proteins. Compared to the gene expression patterns of the 'middle genes' in yeast (Chu et al., 1998, Primig et al., 2000, Mata et al., 2002), the expression of Petunia fragments belonging to this cluster is more repressed in the postmeiotic stage.

Finally, about 244 genes are induced after completion of the meiotic divisions. They putatively represent gametogenesis-related genes, many of which may have unique functions during microspore development. They correspond to the anther-specific transcripts that were identified during a previous cDNA-AFLP transcript profiling experiment on developing *Petunia hybrida* floral organs (Cnudde et al., 2003). A similar cluster of postmeiotically induced genes is present in yeast (Chu et al., 1998, Primig et al., 2000, Mata & Ba¨hler, 2003). However, these genes encode proteins involved in spore maturation and ascus formation, which exhibit low levels of homology with plant genes (Cnudde et al., 2003).

Strong homologies to known meiotic genes from *e.g.*, *Arabidopsis* or *Saccharomyces* that resulted from our experiment include genes like *DMC1*, *ASY1,* and *ASK1*. Few others like *BUB1* and *BUB3* have been identified as essential components of the mitotic and meiotic spindle check point machinery (Amon 1999, Prinz and Amon 1999; Yamaguchi et al., 2003). While *BUB3* has a significant hit (tag 21), no obvious *BUB1* homolog (tag 342) is known in the *Arabidopsis* genome. Weak homologies were found with nucleic acid-modifying enzymes, such as ATP-dependent helicases (tags 222, 230) topoisomerases (tags 283, 319), p23 tubulin binding proteins (tag 445), microtubule associated (tag 77). Fragment 287 is induced late in meiosis and shows a homology to a meiosis-related, testis-specific protein known as cancer-antigen in humans and to a plant Ruv DNA-helicase-like protein. Proteins related to the bacterial RuvB DNA helicase have been shown to catalyze branch migration of Holliday junctions (Shen et al., 2000). In this way, a targeted selection can be carried out to identify candidate gene fragments with a putative function in particular aspects of meiosis.

A number of genes that we found in this study are implicated in processes other than meiosis like flower development, gametogenesis, embryogenesis, microsporogenesis, namely *AtGPAT1, AtPARN, AtADC1.* Many others are related to genes of major biochemical metabolic and signaling pathways for example *AtNADH5, AtBAP1, ATIPT2, ATCIMS* and *AtARF4* that are essential for the cells to survive and grow. However, their expression is also upregulated in meiotic anthers and yet it seems unlikely that they have a meiotic role per se. The identification of genes seemingly unrelated to meiosis may be the result of our sampling method. Exclusive sampling of microsporocytes would enrich the pool of meiosis specific transcripts but is technically challenging and tedious.

Finally we performed RNA *in situ* hybridization in order to validate the expression pattern of the transcripts. The results are in general agreement in all the cases, with some differences. For example, the strong cDNA-AFLP tag expression of *DMC1* in microsporocytes of *Petunia hybrida* is in agreement with the RNA *in situ* hybridization data and the results of *AtDMC1* promoter: GUS protein gene fusions in *Arabidopsis thaliana* (Klimyuk and Jones, 1997). However, the expression in premeiotic stages seen in the anthers using RNA *in situ* hybridization was not seen in cDNA-AFLP expression pattern for *DMC1*. This difference could reflect the difficulty in precisely defining the onset of leptotene.

Further studies, including mutational analyses, are required to elucidate the possible meiotic role of several genes identified in this study. While *Petunia hybrida* is amenable to the microscopy-based sampling and cDNA-AFLP transcript profiling, meiotic research in *Arabidopsis* is attractive due to the

extensive sequence information and the large mutant collections available for this model species. Because the function of the homologs in *Petunia hybrida* and *Arabidopsis thaliana* is likely to be conserved to a great extent in meiotic processes like recombination, synapsis and in the synaptonemal complex components, one can make use of the advantages of Arabidopsis and look for Arabidopsis homologs of candidate Petunia gene fragments with a putative function in meiosis.

In conclusion, the combination of accurately staged anthers with cDNA-AFLP transcript profiling in *Petunia hybrida* is a valuable method to identify genes involved in meiosis. Based on their modulated gene expression pattern, candidate meiosis-related AFLP tags can be selected, while a first indication for a possible function can be obtained by sequence homology and their clustering with known meiotic genes. Our data set provides a starting point for unraveling meiosis at a molecular level in plants. This will allow a knowledge-based selection of novel meiotic genes for further characterization.

**2.5 Acknowledgements**

Veena Hedatale was funded by the sub faculty of Biology, Radboud University Nijmegen and the Graduate School Experimental Plant Sciences, the Netherlands. Filip Cnudde was funded by the Flanders Fund for Scientific Research (FWO), the Flemish Institute for Biotechnology (VIB) and the subfaculty of Biology, Radboud University Nijmegen.

# Chapter 3

## Screening for novel *Arabidopsis* meiotic mutants


*Arabidopsis thaliana* T-DNA insertion lines for segregation analysis

**Abstract**

Meiosis is a conserved process commonly occurring in plants, animals, and fungi making possible the identification of inter-species homologs and study of gene function by mutant analysis. We applied reverse genetics to source genes from expression profile data that are active during microsporogenesis, particularly involved in meiosis and recombination. We screened 100 T-DNA insertion lines within 62 genes to interrogate a meiotic gene function. Three previously characterized meiotic genes and as many as 11 genes important for development were identified. Transcripts with a direct and dedicated role in meiosis were far fewer than expected suggesting that they are either lowly expressed, have multiple roles in the anthers or exhibit a great degree of functional redundancy.

## 3.1 Introduction

The life cycle of flowering plants consists of two phases: the haploid gametophytic phase and the diploid sporophytic phase. Unlike animals, plants have no predetermined germ line cells and their gametes arise by differentiation of the floral meristem. The developmental cues dictating the sub-epidermal L2 layer-derived archesporial cells to generate meiocytes are still a mystery (Scott et al., 2004). Unique to plant meiosis are processes like alternation of phases of a single generation and the formation of an independent microgametophyte, the pollen. Meiosis starts after the G2 phase of the premeiotic cell cycle is completed and results in the formation of four haploid cells. Important aspects of meiotic development that distinguish it from mitotic growth include a highly increased rate of recombination, formation of the synaptonemal complex at the axes of the paired homologous chromosomes, as well as separation of the homologs and sister centromere pairs during meiosis I and II without an intervening S-phase. Homologous recombination is an evolutionarily conserved process that generates allelic diversity and preserves genetic information. Although a number of meiotic mutants have been identified, the specific mechanism of HR still remains largely unknown. In the future, breakthroughs in plant breeding strategies will be possible when we can regulate the timing and the expression of these proteins. It would be advantageous to prevent recombination in selected hybrids or increase recombination efficiency in a targeted manner in crop developmental programs.

During meiosis, homologous chromosomes recombine through a complex process of breakage, exchange and rejoin of DNA strands, using the DNA repair mechanisms that rely on sequence homology to recombine broken ends. The major DNA repair pathway acting during meiosis is the Double Strand Break Repair (DSBR) pathway. A number of plant meiotic proteins in the DSBR pathway have been successfully identified using sequence homology to yeast meiotic proteins. However, comparative genomics and proteomic studies also provide evidence that many proteins acting in meiosis have striking differences

in each organism. The synaptonemal complex proteins exist in most eukaryotic species with chiasmatic meiosis and yet differ in their ultrastructure at the level of the primary sequence (Bogdanov et. al., 2007). Comparing meiosis between all kinds of eukaryotic model species has made it clear that structural and morphological details of the pairing and recombination processes are not fully conserved necessitating us to investigate different organisms to understand the nuances of the meiotic process. Hence, in addition to studying *Arabidopsis* homologs of the yeast and mammalian genes we need more leads to identify unique meiotic genes in plants.

Expression profiling data obtained from flower buds and meiotic anthers in *Arabidopsis*, Rice, *Brassica* and *Petunia* are a promising source for finding new meiotic genes that are unlikely to be found by homology searches alone or forward screens that rely on the reduced fertility phenotypes (Wang et al., 2005; Sanchez-Moran et al., 2005). We applied reverse genetics to source genes from expression profile data that are active during microsporogenesis, particularly involved in meiosis and recombination. In a former study discussed in Chapter 2, approximately 300 genes modulated in expression during male meiosis in *Petunia* have been assembled using cytology-based sampling and cDNA-AFLP transcript profiling (Cnudde et al., 2006). While *Petunia hybrida* is amenable to easy sampling of meiocytes and the cDNA-AFLP approach, *Arabidopsis* offers sequence information and T-DNA insertion lines to study mutants in the genes of interest. In the present study we therefore used our set of partial *Petunia* cDNAs generated during meiosis to identify a subset of *Arabidopsis* genes with the goal to identify new meiotic genes. We validated our homolog identification approach using meiotic DMC1 in *Petunia* and *Arabidopsis,* by comparative sequence analysis and quantitative RT-PCR. We present here the genes that were upregulated during meiosis in the anthers and the results of our mutant screen using T-DNA insertion lines in *Arabidopsis*. This study has brought to light the different group of genes that are expressed in the early phases of male reproductive development.

## 3.2 Materials and Methods

### Plant material

The *Arabidopsis thaliana* T-DNA insertion lines were obtained from the Nottingham Stock Centre (NASC) for SALK, Wisconsin and SAIL lines while the FLAG lines were obtained from Institut National de la Recherche Agronomique (INRA). The Arabidopsis ecotypes Columbia-0 (Col-0) and Wassilewskija (Ws) were used as controls. Seeds of 99 lines were sown on half strength Murashige and Skoog (1/2 MS) medium without sucrose for 14 days and

later grown in the green house under long-day conditions (16 h light/8 h dark) at approximately 22°C in a growth chamber.

**Arabidopsis homolog search**

cDNA-AFLP transcript profiling was used to analyze changes in gene expression during male meiosis in *Petunia hybrida* (Cnudde et al, 2006). All of the 292 partial *Petunia* sequences obtained were subjected to a homology search. The *Petunia* cDNA AFLP tags ranged from 50 to 450bp and close homologs in the EST database of Solanaceous species sometimes provided sequences of improved length. These ESTs were then BLASTed against the non-redundant datasets of *Arabidopsis* in NCBI (http://www.ncbi.nlm.nih.gov/) and TAIR (http://www.arabidopsis.org/Blast/) using the BLAST program (Altschul et al., 1997). Based on sequence similarity (e-value cut off $10^{-6}$) and annotations, *Arabidopsis* homologs indicating a meiotic function were selected. T- DNA insertion lines within these genes were obtained from the SALK collection (http://signal.salk.edu).

**Table 3.1: Insertion line primer information.** LB is left border, RB is right border, (F) is forward, (R) is reverse.

| Primer name | T-DNA primer | Primer (F) | Primer (R) |
|---|---|---|---|
| SALK_003297.01 | LB SALK2 | GAAGTTAGCAGCACCCTTGG | AAAGTCGACCACCACTGGAC |
| SALK_130202.01 | LB SALK2 | ATCGGTTTGAATCCGATAGC | AGTGGTCAATCCTGTGGGAG |
| FLAG_368A11.01 | LBBar2 | CGCCCACTTAATTTCAACAAC | TTGAACTCGGCACATTTTATG |
| SALK_079991.02 | LB SALK2 | CAAGTATAACAAGAAAGCCCGG | CTGAAAGCTCAAATGGTCAGG |
| FLAG_014E06.01 | LBBar2 | AACCTGTTCCGTTGGGATAAC | GAATTCACAGCCCATTTATCG |
| SALK_151687.01 | LB SALK2 | TGAATGGAAACAATCAGGTTTC | TGTTTAGGAATTGTTTTGCGG |
| AT1G55870.01 | SALK LBa1 | AATCGGGTTCCGTCAAGTG | GAGGTGACAGAAGCAGAG |
| At1g64230.01 | SALK LBa1 | GATCCTCCAACTTCCTGCAG | AAGGCAAATGCTTCCATTGCT |
| SALK_110996.01 | LB SALK2 | AATTGCGTCTTTGCTTCCTCC | TTGACTCTTGTTCTAAACGATTC |
| FLAG_634B01.01 | Tag3 RB | TGGTGCTTTGGGATTTCTTC | ATCTTTTGATTGCAGGTGGC |
| SALK_003223.01 | LB SALK2 | ACCCAGTGAGTATGTAGAAC | AAGTGCCCCCTATTGAAAAT |
| SALK_110701.01 | LB SALK2 | AGCACGTAAGCCCAAAACCAG | GCGATGGCTTTGTTGAGTTTG |
| SALK_001041.01 | LB SALK2 | AAACATGTGAGAAAACGAGCG | TGATTTGTATTGCAGTTGGAGG |

| Primer name | T-DNA primer | Primer (F) | Primer (R) |
|---|---|---|---|
| SALK_001077.01 | LB SALK2 | CGAGCGTCATTTGGATTACTC | TTTTGCATTGCTATTGGGTTC |
| FLAG_414B06.02 | LBBar2 | GAGGAGCTTTTCCCACCATAG | TAATGAATCCCTTCTTGCTGC |
| SALK_113285 .02 | LB SALK2 | CTGTTCTTTTATCGGCTTGC | ACCTTTTTGTGCTATGTCCA |
| FLAG_271B04.01 | LBbar2 | CTATGCAGGAACTATGGTCGC | TCATTGAAGGGAGAAGCTCAG |
| FLAG_352B03.01 | LBbar2 | AATACAAAGCCCCTTTTGTGC | CCAATCCAAACCACAATTTTG |
| SALK_046869.02 | LB SALK2 | TCCAACGAAACACACTCTCAG | AAAGCTCTTTTCGAAGATCCG |
| SALK_135289.01 | LB SALK2 | ATAGCAGCGATGGTGATTGTG | ACAATCCTGACAGTAGAAGTTTC |
| FLAG_130A06.01 | LBBar2 | ATGATGCTGAACTGACGATTG | CAGGACCAGATTTTCCTCTCC |
| FLAG_346C07.01 | LBBar2 | ATGGCTTCTATCCAATGGTCC | CTTTTCACAGGAACTTGCTGC |
| SALK_022699.01 | LBSALK2 | TCCCTCTGCAGTTTTGTGAAG | TCTCCGTGATTTGATTATGCC |
| SALK_042029.01 | LB SALK2 | GTTTCACCCTCTGTTCATTGC | CTCTGAAGCAATGTGAAAAAGG |
| SALK_118756.02 | LB SALK2 | GAGATTCCGCTTGGACTATG | GCACTGGAAGATGTAAGAAGAG |
| AT2G30580.02 | SALK LBa1 | GGATGTTGATGAACCATGGG | TGGAATATTTCCATCCCTACC |
| AT2G32800.02 | SALK LBa1 | GTTAAAGCCACCGGTGATG | CGAGCTAAACCAAAATCTCC |
| SALK_126383.01 | LB SALK2 | AATGGGGTTGATGATGTTGAG | TCACGTTTGTCGTAATCCAAAC |
| SALK_050711.01 | LB SALK2 | CATCAATCGTTCAAAACCGG | GAAAAGGGACAAAACCTTGG |
| At2g45290.01 | SALK LBa1 | TCAGCTACGCCGTCACCGAC | GAGACGCAGTTTTCAGAGCC |
| SALK_015554.01 | LBSALK2 | TGAATCGATTTATGTGGTCCTG | TGAGTTCCAACAAAGCAGAATC |
| At3g12610.01 | SALK LBa1 | TCGCCGAGAATCAAATGTCC | GACGACAACGAATCCGGGATC |
| SALK_003718.01 | LB SALK2 | TGCCAAATCCAGTCAATATGTC | TCATCGGAGCTGGAGTTGGTG |
| SALK_003041.01 | LB SALK2 | ACGGATAACAGCACGAGACAG | CTCGTTGAGAGATAACGGCTG |
| SALK_038057.01 | LB SALK2 | GAAAACAAACGTCACCTGCAATG | TGACCAAGAAGACATAGGCGG |
| SALK_069547.01 | LB SALK2 | AACGCGTACACGCCTAATTAC | CCATGAAGAAACGAGGAGATG |
| SALK_148060.01 | LB SALK2 | ACAACGGATTCAAGGCATTTG | TAATTTATCCAAACGCGTTGG |
| FLAG_298F01.01 | LBBar2 | CACTTGGCTCATTATCTTGGC | TGTGACCAGTTTGCAACAGAG |
| FLAG_484A03.01 | LBBar2 | AAAATGGATCCCTTTCATTCG | TAAACCCAAATCAACAGCTGC |

| Primer name | T-DNA primer | Primer (F) | Primer (R) |
|---|---|---|---|
| SALK_012836.01 | LB SALK2 | ATCATGCAAAACGGTCCTCGG | TGGCTAAACCCCCTACATG CTG |
| SAIL_276_E11.01 | LB3 SAIL | TTGAGGTTTTGGCTACGTTTG | TCCCAACAACAGGTTTGTCT C |
| SALK_024090.01 | LBSALK2 | TTGTAACTTATGAAAATTTAGGG GG | AAAAACACAATGCCAACAA CC |
| FLAG_430D09.01 | LBbar2 | TGACCCAAAGTCCATATAGCG | CTATCCTGAGGGAAACTTC GG |
| At3g46740.02 | SALK LBa1 | ATATGGACTTGTGATGGAGGAG | TAGCCACGGACAGAGTACG GA |
| At3g46740.05 | SALK LBa1 | CTGCTTCATTCTTTCTGTTCC | ACCACCAGGACGAATCGAG AC |
| FLAG_076E01.01 | LBBar2 | CCTCGAATCTTCGATTGGAC | CTTGATGACGAGAGCTGCA G |
| FLAG_567H05.01 | Tag3 RB | GCAAATAATTCCATCTTTGAGC | TCTCGTATCCTTGCTCTGCT G |
| SALK_052700.01 | LB SALK2 | CACCTTCCCCTGTTAAGGAAG | CTTTGTTTTCCGGGGAAGTA G |
| SALK_127214.01 | LB SALK2 | TTACCGTAGGGGAAATCGTTC | TTATCCGTTCTTGGGACATT G |
| SALK_058277.01 | LB SALK2 | AGACCTCTTGAAAACATGATGG G | CTCAGCTCACCAACACAAA ATC |
| SALK_089597.02 | LB SALK2 | CTTAGACAACAACACGCCGA | GAGTAGCATAAGCAGTAGA T |
| SALK_052702.01 | LB SALK2 | GGCGTTGAGCTATGAAAACTG | TTGTGTTTGGTTTGTGTATT TCAG |
| FLAG_432H07.01 | LBBar2 | TGTCTCCTCCATTCCATTC | ACCTACGCATCTTTTCTCTC |
| FLAG_543G06.01 | Tag3 RB | TGGATCAACACATTGCTTCAC | GTGAAGCCTGATGCTTTGA AG |
| FLAG_280B07.01 | LBbar2 | GCACCTCTGAGTATCGTACGC | CTTACCACGTCAACAACTG AGG |
| SAIL_150_H01.01 | LB3 SAIL | GACTATGGTGTTATTCGGAG | GAGAAGAGGAAAAGGATG AG |
| SALK_021679.02 | LB SALK2 | ATCTTGGGAATGCAACTCATG | AGGGAATTGAAGATCGAGA GG |
| SALK_082847.01 | LB SALK2 | AATTAATGGACGGCTTGAGC | AAGACCGACAATAATGTTG CC |
| SAIL_393_D12.01 | LB3SAIL | CTTGAAGAGGCTGGTGGCTG | CTCTTGCTCTCAGCCGTCTG |
| At4g04910.01 | SALK LBa1 | TGCGGACGGAGTATTGGT | CCGGAATGTTTGGTCTGG |
| SALK_055584.01 | LBSALK2 | TTTGGTATGGCTTTTACTTCCTG | TGGTCATCTGATATATTGCT TCC |
| FLAG_632G12.01 | Tag3 RB | ATTGTTTGCGCCATTGTCTAC | GAGAGATTGACTCGCATGA AAC |
| At4g16155.02 | SALK LBa1 | CAATCGGTTCTTTCTCTTTC | AACTCCAGCTCCGATAAT |

| Primer name | T-DNA primer | Primer (F) | Primer (R) |
|---|---|---|---|
| At4g16155.01 | SALK LBa1 | GTACTTGCGTTAACAGAGGCTG | ACGGTACAGATCCAGTTGCG |
| FLAG_632H10.01 | Tag3 RB | TCTCTAGGGTTCATCCTCGTG | ACCGACCAGGACAATAGGATC |
| FLAG_272G05.01 | LBBar2 | ATGCTCGTCGGATATGTCATC | AGTGCCAAATATGACTGTCGG |
| FLAG_348G01.02 | LBBar2 | GAGGCAGAGACGCTATCACT | CACAGAGAAGGAAACCAAGG |
| AT4G30020.01 | SALK LBa1 | TGTTTCCTCACTGTGACAG | CGCTCCTATGATCTTCCCATTG |
| At4g30870.02 | SALK LBa1 | CCCAAAGATGAACCAAGTGAC | CTCCAGATTTTCCGACAAGCC |
| At4g31750.02 | SALK LBa1 | TTCTGTTTTGTCATCTTCGAGCC | CTTTTACCGGGAGAGCTTGC |
| At4g31750.01 | SALK LBa1 | CGTGCAGCTGAATATGTGAAG | TGCAACAAGTAAACGGTCACC |
| FLAG_394D05.01 | LBbar2 | TGGATTTCACAACCGACAAG | TGTAAGAGATGCGGAAATTGC |
| FLAG_437D02.02 | LBbar2 | CCAAATTGCTTAAAGACAGCC | AGACTGGAGAAACAAGCAAGG |
| SALK_033070.01 | LB SALK2 | TCACAGGACACCCTCAATTTC | TGGCTTCACAACTGTGTCTTG |
| SALK_023626.01 | LB SALK2 | TTGCTAGCAACCATATCGTCC | GATGTTGTGTTTGGAGGATGG |
| AT5G09850.02 | SALK LBa1 | AAACCAGCAAAGGGATCGAAA | TGGACATTTATCGATACGGCG |
| FLAG_386D01.01 | LBBar2 | CCAAGGACAAAGATCACATGC | TGATGATACCGGAGAGACGAG |
| AT5G19820.02 | SALK LBa1 | GCACGACTACCAAGGAAAATGC | CAGCCAAGCTGGCAATAGAGA |
| SALK_133101.01 | LB SALK2 | GACATTCTCCATATTCCGAC | GATCTTGCTCAGGACTCAGG |
| FLAG_016H09.01 | LBBar2 | TGTTTCTTCATATTCGGCGAG | TGCTGTGGTCACATTCGTTC |
| SALK_008776.01 | LB SALK2 | AACTTTTTCTCTCTTTGCCGC | CGCAATGAGAATCACTGTTTC |
| FLAG_629B06.01 | Tag3 RB | GCTGGTCGCTGACTAAGTTTG | ATCAATGGAGGAGAAAAAGG |
| SALK_024447.01 | LB SALK2 | GGACAATGAAATCTGCTTCC | AGCAAATCTCAAAAACAAGACC |
| SALK_077401.01 | LB SALK2 | GACCTTTGGAATTGAAAATTGG | AGGGAATGGAGCTTGGTATTG |
| SALK_025569.02 | LB SALK2 | CGAGTTTTACTTGCTCTTGCG | TCAAGCGCTACATTGCATATG |
| SALK_108271.02 | LB SALK2 | ACCTCCTTTTAGATTCCCACG | CTCGACTTGAATCGCTTGTTC |

## DNA extraction

DNA preparation of Edwards et al. (1991) was modified as described below. Two leaves of two to three weeks old seedlings were sampled and put in racked, 96-well collection microtubes (Qiagen, Hilden, Germany) with one grinding ball (3-mm diameter) in every collection microtube. The laboratory vibration mill

MM300 (Retsch GmbH and Co, Haan, Germany) was used to disrupt the samples (30 s at 30 Hz). After adding 500 µl of extraction buffer (200 mM of Tris HCl pH 7.5, 250 mM of NaCl, 25 mM of EDTA and 0.5% SDS), the samples were mixed well and left at 55–65ºC for 15 min. The extracts were centrifuged for 10–20 min at 4,000 rpm. Then 400 µl of the supernatant was transferred to fresh collection tubes and mixed with 400 µl of isopropanol. After centrifugation at 6,000 rpm for 10–20 min, the supernatant was poured off and the pellet was washed with 70% ethanol. The ethanol was poured off after 10 min centrifugation at 6,000 rpm and allowed to dry. The pellet was dissolved in 200 µl of water and left in the fridge overnight before use.

### Identifying T-DNA mutants

To select the mutants, 25-30 seeds obtained from NASC were sown and DNA was extracted from the rosette leaves for genotyping. Gene-specific primers (Table 3.1) were designed on both sides of the predicted insertion site using the SIGnAL T-DNA Express Arabidopsis Gene Mapping Tool (http://signal.salk.edu/cgi-bin/tdnaexpress) or designed manually using the program Oligo version 4.0. Depending on the source of the T-DNA lines, appropriate T-DNA specific primers were used (Table 3.2). The PCR profile applied was 94°C for 1m 35 cycles of 94°C for 30s, 55°C for 30s and 72°C for 1m 20s, followed by a final extension at 72°C for 2m. Plants homozygous for the T-DNA insert only form a PCR product with a gene-specific primer in combination with the appropriate T-DNA specific primer while the heterozygous plants contain both alleles and hence amplify the insert and gene-specific products. When mutants were absent in the first screen, seeds from a heterozygous plant were sown and genotyped in the next generation.

**Table 3.2: T-DNA specific primers**
LB is left border; RB is right border

| Primer name | Description | Sequence |
|---|---|---|
| LBa1 | SALK LB | TCACGTAGTGGGCCATCG |
| LB SALK2 | SALK LB | GCTTTCTTCCCTTCCTTTCTC |
| LB3 SAIL | SAIL LB | TAGCATCTGAATTTCATAACCA |
| p745 | Wisconsin LB | AACGTCCGCAATGTGTTATTAAGTTGTC |
| LBBar2 | FLAG LB | CGTGTGCCAGGTGCCCACGGAATAG |
| Tag3 RB | FLAG RB | CTAATACCAGACGTTGCCCGCATAA |

**Pollen viability**

Pollen viability was tested for all mutants and for heterozygotes when no mutants survived in the population screened. To determine the viability of the pollen, anthers prior to dehiscence were stained with Alexander solution (Alexander, 1969). Aborted sterile pollen stain green and the non-aborted fertile pollen stain the protoplasm red to deep red. Male gametophytic lethal mutants show an equal ratio of normal and defective pollen and segregated in a 1:1 ratio for the wild type and insert containing alleles, respectively. Anthers were photographed with an Axiovert camera connected to a Leica phase contrast microscope.

**Silique Analysis**

Siliques were analyzed for the T-DNA lines for which mutants were absent. The silique of a heterozygous plant was opened and examined under a dissecting microscope. Embryo-lethal mutations were detected by the presence of siliques containing normal and defective embryos (1/4) and were expected to segregate in a 1:2 ratio for the wildtype and heterozygotes, respectively (Muller, 1963). Siliques were studied under a binocular microscope and images were captured using a Leitz Orthoplan microscope equipped with a CoolSnap color camera (Roper Scientific) and MetaVue program (Leica Microsystems Imaging Solutions).

**Meiotic chromosome morphology**

Chromosome spreads were analyzed for all pollen defective lines to examine meiotic stages and identify the defective stages. *Arabidopsis* flower buds of mutant lines were fixed in Carnoy's fixative (ethanol: acetic acid 3:1). Chromosomes were spread as described in Ross et al., 1996. Slides were stained with 4'-6-Diamidino-2-phenylindole (DAPI) and examined under a Zeiss Axioplan 2 fluorescence microscope. Images were captured using a CCD camera with GENUS Cytovision software and further processed in Adobe Photoshop.

**Quantitative Real Time PCR (RT-PCR)**

Total RNA from premeiotic, meiotic and post meiotic samples was extracted using NucleoSpin® RNA Plant kit (Clontech Laboratories, Inc., CA, U.S.A). The RNA samples were DNase treated using RQ1 RNase-Free DNase (Promega Corporation, Madison, U.S.A.). First-strand cDNA was synthesized from 1μg DNase-free RNA using the SuperScript III and oligo-dT primer (Invitrogen Corp., Carlsbad, U.S.A.). RT-PCR was done on 40-times diluted cDNA using Biorad's iQ SYBR Green Supermix (3 mM MgCl2). The forward and reverse primers were designed using Beacon Designer 2 software. For PtDMC1, forward primer 5'-ATAAGACTAATGTTCAGGAAGG–3' and reverse primer 5'-

AGCGGAAAGTTAAGATAAGC –3' were used. qPCR was carried out using two-step PCR protocol in BioRad icycler (Bio-Rad Laboratories, CA, U.S.A.).

### 3.3 Results

The male meiosis profiling experiments, performed by Cnudde et al. (2006) produced in total 7408 cDNA-AFLP fragments. A subset of 475 of these exhibited clearly modulated meiosis-specific gene expression patterns. We successfully sequenced 292 of these modulated, partial cDNAs and verified the expression pattern for DMC1 (Cnudde et al. 2006; chapter 2 of this thesis).

**Table 3.3:** Details of Arabidopsis genes and T-DNA insertion lines chosen based on homology to Petunia and Solanaceae ESTs

| Gene # | Tag # | GenBank ID /Sequence | Expression ‡ | BLAST Solanaceae[1] | BLAST Arabidopsis[2] | Homolog | Insertion line |
|---|---|---|---|---|---|---|---|
| | | | | **Significant Homologs** | | | |
| 1 | 99 | EB174628 | 1-4 stronger | gi\|76867215\| Nicotiana tabacum cDNA clone KG9B.003A09, Length=810 Score = 301 bits (152), Expect = 1e-80 , Identities = 297/347 (85%) | gi\|79317271\| calmodulin binding / translation elongation factor AT1G07940 transcript variant AT1G07940.2 mRNA, complete cds length=1990, Score = 444 bits (224), Expect = 4e-123 Identities = 431/500 (86%) | AT1G07940 | SALK_003297 *, SALK_130202 L |
| 2 | 21 | EB174589 | stronger in 1-3 + repression | SGN-U271441 Solanum tuberosum Length = 1,464 Score = 428 bits (216), Expect = 1e-119 Identities = 276/296 (93%) | AT1G49910.1 \| WD-40 repeat family protein / mitotic checkpoint protein, putative Length = 1224 Score = 143 bits (72), Expect = 5e-33 Identities = 334/420 (79%) | AT1G49910 | FLAG_014E06 M, SALK_151687 P |
| 3 | 245 | EB174682 | expression in 1-3 | gi\|52588934 Petunia-DevA-22-C01 5' end, mRNA sequence length=663 Score = 210 bits (106), Expect = 4e-53 Identities = 118/124 (95%) | AT1G55870.1 CAF1 family ribonuclease, Length = 2190 Plus Strand HSPs: Score = 524 (84.7 bits), Expect = 3.5e-18, P = 3.5e-18, Identities = 212/331 (64%) | At1g55870 | SALK_072627 L |

| Gene # | Tag # | GenBank ID /Sequence | Expression ‡ | BLAST Solanaceae[1] | BLAST Arabidopsis[2] | Homolog | Insertion line |
|---|---|---|---|---|---|---|---|
| 4 | 106 | EB174631 | 1-3 stronger | gi\|52589965 Petunia-DevA-14R-C03 5' end, mRNA sequence. Length=533 Score = 246 bits (124), Expect = 3e-64, Identities = 133/137 (97%) | gi\|79320671 ubiquitin conjugating enzyme/ ubiquitin-like activating enzyme AT1G64230 transcript variant AT1G64230.2 mRNA, complete cds Length=885 Score = 268 bits (135), Expect = 3e-70 Identities = 287/338 (84%) | At1g64230 | SALK_034041 M, SALK_040325 * |
| 5 | 106 | | | | | At1g69840 | SALK_110996 *, SALK_001077 P |
| 6 | 407 | EB174787 | expression in 2-5, 4-5 stronger | gi\|39874238 EST755333 Nicotiana benthamiana mixed tissue cDNA library Length=754 Score = 244 bits (123), Expect = 2e-63, Identities = 186/207 (89%) | gi\|30684645 ubiquitin-protein ligase/ zinc ion binding AT2G30580 mRNA, complete cds Length=2005 Score = 65.9 bits (33), Expect = 3e-09, Identities = 66/77 (85%) | AT2G30580 | SALK_017187 * |
| 7 | 407 | | | | | AT2G32800 | SALK_064192 * |
| 8 | 93 | EB174623 | expression in 1-3 | - | AT2G35510.1 Encodes a WWE domain-containing protein with 76% similarity to RCD1. Length = 3654 Plus Strand HSPs: Score = 246 (43.0 bits), Expect = 3.3e-05, P = 3.3e-05 Identities = 78/110 (70%) | At2g35510 | SALK_126383 M |
| 9 | 294 | EB174722 | expression in 1-3 | gi62907999 Cold Sweetening B Solanum tuberosum cDNA clone 38697 3', mRNA sequence Length=669 Score = 335 bits (169), Expect = 7e-91 Identities = 232/254 (91%) | gi\|21404327 Arabidopsis thaliana clone 16208 mRNA, complete sequence Length=771 Score = 194 bits (98), Expect = 4e-48 Identities = 272/330 (82%) | AT2G40110 | SALK_050711 M |

| Gene # | Tag # | GenBank ID /Sequence | Expression‡ | BLAST Solanaceae[1] | BLAST Arabidopsis[2] | Homolog | Insertion line |
|---|---|---|---|---|---|---|---|
| 10 | 14 | EB174582 | stronger in 3-5 | gi\|21921456\| Generation of a set of potato cDNA clones for microarray analyses mixed potato tissues mRNA sequence. Length=721 Score = 258 bits (130), Expect = 9e-68 Identities = 154/162 (95%) | gi\|30689982\| Arabidopsis thaliana transketolase AT2G45290 mRNA, complete cds Length=2598 Score = 81.8 bits (41), Expect = 5e-14 Identities = 116/141 (82%) | At2g45290 | SALK_039795[L] |
| 11 | 434 | EB174807 | expression in 2-5, 3-5 stronger | gi\|32877770\| Nicotiana tabacum cDNA clone BY7336, mRNA sequence. Length=733 Score = 79.8 bits (40), Expect = 3e-14 Identities = 80/94 (85%) | Wu Blast AT5G12940.1 leucine-rich repeat family protein, contains leucine rich-repeat domains Length = 1293 Score = 336 (56.5 bits), Expect = 1.5e-07, P = 1.5e-07 Identities = 158/252 (62%) | AT5G12940 | FLAG_386D01[M] |
| 12 | 434 | | | | gi\|20178285 DNA-damage-repair/toleration protein DRT100 precursor Length=372 Score = 89.0 bits (219), Expect = 4e-18 Identities = 85/258 (32%) | At3g12610 | SALK_104292[L] |
| 13 | 111 | EB174632 | 1-3 stronger | gb\|DN172491.1\| Solanum habrochaites cDNA clone LH__Ea10L20 5', mRNA sequence. Length=712 Score = 182 bits (98), Expect = 9e-45 Identities = 118/131 (90%) | AT3G16950.2 PTLPD1 (LIPOAMIDE DEHYDROGENASE 1) Length = 2137 Score = 525 (84.8 bits), Expect = 3.3e-18, P = 3.3e-18 Identities = 133/165 (80%) | At3g16950 | SALK_003718[M] |
| 14 | | | | gb\|EB174632.1\| VUA659 mixed organs cDNA library Petunia x hybrida cDNA, mRNA sequence. Length=171 Score = 254 bits (137), | gi\|145340279\| dihydrolipoamide dehydrogenase 2, plastidic / lipoamide dehydrogenase 2 (PTLPD2) (AT4G16155) mRNA, complete | At4g16155 | SALK_011050[L], SALK_118337[M] |

| Gene # | Tag # | GenBank ID /Sequence | Expression‡ | BLAST Solanaceae[1] | BLAST Arabidopsis[2] | Homolog | Insertion line |
|---|---|---|---|---|---|---|---|
| | | | | Expect = 2e-66 Identities = 171/171 (100%) | cds Score = 182 bits (92), Expect = 2e-44 Identities = 272/332 (81%) | | |
| 15 | 459 | EB174823 | expression in 3-5 | gi\|11529060\|gb\|BF459903.1\| 068B06 Mature tuber lambda ZAP Solanum tuberosum cDNA 5', mRNA sequence length=691 Score = 40.1 bits (20), Expect = 0.029, Identities = 55/64 (85%) | gi\|20259398\|gb\|AY090986.1\| Arabidopsis thaliana At3g41950 mRNA sequence Length=2747 Score = 1063 bits (536), Expect = 0.0, Identities = 658/691 (95%) | At3g41950 | FLAG_430D09[L] |
| 16 | 115 | EB174635 | 1-3 stronger | gi\|76868920\| Nicotiana tabacum cDNA clone KP1B.101L21, mRNA sequence. Length=863 Score = 157 bits (79), Expect = 2e-37, Identities = 94/100 (94%) | gi\|30692756\|protein translocase AT3G46740 (TOC75) mRNA, complete cds Length=2795 Score = 123 bits (62), Expect = 2e-26 Identities = 263/330 (79%) | At3g46740 | SALK_062094*, SALK_015928[L] |
| 17 | 8 | EB174576 | expression 4-5 | gi\|25035396\| Capsicum annuum cDNA, mRNA sequence length=428Score = 157 bits (79), Expect = 3e-37 Identities = 163/191 (85%) | Wu Blast AT3G47990.1zinc finger (C3HC4-type RING finger) family protein length = 1557 Plus Strand HSPs: Score = 366 (61.0 bits), Expect = 4.9e-11, P = 4.9e-11, Identities = 104/141 (73%) | AT3G47990 | FLAG_239C05[P]/ FLAG_090H05[P] |
| 18 | 283 | EB174717 | 1-3 stronger | SGN-U208484 Petunia hybrida (2 ESTs aligned) Length = 605 Score = 87.7 bits (44), Expect = 8e-18 Identities = 49/51 (96%) | AT3G53430.160S ribosomal protein L12 (RPL12B), Length = 783 HSPs: Score = 1317 (203.7 bits), Expect = 7.8e-55, P = 7.8e-55 Identities = 19/598 (70%) | AT3G53430 | FLAG_076E01[M] |

| Gene # | Tag # | GenBank ID /Sequence | Expression‡ | BLAST Solanaceae[1] | BLAST Arabidopsis[2] | Homolog | Insertion line |
|---|---|---|---|---|---|---|---|
| 19 | 463 | seq463 | expression in 1-3 | EST887217 petunia floral post-pollination cDNA library, Length=640 Score = 63.9 bits (32), Expect = 7e-10 Identities = 36/38 (94%) | gi\|30695240 Arabidopsis thaliana VAP27-1 (VAMP/SYNAPTO BREVIN-ASSOCIATED PROTEIN 27-1); Length=1204 Score = 50.1 bits (25), Expect = 2e-04 Identities = 126/160 (78%) | At3g60600 | SAIL_150_H01[P], SALK_082847*, SALK_021679* |
| 20 | 42 | EB174607 | expression in 1-3 | gi\|76867514\| Nicotiana tabacum cDNA clone KG9B.003N04, mRNA sequence. Length=858 Score = 63.9 bits (32), Expect = 1e-09 Identities = 68/80 (85%) | gi\|30695684\| Arabidopsis thaliana structural constituent of ribosome AT3G62870 mRNA, complete cds Length=1048 Score = 258 bits (130), Expect = 5e-67 Identities = 478/594 (80%), Gaps = 0/594 (0%) | AT3g62870 | SAIL_393_D12[L] |
| 21 | 317 | EB174737 | expression in 1-3 | gb\|EB174737.1\| VUA775 mixed organs cDNA library Petunia x hybrida cDNA, mRNA sequence. Length=353 Score = 652 bits (353), Expect = 0.0 Identities = 353/353 (100%) | gi\|145339982\| NSF (N-ETHYLMALEIMI DE SENSITIVE FACTOR); mRNA, complete cds Score = 50.4 bits (119), Expect = 1e-06 Identities = 25/56 (44%) | At4g04910 | SALK_038536* |
| 22 | 236 | seq236 | expression in 2-3 | gi\|39828315\| potato abiotic stress cDNA library Solanum tuberosum Length=749 Score = 46.1 bits (23), Expect = 3e-04, Identities = 33/35 (94%) | gi\|30680924\|ref\|NM_116965.2\| phosphatase activator AT4G08960 mRNA, complete cds Length=1507 Score = 52.0 bits (26), Expect = 3e-05 Identities = 104/130 (80%) | AT4G08960 | SALK_058277[M], FLAG_632G12* |
| 23 | 43 | seq43 | stronger in 4-5 | gi\|9508338\|gb\|BE462569.1\| EST324851 tomato flower buds 0-3 mm, mRNA, sequence length=427 Score | AT4G20980.1 eukaryotic translation initiation factor 3 subunit 7, Length = 2126 Plus Strand HSPs: Score = 1308 (202.3 bits), | AT4G20980 | FLAG_632H10[M] |

| Gene # | Tag # | GenBank ID /Sequence | Expression‡ | BLAST Solanaceae[1] | BLAST Arabidopsis[2] | Homolog | Insertion line |
|---|---|---|---|---|---|---|---|
| | | | | = 40.1 bits (20), Expect = 0.011 Identities = 20/20 (100%) | Expect = 7.3e-55, P = 7.3e-55, Identities = 340/429 (79%) | | |
| 24 | 76 | seq76 | induction 2-6 | gb\|CV504764.1\| 71330.1 Mixed Floral Solanum tuberosum cDNA clone 71330 5', mRNA sequence. Length=656 Score = 143 bits (77), Expect = 3e-33 Identities = 90/97 (92%) | AT4G30020.1 subtilase family protein Length = 2960 Score = 241 (42.2 bits), Expect = 3.3e-05, P = 3.3e-05, Identities = 85/122 (69%), Positives = 85/122 (69%) | AT4G30020 | SALK_068944 M |
| 25 | 48 | EB174609 | expression in 3-6 | gb\|EB174609.1\| VUA636 mixed organs cDNA library Petunia x hybrida cDNA, mRNA sequence length=125 Score = 176 bits (95), Expect = 3e-43 Identities = 125/125 (100%) | gi\|67633819\| putative protein phosphatase 2C (At5g24940) mRNA, complete cds Length=1344 Score = 468 bits (1204), Expect = 3e-130 Identities = 243/310 (78%) | At4g31750 | SALK_089597 *, SALK_143024 M, SALK_146020 * |
| 26 | 448 | seq448 | 2-3 stronger | gb\|EB174814.1\| VUA852 mixed organs cDNA library Petunia x hybrida cDNA, mRNA sequence. Length=116 Score = 196 bits (106), Expect = 2e-49 Identities = 116/116 (100%) | gi\|79502126\| unknown protein (AT4G39790) mRNA, complete cds Score = 48.1 bits (24), Expect = 5e-04 Identities = 33/36 (91%) | At4g39790 | SALK_033070 * |
| 27 | 98 | EB174627 | 1-5 stronger | gi\|76571957\| Reverse subtractive cDNA library of tomato inoculated with Ralstonia solanacearum Length=962 Score = 113 bits (57), Expect = 2e-24 Identities = 72/77 (93%) | gi\|30692536\| inositol-3-phosphate synthase AT4G39800 (MI-1-P SYNTHASE) mRNA, complete cds Length=1918 Score = 184 bits (93), Expect = 6e-45 Identities = 225/269 (83%) | AT4G39800 | SALK_023626 * |

| Gene # | Tag # | GenBank ID /Sequence | Expression‡ | BLAST Solanaceae[1] | BLAST Arabidopsis[2] | Homolog | Insertion line |
|---|---|---|---|---|---|---|---|
| 28 | 27 | seq27 | expression 3-4 | gi\|46828438\| Tuber Skin Solanum tuberosum cDNA clone 2497 5', mRNA sequence length=684 Score = 30.2 bits (15), Expect = 6.3 Identities = 15/15 (100%) | gi\|22329168\| Arabidopsis thaliana structural constituent of ribosome AT4G34670 mRNA, complete cds Length=1093 Score = 71.9 bits (36), Expect = 5e-11 Identities = 54/60 (90%) | At4g34670 | FLAG_394D05*, FLAG_437D02[M] |
| 29 | 450 | EB174816 | expression in 2-5 | SGN-U207936 Petunia hybrida (4 ESTs aligned) Length = 654 Score = 394 bits (199), Expect = 1e-109, Identities = 206/209 (98%) | AT5G09850.1 transcription elongation factor-related Length = 1967 Score = 538 (86.8 bits), Expect = 7.4e-19, P = 7.4e-19 Identities = 286/455 (62%) | AT5G09850 | SALK_072990[L] |
| 30 | 287 | EB174720 | 3-6 stronger | gi\|66835981\| Swollen Stolon Solanum tuberosum cDNA clone 16360 3', mRNA sequence. Length=812 Score = 91.7 bits (46), Expect = 6e-18 Identities = 76/86 (88%) | Gi\|30688414\| Arabidopsis thaliana nucleoside-triphosphatase/ nucleotide binding AT5G22330 mRNA, complete cds Length=1730 Score = 125 bits (63), Expect = 4e-27 Identities = 111/127 (87%) | AT5G22330 | SALK_133101* |
| 31 | 103 | EB174629 | 4-5 stronger | gi\|78750268\| Cold Sweetening C Solanum tuberosum cDNA clone 97160 5', mRNA sequence. Length=625 Score = 101 bits (51), Expect = 7e-21 Identities = 78/87 (89%) | gi\|42568151\| Arabidopsis thaliana unknown protein AT5G36290 Length=1264 Score = 101 bits (51), Expect = 5e-20 Identities = 201/251 (80%) | AT5G36290 | FLAG_629B06[L] |
| 32 | 416 | EB174794 | stronger 1-3 | gb\|EB683822.1\| Nicotiana tabacum cDNA clone KR3B.113J18, mRNA sequence. Length=628 Score = 292 bits (158), Expect = 5e-78 Identities = 200/219 (91%), | gi\|22327574\| Arabidopsis thaliana minichromosome maintenance family protein / MCM family protein (AT5G44635) mRNA, complete cds Length=2895 | At5g44635 | SALK_025569*, SALK_108271[L] |

| Gene # | Tag # | GenBank ID /Sequence | Expression ‡ | BLAST Solanaceae[1] | BLAST Arabidopsis[2] | Homolog | Insertion line |
|---|---|---|---|---|---|---|---|
| | | | | Gaps = 7/219 (3%) | Score = 168 bits (362), Expect = 9e-46 Identities = 73/105 (69%) | | |
| 33 | 22 | EB175019 | stronger in 2-10 | gi\|32878828\| Nicotiana tabacum cDNA clone BY8495, mRNA sequence. Length=581 Score = 182 bits (92), Expect = 6e-45 Identities = 147/163 (90%) | WuBlast AT5G59270.1 lectin protein kinase family protein, Length = 2007 Score = 346 (58.0 bits), Expect = 4.6e-10, P = 4.6e-10 Identities = 226/383 (59%) | AT5G59270 | SALK_096198*, SALK_096269* |
| 34 | 22 | | | | | AT3G59350 | FLAG_432H07[M], FLAG_543G06[M] |
| 35 | 393 | EB174777 | 3-5 stronger | gb\|EB174777.1\| VUA815 mixed organs cDNA library Petunia x hybrida cDNA, mRNA sequence. Length=222 Score = 388 bits (210), Expect = 6e-107 Identities = 222/222 (100%) | gi\|145359484\| ARF4 (AUXIN RESPONSE FACTOR 4) Score = 65.9 bits (33), Expect = 3e-09 Identities = 93/113 (82%) | AT5G60450 | SALK_070506[M] |
| 36 | 16 | EB174584 | stronger in 1-5 | gi\|52581732\| EST881818 petunia floral post-ethylene cDNA library Petunia x hybrida cDNA clone Petunia-C2H4-6RR-C01 5' end, mRNA sequence Score = 662 bits (334), Expect = 0.0 Identities = 340/342 (99%) | gi\|21554781\|hypersensitive-induced response protein Score = 313 bits (801), Expect = 9e-86 Identities = 163/192 (84%) | AT5G62740 | SALK_111162*, WISCDSLOX489-492B7[P] |
| 37 | 206 | EB174661 | expression in 4-5 | gi\|39883036\| Nicotiana benthamiana mixed tissue cDNA library, mRNA sequence length=676 Score = 63.9 bits (32), Expect = 3e-09 Identities = 76/91 (83%) | gi\|42568773\| Arabidopsis thaliana ubiquitin-protein ligase AT5G64660 mRNA, complete cds Length=1525Score = 63.9 bits (32), Expect = 1e-08 Identities = 35/36 | AT5G64660 | FLAG_270C11[P], FLAG_256A05[P] |

| Gene # | Tag # | GenBank ID /Sequence | Expression ‡ | BLAST Solanaceae[1] | BLAST Arabidopsis[2] | Homolog | Insertion line |
|---|---|---|---|---|---|---|---|
| | | | | | (97%) | | |
| 38 | 30, 89 | EB174620 | expression 1-5 | Score = 188 bits (95), Expect = 6e-47 Identities = 131/143 (91%) | AtDGL1; dolichyl-di-phospho-oligosaccharide-protein glycotransferase-like Score = 145 bits (73), Expect = 4e-33 Identities = 266/329 (80%) | At5g66680 | SALK_063253 [P] |
| | | | | **Less- significant homologs** | | | |
| 39 | 2 | EB174571 | expression 4-5 | - | WU_Blast AT3G59570.1 RabGAP/TBC domain-containing protein Length = 2631 Plus Strand HSPs: Score = 150 (28.6 bits), Expect = 0.42, P = 0.35 Identities = 72/111 (64%) | AT3G59570 | FLAG_280B07 [M] |
| 40 | 18 | EB174586 | expression in 3-5 | SGN-U203420 Capsicum annuum Length = 477Score = 38.2 bits (19), Expect = 0.063 Identities = 19/19 (100%) | AT2G28620.1kinesin motor protein-related Length = 3231 Score = 194 (35.2 bits), Expect = 0.61, P = 0.46, Identities = 230/403 (57%) | AT2G28620 | SALK_042029 [M], SALK_118756 [M] |
| 41 | 51, 25 | EB174610 | expression in 2-5 | gi\|52567856\| After-Cooking Darkening A Solanum tuberosum cDNA clone 66823 5', mRNA sequence length=782 Score = 133 bits (67), Expect = 6e-30 Identities = 147/173 (84%) | gi\|30687496\|ref\|NM_121987.2\| Arabidopsis thaliana lyase AT5G19820 (EMB2734) mRNA, complete cds Length=3922 Score = 44.1 bits (22), Expect = 0.012 Identities = 25/26 (96%) | AT5G19820 | SALK_050129 [L] |
| 42 | 48 | EB174609 | expression in 3-6 | gb\|EB174609.1\| VUA636 mixed organs cDNA library Petunia x hybrida cDNA, mRNA sequence | translesion synthesis polymerase RAD30 like protein | AT5g40270 | SALK_024447 [*], SALK_077401 [L] |

| Gene # | Tag # | GenBank ID /Sequence | Expression ‡ | BLAST Solanaceae[1] | BLAST Arabidopsis[2] | Homolog | Insertion line |
|---|---|---|---|---|---|---|---|
| | | | | length=125 Score = 176 bits (95), Expect = 3e-43 Identities = 125/125 (100%) | | | |
| 43 | 335 | seq335 | expression in 2-5 | - | succinate-semialdehyde dehydrogenase (SSADH1) | At1g79440 | FLAG_634B01[L], SALK_003223[L], SALK_110701[P] |
| | | | | **Gene families** | | | |
| 44 | 280 ddb1a | EB174714 | expression in 1-3 | gi\|83420454\| Nicotiana tabacum cDNA clone KR3B.102P02, mRNA sequence length=839 Score = 131 bits (66), Expect = 8e-30 Identities = 96/105 (91%) | gi\|30680092\| DDB1A; DNA binding / nucleic acid binding AT4G05420 mRNA, complete cds Length=3714 Score = 87.7 bits (44), Expect = e-15 Identities = 92/108 (85%) | AT4G05420 | SALK_055584* |
| 45 | 280 ddb1b | | | | ATDDB1B | AT4G21100 | FLAG_272G05[L], FLAG_348G01[P] |
| 46 | 311 BACH1a | EB174731 | expression in 1-3 | - | AT1G20750.1 helicase-related, similar to BRCA1-binding helicase-like protein BACH1 (GI: 13661819) Homo sapiens) Length = 3540 Expect = 5.4e-05, P = 5.4e-05 Identities = 60/76 (78%), Positives = 60/76 (78%) | AT1G20750 | FLAG_368A11[M], SALK_079991[M] |
| 47 | BACH1b | | | | | AT1G20720 | SALK_101493[P] |
| 48 | BACH1c | | | | | At1g79950 | FLAG_414B06[L], SALK_113285[M] |
| 49 | BACH1d | | | | | At1g79890 | SALK_001041[M], SALK_001077* |

| Gene # | Tag # | GenBank ID /Sequence | Expression‡ | BLAST Solanaceae[1] | BLAST Arabidopsis[2] | Homolog | Insertion line |
|---|---|---|---|---|---|---|---|
| 50 | 278 FKBP06a | EB174712 | expression in 1-3 | gi\|83417166\| Nicotiana tabacum cDNA clone KL4B.101D14, mRNA sequence length=798 Score = 99.6 bits (50), Expect = 5e-20 Identities = 73/81 (90%) | gi\|30694261\| FK506 binding / peptidyl-prolyl cis-trans isomerase AT3G55520 mRNA, complete cds Length=966 Score = 48.1 bits (24), Expect = 8e-04 Identities = 48/56 (85%) | At3g55520 | SALK_052700*, SALK_058277[M], SALK_127214[M] |
| 51 | FKBP06c | | | | | At3g55530 | SALK_052702[M] |
| 52 | FKBP06d | | | | ROF1 | At3g25230 | SALK_024090* |
| 53 | FKBP06e | | | | AtTWD1 | At3g21640 | SALK_012836[M] |
| 54 | FKBP06f | | | | AtPAS1 | At3g54010 | FLAG_567H05[L] |
| 55 | 341, 348 RAD54a | EB174748 | strong in 2-3 | gi\|48431358\| Nicotiana tabacum Pollen PCR-based subtractive library Nicotiana tabacum cDNA clone Peg207BS, mRNA sequence length=740 Score = 165 bits (83), Expect = 2e-39 Identities = 128/142 (90%) | WU Blast i\|18395301\|ref\|NM_ 26270.1\| ATP inding / ATP-ependent helicase/ )NA binding / helicase/ nucleic acid binding AT2G02090 mRNA, complete cds Length=2617 Score = 40.1 bits (20), Expect = 0.18 Identities = 20/20 (100%) | At2g02090 | SALK_135289[M], SALK_046869[L], FLAG_352B03*, FLAG_271B04[L] |
| 56 | RAD54b | | | | | AT3g19210 | SALK_003041*, SALK_038057[M] |
| 57 | RAD54c | | | | | At5g63950 | SALK_152488[M] |
| 58 | RAD54e | | | | | At3g06010 | SALK_015554* |
| 59 | RAD54f | | | | | At2g13370 | FLAG_130A06[M], FLAG_346C07[M] |
| **Insertion lines unavailable within coding region** | | | | | | | |
| 60 | 53 | seq53 | | SGN-U290122 Solanum | AT2G29770.1 \| kelch repeat- | AT2G29770 | - |

| Gene # | Tag # | GenBank ID /Sequence | Expression‡ | BLAST Solanaceae[1] | BLAST Arabidopsis[2] | Homolog | Insertion line |
|---|---|---|---|---|---|---|---|
| | | | | tuberosum (1 EST aligned) Length = 567 Score = 63.9 bits (32), Expect = 4e-10 Identities = 45/48 (93%) | containing F-box family protein, Length = 1363 Score = 173 (32.0 bits), Expect = 8.0, P = 0.9997 Identities = 139/232 (59%) | | |
| 61 | 272 | EB174707 | expression in 1-3 | gb\|EB174707.1\| VUA739 mixed organs cDNA library Petunia x hybrida cDNA, mRNA sequence. Length=335 Score = 584 bits (316), Expect = 1e-165 Identities = 332/332 (100%) | TCP1 t-complex polypeptide 1-homolog (D11351) chaperonin, t-complex protein alpha subunit Length=1718 Score = 69.9 bits (35), Expect = 1e-10 Identities = 160/199 (80%) | At3g20050 | FLAG_298F01[M], FLAG_484A03[M] |
| 62 | 3 | EB174572 | stronger in 1-3 + repression | SGN-U271441 Solanum tuberosum (14 ESTs aligned) Length = 1,464 Score = 428 bits (216), Expect = 1e-119 Identities = 276/296 (93%) | AT3G19590.1 WD-40 repeat family protein / mitotic checkpoint protein; similar to testis mitotic checkpoint protein BUB3 Length = 1395 Plus Strand HSPs: Score = 2846 (433.1 bits), Expect = 3.8e-124, P = 3.8e-124 Identities = 848/1159 (73%), Positives = 848/1159 (73%) | AT3G19590 | SALK_069547[M], SALK_148060[P] |
| 63 | 114 | EB174634 | | SGN-U208323 Petunia hybrida (3 ESTs aligned) Length = 799 Score = 73.8 bits (37), Expect = 2e-13 Identities = 46/48 (95%) | AT5G25450.1 ubiquinol-cytochrome C reductase complex 14 kDa protein, Score = 1063 (165.5 bits), Expect = 1.8e-43, P = 1.8e-43 Identities = 319/434 (73%) | AT5G25450 | - |
| 64 | 223, 246, st19 | EB174666, EB174683 | 1-3 repression | SGN-U207616 Petunia hybrida (3 ESTs aligned) Length = 679 Score = 81.8 bits (41), Expect = 2e-15, Identities = 44/45 (97%) | AT5G22880 histone H2B, putative, Length = 666 Score = 1480 (228.1 bits), Expect = 4.0e-62, P = 4.0e-62 Identities = 398/500 (79%) | AT5G22880 | FLAG_016H09[M], SALK_008776[M] |

| Gene # | Tag # | GenBank ID /Sequence | Expression‡ | BLAST Solanaceae[1] | BLAST Arabidopsis[2] | Homolog | Insertion line |
|---|---|---|---|---|---|---|---|
| | | | | **Not Analyzed** | | | |
| 65 | 358 | EB174761 | expression in 2-3 | gi\|50878647\|gb\|CK714818.1\| LECAD01H08 Seedlings treated with 0.2mM CdCl2 L. esculentum cDNA clone, mRNA sequence length=250 Score = 133 bits (67), Expect = 3e-30 Identities = 100/112 (89%) | Gi\|306781551 acylglycerol-3-phosphate O-acyltransferase/ acyltransferase AT1G01610 (ATGPAT4/GPAT4) mRNA, complete cds, Length=1831 Score = 50.1 bits (25), Expect = 6e-05 Identities = 28/29 (96%) | At1g01610 | |
| 67 | 142 | EB174644 | | SGN-U212207 Petunia hybrida (1 EST aligned) [cluster S] Length = 642 Score = 218 bits (110), Expect = 1e-56 Identities = 114/116 (98%) | AT1G07360.1 zinc finger (CCCH-type) family protein / RNA recognition motif (RRM)-containing protein, similar to SP: O59800 Cell cycle control protein cwf5 {S. pombe}, Length = 1671 Score = 245 (42.8 bits), Expect = 0.0038, P = 0.0038 Identities = 207/362 (57%) | AT1G07360 | |
| 68 | st32, st24 | mshseq32 | expression in 2-5/6 | gi\|52594565\| petunia early fruit development cDNA library length=595 Score = 145 bits (73), Expect = 5e-34, Identities = 73/73 (100%) | Wu Blast AT1G12100.1 \| protease inhibitor/seed storage/lipid transfer protein (LTP) family protein, contains Pfam protease inhibitor/seed storage/LTP family domain Score = 722 (114.4 bits), Expect = 1.3e-27, P = 1.3e-27 Identities = 220/307 (71%) | AT1G12100 | |
| 69 | 461 | EB174825 | expression in 2-5 | gi\|83419619\|Nicotiana tabacum cDNA clone KR3B.001K05, mRNA sequence length=586 Score | gi\|30688564\| aldehyde dehydrogenase/ oxidoreductase AT1G23800 (ALDH2B7) | AT1G23800 | |

| Gene # | Tag # | GenBank ID /Sequence | Expression ‡ | BLAST Solanaceae[1] | BLAST Arabidopsis[2] | Homolog | Insertion line |
|---|---|---|---|---|---|---|---|
| | | | | = 75.8 bits (38), Expect = 5e-13 Identities = 71/78, (91%) | mRNA, complete cds Length=1866 Score = 52.0 bits (26), Expect = 4e-05 Identities = 35/38 (92%) | | |
| 70 | 363, 376 | EB174762, EB174771 | expression in 4-6 | SGN-U215996 Lycopersicon Combined (19 ESTs aligned) Length = 1,630 Score = 133 bits (67), Expect = 6e-31 Identities = 122/141 (86%) | AT1G26440.2 ATUPS5 expressed protein Length = 1698 Score = 1436 (221.5 bits), Expect = 4.7e-113, Sum P(2) = 4.7e-113 Identities = 438/610 (71%) | AT1G26440 | |
| 71 | 31 | seq31 | expression 3-5 | gi\|51296922\|gb\|CO906619.1\| Capsicum annuum cDNA 5', mRNA sequence length=637 Score = 73.8 bits (37), Expect = 3e-12, Identities = 66/76 (86%) | Wu Blast AT1G28695.1 expressed protein, Score = 501 (81.2 bits), Expect = 8.1e-18, P = 8.1e-18 Identities = 205/324 (63%) | AT1G28695; AT1G28700 | |
| 72 | 371 | EB174767 | expression in 4-5 | gi\|48758403\|BP748799 partially normalized diploid tobacco cDNA library Nicotiana sylvestris cDNA clone L-109_A05, mRNA sequence length=374 Score = 71.9 bits (36), Expect = 6e-12, Identities = 49/54 (90%) | gi\|30694308\|ref\|NM_103733.2\| AT1G48370 ROOT HAIRLESS 1 Arabidopsis thaliana oligopeptide transporter Length=2361 Score = 56.0 bits (28), Expect = 1e-06, Identities = 97/120 (80%) | AT1G48370 | |
| 73 | 428 | EB174802 | | SGN-U196301 Capsicum annuum (14 ESTs aligned) Length = 1,172 Score = 109 bits (55), Expect = 8e-24, Identities = 100/110 (90%) | AT1G59900.1 pyruvate dehydrogenase E1 component alpha subunit, mitochondrial (PDHE1-A), Length = 1468Score = 2968 (451.4 bits), Expect = 1.1e-129, P = 1.1e-129, Identities = 842/1124 (74%) | AT1G59900 | |
| 74 | 71 | seq71 | stronger in 4-6 | SGN-U281075 Solanum tuberosum (3 | AT1G62940.1 4-coumarate--CoA ligase family | AT1G62940 | |

| Gene # | Tag # | GenBank ID /Sequence | Expression‡ | BLAST Solanaceae[1] | BLAST Arabidopsis[2] | Homolog | Insertion line |
|---|---|---|---|---|---|---|---|
| | | | | ESTs aligned) Length = 505 Score = 305 bits (154), Expect = 2e-82 Identities = 254/285 (89%) | protein /4-coumaroyl-CoA synthase family protein, Length = 1629 (-) strand HSPs: Score = 746 (118.0 bits), Expect = 1.2e-28, P = 1.2e-28 Identities = 228/322 (70%) | | |
| 75 | 371 | EB174767 | expression in 1-3 | SGN-U219011 Lycopersicon Combined (9 ESTs aligned) Length = 1,589 Score = 54.0 bits (27), Expect = 3e-07, Identities = 35/38 (92%) | AT1G65730.1 oligopeptide transporter OPT family protein, similar to iron-phytosiderophore transporter protein yellow stripe1 (Zea mays) Length = 2371 Score = 2280 (348.1 bits), Expect = 1.0e-134, Sum P (2) = 1.0e-134, Identities = 736/1059 (69%) | AT1G65730 | |
| 76 | 204, 203 | EB174658 | 1-2 expression | | WU Blast AT1G67370.1 meiotic asynaptic mutant 1 (ASY1), identical to meiotic asynaptic mutant 1 Length = 2145 Score = 251 (43.7 bits), Expect = 1.0e-05, P = 1.0e-05 Identities = 75/103 (72%) | AT1G67370 | |
| 77 | 412 | EB174791 | expression in 4-5/6 | | AT1G67730.1 b-keto acyl reductase, putative (GLOSSY8), Length = 1418 Score = 1265 (195.9 bits), Expect = 9.6e-53, P = 9.6e-53 Identities = 517/799 (64%) | AT1G67730 | |
| 78 | 241 | EB174678 | 4-5 expression | - | Wu blast AT1G71830.1 SERK1 leucine-rich repeat family protein / protein kinase family protein Length = | AT1G71830 | |

| Gene # | Tag # | GenBank ID /Sequence | Expression ‡ | BLAST Solanaceae[1] | BLAST Arabidopsis[2] | Homolog | Insertion line |
|---|---|---|---|---|---|---|---|
| | | | | | 2565 Score = 139 (26.9 bits), Expect = 1.3, P = 0.74 Identities = 85/137 (62%) | | |
| 79 | 295 | EB174723 | | - | AT1G76540.1 CDKB2; 1 cell division control protein, putative, Length = 1338 Score = 149 (28.4 bits), Expect = 0.42, P = 0.34 Identities = 125/207 (60%) | AT1G76540 | |
| 80 | 40 | Pt40b_ | expression in 1-5 | gi\|83422139\|gb\|DW004133.1\| KR3B.107N19F.051110T7 KR3B *N. tabacum* cDNA clone Length=683 Score = 165 bits (83), Expect = 6e-40 Identities = 104/111 (93%) | gi\|42563322\| ATTPS1 TREHALOSE-6-PHOSPHATE SYNTHASE Length=4635 Score = 121 bits (61), Expect = 6e-26 Identities = 136/161 (84%) | At1g78580 | |
| 81 | 373 | EB174768 | | SGN-U218226 Lycopersicon Combined (11 ESTs aligned) Length = 2,049 Score = 200 bits (101), Expect = 4e-51, Identities = 149/165 (90%) | AT2G04350.1 long-chain-fatty-acid--CoA ligase family protein/ long-chain acyl-CoA synthetase family protein (LACS8) Length = 2433 Score = 3559 (540.0 bits), Expect = 1.2e-206, Sum P (2) = 1.2e-206 Identities = 1057/1457 (72%) | AT2G04350; AT1G77590 | |
| 82 | 91 | EB174622 | expression in 2-6 | SGN-U269364 Solanum tuberosum (26 ESTs aligned) Length = 2,868 Score = 176 bits (89), Expect = 8e-44, Identities = 184/216 (85%) | AT2G16500.1 arginine decarboxylase 1 Length = 2718 Score = 2432 (370.9 bits), Expect = 3.1e-214, Sum P (4) = 3.1e-214 Identities = 692/940 (73%) | AT2G16500 | |
| 83 | 235 | EB174674 | 3-5 stronger | SGN-U210224 Petunia hybrid, Length = 559 Score = 147 bits (74), Expect = 2e-35 Identities = 76/77 (98%) | AT2G16630.1 proline-rich family protein, contains proline-rich extensin domains Length = 1277, Score = 761 (120.2 bits), Expect = 6.2e- | AT2G16630 | |

| Gene # | Tag # | GenBank ID /Sequence | Expression‡ | BLAST Solanaceae[1] | BLAST Arabidopsis[2] | Homolog | Insertion line |
|---|---|---|---|---|---|---|---|
| | | | | | 30, P = 6.2e-30 Identities = 351/553 (63%) | | |
| 84 | 36 | EB174602 | expressed in 1-3 | gi\|76869992\|gb\|DV160984.1\| Nicotiana tabacum cDNA clone KP1B.104M06, mRNA sequence length=866 Score = 115 bits (58), Expect = 6e-25 Identities = 83/92 (90%) | gi\|18401124\|ref\|NM_128199.1\| 1-phosphatidylinositol-4-phosphate 5-kinase AT2G26420 mRNA, complete cds Length=2118 Score = 69.9 bits (35), Expect = 2e-10 Identities = 86/103 (83%) | AT2G26420 | |
| 85 | 399 | seq399 | 2-3 stronger | SGN-U220531 Lycopersicon Combined (7 ESTs aligned) Length = 890 Score = 236 bits (119), Expect = 1e-61, Identities = 272/327 (83%) | AT2G27510.1 ferredoxin, putative, Length = 754 Score = 809 (127.4 bits), Expect = 7.1e-32, P = 7.1e-32, Identities = 325/505 (64%), Positives = 325/505 (64%) | AT2G27510 | |
| 86 | 184 | seq184 | 1-3 expression | SGN-U207220 Solanum melongena (1 EST aligned) Length = 510 Score = 83.8 bits (42), Expect = 3e-16, Identities = 60/66 (90%) | AT2G27760.1 tRNA isopentenyltransferase 2 / IPP Length = 1622 Score = 318 (53.8 bits), Expect = 8.0e-09, P = 8.0e-09, Identities = 98/138 (71%) | AT2G27760 | |
| 87 | 375 | EB174770 | expression in 4-6 | SGN-U274840 Solanum tuberosum (6 ESTs aligned) Length = 1,040 Score = 60.0 bits (30), Expect = 9e-09 Identities = 40/44 (90%) | AT2G29080.1 FTSH3 encodes an FtsH protease that is localized to the mitochondrion Length = 3000 Score = 1940 (297.1 bits), Expect = 1.5e-83, P = 1.5e-83, Identities = 588/819 (71%) | AT2G29080 | |
| 88 | 397 | EB174780 | expression in 2-5,4-5 stronger | SGN-U268331 Solanum tuberosum (138 ESTs aligned) Length = 1,690 Score = 145 bits (73), Expect = 1e-34 Identities = | AT2G36530.1 LOS2 enolase (2-phosphoglycerate dehydratase) (2-phospho-D-glycerate hydro-lyase) Length = 1740 Score = 4445 | AT2G36530 | |

| Gene # | Tag # | GenBank ID /Sequence | Expression ‡ | BLAST Solanaceae[1] | BLAST Arabidopsis[2] | Homolog | Insertion line |
|---|---|---|---|---|---|---|---|
| | | | | 112/125 (89%) | (673.0 bits), Expect = 1.8e-196, P = 1.8e-196 Identities = 1181/1501 (78%) | | |
| 89 | 302 | EB174726 | | gi\|22788102\| Capsicum annuum cDNA, mRNA sequence. Length=415 Score = 109 bits (55), Expect = 3e-23 Identities = 93/103 (90%) | AT2G41130.1 basic helix-loop-helix (bHLH) family protein, Length = 1091 Score = 192 (34.9 bits), Expect = 0.29, P = 0.26 Identities = 98/156 (62%) | AT2G41130 | |
| 90 | 422, 430 | EB174799, EB174804 | expression in 3-5 | gi\|52596440\| EST888126 petunia fruit ripening cDNA library Petunia x hybrida Length=508 Score = 65.9 bits (33), Expect = 6e-08, Identities = 38/40 (95%) | gi\|18407284\|ref\|NM_130285.1\| ARF1 (ADP-RIBOSYLATION FACTOR 1); GTP binding, complete cds Length=995 Score = 262 bits (132), Expect = 2e-68 Identities = 261/304 (85%) | AT2G47170 | |
| 91 | 438 | EB174809 | expression in 4-5 | gi\|52582211\| EST882057 petunia floral post-ethylene cDNA library Petunia x hybrida cDNA clone Length=588 Score = 69.9 bits (35), Expect = 3e-11, Identities = 64/70 (91%) | gi\|30678283\| AT3G01120 MTO1 (METHIONINE OVERACCUMULATION 1) Length=2234 Score = 121 bits (61), Expect = 5e-26, Identities = 172/209 (82%) | AT3G01120 | |
| 92 | 309 | EB174730 | | SGN-U236988 Lycopersicon Combined (1 EST aligned) Length = 403 Score = 190 bits (96), Expect = 8e-48 Identities = 138/152 (90%) | AT3G01310.2 similar to expressed protein Length = 3352 Score = 369 (61.4 bits), Expect = 4.9e-11, P = 4.9e-11, Identities = 117/162 (72%) | AT3G01310 | |
| 93 | 346 | EB174752 | | SGN-U273549 Solanum tuberosum (8 ESTs aligned) [cluster 3039] Length = 1,097 Score = 107 bits (54), Expect = 2e-23 Identities = 88/100 (88%) | AT3G05545.1 transcription factor, putative / zinc finger (C3HC4 type RING finger) Length = 1668 Score = 268 (46.3 bits), Expect = 0.0010, P = 0.0010, Identities = 110/167 (65%) | AT3G05545 | |

| Gene # | Tag # | GenBank ID /Sequence | Expression‡ | BLAST Solanaceae[1] | BLAST Arabidopsis[2] | Homolog | Insertion line |
|---|---|---|---|---|---|---|---|
| 94 | 59 | seq59 | stronger 3-6 | gi\|39822628\| EST711728 potato abiotic stress cDNA library length=807 Score = 184 bits (93), Expect = 1e-45, Identities = 135/149 (90%) | WU Blast AT3G16200.1 expressed protein Length = 1608 Score = 1346 (208.0 bits), Expect = 1.9e-56, P = 1.9e-56 Identities = 510/772 (66%) | AT3G16200 | |
| 95 | 56, 46, 12 | EB174612, EB174580, EB174580 | expression in 3-6 | gi\|66837509\|gb\|DR035615.1\| 19526.3 Swollen Stolon Solanum tuberosum cDNA clone 19526 3', mRNA sequence. Length=777 Score = 99.6 bits (50), Expect = 1e-19 Identities = 80/89 (89%) | gi\|30686825\| Arabidopsis thaliana ATDMC1 (RECA-LIKE GENE); DNA-dependent ATPase Length=1376 Score = 75.8 bits (38), Expect = 3e-12 Identities = 77/90 (85%) | AT3G22880 | |
| 96 | 296 | EB175236 | | SGN-U278969 Solanum tuberosum (4 ESTs aligned) Length = 763 Score = 119 bits (60), Expect = 8e-27, Identities = 90/100 (90%) | AT3G26670.1 expressed protein Length = 1794 Score = 779 (122.9 bits), Expect = 4.5e-30, P = 4.5e-30, Identities = 201/256 (78%) | AT3G26670 | |
| 97 | st20 | EB174588 | 1-3 stronger | - | WU BLAST AT3G43740.1 leucine-rich repeat family protein, with similarity to somatic embryogenesis receptor-like kinase 2 Length = 844 Score = 675 (107.3 bits), Expect = 7.2e-26, P = 7.2e-26, Identities = 259/397 (65%), Positives = 259/397 (65%) | AT3G43740 | |
| 98 | 261 | seq261 | 1-3 stronger | gi\|10902069\| EST360386 tomato nutrient deficient roots Lycopersicon esculentum cDNA clone P\|439278\|emb\|CAA49144.1\|X69205 | AT3G44660.1 \| HDA10 \| histone deacetylase-related / HD-relate... 38 0.13 AT2G21630.1 \| Symbol: None \| transport protein, putative, similar to | AT3G44660 AT2G21630 AT1G65070 | |

| Gene # | Tag # | GenBank ID /Sequence | Expression‡ | BLAST Solanaceae[1] | BLAST Arabidopsis[2] | Homolog | Insertion line |
|---|---|---|---|---|---|---|---|
| | | | | ribosomal protein {Triticum a, mRNA sequence length=532 Score = 83.8 bits (42), Expect = 2e-15 Identities = 61/65 (93%) | ... 38 0.13 AT1G65070.1 \| Symbol: None \| DNA mismatch repair MutS family protein,... 38 0.13 | | |
| 99 | 172, 298 | EB174646, EB175237 | expression in 4-5 | SGN-U207429 Petunia hybrida (22 ESTs aligned) Length = 1,468 Score = 172 bits (87), Expect = 5e-43, Identities = 94/95 (98%) | AT3G45310.1 cysteine proteinase, putative, similar to AALP protein Length = 1418 Score = 2555 (389.4 bits), Expect = 5.2e-111, P = 5.2e-111, Identities = 761/1051 (72%) | AT3G45310 | |
| 100 | 66 | seq66 | stronger in 7-10 | gi\|39879171\|EST757822 Nicotiana benthamiana mixed tissue cDNA library, Length=650 Score = 129 bits (65), Expect = 4e-29, Identities = 98/109 (89%) | Wu Blast AT3G53000.1 F-box family protein / SKP1 interacting partner 3-related, Length = 1392 Score = 526 (85.0 bits), Expect = 1.7e-18, P = 1.7e-18, Identities = 178/260 (68%) | AT3G53000 | |
| 101 | 414 | EB174792 | | SGN-U273295 Solanum tuberosum (6 ESTs aligned) Length = 765 Score = 194 bits (98), Expect = 2e-49, Identities = 110/114 (96%) | AT3G54560.1 histone H2A.F/Z, Length = 685 Score = 1349 (208.5 bits), Expect = 3.2e-56, P = 3.2e-56 Identities = 443/616 (71%) | AT3G54560 | |
| 102 | 256 | EB174692 | expressed in 1-6/6; 4-5 stronger | gi\|52596365\|EST888089 cDNA clone PetuniaRF-4-H04 5' end, mRNA sequence length=492 Score = 349 bits (176), Expect = 5e-95, Identities = 218/234 (93%) | gi\|30694229\|CER10/ECR; 3-oxo-5-alpha-steroid 4-dehydrogenase/ fatty acid elongase Length=1319, Score = 77.8 bits (39), Expect = 5e-13 Identities = 180/227 (79%) | AT3G55360 | |
| 103 | 318 | EB174738 | | SGN-U219025 Lycopersicon Combined (9 ESTs aligned) Length = 1,404, Score = 188 bits (95), Expect = | AT3G58060.1 cation efflux family protein / metal tolerance protein, putative (MTPc3) Length = 1236 | AT3G58060 | |

| Gene # | Tag # | GenBank ID /Sequence | Expression ‡ | BLAST Solanaceae[1] | BLAST Arabidopsis[2] | Homolog | Insertion line |
|---|---|---|---|---|---|---|---|
| | | | | 1e-47, Identities = 122/131 (93%) | Score = 1222 (189.4 bits), Expect = 2.8e-100, Sum P (2) = 2.8e-100, Identities = 378/527 (71%) | | |
| 104 | 60 | seq60 | 3-10 meiosis-specific | gi\|53787123\| Mixed Floral Solanum tuberosum cDNA clone 71332 5', mRNA sequence. Length=681 Score = 60.0 bits (30), Expect = 5e-08, Identities = 82/98 (83%) | AT3G59510.1 leucine-rich repeat family protein, contains leucine rich-repeat domains, Length = 1260, Score = 579 (92.9 bits), Expect = 4.0e-21, P = 4.0e-21, Identities = 325/531 (61%) | AT3G59510 | |
| 105 | 453 | EB174819 | 4-5 stronger/6 | Gi\|67764989\|Solanum chacoense cDNA, mRNA sequence. Length=845 Score = 54.0 bits (27), Expect = 7e-07 Identities = 43/46 (93%) | gi\|42566120\| Arabidopsis thaliana aldose 1-epimerase AT3G61610 mRNA, complete cds Length=1583 Score = 89.7 bits (45), Expect = 2e-16 Identities = 114/137 (83%) | AT3G61610 | |
| 106 | 11 | pcr11 | stronger in 6-7 | gi\|52595471\|EST886304 petunia leaf cDNA library, mRNA sequence Length=363 Score = 174 bits (88), Expect = 5e-43 Identities = 88/88 (100%) | AT4G05180.1 oxygen-evolving enhancer protein 3, chloroplast, putative (PSBQ2), Length = 1037 Expect = 1.3e-21, P = 1.3e-21 Identities = 205/297 (69%) | AT4G05180 | |
| 107 | 251 | EB174687 | expression in 2-6/6, 4-5 stronger | gi\|52836680\|dbj\|BP532953.1\| Nicotiana tabacum cDNA clone BY29003, mRNA sequence length=381 Score = 242 bits (122), Expect = 1e-62 Identities = 161/174 (92%) | gi\|30681905\| AT4G11820 (BAP1) Length=1724 Score = 48.1 bits (24), Expect = 4e-04 Identities = 36/40 (90%) | AT4G11820 | |
| 108 | 3 | EB174572 | expression 11-12 | - | AT4G15520.1 tRNA/rRNA methyltransferase (SpoU) family protein, Length = 935 Score = 133 (26.0 bits), Expect | AT4G15520 | |

| Gene # | Tag # | GenBank ID /Sequence | Expression ‡ | BLAST Solanaceae[1] | BLAST Arabidopsis[2] | Homolog | Insertion line |
|---|---|---|---|---|---|---|---|
| | | | | | = 2.1, P = 0.87, Identities = 61/92 (66%) | | |
| 110 | 451 | EB174817 | 4-5 stronger/6 | gi\|21925293\| EST616972 potato cDNA clones mixed potato tissues Solanum tuberosum cDNA clone STMHD43 3' end, mRNA sequence length=729 Score = 77.8 bits (39), Expect = 3e-13 Identities = 104/125 (83%) | gi\|30684042\|ref\|NM_117850.2\| palmitoyl-(protein) hydrolase AT4G17470 mRNA, complete cds Length=1168 Score = 65.9 bits (33), Expect = 3e-09, Identities = 69/81 (85%) | AT4G17470 | |
| 111 | 121 | EB174639 | 1-3/6 stronger | gi\|56122578\| cDNAs of Nicotiana attenuata genes activated in trichomes N. attenuata cDNA clone pTRC175 5', mRNA sequence length=390 Score = 335 bits (169), Expect = 7e-91 Identities = 220/237 (92%) | gi\|30687802\| UBC9; complete cds Length=686 Score = 182 bits (92), Expect = 1e-44 Identities = 293/360 (81%) | AT4g27960 | |
| 112 | 410 | EB174790 | expression in 3-6 | SGN-U280839 Solanum Length = 767Score = 93.7 bits (47), Expect = 7e-19, Identities = 153/186 (82%) | AT4G28610.1 myb family transcription factor, putative /phosphate starvation response regulator, putative (PHR1) Length = 1693 Minus Strand HSPs: Score = 945 (147.8 bits), Expect = 2.3e-38, P = 2.3e-38 Identities = 347/510 (68%) | AT4G28610 | |
| 113 | 183 | EB174650 | | SGN-U210274 Petunia hybrida (1 EST aligned) Length = 489 Score = 170 bits (86), Expect = 2e-42 Identities = | AT4G30220.1 small nuclear ribonucleoprotein F, putative /snRNP-F, Length = 476 Score = 797 (125.6 bits), Expect = 3.9e-31, P | AT4G30220 | |

| Gene # | Tag # | GenBank ID /Sequence | Expression‡ | BLAST Solanaceae[1] | BLAST Arabidopsis[2] | Homolog | Insertion line |
|---|---|---|---|---|---|---|---|
| | | | | 90/92 (97%) | = 3.9e-31 Identities = 275/397 (69%) | | |
| 114 | 446 | EB174813 | 4-6 stronger | gi\|48756521\| partially normalized diploid tobacco cDNA library Nicotiana sylvestris cDNA clone L-067_G05, mRNA sequence length=298 Score = 212 bits (107), Expect = 8e-54, Identities = 209/242 (86%) | gi\|30690203\| Arabidopsis thaliana CAT2 (CATALASE 2); complete cds Length=1856 Score = 65.9 bits (33), Expect = 1e-09 Identities = 84/101 (83%) | AT4G35090 | |
| 115 | 141 | EB174643 | stronger in 4-6 | SGN-U198893 Capsicum annuum (2 ESTs aligned) [cluster 2737] Length = 913 Score = 176 bits (89), Expect = 1e-43 Identities = 141/159 (88%) | AT4G35090.1 catalase 2, identical to catalase 2 Length = 1856 Score = 1912 (292.9 bits), Expect = 4.4e-82, P = 4.4e-82 Identities = 546/722 (75%) | AT4G35090 | |
| 116 | 253 | EB174689 | | SGN-U209020 Petunia hybrida (2 ESTs aligned) [cluster 1557] Length = 482 Score = 89.7 bits (45), Expect = 6e-18 Identities = 80/92 (86%) | AT4G38950.1kinesin motor family protein, similar to AtNACK1 kinesin-like protein (GI: 19979627) (Arabidopsis thaliana); Length = 2645 Score = 372 (61.9 bits), Expect = 3.3e-11, P = 3.3e-11 Identities = 198/324 (61%) | AT4G38950 | |
| 117 | 216 | EB174663 | expression in 4-5/6 specific | gi\|39879654\| Nicotiana benthamiana mixed tissue cDNA library, normalized, full-length mRNA sequence length=986 Score = 40.1 bits (20), Expect = 0.045 Identities = 20/20 (100%) | gi\|30679668\| nucleic acid binding AT5G02530 mRNA, complete cds Length=1207 Score = 73.8 bits (37), Expect = 2e-11 Identities = 103/125 (82%) | AT5G02530 | |

| Gene # | Tag # | GenBank ID /Sequence | Expression‡ | BLAST Solanaceae[1] | BLAST Arabidopsis[2] | Homolog | Insertion line |
|---|---|---|---|---|---|---|---|
| 118 | 449 | EB174815 | expression in 1-3 | gi\|52585236\| petunia floral post-ethylene cDNA library Petunia x hybrida cDNA clone Petunia-C2H4-30-A10 5' end, mRNA sequence length=450 Score = 147 bits (74), Expect = 2e-34 Identities = 121/137 (88%) | gi\|30679842\| structural constituent of ribosome AT5G02960 mRNA, complete cds Length=697 Score = 246 bits (124), Expect = 9e-64 Identities = 227/260 (87%) | AT5G02960 | |
| 119 | 128 | EB174642 | expression in 1-5 | | AT5G06750.1protein phosphatase 2C family protein / PP2C family protein, Length = 1602 Score = 134 (26.2 bits), Expect = 2.1, P = 0.88, Identities = 42/65 (64%) | AT5G06750 | |
| 120 | 279 | EB174713 | | SGN-U281870 Solanum tuberosum (3 ESTs aligned) Length = 730 Score = 107 bits (54), Expect = 3e-23, Identities = 111/126 (88%) | AT5G07990.1 flavonoid 3'-monooxygenase / flavonoid 3'-hydroxylase (F3'H) / cytochrome P450 75B1 (CYP75B1) /transparent testa 7 protein (TT7), Length = 1835 Expect = 8.2e-46, P = 8.2e-46 Identities = 365/529 (68%) | AT5G07990 | |
| 121 | 304 | EB174728 | expression in 1-5, 1-4 stronger | SGN-U198003 Capsicum annuum (2 ESTs aligned) Length = 617 Score = 81.8 bits (41), Expect = 4e-15 Identities = 47/49 (95%) | AT5G09810.1 actin 7 (ACT7) / actin 2, Score = 1292 (199.9 bits), Expect = 5.0e-54, P = 5.0e-54 Identities = 304/361 (84%) | AT5G09810 | |
| 122 | 364 | EB174763 | | SGN-U209184 Petunia hybrida (1 EST aligned) [cluster 550] Length = 335 Score = 105 bits (53), Expect = 2e-22 Identities = 112/132 (84%) | gi\|30683150\| DNA binding AT5G10400 mRNA, complete cds Length=664 Score = 83.8 bits (42), Expect = 6e-15 Identities = 78/90 (86%) | At5g10400 | |

| Gene # | Tag # | GenBank ID /Sequence | Expression‡ | BLAST Solanaceae[1] | BLAST Arabidopsis[2] | Homolog | Insertion line |
|---|---|---|---|---|---|---|---|
| 123 | 419 | EB174796 | expression in 1-6/6 2-5 stronger | gi\|39820326\| potato abiotic stress cDNA library Solanum tuberosum cDNA clone POABL92 3' end, mRNA sequence length=742 Score = 99.6 bits (50), Expect = 4e-20 Identities = 71/79 (89%) | Wu Blast AT5G11010.3 pre-mRNA cleavage complex-related, Length = 1362 Score = 514 (83.2 bits), Expect = 5.9e-18, P = 5.9e-18, Identities = 292/473 (61%) | AT5G11010 | |
| 124 | 23 | pcr23 | expression in 2-5 | SGN-U207426 Petunia hybrida (8 ESTs aligned) Length = 1,822 Score = 373 bits (188), Expect = 1e-103 Identities = 195/196 (99%) | gi\|47600740\|emb\| AJ608673.1\| ATMS1cobalamin-independent methionine synthase Length=2326 Score = 500 bits (252), Expect = 2e-139 Identities = 582/692 (84%) | AT5G17920 | |
| 125 | 44 | EB174608 | expression in 1-5 | SGN-U211683 Petunia hybrida Length = 648 Score = 309 bits (156), Expect = 5e-84 Identities = 159/160 (99% | AT5G20080.1 NADH-cytochrome b5 reductase, Length = 1426 Score = 1773 (272.1 bits), Expect = 1.1e-75, P = 1.1e-75, Identities = 491/651 (75%) | AT5G20080 | |
| 126 | 54 | seq54 | expression in 2-5 | gi\|5275374\| EST263741 Lycopersicon esculentum cDNA clone cLEE10C7, mRNA sequence. Length=383 Score = 135 bits (68), Expect = 6e-31 Identities = 98/107 (91%) | Wu Blast ATCG00760.1 \| encodes a chloroplast ribosomal protein L36, a constituent of the large subunit of the ribosomal complex Length = 114Score = 428 (70.3 bits), Expect = 7.6e-14, P = 7.6e-14 Identities = 96/109 (88%) | ATCG00760 | |
| 127 | 37 | EB174603 | expression in 1-5 | SGN-U196611 Capsicum annuum Length = 795 Score = 159 bits (80), Expect = 2e-38 Identities = 173/205 (84%) | AT5G20620.1 polyubiquitin (UBQ4), Length = 1488 Score = 2207 (337.2 bits), Expect = 2.6e-95, P = 2.6e-95 Identities = | AT5G20620 AT5G03240 | |

| Gene # | Tag # | GenBank ID /Sequence | Expression ‡ | BLAST Solanaceae[1] | BLAST Arabidopsis[2] | Homolog | Insertion line |
|---|---|---|---|---|---|---|---|
| | | | | | 575/724 (79%) | | |
| 128 | 265, 285 | EB174700, EB174719 | strong expression in 1-3/6 | gi\|51292006\| Nicotiana tabacum cultivar SKP1 mRNA, complete cds Length=653 Score = 73.8 bits (37), Expect = 9e-14 Identities = 39/40 (97%) | gi\|42568263\|ref\|NM _123584.2\| ASK2 (ARABIDOPSIS SKP1-LIKE 2); ubiquitin-protein ligase AT5G42190 (ASK2) mRNA, complete cds Length=1405 Score = 103 bits (52), Expect = 1e-20 Identities = 148/180 (82%) | At5g42190 | |
| 129 | 9 | EB174577 | expression 2-6 | SGN-U223227 Lycopersicon Combined Length = 1,278 Score = 194 bits (98), Expect = 2e-49 Identities = 132/142 (92%) | Wu BLAST AT5G48000.2 CYP708A2 Length = 1619 Score = 189 (34.4 bits), Expect = 0.0065, P = 0.0065 Identities = 83/132 (62%) | AT5G48000 | |
| 130 | 178 | seq178 | expression in 4-5 | gi\|67767762\| Solanum chacoense cDNA, mRNA sequence Length=863 Score = 54.0 bits (27), Expect = 1e-06 Identities = 36/39 (92%) | WU BLAST AT5G48500.1 Length = 975 Plus Strand HSPs: Score = 320 (54.1 bits), Expect = 1.2e-06, P = 1.2e-06 Identities = 348/613 (56%) | AT5G48500 | |
| 131 | st12 | mshseq12 | expression in 4-5 | gi\|67764989\| Solanum chacoense cDNA, mRNA sequence length =845Score = 81.8 bits (41), Expect = 4e-15 Identities = 51/53 (96%) | AT5G57330.1 aldose 1-epimerase family protein, Length = 1463 Plus Strand HSPs: Score = 1136 (176.5 bits), Expect = 6.2e-47, P = 6.2e-47 Identities = 364/502 (72%) | AT5G57330 | |
| 132 | 90 | EB174621 | very faint; 2-5 stronger /12 | gi\|52586823\|gb\| Petunia-DevA-6-F03 5' end, mRNA sequence. Length=561 Score = 389 bits (196), Expect = 5e-107 Identities = 196/196 (100%) | gi\|30697194\| structural constituent of ribosome AT5G59240 mRNA, complete cds Length=851 Score = 167 bits (84), Expect = 8e-40 Identities = 309/383 (80%) | AT5G59240 | |

| Gene # | Tag # | GenBank ID /Sequence | Expression‡ | BLAST Solanaceae[1] | BLAST Arabidopsis[2] | Homolog | Insertion line |
|---|---|---|---|---|---|---|---|
| 133 | 258, 10 | EB174694 | stronger in 3-6; 11-12 | SGN-U208711 Petunia hybrida Length = 489 Score = 242 bits (122), Expect = 1e-63 Identities = 172/190 (90%) | AT5G61170.1 40S ribosomal protein S19 (RPS19C), Length = 645 Score = 720 (114.1 bits), Expect = 8.7e-28, P = 8.7e-28, Identities = 186/234 (79%) | AT5G61170 | |
| 134 | 390 | EB175241 | expression in 4-5 | SGN-U285494 Solanum tuberosum Length = 755 Score = 202 bits (102), Expect = 1e-51 Identities = 142/156 (91%) | gi\|18424677\|ref\|NP_568967.1\| lyase/ pectate lyase Length=432 Score = 351 bits (901), Expect = 4e-97, Identities = 172/220 (78%) | AT5g63180 | |
| 135 | 85 | seq85 | 1-5 stronger/12 | gi\|62892234\|gb\| Developing Tubers Solanum tuberosum cDNA clone 22753 3', mRNA sequence. Length=289, Score = 151 bits (76), Expect = 1e-35 Identities = 88/91 (96%) | gi\|49256807\|emb\|Y08501.2\|MIATGENA NADH dehydrogenase subunit mitochondrial genome Length=366924 Score = 208 bits (105), Expect = 1e-52 Identities = 115/117 (98%) | ATMG00513 | |
| 136 | 139 | EB175231 | expression in 1-3 | gi\|50892641\| Lycopersicon esculentum var. cerasiforme fruit 12 days post anthesis length=734 Score = 609 bits (307), Expect = 5e-173 Identities = 334/342 (97%) | gi\|1928871\|gb\|U91966.1\|ATU91966 ribulose-1, 5-bisphosphate carboxylase/oxygenase large subunit (rbcL) gene, Length=2187Score = 809 bits (408), Expect = 0.0 Identities = 610/678 (89%) | ATCG00490 | |

‡ Samples 1: premeiotic, 2: leptotene, leptotene-zygotene transition, 3: zygotene 4: late pachytene, metaphase I, 5: dyad stage, telophase II, 6 postmeiotic

1 http://www.sgn.cornell.edu/tools/blast/

2. http://www.arabidopsis.org/Blast/; http://www.ncbi.nlm.nih.gov/

* = No insert at predicted position

M = Mutant

L = Non-Mutants

P = Phenotyped only

A= Sequence data in Appendix 1

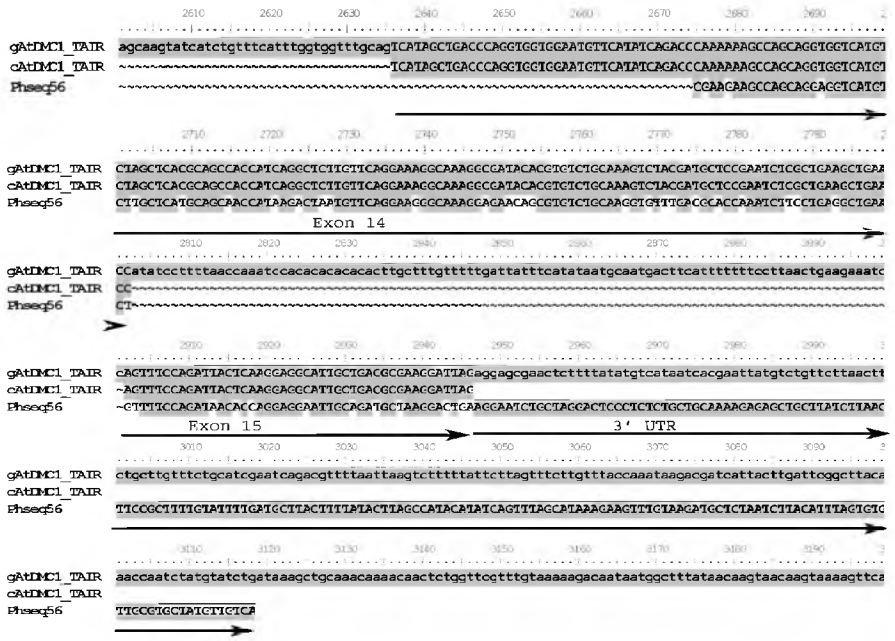


**Fig. 3.1: Alignment of Arabidopsis and Petunia *DMC1* nucleotide sequence.** gAtDMC1= Arabidopsis *DMC1* genomic DNA (GI: 30686825), *cAtDMC1*= Arabidopsis *DMC1* complementary DNA (EB174612), Phseq56 = Petunia *DMC1* EST; Transcript region indicated by ▶.

### Verification of DMC1 expression in Petunia

To verify the results of the profiling experiments, we performed a quantitative RT-PCR experiment on one of the proteins that is known to be crucial for meiosis and recombination, DMC1. The Petunia *DMC1* partial cDNA we identified had 85% sequence identity to the *Arabidopsis DMC*. An alignment of the two sequences (Fig. 3.1) showed that the Petunia sequence spanned the last exon and extended into the unique 3'UTR region. In the cDNA-AFLP experiment performed earlier (Cnudde et al., 2006), *DMC1* was highly expressed during leptotene and zygotene with the expression restricted to early meiotic stages.

To verify this data, quantitative RT-PCR was performed on *DMC1* using Petunia mRNA from the same meiotic stages used in the cDNA-AFLP experiment (Fig. 3.2A). The quantitative RT-PCR data showed that the expression was highest in pre-meiotic and early meiotic stages and decreased thereafter (Fig. 3.2B). At the tissue level, the *Petunia DMC1* was expressed highest in the flower buds but was also high in seedlings (Fig. 3.2C).

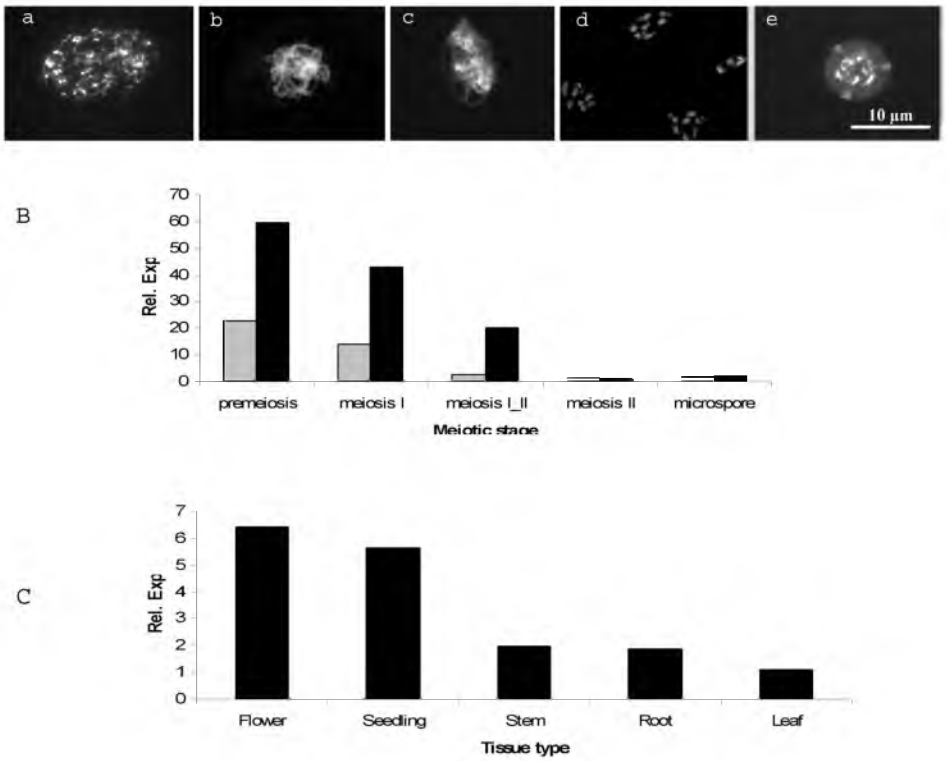


**Fig. 3.2: Quantitative RT-PCR analysis of *Petunia hybrida* DMC1**

A. Representative meiotic stages of bud sampling a. premeiotic, b. meiosis-I, c. meiosis-I & II, d. meiosis-II, e. microspore, scale bar =100µm; B. Relative expression in meiotic tissues compared to GAPDH constitutive

### Arabidopsis homologs

Homologs were sought to the partial sequences by performing BLAST searches against the *Solanaceae* ESTs and non-redundant *Arabidopsis* datasets in NCBI and TAIR (screening performed end 2004). A total of 136 *Arabidopsis* genes (46%) were identified as putative homologs (Table 3.3). Sixty-four of these were selected for further investigation and categorized based on the following criteria. We looked for significant sequence homology (e-value cut off larger than $10^{-6}$) to previously uncharacterized *Arabidopsis* genes and prioritized these for our investigation (see section "Significant homologs" in Table 3.3). We also included low significance hits like At2g02090, AT1G07360 and AT2G41130 that had a domain or a functional annotation to support a possible role in meiosis. A hit was considered to be of low significance when the length of the query sequence was short (60-90 bp) and the sequence identity with the *Arabidopsis* gene was confined to short stretches with a low e-value (see section" Less- significant homologs" in Table 3.3). We found that for some of the hits, the homologs in yeast and mammals were DNA repair and meiosis related genes. A reciprocal

BLAST of these yeast and mammalian genes to the Arabidopsis dataset pointed to multiple *Arabidopsis* genes with conserved domains suggesting that they might be part of a gene family with redundant functions. We selected more than one gene for further analysis (see below) if the hit represented a member of a gene family (see section "Gene families" in Table 3.3). Known meiotic genes that came out of our screen like *DMC1* (Doutriaux et al 1998), *ASY1* (Ross et al., 1997 Caryl et al., 2000), *ASK1* and *ASK2* (Yang et al., 1999; Yang and Ma, 2001) served as positive controls.

**Table 3.4:** Putative functions of characterized Arabidopsis genes identified based on the homolog's meiotic expression in Petunia

| Expression profile ‡ | Arabidopsis gene | Role | Reference |
|---|---|---|---|
| expression in 1-5 | *AT1G78580* | AtTPS1 (trehalose-6-phosphate-synthase); TPS1 may play a major role in cell wall biosynthesis, cell division and cellular metabolism during embryo development. Embryo development is delayed in Attps1 | Gomez et al., 2006 |
| expression in 2-3 | *AT3G22880* | ATDMC1 (RECA-like gene meiotic recombination protein. Mutant produces univalents at prophase I suggesting a role in bivalent formation and chromosome segregation during meiosis | Klimyuk et al., 1997 |
| expression in 3-5 stronger | *AT5G60450* | AtARF4 (Auxin Response Factor 4) required for specification of abaxial cell types. | Pekker et al., 2005 |
| expression in 1-4 stronger | *AT2G16500* | AtADC1 (arginine decarboxylase 1); ADC genes involved in polyamine biosynthesis are essential for seed development | Urano et al., 2005 |
| expression in 1-3 | *AT1G55870* | AtPARN (poly A- specific ribonuclease); CAF1 family ribonuclease degrading polyA specific mRNA with a role in embryogenesis | Reverdatto et al., 2004 |
| expression in 2-3 | *AT1G01610* | AtGPAT1 (glycerol acyltransferase) ; AtGPAT1 deficiency affects tapetal differentiation and plays a pivotal role in pollen development and male fertility | Zheng et al., 2003 |

| | | | |
|---|---|---|---|
| expression in 1-3 | *AT1G75950; AT5G42190* | AtASK1; AtASK2, (Arabidopsis SKP1-Like 1 and 2); E3 ubiquitin ligase SCF complex subunit SKP1/ASK1 gene family involved in flower development, male meiosis and embryogenesis | Wang et al., 2006 |
| expression in 1-2 stronger | *AT1G67370* | AtASY1 (asynaptic 1) involved in homologous chromosome synapsis during meiotic prophase I | Armstrong et al., 2002 |
| expression in 1-3 | *AT4G05420* | DDB1A (damaged DNA binding protein 1); UV-damaged DNA binding factor-like protein | Schroeder et al., 2002 |
| expression in 1-3 stronger | *ATMG00513* | AtNADH5 (NADH dehydrogenase subunit 5); | Knoop et al., 1991 |
| expression in 2-6, 4-5 stronger | *AT4G11820* | AtBAP1 (BON1-associated protein); involved in plant growth homeostasis maintenance | Hua et al., 2001 |
| expression in 1-3 | *AT2G27760* | ATIPT2 (isopentenyltransferase); involved in cytokinin biosynthesis and expressed in proliferating tissues | Miyawaki et al., 2004 |
| expression in 2-5 | *AT5G17920* | ATCIMS (Cobalamin-Independant Methionine Sythesis); methionine biosynthesis | Ferrer et al., 2004 |
| expression in 2-5, 4-5 stronger | *AT2G36530* | LOS2 (Low expression of osmotically responsive); Encodes an enolase, shows light-dependent cold tolerance, phosphorylation state is modulated in response to ABA in seeds | Lee et al., 2002 |
| expression in 4-5 | *AT1G48370* | RHL1 (Root hairless 1); Forms a multiprotein complex with plant topo VI known to have distinct but overlapping roles during the mitotic cell cycle and endoreduplication cycle | Sugimoto-Shirasu et al., 2005 |

‡ Petunia anthers in 1: premeiotic, 2: leptotene, leptotene-zygotene transition, 3: zygotene 4: late pachytene, metaphase I, 5: dyad stage, telophase II, 6: postmeiotic stages

**Arabidopsis mutant screen**

We searched the SIGnAL database (http://signal.salk.edu/cgi-bin/tdnaexpress) for T-DNA insertion lines within the 64 selected genes. Preference was given to insertions disrupting the coding regions whenever possible. Such T-DNA insertion lines were not available for 5 genes. For AT3G19590, AT5G22880 (histone H2B) and At3g20050 (t-complex polypeptide), the insertion was in the 5'UTR region and the corresponding mutants were not affected in their

reproductive development. Since there were no inserts available for AT2G29770 (kelch repeat-containing F-box family protein) and AT5G25450, these genes were eliminated from further analysis. Eventually, 100 T-DNA insertion lines corresponding to 62 genes were available to screen for meiosis-related mutants (Table 3.3). The seeds obtained from the Arabidopsis stock center were sown and segregation of the T-DNA was checked for 85 lines by PCR using a combination of insert-specific and gene-specific primers. Representative flowers and siliques of plants homozygous/heterozygous for the insert were examined for pollen and embryo defects, respectively. The remaining fifteen lines were only phenotyped and did not show any defects in the developing anthers and siliques. Since our interest was in finding meiotic mutants with partial or complete sterility, we did not pursue these further. Below we present the results of this screen in different categories and elaborate on one gene as a representative for each class.

**Elusive T-DNA lines**

The T-DNA insertion could not be detected at the predicted site in 28 lines, which corresponds to approximately one fourth of the lines tested (see T-DNA lines labeled with * in Table 3.3). While most of these lines were fertile, one line (SALK_062094) exhibited pollen defects. The corresponding gene At3g46740 was pursued by screening for mutants with a second insertion line.

*At3g46740*

The homolog of the *Petunia* EST (tag 115) is upregulated in early meiosis (Fig. 3.4A) and is well conserved in *Arabidopsis* with 85% identity and corresponds to the gene At3g46740, a putative translocase (Table 3.3). Genotyping of SALK_062094 did not identify the insert at the predicted position although some of the plants showed reduced fertility. A closer examination revealed siliques with aborted embryos (Fig. 3.4D). Since the T-DNA insert could not be identified using SALK_062094, we tested a second insertion line SALK_015928 where the T-DNA was predicted to be located in the first exon of the gene (Fig. 3.4B). SALK_015928 mutants did not survive and the heterozygous anthers contained a mix of viable and defective pollen. Chromosomal spreads of SALK_062094 and SALK_015928+/- meiotic buds revealed meiotic defects (Fig. 3.4D) like formation of univalents and multivalents instead of bivalents at metaphase-I and chromosome stickiness. In another study the same gene was characterized as TOC75-III, an integral envelope membrane protein and homozygous toc75-III embryos were found to abort embryos at the two-cell stage (Baldwin et al., 2005), thus confirming our findings of lethality.

**Putative homozygous lethals**

The T-DNA insertion could not be detected in the homozygous state for 20 insertion lines (see T-DNA lines labeled "L" in Table 3.3). This might point to the presence of embryo-lethal or gametophytic-lethal mutations (Howden et al., 1998). To identify the nature of the defect we examined the anthers and siliques of all 20 lines. Examination of the anthers using Alexander's stain revealed a mixture of viable and dead pollen for eight heterozygous T-DNA insertion lines (data not shown). These correspond to AT2g02090 (RAD54 family), At1g07940 (elongation factor), At4g08960 (phosphatase activator), At4g21100, At1g79950 (bach1-related), At2g45290 (transketolase), At3g12610
(DRT100) and At3g46740 (translocase). Defective embryos were found in siliques of three T-DNA insertion lines of the genes At5g19820 (EMB2734), At5g09850 (elongation factor) and At5g40270 (RAD30-like).

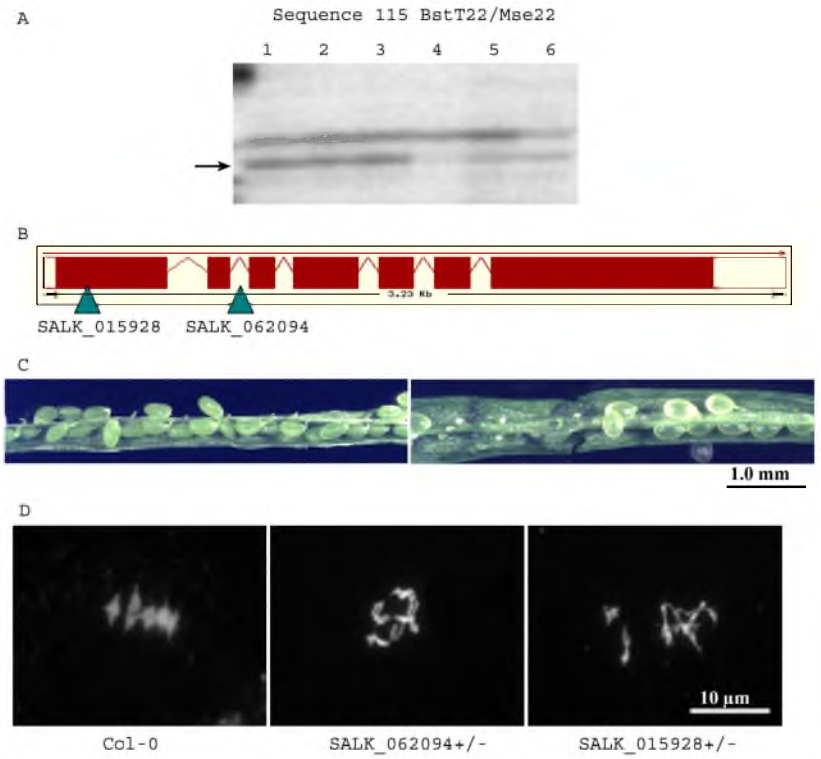


**Fig. 3.3: Overview of gene *At3g46740* investigation.**
A.. Petunia EST cDNA-AFLP expression pattern during meiotic stages 1- premeiotic, 2- leptotene, leptotene-zygotene transition, 3- zygotene 4- late pachytene, metaphase I, 5- dyad stage, telophase II, and 6- postmeiotic B. Schematic representation of At3g46740 gene structure where exons and introns are depicted as blocks and lines respectively, and T-DNA insert locations are indicated using triangles. C. Wildtype (left) and SALK_062094 (right) siliques reveal aborted embryos; scale bar = 1mm .D. DAPI-

stained chromosome undergoing meiosis at metaphase-I in wildtype (left), SALK_062094 (middle) and SALK_015928 heterozygote (right); scale bar = 10µm

Both embryo and pollen defects were seen in At1g55870 (AtPARN). The segregation patterns in two pollen defective lines (At2g02090 and At1g07940) were examined in the next generation to check for gametophytic lethality (1:1 segregation in a selfed heterozygote). Homozygous mutants continued to be absent among the segregants but the lines deviated from the expected 1:1 segregation (data not shown). Since we could not find mutants in these insertion lines, we did not proceed with them.

**Mutants**

Plants homozygous for the T-DNA insertion were identified in 37 lines corresponding to 31 genes (see T-DNA lines labeled "M" in Table 3.3). All 37 lines were examined for pollen defects. If reduced fertility was observed meiotic spreads were made. Out of the 37 mutant lines examined, 33 had normal viable pollen indicating that meiosis was not affected by a mutation in their respective genes. The four defective lines were SALK_143024 (At4g31750), FLAG_386D01 (At5g12940), SALK_012836 (At3g21640) and SALK_118337 (At4g16155). In these lines, chromosomal defects were seen in the heterozygotes but not in the mutants while unexpected segregation ratios were observed in the progeny of the selfed heterozygotes. Moreover, the pollen and chromosomal defects seen in mutants of the genes At5g12940 and At3g21640 were not stably transmitted to the next generation. Pollen of the progeny of a selfed heterozygous FLAG_386D01 plant was normal in mutants and heterozygotes. SALK_012836 had a distorted segregation for progeny of the two heterozygous plants tested (data not shown). The resulting mutants had a dwarf phenotype and were early flowering but the pollen defects were not consistent within the mutant population. Meiotic spreads of the heterozygote revealed univalents and chromosomal rearrangements and hence could not be pursued further (data not shown). The findings from the investigation of the remaining two mutants within the genes At4g16155 and At4g31750 are described in detail below.

*At4g16155*

Petunia sequence tag 111 was expressed strongly from pre-meiosis to early meiosis. The homologs At4g16155 and At3g16950 are two non-redundant lipoamide dehydrogenase (PTLPDs) proteins with 81% identity between them. At4g16155 (PTLPD2) is part of the pyruvate dehydrogenase complex (PDC) in the plastids and PDC is the major source of acetyl-CoA for de novo fatty acid synthesis needed to support the newly grown membrane structures (Lutziger I and Oliver DJ. 2000). Microarray data in *Arabidopsis* indicate that the gene is

expressed in developing organs (Hruz et al., 2008, Genvestigator database). Disruption of At4g16155 was observed in two lines: SALK_118337 and SALK_011050.

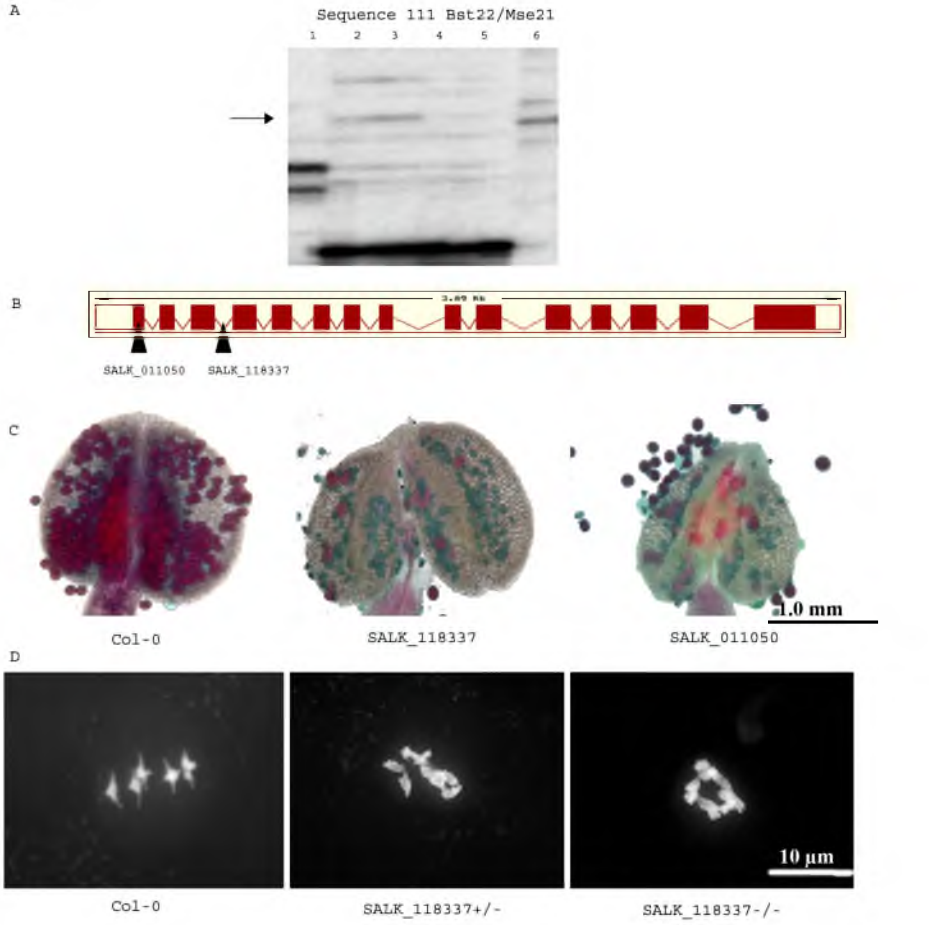


**Fig. 3.4: Overview of gene *At4g16155* investigation.**
A. Petunia EST cDNA-AFLP expression pattern during meiotic stages 1- premeiotic, 2- leptotene, leptotene-zygotene transition, 3- zygotene 4- late pachytene, metaphase I, 5- dyad stage, telophase II, 6- postmeiotic B. Schematic representation of At4g16155 gene structure where exons and introns are depicted as blocks and lines respectively, and T-DNA insert locations are indicated using triangles. C. Alexander staining of wildtype (left), heterozygous SALK_118337 (middle) and heterozygous SALK_011050 anthers (right) with viable pollen (dark), non-viable pollen (light); scale bar= 1 mm D. DAPI-stained chromosome undergoing meiosis at metaphase-I in wildtype (left) and heterozygous SALK_118337 (middle); scale bar =10µm

The insertion in line SALK_118337 is in the third intron of At4g16155 (Fig. 3.4B). SALK_118337 defects were highly irregular from plant to plant with partially defective pollen in the heterozygotes (Fig. 3.4C) while the homozygous mutant lines had normal pollen. There were only three heterozygotes and two

mutants out of 29 plants. Meiosis was abnormal in the heterozygous lines with non-homologous pairing resulting in multivalents and illegitimate associations (Fig 3.4C). A second line SALK_011050 was homozygous lethal. SALK_011050 disrupts the first exon of At4g16155 and 1000bp upstream of the gene At4g16160. Genotyping 48 progeny of a segregating individual revealed 43 heterozygotes, 5 wildtypes and no mutants. There was a clear bias in transmission of the T-DNA allele for both insertion lines tested. T-DNA-induced translocations can equally contribute to the phenotypes described above. In the end the two mutants did not give us any clear evidence of a meiotic function.

*At4g31750*

This gene is a putative serine/threonine phosphatase of the PP2C family. The transcript levels are increased during meiosis as seen by our cDNA-AFLP analysis in *Petunia* (Fig. 3.5A). At4g31750 is a member of the PP2Cc superfamily and homologs in mouse, xenopus and yeast are expressed during meiosis. In another study, PP2C was one of the three *Arabidopsis* cDNA clones that could rescue the meiosis-deficient phenotype of the *S. pombe pde1* mutant, which lacks cAMP phosphodiesterase (Kuromori et al, 1994). Two T-DNA insertions lines, SALK_143024 and SALK_146020 (Fig. 3.5B) were tested to identify mutants. SALK_143024 mutants were extremely slow growing and flowers had wavy petals sometimes showing deformed anthers.

The siliques had a reduced seed set with an average of 20 seeds/silique (n=3). Chromosome spreads of mutant meiocytes revealed meiotic defects that were not uniform (Fig. 3.5D). All Prophase I nuclei had normal pachytenes with no obvious synaptic defects. Early diplotene revealed random associations between the condensing bivalents clearly seen as multivalent associations at metaphase-I. The illegitimate associations between chromosomes were carried into meiosis II. At telophase II, the second plane of division separating the sister chromatids was partial or completely absent with occasionally prematurely separated chromosomes. Tetrads were formed without the second equational division that separates sister chromatids. As a result, dyads were formed with 2 haploids in each cell.

Heterozygotes were genotyped to determine the segregation ratios. However, the majority of the population was heterozygous for the insert in two independent heterozygotes clearly revealing that the segregation was non-mendelian for the T-DNA. In order to confirm the mutant phenotype another independent insertion line, SALK_146020, was genotyped. Unfortunately, in this line, the insert could not be verified at the predicted location. Embryo defects were visible in some of the SALK_146020 plants. We did not pursue additional insertion lines, as only one line that disrupted the 5' UTR region was available at the time of this screen.

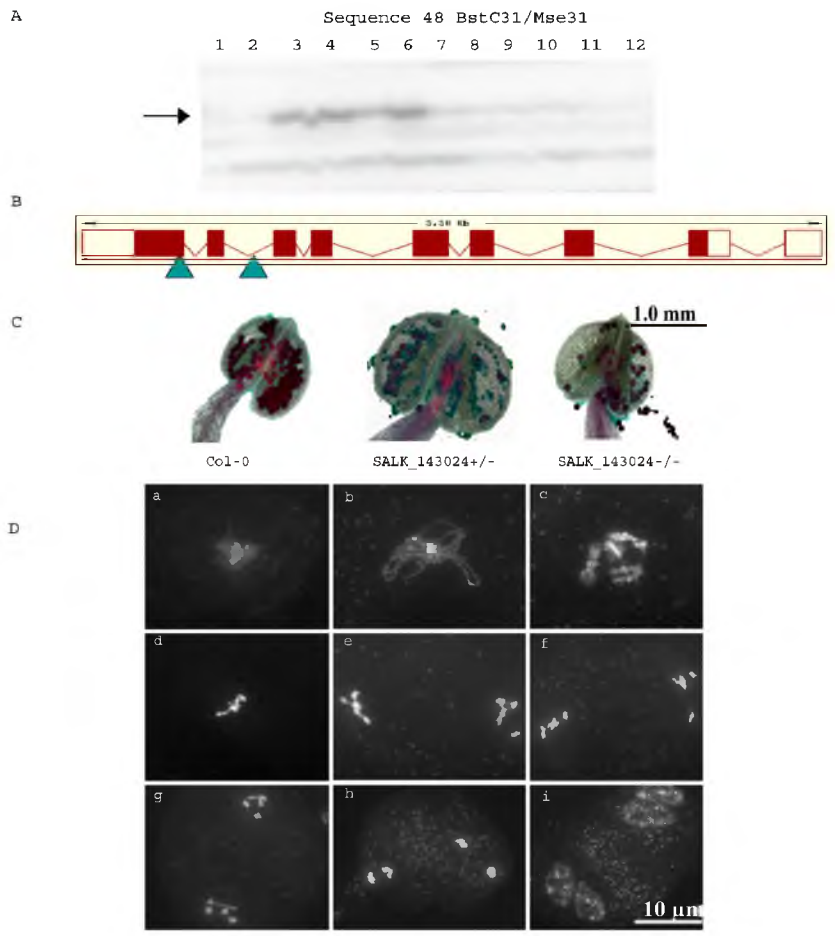


**Fig. 3.5: Overview of gene *At4g31750* investigation.**
Petunia EST cDNA-AFLP expression pattern during meiotic stages 1,2- premeiotic, 3, 4- leptotene, leptotene-zygotene transition, 5, 6- zygotene, 7- late pachytene, 8- metaphase I, 9- dyad, 10- telophase II, 11, 12- postmeiotic B. Schematic representation of *At4g31750* gene structure where exons and introns are depicted as blocks and lines respectively, and T-DNA insert locations indicated using triangles. C. Alexander staining of wildtype (left) with viable pollen (pink) and heterozygous SALK_0143024 (middle), mutant SALK_0143024 anthers (right) with non-viable pollen; scale bar = 1 mm D. DAPI-stained chromosome spreads at meiosis in the SALK_0143024 mutant. a. Zygotene b. Pachytene c. Early diplotene d. Metaphase-I e. Dyad f. Metaphase-II g. Anaphase-II h. Telophase-II i. Tetrad; scale bar = 10µm

### Gene families putatively involved in meiosis

In addition to the direct homologs of the Petunia genes, close members of a few gene families were tested. Gene families were analyzed when a gene seemed

very likely to have a meiotic role based on its homology to a known meiotic gene in yeast or mammals, but did not exhibit a meiotic phenotype when mutated.

**_BACH_ gene family**

Sequence tag 311 (Table 3.3) was expressed from pre-meiotic to pachytene stages with 78% identity to AT1G20750. This gene in *Arabidopsis* is a putative BRCA1-binding helicase-like protein. The human BACH1 gene shares 36% overall identity to two *Arabidopsis* genes, At1g20750 and At1g20720, closely followed by At1g79950 and At1g79890 with 29% identity. All proteins in this family for which functions are known are DNA helicases that participate in the initiation of transcription and nucleotide excision repair as part of the TFIIH complex. Genevestigator microarray (Ath1: 22k array) data indicate that all of them are strongly expressed in sperm cells although they are also expressed in additional cell types (Fig. 3.6A). None of these genes have so far been characterized in Arabidopsis. Mutants were normal in their vegetative and reproductive development with viable pollen in AT1G20750 (SALK_079991, FLAG_368A11) and At1g79890 (SALK_001041). Mutants within At1g79950 (FLAG_414B06) were homozygous lethal. The FLAG_414B06 heterozygote anthers had partially defective pollen. Insertion lines within AT1G20720 were not immediately available and they remain to be tested. We crossed the available mutants, SALK_079991 and SALK_001041, and identified two double mutants amongst 70 F2 progeny, but they were similar to the wildtype.

**_FKBP_ gene family**

Petunia sequence tag 278 (Table 3.3) isolated from meiotic pollen mother cells was expressed from pre-meiotic to pachytene stages (Cnudde et al., 2006). The tag exhibits 90% identity to a tobacco EST that in turn is 85% identical to At3g55520, an uncharacterized *Arabidopsis* gene. The human FKBP6 gene shares 32% identity with At3g55520 and 25-26% identity to At5g48570, At3g25230 (ROF1), At3g21640 (TWD1) and At3g54010 (PAS). Genevestigator microarray (Ath1: 22k array) data indicates that all these genes are expressed in sperm cells except *At3g54010* (gene chip probe ID: 251932) (Fig. 3.6C). The *At3g54010 pas 1* mutants are able to survive only under *in vitro* conditions and form abnormal and sterile flowers (Faure, 1998; Vittorioso et al., 1998). Examination of another mutant allele, FLAG_567H05, within At3g54010 proved to be recessive lethal. At3g25230, has been characterized as ROF1/ FKBP62, a heat-stress induced protein (Aviezer-Hagai et al., 2007). *ROF1* gene expression was observed in the vascular elements of roots, in hydathodes and leaf-trichomes and in stigma, sepals, and anthers. Microarray expression profile of *At5g48570* suggests that it is specifically expressed in sperm cells and in actively dividing tissue. However, a SALK T-DNA insertion line spanning the coding region of

*At5g48570* was unavailable. Hence, these three genes, *At3g54010, At3g25230* and *At5g48570*, were not pursued. Microarray data on At3g55520 shows that the gene's expression is lower in sperm cells compared to other Arabidopsis FKPB-like genes expressed in this cell-type. Mutants of At3g55520 (SALK_127214 and SALK_058277) were fertile with no apparent developmental anomalies thus providing no clues to its function in the anthers. At3g21640 also called *TWISTED DWARF 1 /FKBP42* is a plasma membrane anchored protein. Geisler et al. (2003) show that mutants are reduced in inflorescence and silique size, exhibit disoriented growth in all organs and reduced polar auxin transport important for plant development. The *Attwd1* mutants (SALK_012836) were slow growing and dwarfed and showed delayed bolting compared to the WT. Pollen defects were apparent in both mutants and heterozygotes. Segregation of a selfed heterozygote was non-mendelian in three independent cases with almost all the progeny carrying only the mutant allele. The mutant phenotypes of slow growth and delayed bolting were still visible. However, sterility and pollen defects were not always seen in these lines making it difficult to ascertain that the mutant has a primary meiotic defect.

***RAD54* gene family**

Two identical Petunia partial cDNAs 341 and 348 (Table 3.3) showed strong expression in leptotene and zygotene stages of meiosis-I. The corresponding *Arabidopsis* homolog with 54% identity was AT2g02090 an *SNF2/RAD54* family (*ETL1* subfamily) protein with DEAXHc, HELICc and SNF2_N domains. The yeast RAD54 protein is crucial for strand invasion steps of homologous recombination (Petukhova et al., 1999) and belongs to a large family. We selected the Arabidopsis homologs AT2g02090, At3g19210, At2g13370 and At5g63950 ranging from 41% to 31% identity out of which At3g19210 is the closest homolog of the yeast RAD54 protein. Genevestigator microarray (Ath1: 22k array) data indicates that AT2g02090 is the only gene that is strongly expressed in sperm cells while At3g19210 shows high expression in pollen (Fig. 3.6B). AT2g02090 mutants did not survive in two mutant alleles (SALK_135289 and FLAG_271B04) probably with male gametogenesis defects inferred from the defective pollen found in the heterozygous plants. We genotyped a population of a selfed heterozygous plant to look at segregation ratios and to find mutants. No mutants were found amongst the 81 segregants and the segregation was clearly non-Mendelian with a ratio of 9:72 (wildtype: heterozygote) and not a 1:1 ratio typical of a gametophytic lethal mutant. Mutants of the remaining three genes, At3g19210 (SALK_038057), At2g13370 (FLAG_130A06) and At5g63950 (SALK_151874), were fertile with normal vegetative growth, similar to the wildtype.

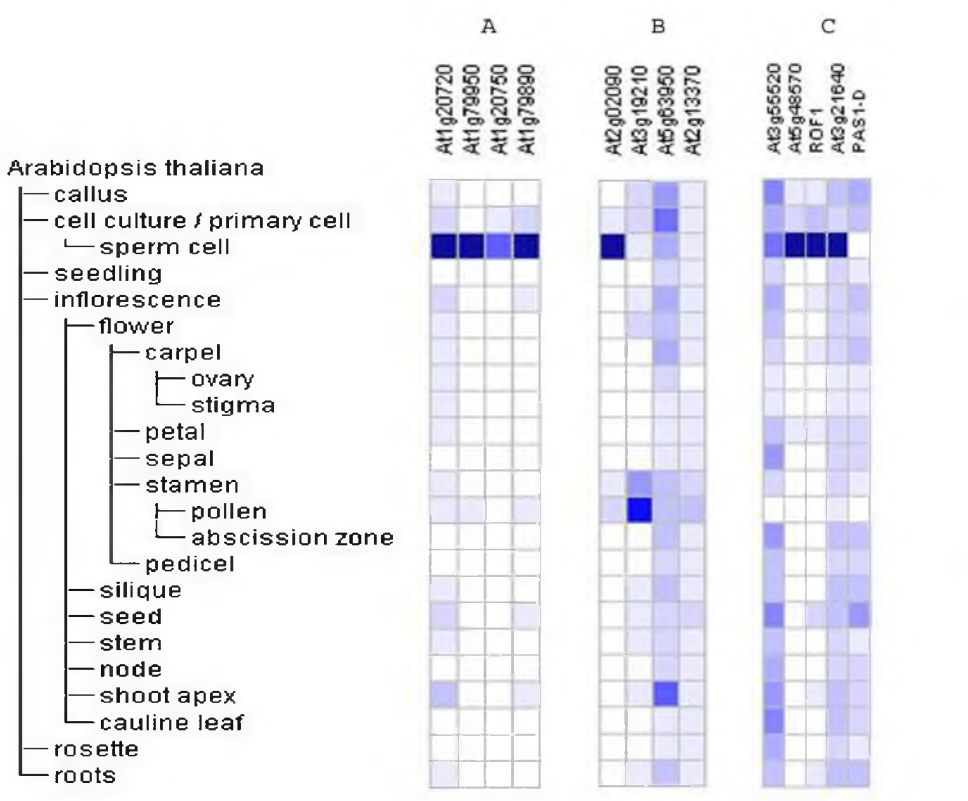


**Fig. 3.6: Genevestigator anatomy meta-profiles of selected Arabidopsis genes. A.** *BACH1* gene family **B.** *RAD54* gene family and **C**. *FKBP* gene family. Arabidopsis 22k array was selected. Heat map color code: dark-light, colors are normalized to the maximum value (the darkest color corresponds to the maximum expression of the gene)

### 3.4 Discussion

We have identified 136 genes in *Arabidopsis* as putative homologs to partial *Petunia* sequences generated from cDNA-AFLP expression profiling of meiotic anthers. In a reverse strategy approach, using T-DNA insertion mutants, a subset of 64 genes was screened for a meiotic phenotype. We were able to identify three previously characterized meiotic genes and a number of genes that seem imperative to development. Although genes that are expressed during meiosis were identified no new meiotic mutants were conclusively obtained from our screen. At4g31750 is probably the only gene implicated in meiosis with a corresponding meiotic defect when disrupted in Arabidopsis. In mouse, *PP2C zeta* is expressed specifically in the testicular germ cells through a SUMO-induced recruitment to *UBC9* (Kashiwaba et al., 2003). In Arabidopsis, this gene has been recently characterized as WIN2, which interacts specifically with the *HWI1* gene in response to *P. syringae* infection (Lee et al., 2008). The mutant

At4g31750 exhibited meiotic defects in which a single plane of division separated two sets of haploid cells at the end of meiosis. This mutant phenotype resembles the second division restitution (SDR) *pc* mutant in potato (Peloquin et al., 1999). Characterization of a second mutant allele with a similar phenotype, must confirm this in the future.

Factors that might have played a role in obtaining these disappointing results include failure to detect lowly expressed genes, sampling methods, co-expression of developmentally important loci, deficiencies associated with T-DNA integration and inability to distinguish the chromosomal aberrations caused by T-DNA from meiosis-related defects. This study has also revealed mutants with aberrant segregation and mutants with no phenotypic alterations, as discussed below.

**Identifying meiotic genes through expression profiling**

One of the major strengths of the cDNA-AFLP technique is that hitherto unknown genes can be identified without prior sequence information or sequence homology to known meiotic genes. Expression profiling with meiocytes is highly challenging, if not impossible, in species like *Arabidopsis* due to the small size of the anthers and the few available meiocytes. In order to focus on meiosis we applied cDNA-AFLP to Petunia, a species with large anthers where sampling is easy compared to *Arabidopsis*. Earlier, expression studies in developing anthers identified new genes involved in meiosis (Wijeratne et al., 2006), but also metabolic, developmental and signaling pathways and transcription factors that mediate light signals to coordinate flowering with anther dehiscence were identified based on proteomics (Kerim et al., 2003). From our screen, we identified 16 Arabidopsis genes whose role has been previously established, including meiotic genes like *DMC1*, *ASY1* and *ASK1*, and others that fall into the above-mentioned pathways (Table 3.4). The profiling technique also poses some disadvantages. Tag length can be a limitation with cDNA-AFLP based ESTs for homolog identification in the desired species and qPCR primer design. Many of the meiosis-related genes have specific and low expression that is induced in particular phases of the cell cycle. It might be for this reason that meiotic genes are underrepresented in public EST datasets available for *Solanaceae* and *Arabidopsis*. This decreases the likelihood of selecting the low expressing meiotic ESTs as also observed in our study.

**Stamen cell types active during meiosis**

Our samples consisted of whole anthers in different stages of development as it is difficult to exclusively sample an adequate quantity of meiocytes in a reliable way. Each anther has four lobes and consists of sporophytic tissue like connective, epidermis, endothecium, middle layer, septum, stromium and

tapetum that surround the developing male sporocytes, also called pollen mother cells (PMCs). The tapetal cells are responsible for synchrony within meiocytes ensuring that their genes are simultaneously upregulated. We found tapetum-specific transcripts like AtGPAT1, known to affect tapetal differentiation and play a pivotal role in pollen development and male fertility (Zheng et al., 2003) and a meiotic serine proteinase (*LeTMP* homolog) required for microsporogenesis. Within microsporocytes, cytoplasmic reorganization occurs along with dedifferentiation of plastids and mitochondria accompanied by a drastic decrease in mRNA and rRNA synthesis (Dickinson, 1987). In Petunia, the tapetal nuclei nourishing the PMCs through connections called plasmodesmata attain DNA levels of 8C indicating high nucleic acid synthesis (Liu and Dickinson, 1989). A high proportion of rice transcripts (>30%) expressed in meiotic anthers consisted of secretory proteins and many that are specific to the tapetum (Huang et al., 2009). Overall, there is an abundance of tapetum-specifc transcripts in the stamens (Scott et al., 1991). Due to high tapetal gene expression, we now suspect that meiotic transcripts might be difficult to detect on cDNA-AFLP gels, especially when their expression is below a threshold level, as defined by clustering programs. This has also been a challenge in investigating the meiotic proteome of *B. napus* using 2-D gels (Sanchez-Moran et al., 2005).

**Expression of developmentally important loci during meiosis**

For most of the Petunia genes, mRNA expression was higher during meiosis but continued to be present post-meiotically. We have identified that developmentally important genes like *AtPARN, AtASK1, AtASK2, AtGPAT1* (Table 3.4) are already expressed during meiosis. A clear example of a post-meiotic gene with a function in meiosis is the *SKP1/ASK1* involved in flower development, male meiosis and embryogenesis (Wang et al., 2006). Yeast sporulation deficient mutant screens show that mutants of 16% of genes differentially expressed during sporulation are also affected in spore production or post germination growth (Deutschbauer et al., 2002). Most rice anther transcripts identified in microspores were also present in increased amounts in mature pollen (Suen et al., 2003; Huang et al., 2009).

About 20% of the tested lines, exhibited lethal phenotypes with a possible effect on gametogenesis and/or embryogenesis. The function of these genes in meiosis remains obscure but some of them are important for embryo and/or gamete development. The role of At3g46740 *(AtTOC75-III),* At1g55870 (*AtPARN*) and At5G19820 (EMB2734) in embryogenesis was described previously. The pollen defects in *AtTOC75-III* +/- anthers and high expression in rapidly dividing tissue confirms that the gene is essential for gametogenesis in addition to having a role in embryo development (Baldwin et al., 2005).

At1g55870 (*AtPARN*) disruption using SALK_072627 heterozygotes showed poor germination and was homozygous lethal with a segregation ratio between 1:2 and 1:3 for the wildtype and T-DNA respectively. *AtPARN* encodes a polyA ribonuclease necessary for early embryo development (Chiba et al., 2004). Its expression during gametogenesis and the appearance of aborted siliques, identified in our study, shows that it is also necessary during microsporogenesis. The corresponding protein in xenopus oocytes, a deadenylating nuclease (DAN), is known to be active during meiotic maturation (Korner et al., 1998). In addition, we found At2g02090, a member of the RAD54 family, to be an essential gene. The RAD54 family has a conserved function in homologous recombination in all species. Most single mutants of RAD54-like genes in Arabidopsis have no phenotype; our candidate AT2g02090 however, selected through expression profiling reveals that it is homozygous lethal with pollen defects in the heterozygotes of two mutant alleles that we tested.

A more elaborate strategy must be employed to confirm gametophytic lethals in our dataset. Crossing the T-DNA heterozygotes to a quartet mutant can identify the male gametophytic lethals. In this mutant, the four meiotic products remain attached to each other, which help to distinguish them from unwanted chromosomal aberrations. The identification of homozygous lethals with defects in both embryogenesis and gametogenesis indicates that some genes are required for both processes. We were not able to convincingly find a 1:1 segregation heterozygous for the T-DNA in the pollen defective homozygous lethal lines. Previous mutant-screens report that the frequency of embryo-defective mutants detected is higher than those affecting gametogenesis. The alarming rate of false positives is due to the inherent complexities associated with using T-DNA lines (reviewed by Meinke et al., 2008).

**Deficiencies associated with T-DNA integration**

The T-DNA was not integrated at the predicted sites in one fourth of the lines screened. A large part of the mutations (20%-30%) are estimated to be caused by partial insertions and deletions that arise from unsuccessful T-DNA integrations (Meinke et al., 2008, Mercier and Grelon, 2008) and considerable effort is required to ensure that the mutant is tagged with an insert. Appropriate insertion lines were not available for five genes. Two of the genes namely At3g20050 and At3g19590 are likely to be important for meiosis and mitosis. At3g20050, encoding the putative Arabidopsis TCP1 protein is highly conserved with 66% identical to the human TCP1. It is expressed highest in haploid cells until the last stage of spermatogenesis (Silver et al., 1987) and associates with the cytoplasmic microtubular structures during mammalian spermatogenesis (Kirchhoff et al., 1990). Male mice carrying these t-alleles are homozygous lethal and sterile in the heterozygotes. These t-haplotype heterozygotes show suppression of

recombination and exhibit preferential transmission of the t-allele to nearly all the progeny (Schimenti, 1972). In yeast, Tcp1p affects microtubule-mediated processes of mitosis and meiosis. It is required for normal development and for actin and microtubule function by interacting with the major cytoskeletal components (Ursic et al., 1991). The second important gene is At3g19590, a putative mitotic checkpoint protein with 5 WD-40 repeats. A search in ExpressionAngler (http://bbc.botany.utoronto.ca/), which is a co-expression analysis database, suggests that it is expressed with the DNA mismatch repair protein, msh6-2, and is similar to genes whose activities peak during cell division in proliferating cells like flower buds and roots.

**Aberrant segregations**

A strong segregation bias was evident in seven segregating lines (At5g12940, At1g07940, At2g02090, At4g16155, At3g21640, At2g28620 and At4g31750). We observed a strong bias towards heterozygosity in SALK_130202 (At1g07940) segregants, with no wildtypes or mutants seen within the 90 plants genotyped. Skewed segregations have been reported in a number of studies where progeny carry chromosomal translocations and inversions that leads to gamete lethality (Koncz and Redei, 1992). Accurate segregation of homologous chromosomes during meiosis requires the coordinated action of chromosome pairing, synapsis, and recombination. Defects in meiosis such as asynapsis, unequal recombination, and illegitimate recombination also result in aneuploidy, duplications, deletions, inversions and translocations. Such chromosomal rearrangements also occur during T-DNA transformation procedures and are therefore not necessarily associated with mutation of the gene in question (Ross et al., 1997). Thus, the meiosis-related `reduced-fertility' trait needs to be distinguished from T-DNA induced variations by using multiple insertion lines within the same gene and observations over several generations.

**Gene families in meiosis**

When close homologs belonging to three gene families, *BACH1*, *FKBP* and *RAD54,* were individually knocked-out, mutants were either lethal or exhibited redundant functions. Since single mutants did not provide evidence of a meiotic role it is necessary to systematically generate double mutants to reveal their function. In cases where putative meiotic genes can be identified on the basis of homology, there can be several potential candidates whose functions have to be established (Caryl et al 2003).

A number of gene scenarios are congruent to what has already been reported by others: SUMO conjugating enzymes have crucial roles in many different biological processes that regulate protein function including protein localization and stability, transcriptional activities, and the regulation of gene

expression. In the basidiomycete *Coprinus cinereus*, Ubc9 interacts with the meiosis-specific RecA homolog, Lim15/Dmc1 (CcLim15), and mediates sumoylation of CcLim15 during meiosis (Koshiyama et al., 2006). Petunia tag 106 corresponds to At1g64230 (AtUBC9) and has a close homolog At4g27960. Predictably, single mutants in *AtUBC9* showed no altered phenotype.

Function of genes within the family might diverge after duplication as in the case of the *ASK* gene family. *AtASK1* has a more obvious role in male meiosis and is only partially substituted by *ASK2* overexpression (Liu et al., 2003). The *Arabidopsis-Mei2-Like* (*AML*) genes comprise a five-member gene family. Only specific multiple mutant combinations displayed sterility and a range of defects in meiotic chromosome behavior (Kaur et al., 2006). Hence, there is no single approach or strategy to analyze gene families.

**Conclusions**

We were able to identify yet unknown genes required for anther development in *Arabidopsis*, by looking at a snapshot of mRNA expression profiles of meiotic *Petunia* anthers and examining the corresponding *Arabidopsis* homologs. Transcripts with a direct and dedicated role in meiosis were far fewer than expected suggesting that they are lowly expressed, or have multiple roles in the anthers and exhibit a great degree of functional redundancy. Gametophytic mutations affecting pollen development were identified in meiotic anthers and suggest that the genes responsible for the mutations might be required during meiosis but this also indicates the possibility that they are subject to post-transcriptional regulatory mechanisms. Single mutants within potential meiotic genes lacked a phenotype and hence have to be analyzed using double or triple mutants within their gene families to reveal their function. This redundancy has not been found in the mammalian counterparts of these genes (Cantor et al., 2001; Crackower et al., 2003; Essers et al., 1997) revealing more and more species-specific variations in the meiotic process.

# Chapter 4

## Meiotic recombination frequency analysis in *Arabidopsis* mutants

**Abstract**

Homologous recombination, an exchange of genetic material between homologs without errors, represents one of the most intriguing aspects of meiosis. Recombination frequency (RF) is a measure of the rate of this genetic exchange. Mutants for a known meiotic crossover (CO)-specific gene-*AtMSH5* and three genes whose meiotic roles are yet to be established: *AtKRP125c*, *AtFKBP20-1* and *AtRECQL4A* were selected to measure RF. Using a visual assay based on fluorescent markers expressed in seeds, we measured homologous meiotic recombination in specific chromosomal regions of Arabidopsis. We observed a drastic reduction in RF of 65% and 80% in the two genetic intervals of the *AtMSH5* mutant. No significant differences in RF were observed in *AtKRP125c*, *AtFKBP20-1* and *AtRECQL4A* mutants. RF measured in plants grown at different locations under controlled conditions shows that it is not greatly affected by the microenvironment. The four single insertion GFP/RFP tester lines we developed with the fluorescent markers located about 20-30 cM apart on chromosomes 1, 3, 4 and 5 can be routinely used to estimate recombination frequencies in a high throughput screen.

## 4.1 Introduction

Meiotic homologous recombination (HR) involves the induction and repair of double strand breaks (DSBs) between paired homologous chromosomes leading to the reciprocal exchange of chromosome parts in a process called Crossing Over (CO). The alternative outcome of HR is a non-crossover (NCO), which includes a DSB repair process that is not accompanied by reciprocal exchange of chromosomal segments. The mechanism that allows homologs to precisely pair up in order to enable CO to occur without errors represents one of the most intriguing aspects of meiosis.

### COs and their chromosomal distribution

Male meiosis in Arabidopsis, from premeiotic S-phase to tetrad stage, takes about 36 hours (Armstrong and Jones, 2003). During meiotic prophase I, a complex series of processes in homologous recombination including chromosome pairing, synaptonemal complex (SC) assembly and crossing-over take place. These processes, which occur in the same spatial and temporal context, are initiated at the transition of leptotene and zygotene, finalized in diplotene (Borner et al., 2004) and last for 20-24 hours in Arabidopsis.

Electron microscopic studies of the SC revealed spherical multiprotein complexes between or at the axes of the synapsed chromosomes (Carpenter, 1979). These structures are called recombination nodules (RNs) and mark the sites of recombination events (Stack and Anderson, 1986a, b; Albini and Jones,

1987; Carpenter, 1987, 1988; Anderson et al., 1997; Zickler and Kleckner, 1999). During zygotene and early pachytene, these RNs are numerous and appear to be randomly distributed along the chromosomes, but most of them disappear during mid pachytene while the remaining nodules become larger and denser stained. At diplotene the chromosome pairs shed their SCs and late RNs are converted into structures that will become visible under the light microscope as chiasmata. These connections that mark the sites of recombined non-sister chromatids are retained until metaphase-I. Sherman and Stack (1995) observed in tomato that the number and distribution of RNs at late pachytene correspond with those of chiasmata at diplotene, and with the estimated number of COs derived from genetic studies in tomato. Hence RNs are considered direct indicators for the occurrence of recombination events. Discrepancies between these recombination estimates for maize were later discussed by Anderson et al. (2003).

In addition to the exchange of genetic material, another important function of chiasmata is to serve as a physical links between the homologs, which is essential for the correct segregation of the homologs at anaphase-I. It explains why even very small bivalents always produce a so-called obligate chiasma. When multiple CO events occur on a bivalent, they mostly keep a certain distance between them, they rarely occur in clusters. This phenomenon of non-random distribution that was found for COs, RNs and chiasmata is referred to as CO or chiasma interference (reviews in de Boer et al., 2006; Drouaud et al., 2007). Using an allelic series of *spo11* mutants, Martini et al., (2006) found that CO numbers were maintained at wild-type levels despite the reduction in numbers of DSBs. CO numbers were maintained at the expense of NCOs, a phenomenon called CO homeostasis (Martini et al., 2006). Work in *C. elegans* shows that the CO numbers and distribution along chromosomes are largely influenced by condensin complexes at the stage of DSB formation (Mets et al., 2009). In addition, a second level of CO regulation in meiosis is evidenced by Youds et al., (2010) who show that RTEL-1 in *C. elegans* enforces interference by channelising DSBs into NCO.

The distribution of chiasmata in plants is generally considered non-random and is confined to the euchromatin regions along the chromosomes (Anderson et al., 2003; Drouaud et al., 2006). A convincing study on related Allium species differing in heterochromatin blocks showed that chiasmata follow the euchromatic regions (Loidl, 1982). In Arabidopsis, a detailed analysis of chromosome 4 shows that CO rates are highly variable (hot and cold spots) across the chromosome and occur at a higher frequency in males compared to females (Drouaud et al., 2006; own results).

**Factors influencing recombination**

Recombination frequencies (RF) can vary due to genetic as well as non-genetic factors. Apart from the genes required for the recombination process itself, factors associated with variations in recombination rates include DNA constitution such as the presence of repetitive sequences and chromosome features. RF variability across genetic backgrounds has also been recorded in many plant species like Arabidopsis, sea beet, Brassica, Petunia, soybean, lima bean, rye, barley and maize (Kraft et al., 1998; Nicolas et al., 2008; Dvorák et al., 1998; Pfeiffer 1993; Allard, 1963;) and in general depends on the actual homology between the homologs.

Genotypes with high RF in certain chromosome regions were found to maintain the increased recombination rates in subsequent generations (Allard, 1963). RF can also dramatically change in chromosomes with altered chromosome structure such as deletions in Petunia (Gerats et al., 1986) and wheat (Qi et al., 2002). This has been further discussed in Wijnker and de Jong (2008). Furthermore, various non-genetic factors influencing RFs have been reported including age, temperature stress, environment (Koren et al., 2002), chemicals, nutritional states (Abdulah and Borts, 2001) and antibiotics (Schewe et al., 1971). Temperature shifts between 19°C – 28°C are known to increase the genetic map length by 2-3 cM in Arabidopsis (Francis et al., 2007). The CO frequency in Arabidopsis changes during development with flowers in the lateral stems having a higher CO rate compared to those in the primary branch (Francis et al., 2007). All these studies reinstate the hypothesis that there is a dynamic relationship between genes, chromosome structure, environment and the frequency of COs.

**Estimating CO frequencies**

The cytological representations of CO events are chiasmata and so, estimates of RF can be obtained from counting chiasmata. This is normally done in diplotene or diakinesis complements, which in plant species with small or middle-sized genomes, is difficult due to the inability of resolving adjacent chiasmata at that stage. Estimation of COs based on the position and number of late RNs is more reliable but the technique is time consuming and only feasible for large chromosome species (Anderson et al., 2003). Immuno-fluorescent tagging of the CO-specific protein MLH1 is an excellent indicator of CO sites, but the labeling is technically challenging and the occurrence of false positives is sometimes a problem (de Boer et al., 2006; Lhuissier et al., 2007). CO frequencies have also been estimated based on genetic recombination data using labor intensive PCR-based molecular markers (Nilsson et al., 1993; Drouaud et al., 2007) as well as morphological markers based on phenotypes (Koornneef et al., 1997), antibiotic

resistance (Barth et al., 2000), visual assays based on recombination between linked fluorescent markers expressed in seeds (Melamed-Bessudo et al., 2005) or the pollen, in a *quartet* mutant background (Francis et al., 2007). In addition, a high throughput method that screens intra-chromosomal recombination events based on glufosinate resistance (due to a reconstituted phosphinotricine N-acetyltransferase) was successful in recovering exclusively germinal recombination events. In this reporter system, DSBs are introduced by *Sce*-I only in germline cells, under a floral specific promoter *APETALA3,* that are repaired by the DSB repair SSA pathway (Wehrkamp-Richter et al., 2009). Genetic estimation of COs depends on the availability of viable products and well-distributed, closely linked markers. A comparison of CO frequency shows a 10% underestimation of CO by chiasma counts over RNs counts (Anderson et al., 2003).

**Mutants with altered recombination frequencies**

Over thirty meiotic mutants have been described in *Arabidopsis* and for many of them, RF has been measured by counting the number of chiasmata in meiotic metaphase-I cells like *Atmsh4*, *Atptd1*, *Atmpa1* and *Atmlh3* (Franklin et al., 2006, Wijeratne et al., 2006, Sanchez-Moran et al., 2004, Jackson et al., 2006) or by using genetic markers for others like *Atmer3*, *Atmsh2*, *Atmus81* (Mercier et al., 2005, Emmanuel et al., 2006, Berkowitz et al., 2007). Impairing genes that are normally recruited to early repair steps of DSBs like *AtMRE11, AtRAD51, AtXRCC3, AtBRCA2, AtRPA2, AtMND1* and *AtAHP2* (Table 1.1, Chapter 1) causes severe chromosome fragmentation ultimately leading to sterility; such mutants cannot be tested further. The effect of mutations on the rate of meiotic CO can be studied only when (at least some) viable gametes are formed. CO and SC formation are allied processes both of which, when disturbed, result in aneuploidy and sterility. Nevertheless, SC mutants are not necessarily affected in COs. For example, the role of the transverse filament protein *AtZIP1* in chiasmata formation remains unresolved, since in the *AtZIP1* mutants, immuno-stained AtMLH1 foci persist which suggest that COs are still formed (Higgins et al., 2005). A screen directly testing for CO events is therefore useful to identify genes affecting RF in plants to varying degrees.

In this study we aim to identify genes affecting RF by screening mutants for altered recombination properties. Using a visual assay based on fluorescent markers expressed in seeds, we measured homologous meiotic recombination in specific chromosomal regions of Arabidopsis. Tester lines harboring Green (GFP) – and Red (RFP) Fluorescent Protein markers (Melamed-Bessudo et al., 2005) were developed for intervals on four of the five chromosomes in Arabidopsis. Mutants for a known meiotic CO-specific gene-*AtMSH5* and three genes whose meiotic roles are yet to be established: *AtKRP125c*, *AtFKBP20-1*

and *AtRECQL4A* were selected. Recombination frequency was compared between the wildtype and the mutants, in at least two chromosomal intervals. Our findings suggest that this assay can be routinely employed to screen for candidate genes involved in the recombination process with relative ease. We also discuss factors influencing recombination rates that need to be considered.

## 4.2 Materials and methods

### Plant material and growth conditions

*Arabidopsis* seeds were surface sterilized with 100% ethanol and 1.5% NaOCl, washed in distilled water and sown on half strength Murashige and Skoog medium without sucrose. The seedlings were transferred after 14 days to a soil-based metro-mix consisting of three-parts of soil (Lentse potground number 4, Hortimea, Cuijk, The Netherlands) with one-part vermiculite (Agro vermiculite number 2, Pull Rhenen B.V., the Netherlands). Plants were grown in a growth room at 23ºC ± 2ºC under long-day conditions (16 h light / 8 h dark). For the experiment comparing the effect of the location on RF, plants were grown under comparable controlled conditions simultaneously at two locations in The Netherlands, namely Radboud University, Nijmegen and KeyGene N.V., Wageningen in growth rooms.

### GFP/RFP tester lines

A chromosome 3 GFP/RFP tester line, C3A, and 8 single GFP or RFP insertion lines (Melamed-Bessudo et al., 2005) were obtained from Dr. Avraham Levy, Israel (Fig. 4.1). Additional meiotic testers were developed for intervals on chromosomes 1, 3, 4 and 5 by crossing the appropriate single GFP/RFP insertion lines. The crossing strategy to obtain additional GFP/RFP tester lines was described previously by Melamed-Bessudo et al. (2005).

### Fluorescence microscopy

GFP/RFP fluorescence in the mature dried seeds was studied under a Leica MZ FLIII stereomicroscope equipped with GFPplant (emission ~ 525nm) and DsRED (emission ~ 590nm) filters (Leica Microsystems, Heerbrugg, Switzerland).

### Mapping the insertions in the tester lines and mutants by PCR

Plants homozygous and heterozygous for the fluorescent markers were confirmed by PCR using a pair of marker-specific primers (Table 4.1) and an insert specific primer LB3: 5'-CGTGGACCGCTTGCTGC-3'. The status of specific meiotic mutants was identified by PCR in T-DNA segregating lines using a pair of gene-specific primers (Table 4.2) and a T-DNA-specific primer Lba1: 5'- TCACGTAGTGGGCCATCG-3'. PCR conditions were 5 min at 94°C

followed by 30 cycles of 94°C for 30s, 59.8°C for 45s, and 72°C for 90s with a final extension at 72°C for 10 min.

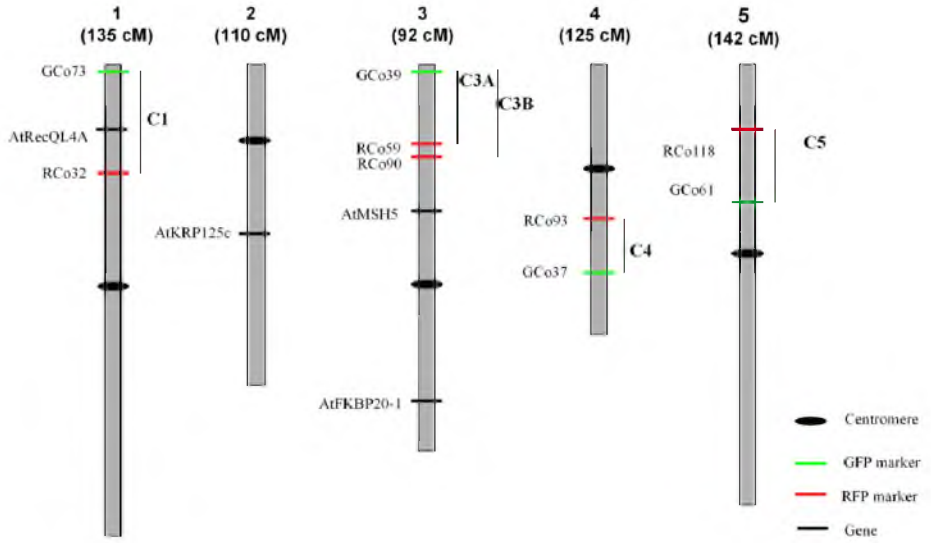


| Tester line | GFP/RFP marker | Position (kb) | Interval size (kb) | Calculated interval size (cM) * | Estimated interval size (cM) ** |
|---|---|---|---|---|---|
| | GCo73 | 210 | | | |
| C1 | RCo32 | 6667 | 6456 | 32 | 23 |
| | GCo39 | 256 | | | |
| C3A | RCo59 | 5361 | 5105 | 25 | 17 |
| | GCo39 | 256 | | | |
| C3B | RCo90 | 5868 | 5611 | 28 | 18 |
| | GCo-37 | 11892 | | | |
| C4 | RCo-93 | 7552 | 4339 | 22 | 23 |
| | GCo61 | 8897 | | | |
| C5 | RCo118 | 4111 | 4786 | 24 | 22 |

**Fig. 4.1** Location of the GFP and RFP markers and their corresponding testerlines (C1, C3A, C3B, C4, C5) and the location of meiotic genes (*AtGRF4, AtRecQL4A, AtKRP125c, AtMSH5, AtFKBP20-1*) on the 5 chromosomes of Arabidopsis. C3A is tester line Col3/4-20 from Melamed-Bessudo et al. (2005). GCo, green fluorescent protein in Columbia; RCo, red fluorescent protein in Columbia. . *Calculations were based on 200kb = 1cM in Arabidopsis; ** the distance between GCo and RCo in cM was deduced based on location of the nearest marker on the Lister and Dean map (1993).

**Table 4.1** Primers to identify GFP and RFP markers in the meiotic tester lines
RCo = RFP marker in Col-0 ecotype, GCo = GFP marker in Col-0 ecotype, F= forward primer, R = reverse primer, LB3 = T-DNA left border primer.

| Primer Name | Sequence | Product size (bp) | |
|---|---|---|---|
| | | F+R | LB3+R |
| RCo32_F | TGCGCGTAGCTCGATCAC | 677 | 234 |
| RCo32_R | TCATCACACGTACAATACCCTTG | | |
| RCo59_2_F | AGCGTCTCACTCACGTACG | 462 | 240 |
| RCo59_2_R | GCTCTCTGCCAACATGAATCG | | |
| RCo118_F | TCGAGAAGAGCGATCCTTACG | 577 | 188 |
| RCo118_R | ATTCCCCAGAACGTCATGGTC | | |
| GCo39_F | TGATACATAAATTAGGGGTGG | 401 | 284 |
| GCo39_R | CAGAGAGAGAGAGAGAGTATT | | |
| GCo61_F | GGTTTCTATGATTGGTGCCAAC | 437 | 337 |
| GCo61_R | CATTCAGAAACACAGACATTAC | | |
| GCo73_F | AATTAA GGTGGCAAGCGAAG | 395 | 296 |
| GCo73_R | GACCGCATTCCTTGGTATGG | | |

**Measurement of meiotic RF**

Meiotic recombination was measured using a seed-based assay (Melamed-Bessudo et al., 2005) in which a pair of genetic markers, GFP and RFP, linked in *cis* may separate following crossing-over. The strategy employed is outlined in Fig 4.2. Specific meiotic mutants were fertilized with pollen of homozygous RFP/GFP tester lines (Fig. 4.2a) and the resulting F1 hybrid was subsequently selfed to create the F2 generation. For each of the mutants-to-be-tested, we selected at least four mutant and four homozygous wild-type F2 plants that were heterozygous for the fluorescent markers. These were then crossed to the male sterile *delayed dehiscence1 (DDE1)* mutant (Sanders et al., 2000) to monitor RF in male meiosis in the resulting seeds (Fig. 4.2b). All resulting siliques were analyzed separately and the data were eventually pooled using approximately 100 seeds per plant. The seeds could be categorized in four classes - one parental class expressing both markers, the other parental class with both markers absent and the two recombinant classes expressing only one of the two markers (see Appendix 3). The RF was calculated as a ratio of the number of recombinants over the total number of seeds investigated.

## 4.3 Results

### Development of GFP/RFP tester lines

Four GFP/RFP tester lines were developed for chromosomes 1, 3, 4 and 5 that contained the GFP/RFP markers in a homozygous or heterozygous state. Details of the tester lines including marker pairs and interval distances (Kb, cM) are presented in Figure 4.1. Except for tester line C1, the homozygous lines were all fertile with healthy pollen. The C1 tester homozygous for the RCo32 marker was extremely slow to grow and stunted with pale stems and leaves. The marker was inserted within the second intron of At1g19290, a pentatricopeptide repeat containing protein (see Appendix 2). Plants heterozygous for the RCo32 marker and homozygous for the Gco73 marker were used for subsequent analysis.

**Table 4.3** Gene information associated with the mutants used in this study

| Gene ID | Gene | Description | Location (kb) | Reference |
|---|---|---|---|---|
| At*MSH5* | AT3G20475 | MutS homolog necessary for meiotic crossover | 7148-7150 | Higgins et al., 2008 |
| At*KRP125c* | AT2g28620 | Kinesin motor protein required for chromosome alignment | 12272-12277 | Bannigan et al., 2007 |
| At*FKBP20-1* | AT3g55520 | FK506 binding / peptidyl-prolyl cis-trans isomerase | 20604-20606 | He et al., 2004 |
| At*RecQL4A* | AT1g10930 | Helicase with anti-CO activity | 3647-3655 | Bagherieh-Najjar et al., 2003 |

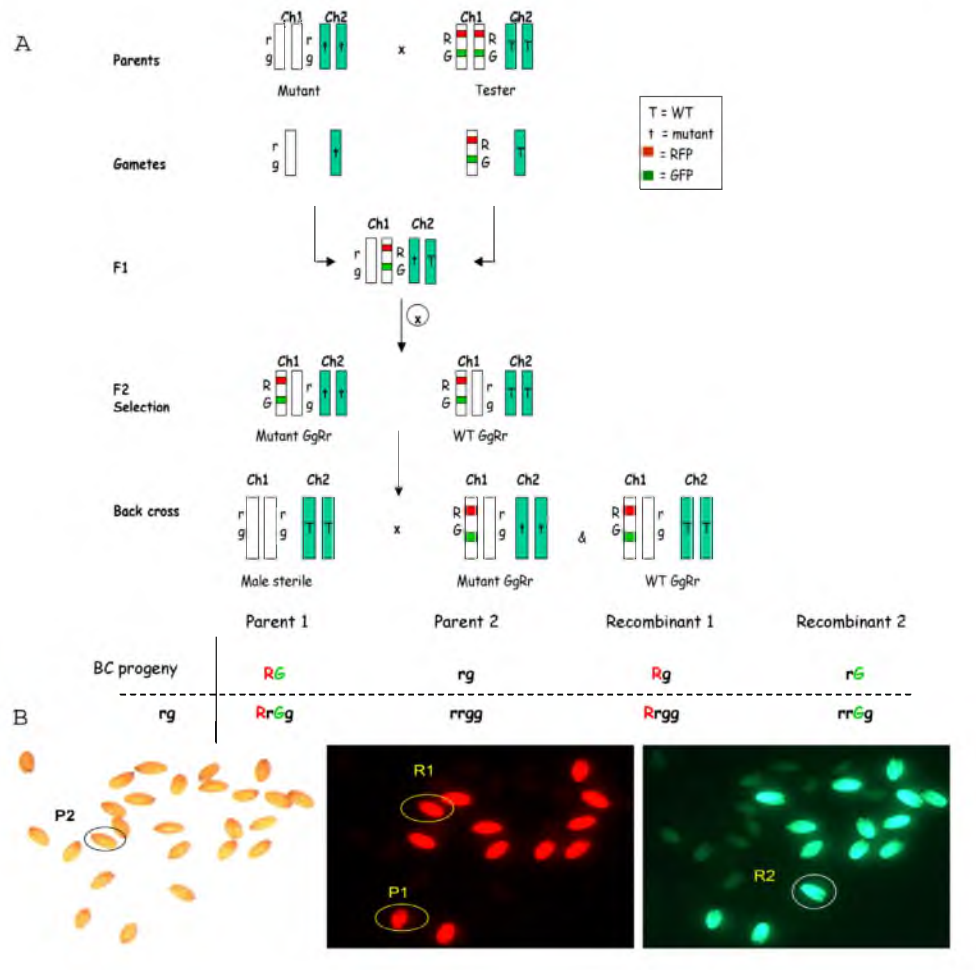


**Fig. 4.2 A seed-based fluorescent assay to estimate meiotic recombination**
a) Schematic representation of the crossing strategy employed to measure recombination Mutants (tt) were crossed to a homozygous GFP/RFP tester line (GR/GR). In the F2 population, mutants and homozygous wildtypes (TT) that were heterozygous for the GFP/RFP markers (GRgr) were selected for crossing to a male sterile plant; b) Detecting recombinants and parental classes (encircled), by fluorescence.

### Mutant recombination frequency analysis

The information concerning the four mutants selected for this study is summarized in Table 4.3. Recombination frequencies were measured in two intervals for every mutant and compared to wild type frequencies. The interval was selected on a different chromosome arm with respect to the location of the T-DNA of the mutant (Fig. 4.1), because the presence of the T-DNA insertions in relatively close proximity could influence recombination. Besides, it would be

complicated to select a homozygous mutant, heterozygous for the tester loci, if all would be located in close proximity on the same chromosome.

***Atmsh5* mutant**

The *AtMSH5* gene (AT3G20475) represents a *MutS* homolog that together with *AtMSH4* participates in CO formation (Table 4.3). The *AtMSH5* mutant (SALK_026553) exhibits a highly reduced male and female fertility. Seed set was poor giving less than 100 seeds per plant despite extensive crossing. The average RF in the chromosome-1 interval was 9.8 cM in *Atmsh5* (501 seeds from 11 plants) compared to 28 cM in the wildtype (809 seeds from 7 plants) (Fig. 4.3a). A t-test between WT and mutant showed that the difference in RF means was significant (P-value = 0.00004). On chromosome-5, the average RF was 3.5 cM in *Atmsh5* (297 seeds from 3 plants) compared to 18.2 cM in the wildtype (559 seeds from 4 plants) (Fig. 4.3b). The t-test showed that the mean RF was once again significantly different (P-value = 0.003). This corresponds to a 65% and 80% reduction of RF respectively, in the two genetic intervals of the *AtMSH5* mutant.

***Atkrp125c* mutant**

The *AtKRP125c* gene (At2G28620) encodes a kinesin motor protein required for spindle movement during mitosis (Table 4.3). A Petunia partial transcript was expressed specifically from zygotene until telophase II of meiosis (Cnudde et al., 2006). *AtKRP125c* was identified as the homolog of this Petunia EST (Chapter 2). *AtKRP125c* mutants (SALK_042029) were fertile with a normal seed set. The average RF in the chromosome-3A interval was 29.7 cM in the *AtKRP125c* mutant (651 seeds from 3 plants) compared to 28.1 cM in the wildtype (927 seeds from 4 plants) (Fig. 4.3c). The difference was not significant in a t-test comparing the RF means (P-value = 0.389). On chromosome-5 the average RF was 22.8 cM in *Atkrp125c* (180 seeds from 1 plant) compared to 18.2 cM in the wildtype (649 seeds from 4 plants) (Fig. 3d). The difference was not significant in a t-test comparing the RF means (P-value = 0.358). The recombination frequency thus appears to remain unaltered in the *AtKRP125c* mutant for both intervals tested.

***Atfkbp20-1* mutant**

The *AtFKBP20-1* (At3g55520) gene encodes a conserved peptidyl-prolyl cis-trans isomerase (PPIases) (Table 4.3). Its homolog in Petunia is expressed from pre-meiotic stage to pachytene (Cnudde et al., 2006). *AtFKBP20-1* mutants (SALK_058277) were fertile and did not have any obvious morphological defects. In the chromosome-1 interval the RF was 29 cM in the mutant (682 seeds from 4 plants) compared to 31.7 cM in wild type (412 seeds from 4 plants) (Fig. 4.3e). The difference was not significant in a t-test comparing the RF means

(P-value = 0.450). In the chromosome-5 interval the RF was 19.1 cM in the mutant (711 seeds from 5 plants) and 16.3 cM in wild-type (495 seeds from 4 plants) (Fig. 4.3f). The difference was not significant in a t-test comparing the RF means (P-value = 0.231). The recombination was not significantly different in the tested intervals for the *AtFKBP20-1* mutant.

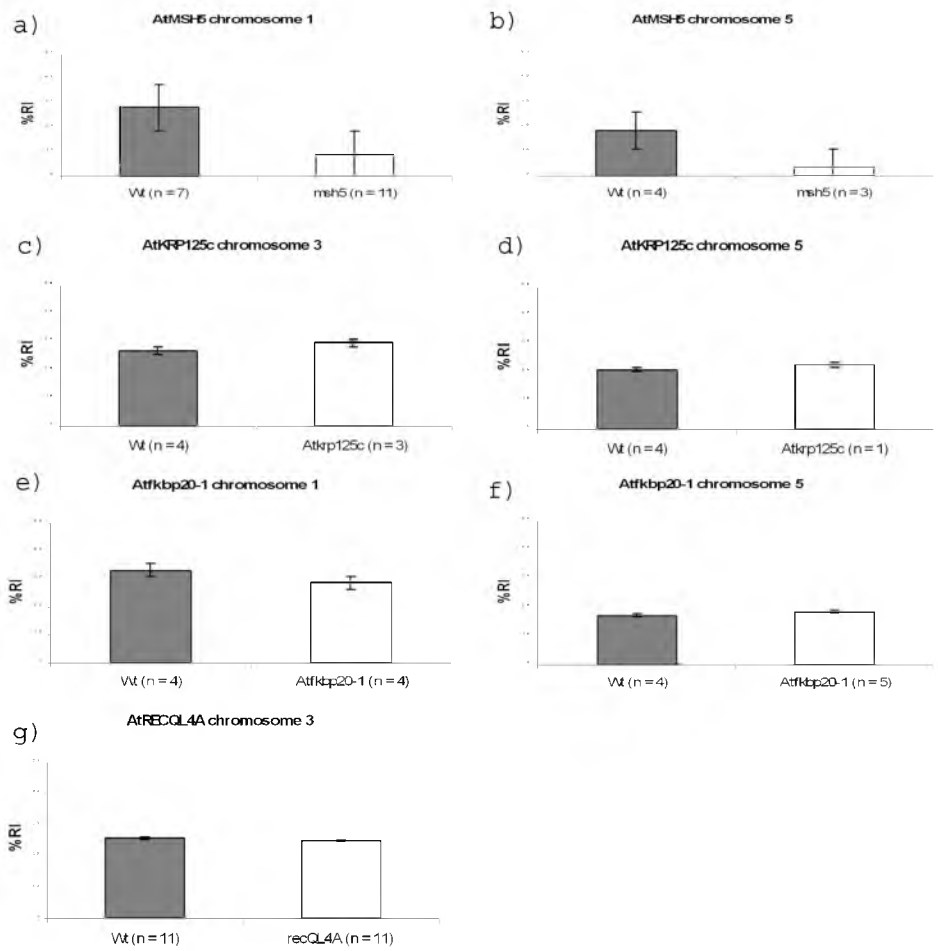


**Fig. 4.3 A comparison of recombination frequencies (RF) between wild type and mutant plants examined in different chromosome intervals of Arabidopsis** At*msh5* (a-b); At*krp125c* (c-d); At*fkbp20-1*(e-f); At*recQl4A* (g). n = number of plants analyzed; Error bars indicate standard error.

### *AtrecQL4A* mutant

*AtRECQL4A* (AT1g10930) is an *SGS1* homolog that prevents excess recombination (Table 4.3). *AtRECQL4A* mutants (SALK_030897) were fertile and phenotypically similar to the wildtype. RF in the chromosome-3A interval was 25.6 cM in the *AtRECQL4A* mutant (1409 seeds from 11 plants) compared

to 25.5 cM in the wildtype (1283 seeds from 11 plants) (Fig. 4.3g). The difference was not significant in a t-test comparing the RF means (P-value =0.503). Thus the recombination rate in the *AtRECQL4A* mutant was similar to the wildtype.

**Recombination and micro-environment**

We compared RF at two locations simultaneously under controlled conditions. The recombination frequency was measured in the chromosome-3A interval of *AtRECQL4A* mutant lines in growth chambers at two different greenhouses located at Radboud University, Nijmegen (RU) and KeyGene N.V., Wageningen (KG).

The *AtRECQL4A* mutants at RU had an average recombination of 28 cM (606 seeds from 4 plants) compared to 25.3 cM in the wild type (671 seeds from 4 plants). At KG the average recombination was 24.3 cM in *AtrecQl4A* mutants (803 seeds from 7 plants) compared to 25.5 cM in the wildtype (1283 seeds from 11 plants). There was a difference of only 3.8 cM in the mutant's recombination frequency across the two locations and no difference for the wildtype (Fig. 4.4).

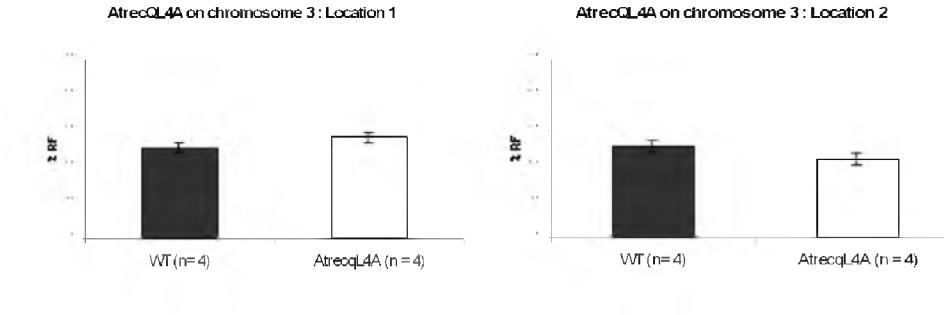


**Fig. 4.3 A comparison of recombination frequencies (RF) between wild type and mutant plants examined in different chromosome intervals of Arabidopsis** At*msh5* (a-b); At*krp125c* (c-d); At*fkbp20-1*(e-f); At*recQl4A* (g). n = number of plants analyzed; Error bars indicate standard error.

**4.4 Discussion**

We used *cis*-linked fluorescent markers to visually assay CO events in *Arabidopsis thaliana* mutants. This assay, established by Melamed-Bessudo et al. (2005), is based on segregation of GFP and RFP markers that can be scored in seeds. Single insertion GFP/RFP lines with the fluorescent markers located about 20-30 cM apart were selected and crossed to develop four new GFP/RFP tester lines in the Col-0 background for Arabidopsis chromosomes 1, 3, 4 and 5. The RF values were estimated in at least two intervals of the genome for four mutants and compared with the wildtype. By analyzing backcross progeny that were

crossed to a male sterile female parent we followed male CO events in the mutants compared to wildtype.

This seed-based assay allows us to efficiently estimate recombination frequencies in a high throughput screen. A larger collection of tester lines, with more closely linked GFP/RFP markers will allow testing in smaller intervals. If this assay ascertains a gene's role in recombination it is advisable to analyze recombination genome-wide with greater accuracy. The strategy adopted allows relative ease with which one can analyze progenies, comparable to the tetrad analysis based on pollen-expressed fluorescent proteins (Francis et al., 2007). However, it cannot measure gene conversion and analyze recombination directly in the gametes, which are the strengths of the tetrad analysis. Analysis of genes directly influencing recombination can be challenging with this method as the high sterility in these mutants reduces the number of successful backcrosses and the resulting seed set. Inherent to assays that use transgenic markers we cannot rule out the influence a T-DNA might have on chromatin structure.

We observed a drastic reduction in RF of 65% and 80% in the two genetic intervals of the *AtMSH5* mutant which is comparable to the 87% reduction in chiasma frequency as scored from metaphase I complements by Higgins et al. (2008). Far greater differences in CO rates were obtained from the recombination data compared to chiasma counts by Nilsson et al., 1993 and Moran et al., 2001, while they were equal when King et al., (2002) compared RF using AFLP markers to chiasmata counted using genomic *in situ* hybridization. Nevertheless, the drastic reductions seen in *Atmsh5* are in the same order of magnitude in both cases, suggesting that the genetic fluorescence marker assay is an effective method to measure CO events.

The normal viability and unaltered meiotic recombination of *AtKRP125c* mutants shows that the gene is dispensable for gametogenesis with no unique role in recombination. *AtKRP125c* has a definite role in stabilizing the mitotic spindle in plants as evidenced by localization of AtKRP125c-GFP to interphase and mitotic cells together with disrupted interphase cortical microtubules in the mutant (Bannigan et al., 2007). Expression of the gene in Petunia meiocytes suggests that it might be associated with the microtubules and does not actively participate in recombination during meiosis.

No significant differences in RF were observed in *AtFKBP20-1* mutants. The FKBP gene family in Arabidopsis consists of 23 genes of which a subgroup including *AtFKPB20-1* is putatively involved in stress response (Geisler and Bailey, 2007). It contains a nuclear targeting signal and the FKBP06 binding domain and belongs to the FKBP-C superfamily (Harrar et al., 2001; He et al., 2004). The human FKBP06 plays an essential role in male fertility and homologous chromosome pairing in meiosis (Crackower et al., 2003). There is evidence for a role of FKBPs in gametogenesis from some animal species:

*FKBP06*-disrupted mice show spermatogenic defects (Crackower et al., 2003) or affect oogenesis in the Drosophila *SHU* (*FKBP*) mutant (Munn and Steward, 2000). Single mutants of *AtFKPB20-1* do not show any defects in gametogenesis or homologous recombination possibly either due to functional redundancy or because it simply has no involvement in meiosis.

The single RecQ gene found in bacteria and yeast has diversified into a gene family in humans and plants. RecQ's in eukaryotes maintain genomic stability by coordinating replication and recombination (Jessop et al., 2006). The Arabidopsis mutant *AtrecQL4A* is sensitive to DNA- damaging agents like MMS, cisplatin and shows enhanced somatic intrachromosomal HR (Bagheriegh-Najjar et al., 2005, Hartung et al., 2007). However, *AtrecQL4A* mutants were not altered in meiotic HR compared to the wildtype. Arabidopsis possesses seven *RecQ*-like genes out of which two closely related RecQ helicases, namely *AtRecQL4A* and *AtRecQL4B*, each with contrasting roles in mitotic HR (Hartung et al., 2007). *SGS1*, the only known yeast RecQ helicase, when disrupted shows a modest 1.6 fold higher CO recombination frequency compared to the wildtype but dramatically increases up to 8-fold in *sgs1/zmm* double mutants (Jessop et al., 2006). This implies that SGS1 prevents CO formation in cells lacking ZMM proteins or that ZMM proteins protect designated CO sites from SGS1 activity. It would be interesting to see if meiotic recombination is affected in *AtRecQL4B* single mutants and if CO is partially restored in recQ double mutants with *Atmer3*, *Atmsh5* or *Atzip1*.

As has been discussed in the introduction, COs are not uniformly distributed over the chromosomes and their distribution is dependent on various genetic and environmental influences (Nag et al., 1989; Mizuno et al., 2001). The recombination rates within the intervals tested varied between the experiments carried out at different times but the relative differences between the wildtype and mutants remained similar. For the chromosome 3 interval C3A, the wildtype RF ranged from 12.3 to 32.8 cM with an average of 23.4 cM across all experiments (data not shown). These data deviate from the expected 17 cM according to Lister and Dean (1993). The RF was comparable across locations where plants were grown under controlled conditions in climate chambers and the microenvironment therefore in this case seems to not significantly affect the results as was initially speculated (Melamed-Bessudo et al., 2005). RF values might be influenced more by seasonal/temperature changes than by the microenvironment. Huge variations in recombination due to differences in planting dates were also observed in lima bean hybrids (Allard et al., 1963) but these fluctuations could not be associated with the special environmental conditions existent at the time of meiosis. Recombination is influenced by multiple factors and hence control crosses always need to be performed at the same time and under the same conditions as mutant crosses.

Central to meiosis is the specialized process of homologous recombination by the formation of COs. Because of the recent advances in cytological and molecular-based techniques, good progress is made with respect to understanding meiotic COs, *i.e.* form, distribution, number, their regulation and choice of sequence partner for exchange. Recent advances in research related to homologous recombination show that CO formation and its control involve multiple pathways, with considerable variation among model organisms. We need to screen and identify more Arabidopsis genes specifically involved in homologous recombination to unravel the mechanisms of this fundamentally important process and utilize it for crop improvement.

# Chapter 5

## Characterization of the *Arabidopsis thaliana* X-ray sensitive mutant *xrs4*

**Abstract**

A functional analysis of the *xrs4* mutant is of interest to understand some of the fundamental aspects of DNA damage repair in plants. Morphological characterization of *xrs4* established that the mutant has pleiotropic developmental defects related to meiosis, pollen mitosis and embryo development. Putative changes in RF due to mutant *xrs4* allele were measured within a small interval on chromosome 3. The overall RF was not altered in the mutant compared to the wildtype but a large plant-to-plant variation was observed. We mapped the *xrs4* mutation to the top of chromosome 5 in a 62 kb region between positions 1182 and 1244 kb containing 18 genes.

## 5.1 Introduction

DNA is predisposed to damage by exogenous and endogenous treatments including ionizing radiation and mutagenic chemicals. Cells respond to this damage by arresting the cell cycle through damage check points. They subsequently employ appropriate DNA repair mechanisms without which the cells would undergo apoptosis. For the repair of a special class of DNA damage, double stranded breaks (DSBs), two pathways are predominantly active: non-homologous end joining (NHEJ) and homologous recombination (HR). In NHEJ, two free DNA ends simply fuse quite often resulting in the loss or modification of nucleotides. The HR pathway requires extensive DNA sequence homology for repair and copies the information from the intact DNA template. During the pre-synthesis gap or G1 phase NHEJ is employed. In the S-phase, both NHEJ and HR are used, while during the G2 phase HR predominates. The DNA strand that has to be repaired and its homologous template are brought in close proximity of each other by cohesins that physically link sister chromatids (Watrin and Peters, 2009). Sister chromatid cohesion (SCC) is therefore established during DNA replication in S phase, G2 phase and early mitosis and seems to be essential for DNA damage repair by HR.

Central to meiotic HR is the process of exact chromosome segregation, without which chromosomes would be unequally distributed, leading to genome instability and aneuploidy. Accurate chromosome segregation during the nuclear divisions is enabled by the formation of chiasmata and the sequential release of SCC to form four haploid gametes from a diploid spore mother cell. The release of sister chromatid cohesion along the chromosome arms at anaphase-I allows proper segregation of the homologs (Strom et al., 2007) while the release of centromeric cohesion at anaphase-II allows paration of sister chromatids (Rabitsch et al., 2004). Knowledge of the genes participating in chromosome segregation is still limited.

Recombination-mediated DNA repair in eukaryotes involves the RAD52 protein complex that participates in both meiotic and mitotic HR. Mutants of

these genes are in general sensitive to ionizing radiation and usually exhibit recombination deficiencies. Masson et al. (1997) developed a simple screening method for the isolation of *Arabidopsis* mutants hypersensitive to X-ray irradiation in order to study recombination pathways in plants. They identified nine mutants specifically hypersensitive to X-ray-induced DNA damage that were named X-ray sensitive (*xrs*). One of these mutants, designated *xrs4*, exhibits a phenotype that shows hypersensitivity to both X-ray radiation and the DNA damaging agents, mitomycin C (MMC) and methyl methanesulfonate (MMS). This phenotype was combined with a reduction in homologous extrachromosomal recombination (ECR) efficiency and enhanced meiotic recombination (Masson et al., 1997). Although this unusual but interesting mutant meets the expectation of a RAD52 mutant with respect to sensitivity to DNA damaging agents, it shows reduced mitotic recombination and increased meiotic recombination thus exhibiting enigmatically opposite effects in these allied processes. The locus was genetically mapped on chromosome 4 (Masson et. al 1997).

A functional analysis of *xrs4* is of interest to understand some of the fundamental aspects of DNA damage repair in plants. In this study we characterize the defects in this mutant with respect to male gametogenesis and measure the effect of the mutant on meiotic recombination. We have mapped the mutant to a narrow genetic interval and made an attempt to identify the corresponding gene by map-based cloning.

## 5.2 Materials and Methods

### Plant material and growth conditions

The original *xrs4* mutant was isolated from ethyl methanesulfonate-mutagenized (EMS) *Arabidopsis thaliana* cv. Landsberg *erecta* (L*er*) (Masson and Paszkowski, 1997). Seeds of the *xrs4* mutant were kindly provided by Dr. J. E. Masson, INRA, Colmar, France. The T-DNA insertion lines from the SALK Institute (SALK), University of Wisconsin (WiscDxLox) and Syngenta Arabidopsis Insertion Library (SAIL) collections were obtained from the Nottingham Stock Centre (NASC). Seeds were surface sterilized with absolute ethanol and 1.5% NaOCl, respectively, then rinsed with distilled water and sown on half strength Murashige and Skoog medium without sucrose. The seedlings were transferred after 14 days to a soil-vermiculite (3:1) mix. Plants were grown in a growth room at 23°C ±2°C under long-day conditions (16 h light/8 h dark).

### Light microscopy

Flower buds measuring 1.2 mm, 0.8 mm, 0.4 mm, 0.25 mm, respectively, were collected from the *xrs4* mutant and wildtype L*er* plants to examine anther development from stages 5 to 14 (Sanders et al., 1999). Buds were fixed in 2%

gluteraldehyde in 50mM phosphate buffer (pH 7.2) for 2h. Tissues were then rinsed three times with phosphate buffer and postfixed in 1% $OsO_4$ for 1h. Subsequently, samples were dehydrated through an ethanol series (10-30-50-70-90-98%) for 30 min each. Tissues were treated twice with 100% propylene oxide for 30 min and subsequently in 25% Spurr's resin in propylene oxide for 4h and in 50% Spurr's resin in propylene oxide overnight in a fume hood, and finally in fresh 100% Spurr's resin for 4-8h. Individual samples were carefully positioned in flat silicone-embedding molds filled with Spur's resin with longest axes perpendicular to the section axis before polymerization at 60ºC overnight. Semi-thin 1 μm sections were made with the MT5000 Sorvall ultramicrotome (Dupont). Sections were stained with Toluidine blue 0.25% to 1% (w/v), mounted with DePex (Sigma), and observed under a Leitz Orthoplan microscope equipped with a CoolSnap color camera (Roper Scientific) and MetaVue software (Leica Microsystems Imaging Solutions).

**Scanning Electron microscopy (Cryo SEM)**

Samples of open flowers with intact anthers from L*er* (wildtype) and *xrs4* (mutant) plants were mounted in a slush containing aluminum and graphite, degassed and plunged in liquid nitrogen and finally devapourized in vacuum using the Oxford Alto 2500 cryosystem (Catan). Images were captured using the JOEL JSM-6330F field emission scanning electron microscope (JEOL, Tokyo, Japan).

**Pollen size measurements**

Pollen of the *xrs4* mutant was compared to L*er* wildtype for size and morphological differences. Pollen from mature flowers was suspended in a drop of lactophenol acid fuchsin staining solution (Sass, 1964) on a microscopic slide. Digital photographs of pollen grains were captured with a CCD camera and morphometric measurements were performed on the images using ImageProPlus ver6.0.

**Examination of ovules by Confocal Laser Scanning Microscopy (CLSM)**

We selected flowers in stage 12 of flower development corresponding to stage FG07 in female gametophyte development (Christensen et al., 1998). During this stage, anthers are yellow in color but anthesis has not occurred and petals are still white. Pistils of two mutant *xrs4* plants were examined and compared to wildtype (L*er*). Flowers were emasculated and pistils were removed after 2 days for analysis by CLSM. The pistils were gently slit to allow easy penetration of the fixative. They were fixed in a solution of 4% gluteraldehyde in 100mM sodium phosphate buffer (pH 7.2) for 2h. Vacuum of about 200 torr was applied for 30 min to the samples until they sank to the bottom. The pistils were then

dehydrated in an ethanol series for 10 min each, and then cleared in a 2:1 mixture of benzyl alcohol: benzyl benzoate for 45 min. Pistils were mounted in immersion oil on a glass slide with a cover slip and sealed with finger nail polish. The CLSM analysis was done using a Leica TCS-SP5 microscope with a laser set at wavelength of 561nm.

**Meiotic chromosome morphology**

Flower buds of *xrs4* mutant and L*er* were fixed in freshly prepared Carnoy's fixative (ethanol: acetic acid 3:1) and spread on a clean glass slide as described by Ross et al. (1996). For chromosome preparations the fixed buds were rinsed in water three times and two times with 10mM citrate buffer pH 4.5. The cell walls were digested for 3h in a pectolytic enzyme mix (0.3% Pectolyase, 0.3% Cellulase RS, 0.3% Cytohelicase prepared in 10mM citrate buffer pH 4.5). The buds were then rinsed in citrate buffer and transferred to water (4°C) for further use. Buds were tapped in a tiny drop of water to separate the cells from their tissues and macerated with 55% acetic acid on a hot plate at 55°C for 30 seconds. Ice-cold Carnoy's fixative was added carefully followed by a brief rinse in 98% ethanol. Slides were dried and then counter -stained with 20 µl of 0.2 µg/mL DAPI (4'-6-Diamidino-2-phenylindole) and examined under the Zeiss Axioplan 2 fluorescence microscope. Images were captured using a Photometrics Sensys 1305×1024 pixel CCD camera. Image processing was performed with the Applied Imaging CytoVision Genus software (Applied Imaging Corporation).

**Measuring meiotic recombination frequency**

The growth conditions, strategy and details of primers and tester line used in this study are described in Chapter 4. The chromosome-3 tester (C3A), homozygous for the GFP/RFP markers in the Col-0 ecotype, was crossed to the mutant in the L*er* background. The resulting F1 generation was selfed. From the F2 generation, the mutants as well as wild types were selected phenotypically. Wild-type plants could either be homozygous wild type or heterozygous. Plants heterozygous for the C3A markers GCo39 and RCo59 were identified by PCR. The gene-specific primers were designed based on the position of the T-DNA associated with the GFP/RFP marker. LB3 was used as the T-DNA insert-specific primer. The selected plants were then backcrossed to the male sterile *delayed dehiscence1* (*dde1*) mutant (Sanders et al., 2000). We measured recombination between red (RFP) and green (GFP) fluorescent markers that were scored visually under fluorescence (see materials and methods of Chapter 4).

**Mapping the xrs4 locus**

The *xrs4* mutant in L*er* background was crossed with the Col-0 ecotype and mutants were selected from the F2 mapping population. DNA was extracted from

the *xrs4* mutants and the locus was mapped by AFLP marker analysis (Peters et al. 2004). The primers developed by Peters et al (2001) include the following restriction enzymes SacI (5'-GAC TGC GTA CAA GCT C-3') and MseI (5'-GAT GAG TCC TGA GTA A-3') and two selective nucleotides. The selected primer combinations are listed in Table 5.1a. Fine mapping was carried out by analyzing InDel markers from the Cereon Arabidopsis Polymorphism collection (Cereon Genomics; http://www.arabidopsis.org/browse/Cereon/index.jsp) and by designing SNP primers within this interval. Table 5.1b shows the InDel and SNP primers used so far for the map-based cloning procedure.

**Table 5.1a:** AFLP primer combinations used for coarse mapping using polymorphic markers between Col-0 and Ler, spanning the five chromosomes of Arabidopsis

| | **Selective nucleotides** | |
|---|---|---|
| **Marker code** | ***Sac*I+2** | ***Mse* I+2** |
| SM34 | AA | TG |
| SM57 | AG | AC |
| SM61 | AT | GA |
| SM91 | AT | TA |
| SM99 | CC | GG |
| SM194 | CG | AG |
| SM228 | TA | AC |
| SM230 | TG | AT |
| SM247 | TG | CC |
| SM34 | TT | CG |

**Table 5.1b:** InDel primers used for the fine mapping of xrs4 on chromosome 5

| **Marker name** | **BAC clone** | **BAC No.** | **Position** | **Primer forward (F)** | **Primer reverse (R)** |
|---|---|---|---|---|---|
| 478385 | F15A17 | 10 | 698566 | ACCCAAACTTGGCT CACAAC | AGCAAATATTC ACGCCATGC |
| 478395 | F17C15 | 12 | 967450 | CAGAGAGACTCCAT TGCATC | ATATCAGTCCC ACGACATCG |
| cer455551 | MED24 | 13 | 1034937 | AAATCGAGGCACTG TTTTGG | CCCAAGCACAC CTACAAGTC |
| 479319 | T32M21 | 17 | 1257137 | CGGTGAGTACTTTT GTTTGTG | CCGTTGCTTAG AACATTTGC |
| 479329 | T32M21 | 17 | 1287146 | | |

| | | | | | |
|---|---|---|---|---|---|
| | | | | GCTTTTTGATTCGAGAATTTC | TTGCCAACATTTCCCTTTTC |
| 477713 | T1E3 | 18 | 1317050 | AGAACCAGATGATCCAAGTCC | ATCCACCAATGCTACGTTCC |
| cer457348 | MUK11 | 19 | 1409671 | TCTCACCACCCATCAGTTCA | GAGCCTCCTCCGTCTATTCA |
| cer457317 | MUG13 | 21 | 1449695 | GACGCCATCATTCACTCTC | CCATTATGTTCTTTTTCTTCC |
| cer455774 | MHF15 | 29 | 1898165 | TGAGCACCAATSAAGGTTTCC | CTAGGGGGAGTGATCAATGG |

**Table 5.1c:** SNP primers

| **Marker name** | **BAC clone** | **BAC No.** | **Position** | **Primer forward Columbia-specific (C_F), Landsberg-specific forward (L_F)** | **Primer reverse (R)** |
|---|---|---|---|---|---|
| 477322[a] | F8F6 | 14 | 1,102,032 | C_F: TGTCCCACATTGAACACTCTGGA<br>L_F: TGTCCCACATCGAACACTCTGTT | AGCCTCCTTCAAATTCTCCATCA |
| 1155042[b] | F21E1 | 15 | 1,155,042 | C_F: GCTTTAATTAAACCTTTTCGTA<br>L_F: GCTTTAATTAAACCTTTTTGCG | ACGCGATTCAAAGGGTGTTG |
| 1198390[c] | T19N18 | 16 | 1,198,390 | C_F: GGTATGTAGTTATTCACCATCTCTTGATA<br>L_F: GGTATGTAGTTATTCACCATCTCTTAACG | CATTTTCTTCCTCGCTCTCATCATAAAGG |
| 478978[a] | T32M21 | 17 | 1,244,492 | C_F: GAAAGGACCAATTGGGTTATGAAT<br>L_F: GAAAGGACCAATTGGGTTATGCTC | TCACTGAAAGCATCTTGAGCAGGT |
| 478750[a] | T32M21 | 17 | 1,272,906 | C_F: CATAAATGGAGCAACAGTTAGAGGGG<br>L_F: CATAAATGGAGCAACAGTTAGAGGGC | R: GGATTTCAGTCATGGCGTGCTGC |

a: Cereon collection
b: Nordborg lab
c: Solexa collection

**Screening T-DNA mutant collections for xrs4-like phenotype**

The *Arabidopsis thaliana* T-DNA insertion lines SALK, WiscDsLox, SAIL lines were obtained from the Nottingham Stock Centre (NASC, University of Nottingham, United Kingdom) and the FLAG lines were obtained from the Institut National de la Recherche Agronomique (INRA, Versailles, France). Details of genes, corresponding insertion lines, gene-specific and insert-specific primers used are presented in table 5.2. Mutants were examined for phenotypic, developmental and fertility defects. The anthers of the selected mutants were stained with Alexander solution (Alexander, 1969) to test for pollen viability.

**Sequencing At5g04320**

The L*er* sequence spanning this gene was partially available in fragments from the Monsanto-Cereon database and was tiled and aligned for comparison. Both L*er* and *xrs4* mutant DNA were amplified using primers designed on Col and sequenced in both directions. PCR primers were designed to amplify overlapping segments of about 500 bp spanning the 2 kb region. These segments were then cloned into the pGEM-T vector and sequenced. The sequences were then assembled using Bioedit program and *xrs4* was compared to the L*er* wild-type plant.

**Table 5.2:** Primers used for genotyping T-DNA lines

| Gene locus | T-DNA insertion line | Primer name | Forward primer | Reverse primer |
|---|---|---|---|---|
| AT5G04270 | SALK_107820C | SALK_107820C.0 | TGATATGGTAACCGAATCGA | GTTATTTCTACAATTGGGTATG |
| " | SAIL_145_F05 | SAIL_145_F05.01 | TGATATGGTAACCGAATCGA | TCAACAATAAGTAAGCCAATAC |
| AT5G04280 | SALK_048738 | SALK_048738.01 | CCTGTTGGTGGTTTTTCTTCA | AAACAGGTCCGCAAACTAATC |
| AT5G04290 | SALK_001305 | SALK_001305.01 | ATTTCCAAAGGCCCATCCGAG | ATTACACGGCAGAGATACCCC |
| AT5G04310 | SAIL_1149_C06 | SAIL_1149_C06.0 | ATCAATAGGTGCGGTGTAACGG | ATATCCAAATCACCGGCCATG |
| AT5G04320 | SALK_026139 | At5g04320.01 | TTATCACGGTTTTAGGCAAC | CTTTGATTGGGGACTCTGAA |
| " | SALK_027486 | At5g04320.01 | TTATCACGGTTTTAGGCAAC | CTTTGATTGGGGACTCTGAA |
| " | FLAG_570B05 | At5g04320.01 | TTATCACGGTTTTAGGCAAC | CTTTGATTGGGGACTCTGAA |

| Gene locus | T-DNA insertion line | Primer name | Forward primer | Reverse primer |
|---|---|---|---|---|
| AT5G04330 | SALK_064404 | SALK_064404.01 | AATTATTCCCCTT CAGATCCG | GAAAGCCCGAA AATCTCTAG |
| AT5G04350/ 60 | SALK_151314 | SALK_151314 .01 | TTATTGGCTTATG CATTGGCG | TTGTTGGTGTC AGTGTCAGTG |
| AT5G04370 | SAIL_300_D1 1 | SAIL_300_D11.01 | CTCCAGCAATTCT CTTCTTC | CTTAGAGAGCC AATGGAGACC |
| " | SALK_001690 | SALK_001690.01 | AAGAACACAAAG GACCTGATG | ACGCAGTTTAA GGAATGTCGC |
| AT5G04380 | GK-571C09 | GK-571C09.01 | CAGGTGTGATTGT AAAAGTGA | TGTGTTGAAAT CGTTAGTAGG |
| AT5G04410 | SALK_025098 | SALK_025098.01 | CCGACGGATGAG GAACTTGTT | AAAACTTACTT GTGGCACACC |
| - | SAIL T-DNA left border | LB3 SAIL | TAGCATCTGAATT TCATAACCA | |
| - | SALK T-DNA left border | LBSALK2 | GCTTTCTTCCCTT CCTTTCTC | |
| - | GABI-Kat | LB_GabiKat | ATTGACCATCATA CTCATTGC | |
| - | FLAG T-DNA left border | LBbar2 | CGTGTGCCAGGT GCCCACGGAATA G | |

## 5.3 Results

### *xrs4* mutant characterization

### Phenotype

The *xrs4* (in L*er* background) exhibits slow growth beyond the rosette stage, with reduced organ size, reduced seed set, compressed inflorescences, reduced apical dominance and overall developmental delay when compared to wildtype plants (Fig. 5.1). Stem and buds were rather pale suggesting lower chlorophyll content and the rosette leaves of the bolted plants were red in color most likely due to the accumulation of anthocyanins. The inflorescence developed slowly and was late flowering. The mutant flowered for a longer time and produced short siliques characteristic of sterile and semi-sterile mutants. The selfed progeny of homozygous *xrs4* plants appeared indistinguishable from the parents, and the phenotype was stable as observed over four generations.

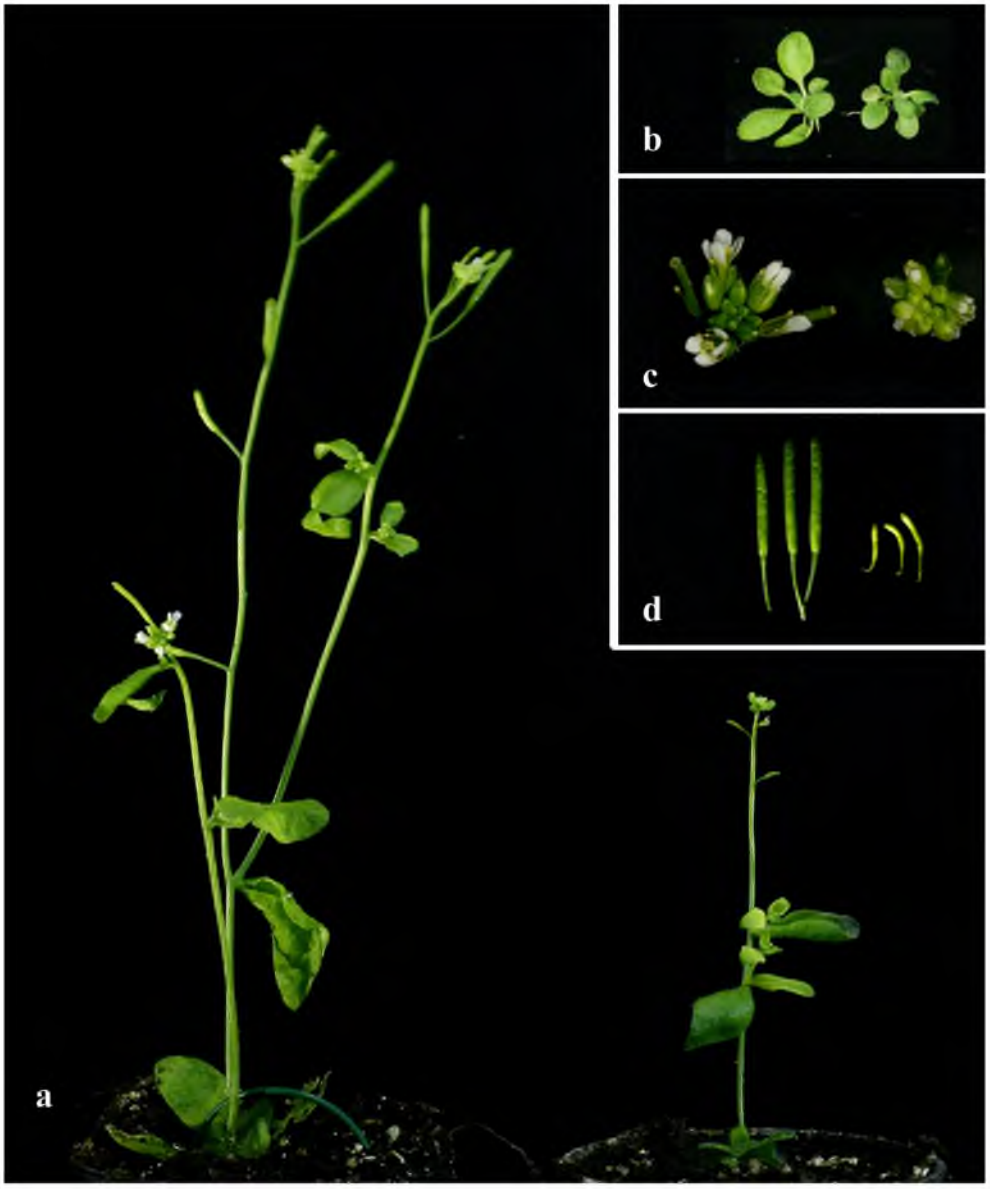


**Fig. 5.1: Comparison of plant morphology** between L*er* wildtype (left) and *xrs4* mutant (right) of (a) young plant, (b) rosettes, (c) inflorescence and (d) siliques.

**Genetic transmission, and fertility**

Siliques of *xrs4* plants were smaller with a highly reduced seed set of 5.7 seeds/silique (n=20) compared to 42.1 seeds/silique (n=10) in wildtype. The *xrs4* in the L*er* background (containing the *erecta* (*er*) mutation) was crossed to Col-0 wildtype. An F2 of 215 plants segregated in the expected Mendelian ratio for a

dihybrid cross (9:3:3:1 segregation) for *xrs4* and *er* ($\chi^2$=0.19 and P=0.98). This indicates that the *xrs4* phenotype is caused by a single, nuclear recessive mutation not linked to the *erecta* gene. The *xrs4* plants in the F2 population that carried a dominant *ERECTA* allele exhibited greater sterility defects. Their anthers were small with mostly non-viable pollen and sterile siliques.

**Female gametophytic development is affected**

To investigate the cause of the fertility defect in *xrs4* mutants we made reciprocal crosses between the mutant and L*er* wildtype. Crosses of the wildtype L*er* with *xrs4* pollen produce F1 siliques with 30-40 seeds/silique (n=4), which is about the same as in the wild type. Reciprocal crosses with *xrs4* as the female parent produced stunted siliques with two to three seeds/silique (n=4) indicating that the female gametophyte was affected. To verify this, we analyzed the ovules in developing siliques of the mutant in three plants at stage FG07 (Christensen et al., 1998) using Confocal Laser Scanning Microscopy (CLSM). The wildtype unfertilized female gametophyte at stage FG07 normally contains a large vacuole and four nuclei, for the egg cell, central cell and two synergid cells (Fig. 5.2a). The aberrant ovules of the mutant lacked these cell types and showed no differentiation of the embryo sac, which usually lacked a vacuole and eventually degenerated (Fig. 5.2b). In pistils of *xrs4* mutants, harvested 48h after emasculation, we observed a mixture of normal and aberrant embryos (data not shown). The *xrs4* mutation affects the female gametophyte and many of the ovules do not complete megagametogenesis.

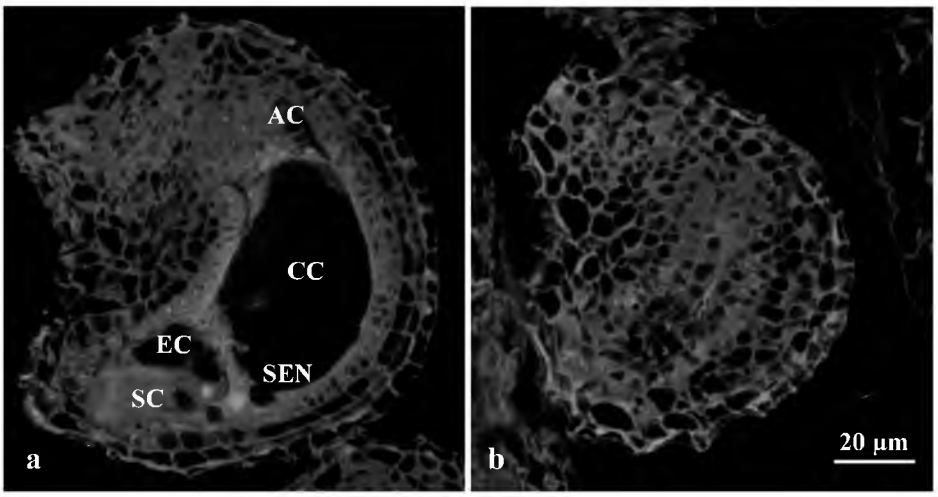


**Fig. 5.2: Ovule development in the *xrs4* mutant**

CLSM projection of 1µm section of the female gametophyte: (a) normal ovule and (b) abnormal *xrs4*-mutant ovule, scale bar = 20 µm..**Abbreviations:** *AC* antipodal cell, *CC* central cell, *EC* egg cell, *SC* synergid cell, *SEN* secondary endosperm nucleus.

**Pollen defects are seen in sporophytic and gametophytic phases**

Examination of the anthers by Alexander stain (Fig. 5.3a-b) revealed non-viable pollen in the *xrs4* mutant (Fig. 5.3a), while scanning electron micrographs of the anthers (Fig. 5.3c-d) showed collapsed pollen and a large anther-to-anther variation in the number of *xrs4* mutant pollen (Fig 5.3d). Morphometric measurements of SASS stained pollen (Fig. 5.3e-f) were taken to determine the pollen area: 40–60% of the *xrs4* pollen was outside the normal pollen size range (Fig 5.3f).

To further define the cause of the sterility, pollen morphology was studied in the anthers at different stages of development. Normal pollen mother cells undergo meiosis at stage 6 within a locule and are surrounded by a layer of tapetal cells. At stage 7, meiosis is complete, resulting in a tetrad of four haploid microspores. The microspores are released from the tetrad at stage 8 followed by callose wall and tapetum degeneration through stages 10 and 11 (Twell, 1998; Sanders et al., 2000; Ma, 2005).

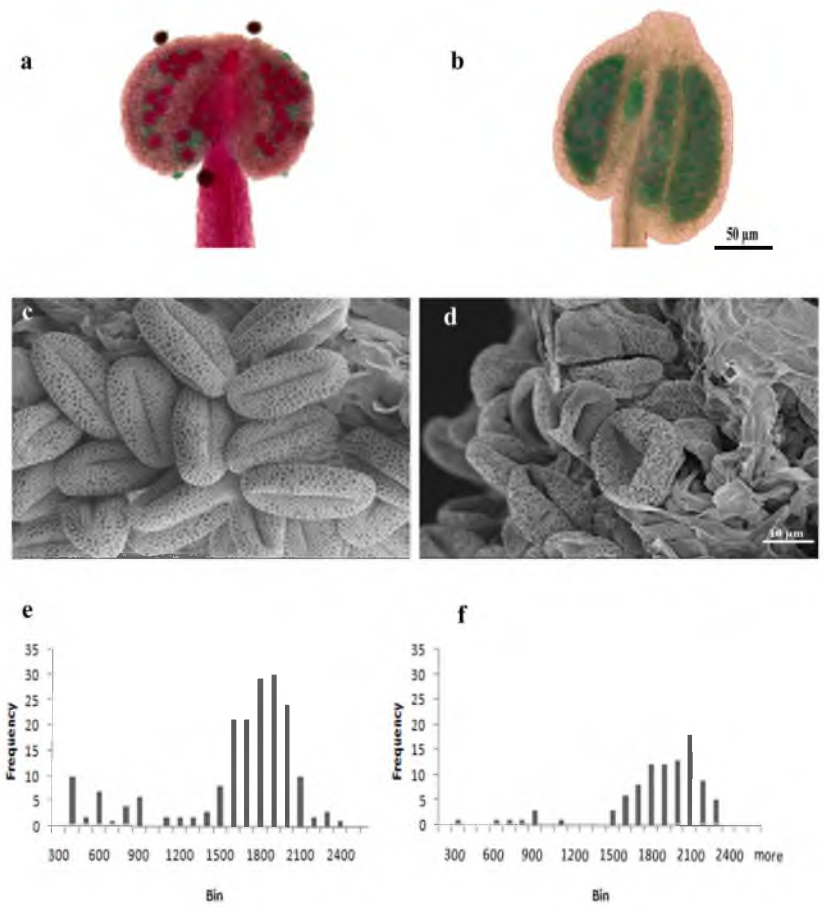


**Fig. 5.3: Pollen morphology of L*er* wild type** (left) and *xrs4* mutant (right). (a-b) Alexander stained pollen from mature anthers that stain deep red when viable and green when non-viable; (c-d) Scanning electron microscopy images of mature pollen grains at 2000x magnification shows shrunken and dead pollen in *xrs4*, Scale bar = 10µm; (e-f) Pollen size range distribution using SASS stained pollen grains.

Microspores of the *xrs4* mutant occasionally showed no nuclear staining indicating that such cells were already anucleate. The microspores contained darkly stained split vacuoles that occupied most of the cell space surrounded by the nuclear material (Fig. 5.4b). In wild type, a single large vacuole develops in the microspore immediately before division at pollen mitosis I (Fig. 5.4a). Pollen mitosis occurs at stage 12 during which the nucleus moves to the poles and undergoes an asymmetric division producing tricellular haploid pollen with two sperm nuclei and a vegetative nucleus. The large vacuole normally disintegrates in wildtype mature pollen (Fig. 5.4c). In contrast, large multiple

vacuoles persisted in *xrs4* mature pollen (Fig. 5.4d) suggesting that the cells were arrested at this stage.

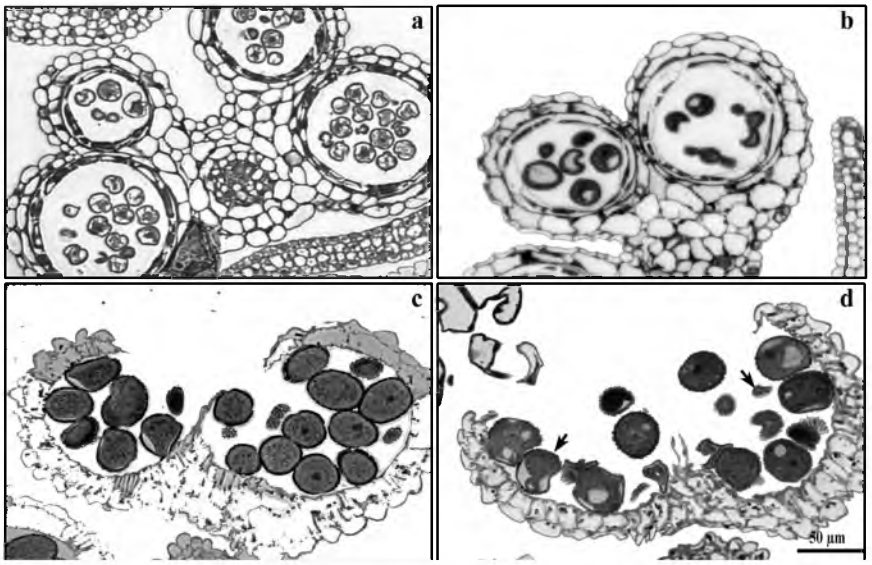


**Fig. 5.4: Post-meiotic development and pollen mitosis** in L*er* wild type (a,c) and *xrs4* mutant (b,d). Light microscopy sections of anther primordial cells of stage 8 microspores in 0.6-0.8mm buds (a-b) and stage 12 mature pollen in 1.0-1.2mm buds (c,d), Scale bar = 50µm. Arrow indicates a defective pollen

## Meiosis

In the *xrs4* mutant, the number of meiotic cells is greatly reduced. Progression is similar to the wildtype through the prophase-I stages leptotene, zygotene, pachytene and diplotene. The most predominant stages found in meiotic materials were pachytene, metaphase-I and tetrads. Chromosome pairing during the pachytene stage is normal (Fig. 5.5c) and no univalents are seen during diakinesis or metaphase-I (Fig. 5.5e-g). Bivalents at diakinesis and metaphase-I clearly display an aberrant morphology, with chiasmata in general closer to the centromeres, and often clumping together, while not clearly orienting to the spindle in a single plane as in the wildtype (Fig. 5.5g). Aberrant chromosome segregation was observed in the dyad stage (Fig. 5.5i) but the most striking defect is seen in meiosis-II. The haploid chromosome distribution is disturbed in the mutant resulting in triads, tetrads with bridges and polyads (Fig. 5.5l). Pollen mother cells at meiosis-II often displayed missegregation of chromatids that may result in defective tetrad formation.

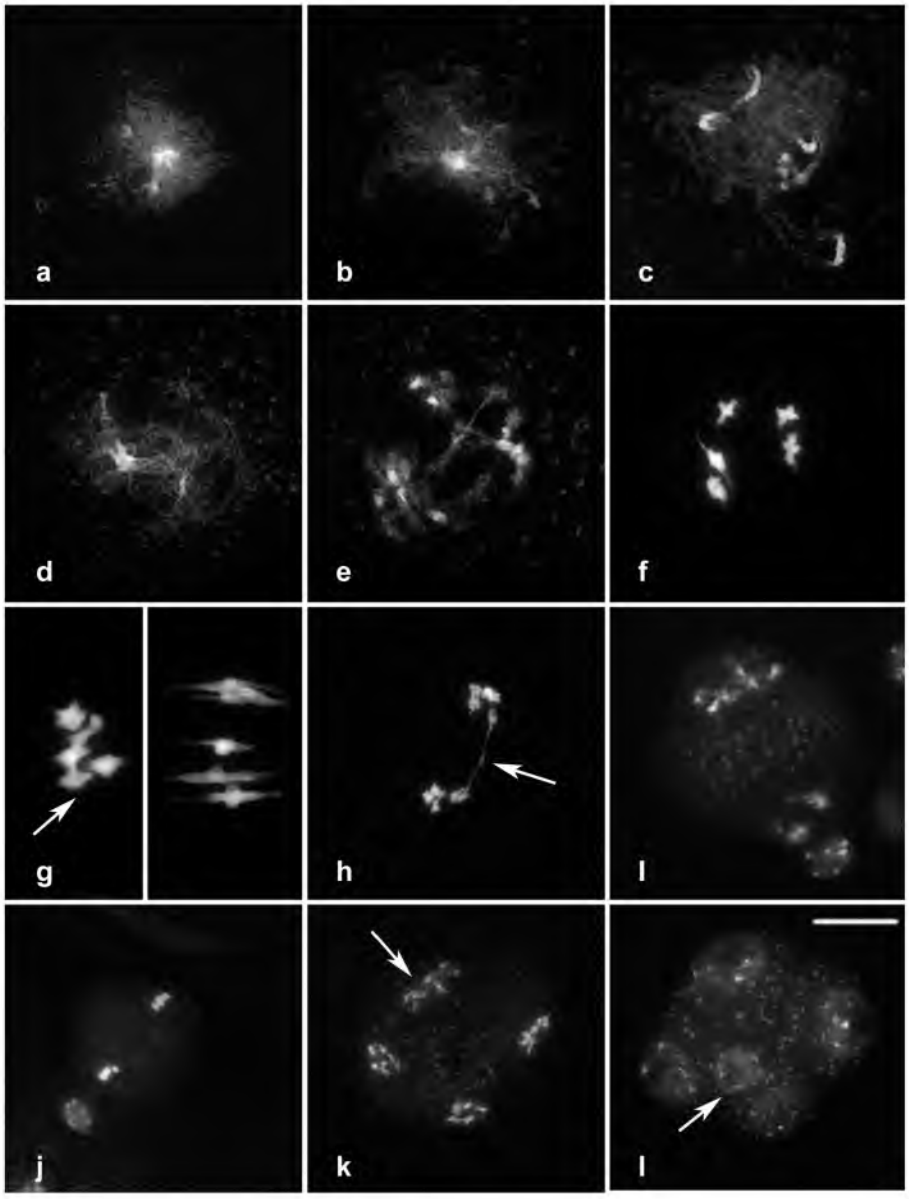


**Fig. 5.5: Meiotic progression in xrs4 mutant**
**a-b** Early prophase-I, **c** pachytene, **d** diplotene, **e-f** diakinesis, **g** metaphase-I in xrs4 (left) and Ler (right), **h** anaphase-I with chromosome bridges, **i** dyad showing unequal distribution of homologs, **j** metaphase-II, **k** anaphase-II with unequal distribution of sister chromatids, **l** defective tetrad formation resulting in polyads, scale bar = 10 µm, arrows point to chromosomal aberrations.

### Meiotic recombination frequency is not altered in the *xrs4* mutant

Analysis of recombination frequencies (RF) in GFP/RFP intervals on chromosomes 1, 3 and 5 was only successful for chromosome 3.

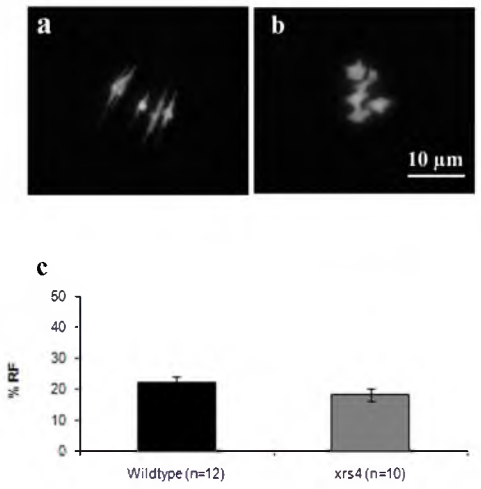


**Fig. 5.6: Effect of xrs4 on meiotic recombination a)** Comparison of bivalent morphology between Ler (left) and xrs4 (right) **b)** A comparison of recombination frequencies (RF) between wild type and xrs4 mutant plants in chromosome 3a interval of Arabidopsis; scale bar = 10 µm; n = number of plants analyzed; Error bars indicate standard error.

Due to (partial) sterility of the *xrs4* mutant many of the crosses performed to study RF failed. *xrs4* mutants homozygous for the *er* locus had anthers with varying degrees of pollen fertility. Crosses to the male sterile *dde1* mutant were relatively more successful than with *xrs4* mutants in an *ER* background. The RF was measured in BC1F1 seeds of twelve wild-type (1573 seeds) and ten *xrs4*-mutants (1024 seeds) plants. The average RF was 17 cM in *xrs4* compared to 21 cM in the wildtype plants (Fig. 5.6a). RF varied over a wide range in the mutant with a variance of 44.3. The population means (p-value = 0.04209, one-way ANOVA) and variance (p-value = 0.0075, Levene's homogeneity of variance test) were significantly different.

**Genetic mapping of xrs4**

The *xrs4* mutant was first mapped using a small set of 24 *xrs4* mutants that were phenotypically selected from an F2 mapping population. Ten AFLP primer combinations, containing a total of 88 markers that are well distributed across the 5 chromosomes, were performed. This analysis placed the XRS4 locus in the top arm of chromosome 5, with two flanking markers spanning a 3.6 Mb region. Another 156 mutant individuals were subsequently analyzed with the flanking and internal markers and the *xrs4* region was further delimited to 499 kb between AFLP markers SM247_252 situated at position 979,129 bp and SM61_268 at position 1,477,827 bp. Fine mapping of *xrs4* was continued with InDel and SNP markers on a population of about 1800 F2 individuals. The gene carrying the *xrs4* mutation was localized in a 62.5 kb region between SNP markers 1182032 and 478978 at positions 1,182,032 bp and 1,244,493 bp, respectively. Thus the genetic region containing the *xrs*4 locus was narrowed down to a 62.5 kb window on BAC T19N18 (Fig. 5.7B).

### Candidate genes for *xrs4*

We identified eighteen putative candidate genes in the region harbouring the *xrs4* mutation (Table 5.3). Three of these have previously been characterized: AT5G04275/ *miR172* a microRNA involved in flower development (Zhao et al., 2007), AT5G04360/ATPU1 involved in starch degradation (Delatte et al., 2006) and AT5G04340/ ZAT6, a C2H2 zinc finger which regulates Pi status of the plant and is involved in nutrition and development (Devaiah et al., 2007). For the remaining fifteen genes the available T-DNA insertion lines were examined for mutant phenotypes, while their microarray expression data were analyzed as well.

**Table 5.3:** Information on the genes in the 65.5 kb region narrowed down by map-based cloning

| Sl. No. | Gene Locus | Chromosomal Location (bp) | Description |
|---|---|---|---|
| 1 | AT5G04267 | 1182164 - 1182295 | Unknown protein |
| 2 | AT5G04270 | 1182719 - 1184766 | Zinc ion binding protein, similar to DHHC type zinc finger. The presence of the DHHC domain suggests an important function in the cell. |
| 3 | AT5G04275 | 1188212-1188300 | Encodes a microRNA involved in flower development and meristem determinacy, targets several genes containing AP2 domains including AP2. |
| 4 | AT5G04280 | 1192275-1195663 | Zinc finger-containing RNA-binding proteins. Exhibits an RNA chaperone activity during the cold adaptation process |
| 5 | AT5G04290 | 1196070-1202654 | KOW domain-containing transcription factor family protein. The KOW domain is the mediator between NusG proteins (involved in transcription termination) and ribosomal proteins. |
| 6 | AT5G04310 | 1203204 - 1207353 | Pectate lyase family protein; similar to PMR6 (POWDERY MILDEW RESISTANT 6), suggesting a pectin degrading activity for PMR6, which is what alters the cell wall's composition. |
| 7 | AT5G04320 | 1209198 - 1212577 | Unknown protein, contains InterPro Shugoshin C-terminal domain. |

| Sl. No. | Gene Locus | Chromosomal Location (bp) | Description |
|---|---|---|---|
| 8 | AT5G04330 | 1212603 - 1214440 | Cytochrome P450, similar to FAH1 (FERULATE-5-HYDROXYLASE 1), catalyzes reactions of the general phenylpropanoid pathway. The products of the general phenylpropanoid pathway are critical to plant survival and include UV- absorptive plant secondary metabolites and lignin. |
| 9 | AT5G04340 | 1216132 - 1217107 | ZAT6, a zinc finger transcription factor that is responsive to phosphor stress and a repressor of primary root growth. |
| 10 | AT5G04347 | 1219878 - 1220270 | Similar to self-incompatibility protein-related, AT5G04350, contains InterPro domain Plant self-incompatibility S1. |
| 11 | AT5G04350 | 1220830-1221270 | Self-incompatibility S1 protein-related, involved in self-incompatibility. |
| 12 | AT5G04360 | 1203204 - 1207353 | ATPU1, encodes an enzyme thought to be involved in the hydrolysis of the a-1, 6 linkages during starch degradation in seed endosperm. Located in the chloroplast. |
| 13 | AT5G04370 | 1231698-1234148; 1231752-1234148 | NAMT1, a member of the Arabidopsis SABATH methyltransferase gene family, a gene family coding for methyltransferases and zinc fingers. |
| 14 | AT5G04380 | 1234884 - 1236318 | S-adenosyl-L-methionine: carboxyl methyltransferase family protein, similar to NAMT1 (AT5G04370), contains InterPro domain SAM dependent carboxyl methyltransferase. |
| 15 | AT5G04386 | 1238104 - 1238220 | Unknown protein. |
| 16 | AT5G04390 | 1239101-1240518 | Zinc finger (C2H2 type) family protein. The A. thaliana zinc finger proteins are known to be involved in transcriptional regulation. |
| 17 | AT5G04400 | 1241556 - 1243359 | ANAC077 transcription factor, No apical meristem (NAM) protein, Mutated NAM genes fail to form shoot apical meristems indicating that NAM plays a role in determining the position of the shoot apical meristem and primordia in this plant. |

| Sl. No. | Gene Locus | Chromosomal Location (bp) | Description |
|---|---|---|---|
| 18 | AT5G04410 | 1243759-1246685 | NAC2/ ANAC078 NAC family member, hypothetical transcriptional regulator comparable to AT5G04400. |

T-DNA lines of the candidate genes were selected to see if any one of their corresponding mutant phenotypes resembled the *xrs4* phenotype. Appropriate T-DNA lines were not available for three genes, namely AT5G04267, AT5G04390 and AT5G04400 while only GABI-KAT lines were available for AT5G04347 and AT5G04386. T-DNA insertion lines were selected within the ten remaining genes. We found mutants in the homozygous state that disrupted the coding region of genes AT5G04280, AT5G04330, AT5G04310, AT5G04410, AT5G04290, AT5G04380 and in the 5' UTR of AT5G04320 and AT5G04270. Only one of these mutants (SAIL_1149_C06) corresponding to AT5G04310, a putative pectate lyase, had a phenotype. Most mutants did not survive and the only escape mutant we found had flowers in which the four pollen grains remained attached to each other, similar to other *quartet* (qrt) mutants. Mutant seeds failed to germinate and the mutant thus could not be maintained as a homozygous line. In *qrt* mutants, failure to degrade pectin components leaves the pollen tetrad intact (Preuss et al., 1994; Copenhaver et al., 1998, Rhee and Somerville, 1998). Mutant alleles of AT5G04370 (SAIL_300_D11, and SALK_001690) were lethal indicating that this putative methyltransferase represents an essential function. None of the mutants that have been screened so far exhibited an *xrs4*-like phenotype.

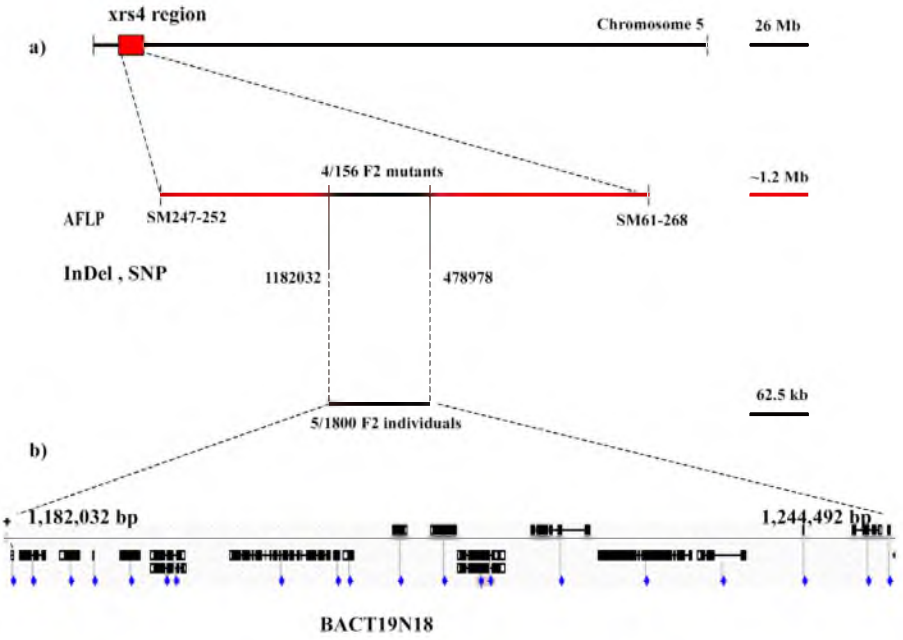


**Fig. 5.7: Fine mapping of *xrs4* A.** The AFLP analysis of 156 F2 mutants gave 4 recombinants and defines the mutation to a 499 kb region between marker SM247_252.1 (979,129 bp) and SM61_268.4 (1,477,827 bp). Additional screens showed 5 recombinants amongst 1800 F2 plants with InDel and SNP PCR markers to further delimits the gene to a 62.5 kb region between SNP markers 1182032 and 478978 at positions 1,182,032 bp and 1,244,493 bp. **B**. The region of BAC T19N18 that contains the 18 genes and their splice variants

**Expression analysis**

Analysis of the expression patterns of the 18 genes in Genvestigator (https://www.genevestigator.ethz.ch) showed that 13 of them were present on the Arabidopsis microarray chip ATH22K (Fig. 5.8). The genes AT5G04340, AT5G04380, AT5G04390 and AT5G04290 are not significantly expressed in male meiocytes while high expression was indicated for genes AT5G04410, AT5G04320, AT5G04360, AT5G04300 and AT5G04280 (ontology term: sperm cell). AT5G04390 expression is high in pollen. RT-PCR of AT5G04310 (PLL12) shows that this gene is expressed in roots, stems, leaves and flowers (Palusa et al., 2007).

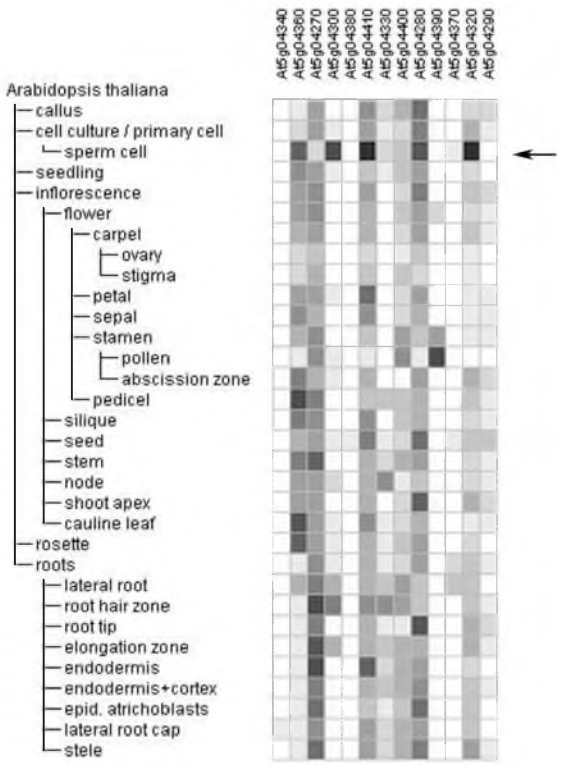


**Fig. 5.8: Genevestigator microarray expression data for nine genes in the different parts of the Arabidopsis plant**. Arabidopsis 22k array was selected. Color code: dark to light colors are normalized to the maximum value (the darkest color corresponds to the maximum value of an expression vector.

### At5g04320

The *xrs4* mutant's chromosome segregation defect in meiosis warrants a close examination of the candidate At5g04320. Computational identification of At5g04320 homologs reveals that it belongs to the shugoshin (SGO) family. SGOs play an important role in chromosome segregation (Yamagishi et al., 2008) and are conserved only in their N-terminal and C-terminal regions. There are 2 shugoshin-like genes in all species, analyzed so far, including Arabidopsis. These are AT3G10440 (SGO1) and At5g04320 (SGO2), neither of which has so far been characterized. T-DNA insertion lines disrupting the 5'UTR of At5g04320 were tested. All three mutants, FLAG_570B05, SALK_027486 and SALK_026139 were fertile and similar to wildtype. Insertion lines are not available within the coding regions of neither SGO1 nor SGO2.

Sequencing of the At5g04320 region including its promoter region, covering 1500bp in L*er*, and *xrs4* (see Materials and Methods) revealed no differences between the sequences. The gene has 15 exons and 14 introns. The L*er* and Col-0 sequence for At5g04320 (TAIR: http://www.arabidopsis.org)

share 95% identity at the nucleotide level and 98% identity at the protein level. Alternative splice sites are predicted with three possible mRNA transcripts for this gene (Aceview **http://www.ncbi.nlm.nih.gov/IEB/Research/Acembly/**).

**5.4 Discussion**

The highly reduced fertility, hypersensitivity to X-rays and DNA-damaging agents and the reported alterations in mitotic/meiotic recombination properties of *xrs4*, are in agreement with some of the universal characteristics of mutants of the RAD52 epistatic group. However, the converse influence of *xrs4* on mitotic and meiotic recombination warrants a detailed characterization of the mutant and the underlying gene.

A morphological characterization of the *xrs4* mutant revealed the nature of the mutant defects. The mutant grew slowly with reduced plant organ size and was late flowering. The plants flowered for a significantly longer period characteristic of sterile mutants (Garcia et al., 2003). We tracked different stages of pollen formation in *xrs4* and found that the first defects appear late in meiosis-I. The first detectable phenotype is that the bivalents do not align properly at the metaphase-I plate, indicating that chromosome movement at early metaphase-I is affected. In addition, homolog separation is asynchronous and unequal in meiosis-II leading to the formation of imbalanced tetrads. The penetrance of the defect was only partial and surviving microspores continued into gametogenesis. Defective pollen mitosis resulted in anucleate apoptotic cells and cells with persistent large vacuoles. There seems to be a disruption of the mechanisms required to position the microspore nucleus to allow correct nuclear division in pollen mitosis-I of gametogenesis. However, at least 40% of the pollen developed normally and were fully capable of fertilizing wildtype ovules. Even after fertilization, some of the embryos were anucleate and aborted very early, resulting in a highly reduced seed set, close to 10% of the wildtype. The *xrs4* mutant therefore showed pleiotropic developmental defects related to meiosis, pollen mitosis and embryo development.

Earlier mapping efforts (Masson et al., 1997b) placed xrs4 on chromosome 4. We mapped the *xrs4* mutation to the top of chromosome 5 in a 62 kb region between positions 1182 and 1244 kb that harbors eighteen genes. Taking leads from published gene information, publicly available microarray expression profile data and our T-DNA screening we could eliminate nine genes - AT5G04275, AT5G04360, AT5G04340, AT5G04280, AT5G04330, AT5G04310, AT5G04410, AT5G04290 and AT5G04380. Apart from these the two mutant alleles of AT5G04370 were homozygous lethal proving that this is an essential gene. However, we cannot verify if *xrs4* (knock down) and this lethal mutant (knock out) correspond to one and the same gene: *xrs4* is an EMS mutant. EMS generally induces point mutations resulting in weak non-lethal alleles of

altered or reduced function. We were not able to find appropriate T-DNA lines for some genes and mutants remain to be generated by alternative methods like RNAi or TILLING for AT5G04320, AT5G04390, AT5G04400 and AT5G04270.

Putative changes in RF, due to mutant *xrs4* allele, were measured within a small interval on chromosome 3. The overall RF was not altered in the mutant compared to the wildtype but a large plant-to-plant variation was observed. Masson and Paszkowski, (1997) report a significant increase in RF for *xrs4*. One possible explanation for this difference is a probable change in CO position in these mutants. In *C. elegans* the *rec-1* mutant shows such a shift in crossover position from telomeres to the middle of the chromosome (Zetka and Rose, 1995) without affecting the overall number of COs. To gain more clarity of how recombination is altered in *xrs4*, crossover distribution needs to be estimated genome-wide or across several intervals of a chromosome.

AT5G04320, the putative shugoshin homolog, seems to be the most probable *xrs4* candidate. Sequencing the gene region of the mutant *xrs4* allele did not yet show any differences compared to wild type. The meiotic chromosome segregation defects are similar to those reported for mutants of *shugoshin* homologs in maize and yeast, suggesting a conserved role for this gene in chromosome segregation. Shugoshin functions as a protector of centromeric cohesin during meiosis in yeast (Kitajima, et al., 2004; Rabitsch et al., 2004) and maize (Hamant et al., 2005) and during mitosis in higher eukaryotes (Salic et al., 2004; Katis et al., 2004)). In maize *ZmSGO1* localizes to centromeres and pericentric heterochromatin during meiosis I. The protein is expressed from leptotene to diakinesis in M-I but not in M-II. The mutant *Zmsgo1* exhibits sterility and meiotic defects in which centromeric cohesion is released precociously before metaphase II. Recombination was not altered in SGO mutants reported so far. In yeast, deletion of *SGO1* did not have a global effect on homologous recombination, although it leads to an increase in spontaneous Rad52-YFP Foci (Alvaro et al., 2007). Both *xrs4* and *SGO* play a role in mitosis. It has been shown in yeast and mouse that SGO1 and SGO2 are components of the kinetochore microtubule tension-sensing machinery, which is active during meiosis II and mitosis. SGO depletion can activate the spindle checkpoint and induce mitotic arrest. Verification of the *SGO* mutant phenotype has proved to be difficult. The three T-DNA mutant alleles available for AT5G04320 were all disrupted in the 5' UTR region and had a normal phenotype. A mutant that disrupts the coding region remains to be tested. Two splice variants have been predicted for the gene. In *Arabidopsis,* over 20% of genes are known to undergo alternative splicing to produce two or more transcripts (Wang & Brendel, 2006). Different transcripts of *SGO* orthologs are produced by alternate splicing in *Mei-S332* of Drosophila (Kerrebrock et al., 1995), and *SGO1* of mouse and human

cells (McGuinness et al., 2005). All these evidences suggest a role for this gene in both meiosis and mitosis, making it in itself interesting for further characterization.

**Future work**

From the characterization of *xrs4* we have established that the mutant exhibits defects in both meiosis and mitosis. Many of the genes in the fine-mapped region on chromosome 5 are predicted to play a role in cell division and are active in meristematic tissues (Table 5.3). Nine genes remain to be screened by mutagenesis approaches like TILLING, T-DNA insertions or RNAi for genes *AT5G04320, AT5G04267, AT5G04270, AT5G04347, AT5G04350, AT5G04370, AT5G04390, AT5G04400* and *AT5G04386*. Sequencing and complementation remains to be tested within prioritized genes *AT5G04400, AT5G04370* and *AT5G04390*. In addition, examination of centromere cohesion by immunostaining and FISH analysis will help to further establish the nature of the meiotic defect in *xrs4*.

# Chapter 6

## Effect of *atmlh3* on crossover frequency and the expression of its promoter in germline cells

**Abstract**

DNA mismatch repair (MMR) is mediated by MutS and MutL proteins. In Arabidopsis, the MutL homologs AtMLH1 and AtMLH3 promote meiotic crossover (CO). The aim of this study is to understand the role of MLH3 during meiosis in Arabidopsis. The effect of the AtMLH3 gene on recombination frequency was tested by measuring RF in the mlh3 mutant. We found a significant reduction of recombination rates of 68% in the chromosome 3 GFP-RFP interval but a much smaller decrease of 30% in the chromosome 5 interval. The MutS proteins affect CO formation more than MutL as we see a 79 % reduction of COs in Atmsh5 compared to 32% in Atmlh3. The confinement of AtMLH3 expression to reproductively active tissue is attractive to test for germ-line specific expression of its promoter. Using transgenic pMLH3-GUS plants we examined the detailed expression pattern of the AtMLH3 gene. Floral meristematic tissue and meiotically active anthers showed high expression that was gradually reduced in older buds. No expression was seen in 2-week-old seedlings, roots, leaves and mature flowers.

## 6.1 Introduction

DNA mismatch repair (MMR) is responsible for post-replicative DNA repair and is conserved in all organisms. The key protein groups involved include the MutS proteins MSH4 and MSH5 that bind to mismatched DNA, MutH endonucleases, found only in prokaryotes so far, that nick the newly synthesized strand, and the MutL proteins MLH1, MLH3, PMS1 that help MutH to interact with MutS (reviewed by Jiricny, 2000). The MutL proteins form heterodimers interacting with two to four proteins but always require MLH1 for the interaction. From studies in yeast we know that the MLH1-PMS1 heterodimer participates in mismatch correction during mitosis and meiosis while MLH1-MLH3 promote meiotic crossover (CO). Their time of action in the cell cycle correlates well with the changes in expression of their corresponding genes (Wang et al., 1999). MLH1 is required for 90-95% of COs in mouse (Guillon et al., 2005) compared to 30-35% of CO in yeast (Hunter and Borts, 1997). In *Arabidopsis*, the three MutL homologs identified so far include AtPMS1, AtMLH1 and AtMLH3. AtPMS1 is required for microsatellite stability during mismatch repair (Alou et al., 2004). AtMLH1 corrects errors and prevents recombination between divergent sequences during mitotic recombination (Dion et al., 2007). AtMLH3 is required for CO stability in meiotic recombination and the absence of AtMLH3 delays prophase-I progression and results in a 60% reduction of crossovers (Jackson et al., 2006). Chiasma frequencies in the At*mlh3* mutant follow a binomial distribution supporting a model where the sites designated for CO could resolve as CO or non-crossover (NCO) (Higgins et al., 2006).

The MLH1 and MLH3 proteins co-localize from middle to late pachytene of meiotic prophase and participate in CO formation (Franklin et al., 2006; Guillon et al., 2005; Marcon and Moens, 2003). RT-PCR data (Jackson et al., 2006) reveals that *AtMLH3* is expressed in buds but not in leaves and stem unlike *AtMLH1*, which is expressed constitutively. These data suggest that AtMLH3 might be specifically expressed in germline cells. A number of promoters have been tested for germ-line specific expression including promoters of *AtSDS1*, *APETALA1* and *AtSUPERMAN* (Verweire et al, 2007). Among the promoters characterized from genes functioning at various stages of pollen development, expression of *AtDMC1* (Klimyuk and Jones et al., 1997), *AtSDS1* (Azumi et al., 2002) and *AtMEI1* (Kaur et al., 2006) are found in meiocytes but are also not entirely meiosis specific. The promoter of *AtSDS1* is expressed in carpels and stamens of young flower buds in stages 4-10 (Smith et al., 1990) as well as in shoot and root tips (Verweire et al, 2007). The confinement of *AtMLH3* expression to reproductively active tissue is attractive to test for germ-line specific expression of its promoter.

The aim of this study is to understand the role of *MLH3* during meiosis in Arabidopsis. We investigated the expression pattern of *AtMLH3* promoter in different tissues to test its suitability as a meiosis/germline specific promoter. In addition, we compared the recombination frequency (RF) in two genetic intervals between *Atmlh3* mutant, the heterozygote and its wild type to understand its role in crossing-over. In chapter 3 a comparison of the RFs with other meiotic genes was presented as well.

## 6.2 Materials and Methods

### Plant material and growth conditions

*Arabidopsis thaliana* ecotype Columbia-0 (Col-0), male sterile *delayed dehiscence 1* (*dde1*) (Sanders et al., 2000) and two T-DNA insertion lines in gene AT4G35520, SALK_015849 (*Atmlh3*-1) and SALK_041465 (*Atmlh3*-2), were used for the analysis. Seeds were surface sterilized with absolute ethanol and 1.5% NaOCl, respectively, and sown on half strength Murashige and Skoog medium without sucrose for germination. Seedlings were transferred after 14 days to a soil-based mix. Plants were grown in a growth room at 23°C± 2°C under long-day conditions (16 h light/8 h dark).

### Genotyping of T-DNA lines for mlh3 mutants

T-DNA insertion lines *mlh3-1* and *mlh3-2* were obtained from the Nottingham Arabidopsis Stock Center (NASC). The T-DNA insert is located in exon 9 (*mlh3*-1) and exon 22 (*mlh3*-2) within the gene At4g35520. Both are null mutants as evidenced by the absence of the protein (Jackson et al., 2006). DNA

extraction was done as described in Cnudde et al. (2005). Genotyping was performed to identify homozygous mutants. The gene-specific primer pairs used for the analysis of *mlh3-1* were 5'-TTGATATCGAAAGGTGCGTTC-3' (forward) and 5'-CTTGTCTATCACCTTTTGCCAG-3' (reverse) and for *mlh3-2* were 5'-TGACATTAAAGGTACTGCCGG-3' (forward) and 5'-TCTCTGCGTTGTAAGCCATG-3' (reverse) along with the T-DNA left border specific primer LBa1 5'- TCACGTAGTGGGCCATCG -3 '.

***Meiotic Recombination***

Meiotic recombination was measured using a seed-based assay (Melamed-Bessudo et al, 2005) in which a pair of linked genes, expressing the green fluorescent protein (GFP) and red fluorescent protein (RFP), respectively, segregates upon a crossing over event between the genes. Pollen of tester lines C3 and C5 (described in Chapter 4) was used to fertilize *mlh3-1* and *mlh3-2* mutants. From the F2 population, plants homozygous for *MLH3* (wildtype) and heterozygous for GFP and RFP were selected. As we did not find mutants with the GFP/RFP markers in heterozygous state among the F2 individuals, the F1 was backcrossed to the *mlh3* mutant and GFP/RFP markers in heterozygous state were selected by PCR. The selected mutant and wild-type plants were backcrossed to the male sterile *dde1* mutant. The primary bolts of *dde1* were excised and flowers on the secondary and tertiary bolts were pollinated with flowers from the selected plants. The dried seeds of resulting siliques were used to compare the recombination frequency (RF) between the fluorescent visible markers in the mutant and wild-type genetic background.

***Generation of* pMLH3::GUS/GFP *transformants***

The promoter region spanning 1424 bp upstream of At4g35520 (AtMLH3) was amplified by PCR from genomic DNA along with the GATEWAY cloning sites attB1 and attB2, respectively. The primers used were: AtMLH3, sense 5′-aaaaagcaggctGATAGTCGGTTTTGATAGG-3′ and antisense 5′-agaaagctgggtCTCAGGATTATCGGACTG-3′. The adaptor containing fragments were cloned into the vector pKGWFS7.0 and the insertion of the promoter region was confirmed by partial sequencing. The resulting vectors consisted of the promoter in front of two reporter genes encoding GFP and GUS (egfp/uidA gene fusion). After mobilizing the constructs in *Agrobacterium tumefaciens*, *A. thaliana* Col-0 plants were transformed using the floral dip method (Clough and Bent, 1998). Transformants were screened for resistance to kanamycin (30μg/ml) and selected for analysis. The presence of the NPTII marker in the kanamycin resistant T1 plants was verified by PCR using NPTII-F 5'-GTCCCGCTCAGAAGAACT-3' and NPTII-R 5'-

GGCACAACAGACAATCGG-3' primers that corresponds to a 706 bp PCR fragment .

***Histochemical localization of GUS in transgenic plants***

Histochemical staining for GUS activity was done on tissue of T2 transformants treated with GUS staining buffer (0.1% Triton X-100, 2mM $Fe^{2+}CN$, 2mM $Fe^{3+}CN$, 1mM X-Gluc in 50 mM phosphate buffer, pH 7.0) for 24-48 h at 37°C. Bleaching was carried out in 70% ethanol at $25^{0}$C. The samples were observed under a Zeiss Axiovert 135 microscope using DIC optics.

## 6.3 Results

### The effect of the *MLH3* gene on recombination frequency

We used a seed-based assay (Melamed-Bessudo et al, 2005) to measure the RF between a pair of c*is*-linked GFP and RFP markers on chromosomes 3 and 5, respectively (see also chapter 4). The effect of the *MLH3* gene on RF was studied in two mutant alleles of *AtMLH3*. The RFs of the wild-type (+,+), heterozygous (+,-) and mutant (-,-) plants are shown in Fig. 6.1. The RF in the chromosome 3 interval for wildtype *AtMLH3* was 25cM, compared to 10cM in *Atmlh3-1*+/- and 9 cM in *Atmlh3-1*-/- Fig 6.1A. The RF was similarly reduced to 7 cM in both *Atmlh3-2*+/- and *Atmlh3-2*-/- Fig 6.1B. A t-test for *Atmlh3-1*, between wildtype and heterozygote (P-value = 0.00004), wildtype and mutant (P-value = 0.00038) showed a significant difference in RF means. A similar examination was done in the chromosome 5 interval. The *AtMLH3* wildtype RF was 19cM compared to 15cM in *Atmlh3-1*+/- and 11 cM in *Atmlh3-1-/-* Fig. 6.1 C. For the second mutant allele RF was 17 cM in *Atmlh3-2*+/- and 13 cM in *Atmlh3-2*-/- plants Fig. 6.1 D. A t-test for *Atmlh3-2*, between wildtype and heterozygote (P-value = 0.521), wildtype and mutant (P-value = 0.0702) showed a significant difference in the mean RF of only the mutant.

### Analysis of *AtMLH3* promoter expression

The 1424 bp promoter sequence upstream of *At4g35520* was cloned into the pKGWFS7.0 plasmid carrying the GUS-GFP fused coding regions and transformed into *Arabidopsis* Col-0 plants (Fig. 6.2A). Transformation success rate was higher in batches of siliques derived from young meiotic buds (data not shown). Twenty one pMLH3::GUS/GFP primary transformants were kanamycin resistant in a population of approximately 2500 T1 seedlings. Seventeen lines displaying kanamycin resistance were tested further and 15 of these also showed the nptII PCR product (Fig. 6.2B). T2 seeds from eight T1 events were scored for kanamycin sensitivity to identify those with single and multiple loci insertions (Table 6.1). The transformants pMLH3-1, -10 and -21 segregated in a

3(resistant): 1(sensitive) ratio for kanamycin, expected for single insertion events.

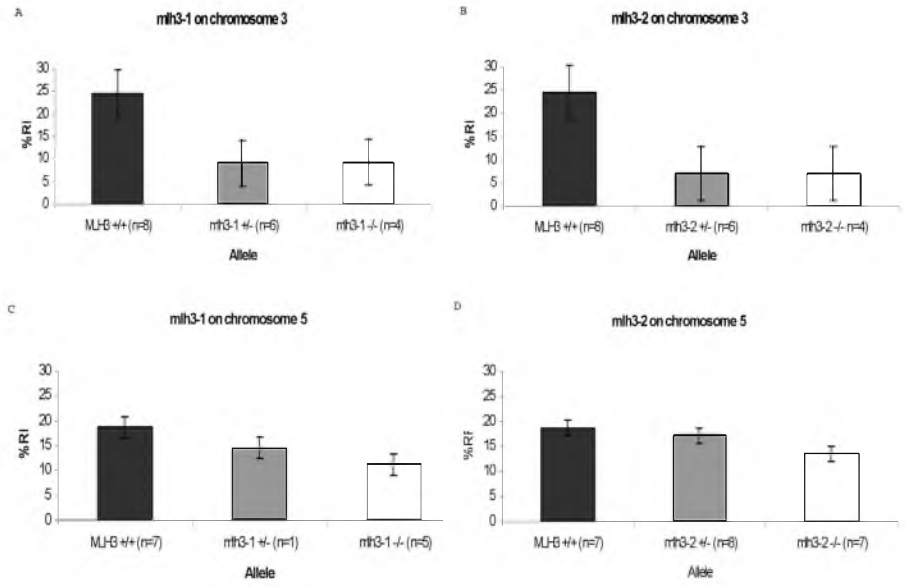


**Fig. 6.1: The effect of two mutant alleles of the *MLH3* gene on recombination frequency (RF).** RF within chromosomal intervals on chromosome 5 (A, B) and chromosome 3 (C, D) were compared between the wild type (black), heterozygous (gray) and mutant (white) plants. %RF was calculated as the ratio of total no. of recombinants to total no. of seeds analyzed x 100; n = the no. of individual plants analyzed, error bars indicate standard error (SE).

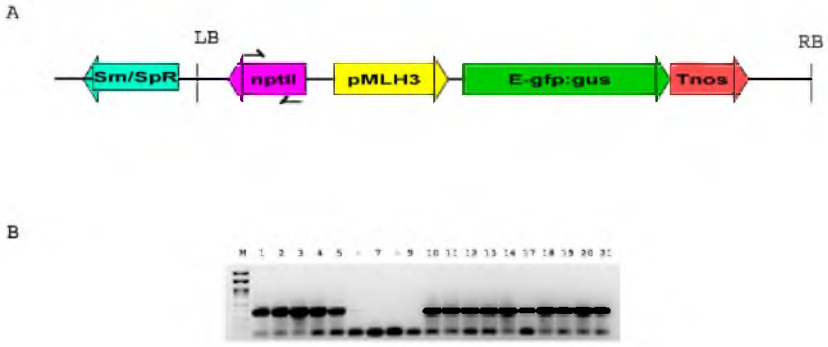


**Fig. 6.2 A. Schematic representation of the promoter construct transformed into Col-0 ecotype**. Sm/SpR-spectromycin/Spectinomycin resistance gene, nptII neomycin phosphotransferase gene for Kanamycin resistance, pMLH3-1500bp promoter of AtMLH3; E-gfp:gus –GFP and GUS fusion gene; Tnos- Nos terminator. **B.** Confirmation of transformation by PCR using nptII specific primers in T1 plants.

**Table 6.1:** Segregation of primary transformants on kanamycin selection medium

| T1 generation | Seeds sown | Seeds germinated | K (r) | K (s) | K(r/s) | $X^2$ (df = 1) |
|---|---|---|---|---|---|---|
| pMLH3-1 | 28 | 28 | 23 | 5 | 4.6 | 0.76 |
| pMLH3-3 | 35 | 33 | 11 | 22 | 0.5 | 30.53 |
| pMLH3-10 | 28 | 27 | 20 | 7 | 2.9 | 0.003 |
| pMLH3-13 | 20 | 17 | 17 | 0 | - | 1.41 |
| pMLH3-17 | 44 | 41 | 26 | 15 | 1.7 | 2.93 |
| pMLH3-18 | 25 | 25 | 25 | 0 | - | 8.33 |
| pMLH3-19 | 39 | 39 | 32 | 7 | 4.6 | 1.02 |
| pMLH3-21 | 32 | 32 | 25 | 7 | 3.6 | 0.16 |

K (r) is kanamycin-resistant plants
K (s) is kanamycin-sensitive plants
K(r/s) is ratio of kanamycin-resistant to kanamycin-sensitive plants
$X^2$ is the chi-square value that fits 3:1 segregation for a single insertion event

### Tissue-specificity of the pMLH3 driven GUS expression

Out of the 21 primary transformant lines tested, no GUS activity was found in lines pMLH3-1 and -17. Events pMLH3-3, -10, -13, -18, -19 and -21 were analyzed for stable GUS expression in the T2 generation. For all tested transformants, we consistently found no expression of the GUS reporter in the seedlings, leaves and roots (Fig. 6.3A). Expression of GUS was highest in the young buds, progressively decreased in older buds containing mature pollen and was absent in opened flowers. Within the young buds, GUS accumulated in the anthers (Fig 6.3A). Dissection of the bud revealed that the GUS activity was confined to the pollen mother cells within anthers (Fig. 6.3B). However, GUS expression was not seen in the pistils of even the highest GUS-expressing lines like pMLH3 -18 and -19.

## 6.4 Discussion

The goal of our project was to examine recombination frequency in the CO pathway mutant *Atmlh3* and to initiate the isolation and characterization of a meiosis-specific promoter.

### AtMLH3 is crucial for class-I crossovers

We found a significant reduction of recombination rates of 68% in the chromosome 3 GFP-RFP interval (see Chapter 4) but a much smaller decrease of 30% in the chromosome 5 interval. Strikingly, the recombination frequency within the chromosome 3 region is reduced in both *mlh3*+/- and *mlh3*-/- lines. The average RF for *mlh3*-/- is 6cM; *mlh3* +/- is 5cM and WT is 25cM. The

reason why the two intervals are affected to a different extent in this mutant is not clear. Furthermore, a phenotype where the heterozygote is affected in meiotic recombination to a similar extent as the mutant has not been reported before. The possibility that the double holliday junctions (dHJs) are likely to be resolved as non-crossovers, in the absence of *AtMLH3*, needs to be tested. One possible explanation is that haploinsufficiency in *AtMLH3* +/- leads to lower amounts of the protein resulting in reduced CO. This phenomenon has been reported, where lower level of BRCA2 protein in the heterozygous carrier *BRCA2* +/-, is correlated with an increase in DNA double strand breaks and an impaired DSB repair (Arnold et al., 2006).

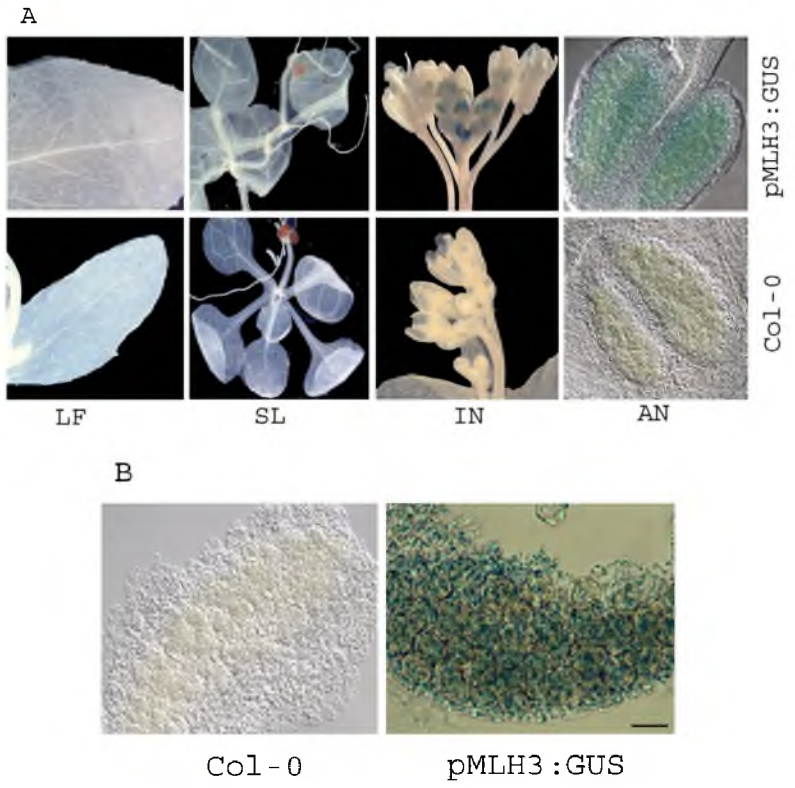


**Fig. 6.3: Histochemical GUS staining in Col-0 control (bottom) and *pMLH3*-reporter transgenic (top) plants**. A. The images shown are representative for all transgenic events studied. LF= Leaf, SL= Seedling, IN = Inflorescence, AN = Stage 9 anther; Scale bar =1mm B. Examination of microspores of GUS stained control (Col-0) and p*MLH3*-reporter transgenic plants by DIC microscopy. Scale bar =50µm.

**MutS affects CO formation more than MutL in *Arabidopsis***

Mismatch repair (MMR) involving MutS and MutL proteins is conserved across species. The disruption of MutS genes like *AtMSH5* and *AtMSH4* reduces seed set to 3.5 seeds/silique (Higgins et al., 2004; Higgins et al., 2008) while disruption of *MutL* genes reduces seed set to 9 seeds/silique in *Atmlh1* (Dion et

al., 2007) and only by 50% in *Atmlh3* with 23.8 seeds/silique. Thus in Arabidopsis, there seems to be a greater fertility defect with the loss of *MutS* compared to *MutL* genes. A comparison of the RF within the chromosome 5 interval between the two mutants At*msh5* and At*mlh3* reveals more. An average RF of 4cM in *Atmsh5* and 13cM in *Atmlh3* was seen compared to 19cM in the Col-0 wildtype. This reflects a 79 % reduction of crossovers in *Atmsh5* compared to 32% in *Atmlh3*. The drastic reduction in RF for *Atmsh5* was consistent across a second interval on chromosome 1. However, the *Atmlh3* mutant showed a much greater RF reduction of 67% in the chromosome 3 region compared with what was observed for chromosome 5 of the same mutant. The reduction in recombination in *Atmlh3* is different across the two intervals of the genome but recombination in general seems to be affected less when compared to At*msh5*, implying the different roles of the *MutL* and *MutS* homologs during meiotic recombination. This suggests that *MSH5* is critical for CO formation while *MLH3* might be required to maintain the dHJ configuration along with *MLH1* for resolution of the dHJ to COs. Meiotic recombination frequency has so far not been tested in *Atmlh1* mutants. *MLH3* together with *MLH1* accounts for ~85-90% interference-sensitive COs in mouse (Svetlanov et al., 2008). The interference-insensitive *Mus81* pathway possibly generates the remaining 15% of the COs. This implies that at least 1/4$^{th}$ of the residual 40% CO activity seen in *Atmlh3,* is generated by an unknown pathway. *AtMLH3* might be responsible for creating positive-interference during CO formation. The contribution of *Mus81* pathway for CO is known to vary between genomic intervals (De Los Santos et al., 2003) and its contribution might be greater in the absence of *MLH3*. Alternatively, plants might have other ways to cope with aberrant meiosis and the function of *MLH3* might be partially taken over by another protein. In yeast, the *Mlh1-Mlh3* heterodimer complex is specifically involved in meiotic recombination as evidenced by yeast 2 hybrid and co-immunoprecipitation studies (Wang et al., 1999). During meiosis the Mlh1-Mlh3 heterodimer complex stabilizes a limited number of late recombination nodule sites to facilitate crossing over, while the other sites are repaired to result in non-crossovers.

***p*MLH3 *driven* GUS *expression is germline-specific***

Earlier studies have shown the timing of expression of the MMR genes in Arabidopsis. *AtMSH4* and *AtMSH5* colocalize at leptotene (Higgins et al., 2008) followed by *AtMLH3* that appear at early zygotene and persist until late pachytene. AtMLH1 marks the sites of CO in an MLH3-dependent manner (Franklin et al., 2006). We already know that the expression of AtMSH4, AtMSH5 and AtMLH1 is not exclusive to meiosis. We looked at the specificity of expression of the *AtMLH3* promoter in various tissues to test its suitability as a germline-specific promoter. Transgenic *Arabidopsis* plants harboring *AtMLH3*

promoter and the reporter gene β-glucuronidase (p*MLH3-GUS*) were used to study the detailed expression pattern of the *AtMLH3* gene. Expression was highest in floral meristematic tissue and in meiotically active anthers of developing buds and lower in older buds. No expression was seen in 2-week-old seedlings, roots, leaves and mature flowers. AtMLH3 is a meiosis specific protein that is active is dividing reproductive cells and during meiotic CO and must be expressed during both male and female meiosis. However, unlike the pollen mother cells (PMCs) of the anthers, during female megasporogenesis, only one of the four meiotic products (megaspores) survives (Siddiqi et al., 2001). The timing of meiosis is also different- meiosis in embryo sac mother cells (EMCs) initiates when the PMCs reach the tetrad stage (Armstrong and Jones, 2001). In addition, genome-wide expression analysis of *AtMLH3* sourced from NCBI *Aceview database* (www.ncbi.nlm.nih.gov/*AceView*), indicates that *AtMLH3* is expressed at a low level corresponding to only 6.3% of the average gene expression (Thierry-Mieg and Thierry-Mieg, 2006). This makes it difficult to precisely follow low levels of expression visually during female meiosis. The low level of p*MLH3* driven *GUS* expression seen only in the pollen mother cells might indicate that the native gene is expressed at very low levels in the cell during meiosis or that the promoter lacks the enhancer elements necessary for strong expression.

*AtMLH3* appears to be meiosis-specific in its function and its promoter might be suitable for directing the expression of genes at precise stages of meiotic development (e.g., during recombination). The efficiency of the *MLH3* promoter needs to be tested with a gene of interest. An interesting candidate to test is the yeast *RAD52* gene. While most of the HR proteins are conserved across organisms at the level of the primary sequence an exception is RAD52, the key HR protein in yeast. In the future, over-expression of yeast *RAD52* driven by the *MLH3* promoter might enhance efficiency of HR in plants. Robust germline specific promoters would enable stable transmission of transgenes over generations and can control expression of specific genes during gametogenesis. This was applied by Wehrkamp-Richter et al., (2009) in a high throughput assay to measure meiotic HR, where a meganuclease *Sce*-I when expressed from a floral specific promoter APETALA, resulted in a four-fold greater recovery of HR events.

# Chapter 7

Summary and perspectives/ Samenvatting

Key events of meiosis include chromosome pairing, recombination and segregation and are essentially the same for all eukaryotes. An ever-increasing number of genes involved in meiosis and recombination are being identified but our understanding of the mechanism of homologous recombination and crossing over is still nascent. Arabidopsis meiotic research has progressed dramatically in the last decade thanks to the plethora of mutant resources and ingenious developments in cytogenetic techniques. In Chapter 1, I present an overview of the genes known to be involved in the Double Strand Break repair and Homologous Recombination pathways. Some of these HR genes have roles in both mitosis and meiosis. A comparison of yeast, mouse and *Arabidopsis* meiotic mutants shows functional differences in the orthologs.

Most of the meiotic genes were identified because of the high levels of sequence similarity among eukaryotes, but for genes with limited sequence conservation, new experimental approaches are required. In Chapter 2, a strategy is presented on the cDNA-AFLP technology of *Petunia* meiotic anthers for capturing novel meiotic genes. The experiment generated around 7,400 transcript fragments of which 475 were modulated in expression during meiosis. Cluster analysis based on quantification of expression profiles categorized transcripts into five clusters, i.e., premeiotic, early meiotic, late meiotic, post-meiotic and down regulated in late meiosis. Homology was sought to the 293 sequenced partial tags out of which functional classification was possible for 30% of the ESTs. Homologies with known meiotic genes from plants, yeast and mammals showed that the screening was, in principle, effective. *In-situ* hybridization experiments confirmed the gene expression patterns for five selected genes validating our cDNA-AFLP results while adding spatial information. Although the cDNA-AFLP transcript profiling has been shown to be in general sensitive and effective, well-known meiotic genes appeared to be underrepresented within 6% of the meiotic transcript pool. Some of the disadvantages in the analysis of these ESTs include presence of unique transcripts generation of very short sequences and occurrence of lowly expressed tags. In addition, whole anthers were sampled reducing the possibility of finding exclusively meiotic transcripts. Similar studies in *Brassica* have shown that there is an extremely low protein yield of ~1.2 µg/bud from meiocyte extracts (Sanchez-Moran et al., 2005). Obtaining exclusive meiotic tissue and employing sensitive and unambiguous techniques for the identification of significant transcripts is therefore crucial for greater success in future experiments.

Obviously, the next step was to investigate the function of the genes we identified in *Petunia*, using reverse genetic approaches. The first option was to find the full-length transcript in *Petunia* followed by mutagenesis; the second was the identification of the putative *Arabidopsis* ortholog. Meiotic research in *Arabidopsis* is attractive due to the availability of extensive sequence information and large mutant collections. We therefore screened for new meiotic mutants in 62 *Arabidopsis* genes using 103 T-DNA insertion lines (Chapter 3). Previously characterized meiotic genes that feature in our dataset include *AtDMC*1, *AtASY*1 and *AtASK*1. The majority

of the characterized genes that featured in our dataset were associated with metabolic and signaling processes, which was consistent with the findings of similar screens in Brassica, mouse and yeast (Sanchez-Moran et al., 2005, Maratou et al., 2004, Rabitsch et al., 2001). While most mutants were phenotypically wild type, meiotic defects were seen in the heterozygote and mutant T-DNA lines of the At4g16155 and At4g31750 genes. Reduced fertility can reflect the consequences of the meiotic impairment but can also be caused by translocations resulting from T-DNA integration and hence need further investigation. In addition, mutations in 11 genes were homozygous lethal implying that they represent essential functions. Single mutants in *Arabidopsis* did not reveal any meiotic defects for some of the genes that are homologs of meiotic genes in other species. We suspect that functional redundancy exists within the *BACH, FKBP* and *RAD54* gene families in this species. This investigation has given us an insight into the types of genes that become active in meiotic stages of anther development.

The specialized process of homologous recombination during meiosis involves the coordinated action of a number of genes. There remains much to be learnt about the molecular basis of recombination. We assayed meiotic recombination frequencies between tightly linked fluorescent markers for four Arabidopsis mutants (Chapter 4). Tester lines with cis-linked fluorescent markers were developed for four chromosomal intervals and can be used to test RF in more mutants in the future. We found a drastic reduction in recombination frequency (RF) of 75% in the *Atmsh5* mutant that participates in crossover formation. RF was not altered in the mutants *Atkrp125c, Atfkbp20-1 and AtrecQL4A.*

We then embarked on the characterization of a meiotic mutant that was isolated by a forward genetics approach. The *x-ray-sensitive 4* (*xrs4*) mutant was identified as a meiotic hyper-recombination mutant by Masson and coworkers (1997). In Chapter 5, we systematically characterized the *xrs4* mutant cytologically and identified defects in meiosis-II, pollen mitosis and female gametophyte development. Overall RF was not altered in the mutant in contrast to previously presented results. A large plant-to plant variation of RF and altered bivalent morphology at metaphase-I was observed. Future experiments must aim to test if there is a shift in CO distribution. The *xrs4* mutation could be located in a 62.5 Kb window on chromosome 5 with 18 genes. Ten candidate genes were eliminated because insertion mutants did not show a phenotype. Efforts are underway to identify the corresponding gene as one amongst the eight remaining candidates: AT5G04267, AT5G04270, AT5G04347, AT5G04350, AT5G04370, AT5G04390, AT5G04400 and AT5G04386.

AtMLH1 participates in the interference sensitive Class I CO pathway in an AtMLH3-dependant manner. We scrutinized the effect of *atmlh3* on meiotic recombination and the expression of its promoter in germline cells as described in Chapter 6. Only an intermediate reduction of 60% in RF was seen in the *Atmlh3* mutant showing that this *MutL* gene affects CO formation to a lesser extent than the MutS gene, *AtMSH5*, in Arabidopsis. Intriguingly, in heterozygous *Atmlh3* plants the

RF was similar to that of the mutant. We found the expression of *AtMLH3* to be meiosis-specific in the anthers making it a good germline specific promoter.

Alteration of recombination i.e., increasing, decreasing or abolishing recombination is useful in trait introgression into cultivars, positional cloning, marker assisted breeding and potentially fixing favorable gene combinations in plant varieties (Barth et al., 2001). Crossover formation between non-homologous chromosomes as seen in mutants *ph1*, *ph2*, *rad51*, *zyp1a/ zyp1b*, *sy10* can facilitate transfer of monogenic and polygenic traits from the wild germplasm into cultivated varieties (with genetic barriers). Thus, there is value in characterizing meiotic mutants to understand fundamental aspects of sexual reproduction. In addition, these mutants are useful tools in crop research particularly in the areas of developing breeding methods, and understanding evolution of polyploid species. Specific screens to test RF alone can identify mutants altered in recombination. In conclusion, this thesis is an investigation of the genes participating in meiosis and recombination in flowering plants like Petunia and Arabidopsis.

# Samenvatting

Belangrijke stappen tijdens de meiose, zoals chromosoomparing, recombinatie en segregatie verlopen in essentie identiek voor alle eukaryoten. Hoewel steeds meer genen betrokken bij meiose en recombinatie geïdentificeerd worden, staat ons begrip van het mechanisme van homologe recombinatie en crossing-over (CO) nog in de kinderschoenen. Dankzij het grote aantal beschikbare mutanten en ingenieuze ontwikkelingen in cytogenetische technieken heeft het onderzoek naar meiose in Arabidopsis de laatste tien jaar grote vooruitgang geboekt. In Hoofdstuk 1 geef ik een overzicht van de genen waarvan bekend is dat ze betrokken zijn bij het herstel van dubbelstrengsbreuken in DNA strengen en homologe recombinatie (HR). Enkele van deze HR-genen spelen een rol in zowel mitose als meiose. Een vergelijking van meiotische mutanten van gist, muizen en Arabidopsis toont aan dat er sprake is van functieverschillen tussen orthologe genen.

De meeste meiotische genen konden worden geïdentificeerd aan de hand van grote gelijkheid in de sequentie in eukaryoten, maar voor genen met een beperkte sequentieconservering zijn nieuwe experimentele benaderingen noodzakelijk. In Hoofdstuk 2 wordt een strategie voorgesteld om nieuwe meiotische genen te ontdekken door het toepassen van de cDNA-AFLP-techniek op meiotische antheren van Petunia. Het experiment resulteerde in ongeveer 7400 transcriptiefragmenten, waarvan er 475 in expressie werden gemoduleerd tijdens de meiose. Clusteranalyse gebaseerd op de kwantificatie van expressieprofielen deelde deze 475 transcripten in vijf clusters in: pre-meiotisch, vroeg-meiotisch, laat-meiotisch, post-meiotisch en neerwaarts-gereguleerd in de laat-meiotische fase. Van de 475 transcriptiefragmenten werden er 293 succesvol gesequenced, waarvan door middel van homologie 30% functioneel geklassificeerd kon worden. Homologie met bekende meiotische genen van planten, gisten en zoogdieren toonde aan dat de screening in principe effectief was. *In situ* hybridizatie-experimenten bevestigden de genexpressiepatronen van vijf geselecteerde genen waarmee de cDNA strategie gevalideerd werd. Hoewel is aangetoond dat cDNA-AFLP-transcriptieprofilering doorgaans sensitief en effectief is, leken bekende meiotische genen ondervertegenwoordigd te zijn. Enkele uitdagingen in de analyse van de transcriptiefragmenten omvatten de aanwezigheid van unieke maar zeer korte transcripten met weinig sequentie-informatie en het voorkomen van fragmenten die zeer laag tot expressie komen. Daarenboven werden complete meeldraden gesampled, waardoor de kans op het vinden van exclusief-meiotische transcripten werd verkleind. Vergelijkbare studies in Brassica hebben aangetoond dat er een extreem lage opbrengst van ongeveer 1,2 microgram eiwit/knop is (Sanchez-Moran et al., 2005). Om toekomstige experimenten vaker te doen slagen is het verkrijgen van exclusief meiotisch weefsel (meiocyten) en het gebruik van sensitieve, eenduidige technieken voor de identificatie van meiotische transcripten derhalve cruciaal.

De voor de hand liggende volgende stap was onderzoek naar de functie van de genen die werden geïdentificeerd in Petunia met gebruikmaking van reverse

genetische benaderingen. Een eerste optie was het vinden van het volledige transcript in Petunia, gevolgd door mutagenese, een tweede de identificatie van de orthologe genen in Arabidopsis. Onderzoek van meiose in Arabidopsis is aantrekkelijk vanwege de beschikbaarheid van uitgebreide sequentie-informatie en grote mutantencollecties. Derhalve werden 62 Arabidopsis genen gescreend op nieuwe meiotische mutanten door gebruik te maken van 103 T-DNA insertielijnen (Hoofdstuk 3). Reeds gekarakteriseerde meiotische genen die ook in onze dataset voorkomen, omvatten *AtDMC1*, *AtASY1* en *AtASK1*. De meerderheid van de gekarakteriseerde genen in de dataset waren geassocieerd met metabolische en signaalprocessen, hetgeen consistent was met de resultaten van vergelijkbare screenings in Brassica, muizen en gist (Sanchez-Moran et al., 2005, Maratou et al., 2004, Rabitsch et al, 2001). Hoewel de meeste mutanten fenotypisch gezien wild type waren, werden meiotische defecten vastgesteld in de heterozygote en gemuteerde T-DNA-lijnen van de genen At4g16155 en At4g31750. Verminderde vruchtbaarheid kan het resultaat zijn van meiotische beschadiging, maar kan ook worden veroorzaakt door translocaties als gevolg van T-DNA-integratie, en dient derhalve verder te worden onderzocht. Hiernaast bleken mutaties in 11 genen homozygoot lethaal, wat aan lijkt te tonen dat ze essentiële functies vertegenwoordigen. Sommige enkelvoudige mutanten in Arabidopsis toonden geen meiotische defecten ondanks het feit dat het om homologen van meiotische genen in andere soorten gaat. We vermoeden dat er sprake is van functionele redundantie binnen de *BACH*, *FKBP* en *RAD54* genenfamilies in deze soort. Overall heeft dit onderzoek meer inzicht opgeleverd in genen die actief worden tijdens de meiotische fases van de antherenontwikkeling.

Het proces van homologe recombinatie gedurende meiose omvat gecoördineerde actie van diverse genen. Over de moleculaire basis van recombinatie is nog veel onbekend. Wij toetsten de meiotische recombinatiefrequenties (RF) tussen gekoppelde fluorescentie markers in vier Arabidopsismutanten (Hoofdstuk 4). Er werden testlijnen ontwikkeld met cis-gekoppelde fluorescentie markers voor vier chromosomale intervallen die ook in de toekomst kunnen worden gebruikt om RF in andere mutanten te onderzoeken. Een drastische reductie van 75% werd vastgesteld in de RF in de *Atmsh5* mutant die een rol speelt in CO-formatie. RF was onveranderd in de mutanten *Atkrp125c*, *Atfkbp20*-1 en *AtrecQL4A*.

Vervolgens werd begonnen met de karakterisering van een meiotische mutant die door middel van een forward genetische aanpak was geïsoleerd. De x-ray-sensitive 4 (*xrs4*) mutant werd door Masson et al (1997) als een meiotische hyper-recombinatie mutant geïdentificeerd. In Hoofdstuk 5 wordt een systematische cytologische karakterisering gegeven van de *xrs4* mutant en worden defecten in meiosis-II, pollen mitose en vrouwelijke gametofietenontwikkeling geïdentificeerd. In tegenstelling met eerder gepresenteerde resultaten bleef de RF globaal gesproken onveranderd. Er werd een grote variatie in RF tussen de planten vastgesteld, alsmede een veranderde morfologie van bivalenten in metafase-I. Toekomstig onderzoek zal zich moeten richten op het vaststellen of er een verschuiving plaatsvindt in CO-

distributie. De *xrs4*-mutatie kon worden gelocaliseerd binnen een 62.5 Kb-gebied op chromosoom 5 dat 18 genen bevat. Tien mogelijke genen werden uitgesloten omdat insertiemutanten geen fenotype vertoonden. Er wordt getracht het corresponderende gen te identificeren als een van acht overgebleven kandidaten: AT5G04267, AT5G04270, AT5G04347, AT5G04350, AT5G04370, AT5G04390, AT5G04400 en AT5G04386.

*AtMLH1* is, op *AtMLH3*-afhankelijke wijze, betrokken bij het interferentiegevoelige Class-1 CO pathway. Het effect van *atmlh3* op meiotische recombinatie en de expressie van zijn promotor in germline cellen werd in detail onderzocht en in Hoofdstuk 6 beschreven. In de *Atmlh3* mutant werd slechts een middelmatige reductie van 60% in RF vastgesteld, hetgeen aantoont dat dit MutL gen de CO-formatie in geringere mate beïnvloedt dan het MutS gen *AtMSH5*. Intrigerend was dat de RF in heterozygote *Atmlh3* planten identiek is aan die van de mutant. We constateerden dat de expressie van *AtMLH3* in de antheren meiose-specifiek is, wat het tot een goede germline-specifieke promotor maakt.

Verandering van recombinatie, dat wil zeggen, een toename, afname of niet plaatsvinden van recombinatie is nuttig voor de introgressie van gewenste kenmerken in cultivars, map-based cloning en teelt met behulp van markers, en kan helpen bij het fixeren van voordelige gencombinaties (Barth et al., 2001). CO formatie tussen niet-homologe chromosomen zoals in de mutanten *ph1*, *ph2*, *rad51*, *zyp1a*, *zyp1b* en *sy10* kan de overdracht van mono- en polygenetische eigenschappen van het wild-germplasm naar gecultiveerde variëteiten (met genetische barrières) faciliteren. Om fundamentele aspecten van sexuele voortplanting te begrijpen is het dus waardevol meiotische mutanten te karakteriseren. Daarenboven vormen deze mutanten nuttige instrumenten in het onderzoek naar landbouwgewassen, met name bij de ontwikkeling van teeltmethodes, alsook voor een beter begrip van de ontwikkeling van polyploïde soorten. Specifieke screens om RF te testen zouden mutanten kunnen identificeren die in recombinatie zijn veranderd. Samengevat, dit proefschrift is een onderzoek naar de genen die participeren in meiose en recombinatie in bloeiende planten zoals Petunia en Arabidopsis.

# References

Abe K, Osakabe K, Nakayama S, Endo M, Tagiri A, Todoriki S, Ichikawa H, Toki S. 2005. Arabidopsis RAD51C gene is important for homologous recombination in meiosis and mitosis. Plant Physiol 139(2):896-908.

Abirached-Darmency M TE, De Jong JH. 1991. The effect on meiotic synapsis of a recombination modulator in Petunia hybrida. Genome 35:443-453.

Albini SM, Jones GH. 1987. Synaptonemal complex spreading in Allium cepa and A. fistulosum I. The initiationand sequence of pairing. Chromosoma 95:324–338.

Alexander MP. 1969. Differential staining of aborted and nonaborted pollen. Stain Technol 44(3):117-122.

Allard RW. 1963. Evidence for Genetic Restriction of Recombination in the Lima Bean. Genetics 48(10):1389-1395.

Allers T, Lichten M. 2001. Differential timing and control of noncrossover and crossover recombination during meiosis. Cell 106(1):47-57.

Alou AH, Azaiez A, Jean M, Belzile FJ. 2004. Involvement of the Arabidopsis thaliana AtPMS1 gene in somatic repeat instability. Plant Mol Biol 56(3):339-349.

Altschul SF, Madden TL, Schaffer AA, Zhang J, Zhang Z, Miller W, Lipman DJ. 1997. Gapped BLAST and PSI-BLAST: a new generation of protein database search programs. Nucleic Acids Res 25(17):3389-3402.

Alvaro D, Lisby M, Rothstein R. 2007. Genome-wide analysis of Rad52 foci reveals diverse mechanisms impacting recombination. PLoS Genet 3(12):e228.

Amon A. 1999. The spindle checkpoint. Curr Opin Genet Dev 9(1):69-75.

Anderson LK, Doyle GG, Brigham B, Carter J, Hooker KD, Lai A, Rice M, Stack SM. 2003. High-resolution crossover maps for each bivalent of Zea mays using recombination nodules. Genetics 165(2):849-865.

Armstrong SJ, Caryl AP, Jones GH, Franklin FC. 2002. Asy1, a protein required for meiotic chromosome synapsis, localizes to axis-associated chromatin in Arabidopsis and Brassica. J Cell Sci 115(Pt 18):3645-3655.

Armstrong SJ, Franklin FC, Jones GH. 2001. Nucleolus-associated telomere clustering and pairing precede meiotic chromosome synapsis in Arabidopsis thaliana. J Cell Sci 114(Pt 23):4207-4217.

Armstrong SJ, Jones GH. 2003. Meiotic cytology and chromosome behaviour in wild-type Arabidopsis thaliana. J Exp Bot 54(380):1-10.

Arnold K, Kim MK, Frerk K, Edler L, Savelyeva L, Schmezer P, Wiedemeyer R. 2006. Lower level of BRCA2 protein in heterozygous mutation carriers is correlated with an increase in DNA double strand breaks and an impaired DSB repair. Cancer Lett 243(1):90-100.

Arora C, Kee K, Maleki S, Keeney S. 2004. Antiviral protein Ski8 is a direct partner of Spo11 in meiotic DNA break formation, independent of its cytoplasmic role in RNA metabolism. Mol Cell 13(4):549-559.

Aten JA, Stap J, Krawczyk PM, van Oven CH, Hoebe RA, Essers J, Kanaar R. 2004. Dynamics of DNA double-strand breaks revealed by clustering of damaged chromosome domains. Science 303(5654):92-95.

Azumi Y, Liu D, Zhao D, Li W, Wang G, Hu Y, Ma H. 2002. Homolog interaction during meiotic prophase I in Arabidopsis requires the SOLO DANCERS gene encoding a novel cyclin-like protein. Embo J 21(12):3081-3095.

Bagherieh-Najjar MB, de Vries OM, Hille J, Dijkwel PP. 2005. Arabidopsis RecQI4A suppresses homologous recombination and modulates DNA damage responses. Plant J 43(6):789-798.

Baker SM, Bronner CE, Zhang L, Plug AW, Robatzek M, Warren G, Elliott EA, Yu J, Ashley T, Arnheim N, Flavell RA, Liskay RM. 1995. Male mice defective in the

DNA mismatch repair gene PMS2 exhibit abnormal chromosome synapsis in meiosis. Cell 82(2):309-319.

Baker SM, Plug AW, Prolla TA, Bronner CE, Harris AC, Yao X, Christie DM, Monell C, Arnheim N, Bradley A, Ashley T, Liskay RM. 1996. Involvement of mouse Mlh1 in DNA mismatch repair and meiotic crossing over. Nat Genet 13(3):336-342.

Baldwin A, Wardle A, Patel R, Dudley P, Park SK, Twell D, Inoue K, Jarvis P. 2005. A molecular-genetic study of the Arabidopsis Toc75 gene family. Plant Physiol 138(2):715-733.

Bannigan A, Scheible WR, Lukowitz W, Fagerstrom C, Wadsworth P, Somerville C, Baskin TI. 2007. A conserved role for kinesin-5 in plant mitosis. J Cell Sci 120(Pt 16):2819-2827.

Barth S, Melchinger AE, Devezi-Savula B, Lubberstedt T. 2000. A high-throughput system for genome-wide measurement of genetic recombination in Arabidopsis thaliana based on transgenic markers. Funct Integr Genomics 1(3):200-206.

Berchowitz LE, Francis KE, Bey AL, Copenhaver GP. 2007. The role of AtMUS81 in interference-insensitive crossovers in A. thaliana. PLoS Genet 3(8):e132.

Bleuyard JY, Gallego ME, Savigny F, White CI. 2005. Differing requirements for the Arabidopsis Rad51 paralogs in meiosis and DNA repair. Plant J 41(4):533-545.

Bleuyard JY, White CI. 2004. The Arabidopsis homologue of Xrcc3 plays an essential role in meiosis. Embo J 23(2):439-449.

Bogdanov YF, Grishaeva TM, Dadashev SY. 2007. Similarity of the domain structure of proteins as a basis for the conservation of meiosis. Int Rev Cytol 257:83-142.

Borner GV, Kleckner N, Hunter N. 2004. Crossover/noncrossover differentiation, synaptonemal complex formation, and regulatory surveillance at the leptotene/zygotene transition of meiosis. Cell 117(1):29-45.

Breyne P, Dreesen, R., Cannoot, B., Rombaut, D., Vandepoele, K., Rombauts, S., Vanderhaeghen, R., Inzé, D., Zabeau, M. 2003. Quantitative cDNA-AFLP analysis for genome-wide expression studies. Mol Gen Genomics 269:173-179.

Breyne P, Dreesen R, Vandepoele K, De Veylder L, Van Breusegem F, Callewaert L, Rombauts S, Raes J, Cannoot B, Engler G, Inze D, Zabeau M. 2002. Transcriptome analysis during cell division in plants. Proc Natl Acad Sci U S A 99(23):14825-14830.

Bundock P, Hooykaas P. 2002. Severe developmental defects, hypersensitivity to DNA-damaging agents, and lengthened telomeres in Arabidopsis MRE11 mutants. Plant Cell 14(10):2451-2462.

Bundock P, Hooykaas P. 2002. Severe developmental defects, hypersensitivity to DNA-damaging agents, and lengthened telomeres in Arabidopsis MRE11 mutants. Plant Cell 14(10):2451-2462.

Cantor SB, Bell DW, Ganesan S, Kass EM, Drapkin R, Grossman S, Wahrer DC, Sgroi DC, Lane WS, Haber DA, Livingston DM. 2001. BACH1, a novel helicase-like protein, interacts directly with BRCA1 and contributes to its DNA repair function. Cell 105(1):149-160.

Carney JP MR, Olivares H, Davis EM, Le Beau M, Yates JR 3rd, Hays L,, Morgan WF PJ. 1998. The hMre11/hRad50 protein complex and Nijmegen breakage syndrome: linkage of double-strand break repair to the cellular DNA damage response. Cell. p 477-486.

Carpenter AT. 1979. Synaptonemal complex and recombination nodules in wild-type Drosophila melanogaster females. Genetics 92(2):511-541.

Carpenter AT. 1987. Gene conversion, recombination nodules, and the initiation of meiotic synapsis. Bioessays 6(5):232-236.

Carpenter ATC. 1988. Thoughts on recombination nodules, meiotic recombination, and

chiasmata. Genetic Recombination, edited by R Kucherlapati and G R Smith American Society of Microbiology, Washington, DC:529-548.

Caryl AP, Armstrong SJ, Jones GH, Franklin FC. 2000. A homologue of the yeast HOP1 gene is inactivated in the Arabidopsis meiotic mutant asy1. Chromosoma 109(1-2):62-71.

Chan KG, Mayer M, Davis EM, Halperin SA, Lin TJ, Lee SF. 2007. Role of D-alanylation of Streptococcus gordonii lipoteichoic acid in innate and adaptive immunity. Infect Immun 75(6):3033-3042.

Chelysheva L, Gendrot G, Vezon D, Doutriaux MP, Mercier R, Grelon M. 2007. Zip4/Spo22 is required for class I CO formation but not for synapsis completion in Arabidopsis thaliana. PLoS Genet 3(5):e83.

Chen C, Marcus A, Li W, Hu Y, Calzada J-PV, Grossniklaus U, Cyr RJ, Ma H. 2002. The Arabidopsis ATK1 gene is required for spindle morphogenesis in male meiosis. Development 129(10):2401-2409.

Chiba Y, Johnson MA, Lidder P, Vogel JT, van Erp H, Green PJ. 2004. AtPARN is an essential poly(A) ribonuclease in Arabidopsis. Gene 328:95-102.

Christensen CA, Subramanian S, Drews GN. 1998. Identification of gametophytic mutations affecting female gametophyte development in Arabidopsis. Dev Biol 202(1):136-151.

Chu S, DeRisi J, Eisen M, Mulholland J, Botstein D, Brown PO, Herskowitz I. 1998. The transcriptional program of sporulation in budding yeast. Science 282(5389):699-705.

Cnudde F, Gerats T. 2005. Meiosis: inducing variation by reduction. Plant Biol (Stuttg) 7(4):321-341.

Cnudde F MC, Porceddu A, Pezzotti M, Gerats T. 2003. Transcript profiling on developing Petunia hybrida floral organs. Sex Plant Reprod 16:77-85.

Copenhaver GP, Browne WE, Preuss D. 1998. Assaying genome-wide recombination and centromere functions with Arabidopsis tetrads. Proc Natl Acad Sci U S A 95(1):247-252.

Copenhaver GP, Housworth EA, Stahl FW. 2002. Crossover interference in Arabidopsis. Genetics 160(4):1631-1639.

Cotsaftis O, Guiderdoni E. 2005. Enhancing gene targeting efficiency in higher plants: rice is on the move. Transgenic Res 14(1):1-14.

Cox KH GR. 1988. Analysis of plant gene expression. Plant Molecular Biology: A Practical Approach Oxford: IRL Press:1Y34.

Crackower MA, Kolas NK, Noguchi J, Sarao R, Kikuchi K, Kaneko H, Kobayashi E, Kawai Y, Kozieradzki I, Landers R, Mo R, Hui CC, Nieves E, Cohen PE, Osborne LR, Wada T, Kunieda T, Moens PB, Penninger JM. 2003. Essential role of Fkbp6 in male fertility and homologous chromosome pairing in meiosis. Science 300(5623):1291-1295.

Cromie GA, Smith GR. 2007. Branching out: meiotic recombination and its regulation. Trends Cell Biol 17(9):448-455.

Culligan KM, Britt AB. 2008. Both ATM and ATR promote the efficient and accurate processing of programmed meiotic double-strand breaks. Plant J 55(4):629-638.

de Boer E, Dietrich AJ, Hoog C, Stam P, Heyting C. 2007. Meiotic interference among MLH1 foci requires neither an intact axial element structure nor full synapsis. J Cell Sci 120(Pt 5):731-736.

de Boer E, Stam P, Dietrich AJ, Pastink A, Heyting C. 2006. Two levels of interference in mouse meiotic recombination. Proc Natl Acad Sci U S A 103(25):9607-9612.

De Jong JH, Oud J.L. 1979. Location and behaviour of constitutive heterochromatin during meiotic prophase in Beta vulgaris L. Genetica 51:125-133.

de los Santos T, Hunter N, Lee C, Larkin B, Loidl J, Hollingsworth NM. 2003. The

Mus81/Mms4 endonuclease acts independently of double-Holliday junction resolution to promote a distinct subset of crossovers during meiosis in budding yeast. Genetics 164(1):81-94.

De Muyt A, Pereira L, Vezon D, Chelysheva L, Gendrot G, Chambon A, Laine-Choinard S, Pelletier G, Mercier R, Nogue F, Grelon M. 2009. A high throughput genetic screen identifies new early meiotic recombination functions in Arabidopsis thaliana. PLoS Genet 5(9):e1000654.

De Muyt A, Vezon D, Gendrot G, Gallois JL, Stevens R, Grelon M. 2007. AtPRD1 is required for meiotic double strand break formation in Arabidopsis thaliana. Embo J 26(18):4126-4137.

De Smet F, Mathys J, Marchal K, Thijs G, De Moor B, Moreau Y. 2002. Adaptive quality-based clustering of gene expression profiles. Bioinformatics 18(5):735-746.

de Vries FA, de Boer, E., van den Bosch, M., Baarends, W. M., Ooms, M., Yuan, L., Liu, J. G., van Zeeland, A. A., Heyting, C. and Pastink, A. 2005. Mouse Sycp1 functions in synaptonemal complex assembly, meiotic recombination, and XY body formation. Genes Dev 19:1376-1389.

Delatte T, Umhang M, Trevisan M, Eicke S, Thorneycroft D, Smith SM, Zeeman SC. 2006. Evidence for distinct mechanisms of starch granule breakdown in plants. J Biol Chem 281(17):12050-12059.

Deutschbauer AM, Williams RM, Chu AM, Davis RW. 2002. Parallel phenotypic analysis of sporulation and postgermination growth in Saccharomyces cerevisiae. Proc Natl Acad Sci U S A 99(24):15530-15535.

Devaiah BN, Nagarajan VK, Raghothama KG. 2007. Phosphate homeostasis and root development in Arabidopsis are synchronized by the zinc finger transcription factor ZAT6. Plant Physiol 145(1):147-159.

Deveaux Y, Alonso B, Pierrugues O, Godon C, Kazmaier M. 2000. Molecular cloning and developmental expression of AtGR1, a new growth-related Arabidopsis gene strongly induced by ionizing radiation. Radiat Res 154(4):355-364.

Dion E, Li L, Jean M, Belzile F. 2007. An Arabidopsis MLH1 mutant exhibits reproductive defects and reveals a dual role for this gene in mitotic recombination. Plant J 51(3):431-440.

Doutriaux MP, Couteau F, Bergounioux C, White C. 1998. Isolation and characterisation of the RAD51 and DMC1 homologs from Arabidopsis thaliana. Mol Gen Genet 257(3):283-291.

Drouaud J, Camilleri C, Bourguignon PY, Canaguier A, Berard A, Vezon D, Giancola S, Brunel D, Colot V, Prum B, Quesneville H, Mezard C. 2006. Variation in crossing-over rates across chromosome 4 of Arabidopsis thaliana reveals the presence of meiotic recombination "hot spots". Genome Res 16(1):106-114.

Drouaud J, Mercier R, Chelysheva L, Berard A, Falque M, Martin O, Zanni V, Brunel D, Mezard C. 2007. Sex-specific crossover distributions and variations in interference level along Arabidopsis thaliana chromosome 4. PLoS Genet 3(6):e106.

Dvorak J, M.-C. Luo and Z.-L. Yang. 1998. Restriction fragment length polymorphism and divergence in the genomic regions of high and low recombination in self-fertilizing and cross-fertilizing Aegilops species. Genetics 148:423-434.

Edwards K, Johnstone C, Thompson C. 1991. A simple and rapid method for the preparation of plant genomic DNA for PCR analysis. Nucleic Acids Res 19(6):1349.

Eisen MB, Spellman PT, Brown PO, Botstein D. 1998. Cluster analysis and display of genome-wide expression patterns. Proc Natl Acad Sci U S A 95(25):14863-14868.

Elmayan T, Proux F, Vaucheret H. 2005. Arabidopsis RPA2: a genetic link among transcriptional gene silencing, DNA repair, and DNA replication. Curr Biol 15(21):1919-1925.

Emmanuel E, Yehuda E, Melamed-Bessudo C, Avivi-Ragolsky N, Levy AA. 2006. The role of AtMSH2 in homologous recombination in Arabidopsis thaliana. EMBO Rep 7(1):100-105.

Essers J, Hendriks RW, Swagemakers SM, Troelstra C, de Wit J, Bootsma D, Hoeijmakers JH, Kanaar R. 1997. Disruption of mouse RAD54 reduces ionizing radiation resistance and homologous recombination. Cell 89(2):195-204.

Faure JD, Vittorioso P, Santoni V, Fraisier V, Prinsen E, Barlier I, Van Onckelen H, Caboche M, Bellini C. 1998. The PASTICCINO genes of Arabidopsis thaliana are involved in the control of cell division and differentiation. Development 125(5):909-918.

Feng XL, Ni WM, Elge S, Mueller-Roeber B, Xu ZH, Xue HW. 2006. Auxin flow in anther filaments is critical for pollen grain development through regulating pollen mitosis. Plant Mol Biol 61(1-2):215-226.

Ferrer JL, Ravanel S, Robert M, Dumas R. 2004. Crystal structures of cobalamin-independent methionine synthase complexed with zinc, homocysteine, and methyltetrahydrofolate. J Biol Chem 279(43):44235-44238.

Francis KE, Lam SY, Harrison BD, Bey AL, Berchowitz LE, Copenhaver GP. 2007. Pollen tetrad-based visual assay for meiotic recombination in Arabidopsis. Proc Natl Acad Sci U S A 104(10):3913-3918.

Franklin FC, Higgins JD, Sanchez-Moran E, Armstrong SJ, Osman KE, Jackson N, Jones GH. 2006. Control of meiotic recombination in Arabidopsis: role of the MutL and MutS homologues. Biochem Soc Trans 34(Pt 4):542-544.

Fries R. 1911. Die Arten der Gattung Petunia. Kungl. Svenska Vetenskapsakademiens Handlingar 46. Uppsala: Almqvist & Wikells.Gallego ME, Jeanneau M, Granier F, Bouchez D, Bechtold N, White CI. 2001. Disruption of the Arabidopsis RAD50 gene leads to plant sterility and MMS sensitivity. Plant J 25(1):31-41.

Garcia V, Bruchet H, Camescasse D, Granier F, Bouchez D, Tissier A. 2003. AtATM is essential for meiosis and the somatic response to DNA damage in plants. Plant Cell 15(1):119-132.

Geisler M, Bailly A. 2007. Tete-a-tete: the function of FKBPs in plant development. Trends Plant Sci 12(10):465-473.

Geisler M, Kolukisaoglu HU, Bouchard R, Billion K, Berger J, Saal B, Frangne N, Koncz-Kalman Z, Koncz C, Dudler R, Blakeslee JJ, Murphy AS, Martinoia E, Schulz B. 2003. TWISTED DWARF1, a unique plasma membrane-anchored immunophilin-like protein, interacts with Arabidopsis multidrug resistance-like transporters AtPGP1 and AtPGP19. Mol Biol Cell 14(10):4238-4249.

Gerats AGM, Vlaming d, Maizonnier D. 1984. Recombination behaviour and gene transfer in Petunia hybrida after pollen irradiation. Mol Gen Genet 198:57-61.

Geuting V, Kobbe D, Hartung F, Durr J, Focke M, Puchta H. 2009. Two Distinct MUS81-EME1 Complexes from Arabidopsis Process Holliday Junctions 10.1104/pp.109.136846. Plant Physiol 150(2):1062-1071.

Gherbi H, Gallego ME, Jalut N, Lucht JM, Hohn B, White CI. 2001. Homologous recombination in planta is stimulated in the absence of Rad50. EMBO Rep 2(4):287-291.

Gomez LD, Baud S, Gilday A, Li Y, Graham IA. 2006. Delayed embryo development in the ARABIDOPSIS TREHALOSE-6-PHOSPHATE SYNTHASE 1 mutant is associated with altered cell wall structure, decreased cell division and starch accumulation. Plant J 46(1):69-84.

Greenberg RA. 2006. BRCA mutations and childhood cancer. Cancer Biol Ther 5(9):1103-1104.

Grelon M, Vezon D, Gendrot G, Pelletier G. 2001. AtSPO11-1 is necessary for efficient meiotic recombination in plants. Embo J 20(3):589-600.

Guillon H, Baudat F, Grey C, Liskay RM, de Massy B. 2005. Crossover and noncrossover pathways in mouse meiosis. Mol Cell 20(4):563-573.

Hamant O, Golubovskaya I, Meeley R, Fiume E, Timofejeva L, Schleiffer A, Nasmyth K, Cande WZ. 2005. A REC8-dependent plant Shugoshin is required for maintenance of centromeric cohesion during meiosis and has no mitotic functions. Curr Biol 15(10):948-954.

Harrar Y, Bellini C, Faure JD. 2001. FKBPs: at the crossroads of folding and transduction. Trends Plant Sci 6:426-431.

Hartung F, Suer S, Bergmann T, Puchta H. 2006. The role of AtMUS81 in DNA repair and its genetic interaction with the helicase AtRecQ4A. Nucleic Acids Res 34(16):4438-4448.

Hartung F, Suer S, Knoll A, Wurz-Wildersinn R, Puchta H. 2008. Topoisomerase 3alpha and RMI1 suppress somatic crossovers and are essential for resolution of meiotic recombination intermediates in Arabidopsis thaliana. PLoS Genet 4(12):e1000285.

Hartung F, Suer S, Puchta H. 2007. Two closely related RecQ helicases have antagonistic roles in homologous recombination and DNA repair in Arabidopsis thaliana. Proc Natl Acad Sci U S A 104(47):18836-18841.

He Z, Li L, Luan S. 2004. Immunophilins and parvulins. Superfamily of peptidyl prolyl isomerases in Arabidopsis. Plant Physiol 134(4):1248-1267.

Heitzeberg F, Chen IP, Hartung F, Orel N, Angelis KJ, Puchta H. 2004. The Rad17 homologue of Arabidopsis is involved in the regulation of DNA damage repair and homologous recombination. Plant J 38(6):954-968.

Helleday T. 2003. Pathways for mitotic homologous recombination in mammalian cells. Mutat Res 532(1-2):103-115.

Higgins JD, Armstrong SJ, Franklin FC, Jones GH. 2004. The Arabidopsis MutS homolog AtMSH4 functions at an early step in recombination: evidence for two classes of recombination in Arabidopsis. Genes Dev 18(20):2557-2570.

Higgins JD, Buckling EF, Franklin FC, Jones GH. 2008. Expression and functional analysis of AtMUS81 in Arabidopsis meiosis reveals a role in the second pathway of crossing-over. Plant J 54(1):152-162.

Higgins JD, Sanchez-Moran E, Armstrong SJ, Jones GH, Franklin FC. 2005. The Arabidopsis synaptonemal complex protein ZYP1 is required for chromosome synapsis and normal fidelity of crossing over. Genes Dev 19(20):2488-2500.

Higgins JD, Vignard J, Mercier R, Pugh AG, Franklin FC, Jones GH. 2008. AtMSH5 partners AtMSH4 in the class I meiotic crossover pathway in Arabidopsis thaliana, but is not required for synapsis. Plant J 55(1):28-39.

Hollingsworth NM, Brill SJ. 2004. The Mus81 solution to resolution: generating meiotic crossovers without Holliday junctions. Genes Dev 18(2):117-125.

Honys D, Twell D. 2003. Comparative analysis of the Arabidopsis pollen transcriptome. Plant Physiol 132(2):640-652.

Howden R, Park SK, Moore JM, Orme J, Grossniklaus U, Twell D. 1998. Selection of T-DNA-tagged male and female gametophytic mutants by segregation distortion in Arabidopsis. Genetics 149(2):621-631.

Hruz T LO, Szabo G, Wessendorp F, Bleuler S, Oertle L, Widmayer P, Gruissem W and Zimmermann, P. 2008. Genevestigator V3: a reference expression database for the meta-analysis of transcriptomes. Advances in Bioinformatics 2008:1687-8027.

Hua J, Grisafi P, Cheng SH, Fink GR. 2001. Plant growth homeostasis is controlled by the Arabidopsis BON1 and BAP1 genes. Genes Dev 15(17):2263-2272.

Huang MD, Wei FJ, Wu CC, Hsing YI, Huang AH. 2009. Analyses of advanced rice anther transcriptomes reveal global tapetum secretory functions and potential proteins for lipid exine formation. Plant Physiol 149(2):694-707.

Hunter N, Borts RH. 1997. Mlh1 is unique among mismatch repair proteins in its ability to promote crossing-over during meiosis. Genes Dev 11(12):1573-1582.

Hwang SY, Oh B, Knowles BB, Solter D, Lee JS. 2001. Expression of genes involved in mammalian meiosis during the transition from egg to embryo. Mol Reprod Dev 59(2):144-158.

Iguchi N, Tobias JW, Hecht NB. 2006. Expression profiling reveals meiotic male germ cell mRNAs that are translationally up- and down-regulated. Proc Natl Acad Sci U S A 103(20):7712-7717.

Irish V, Sussex I. 1990. Function of the apetala-1 gene during Arabidopsis floral development. Plant Cell 2(8):741-753.

Ito T, Sakai H, Meyerowitz EM. 2003. Whorl-specific expression of the SUPERMAN gene of Arabidopsis is mediated by cis elements in the transcribed region. Curr Biol 13(17):1524-1530.

Jackson N, Sanchez-Moran E, Buckling E, Armstrong SJ, Jones GH, Franklin FC. 2006. Reduced meiotic crossovers and delayed prophase I progression in AtMLH3-deficient Arabidopsis. Embo J 25(6):1315-1323.

Jacobsen EA, Taranova AG, Lee NA, Lee JJ. 2007. Eosinophils: singularly destructive effector cells or purveyors of immunoregulation? J Allergy Clin Immunol 119(6):1313-1320.

Jessop L, Rockmill B, Roeder GS, Lichten M. 2006. Meiotic chromosome synapsis-promoting proteins antagonize the anti-crossover activity of sgs1. PLoS Genet 2(9):e155.

Jiricny J. 2000. Mediating mismatch repair. Nat Genet 24(1):6-8.

Jolivet S, Vezon D, Froger N, Mercier R. 2006. Non conservation of the meiotic function of the Ski8/Rec103 homolog in Arabidopsis. Genes Cells 11(6):615-622.

Karathanasis E, Wilson TE. 2002. Enhancement of Saccharomyces cerevisiae end-joining efficiency by cell growth stage but not by impairment of recombination. Genetics 161(3):1015-1027.

Katis VL, Galova M, Rabitsch KP, Gregan J, Nasmyth K. 2004. Maintenance of cohesin at centromeres after meiosis I in budding yeast requires a kinetochore-associated protein related to MEI-S332. Curr Biol 14(7):560-572.

Katis VL, Galova M, Rabitsch KP, Gregan J, Nasmyth K. 2004. Maintenance of cohesin at centromeres after meiosis I in budding yeast requires a kinetochore-associated protein related to MEI-S332. Curr Biol 14(7):560-572.

Kaur J, Sebastian J, Siddiqi I. 2006. The Arabidopsis-mei2-like genes play a role in meiosis and vegetative growth in Arabidopsis. Plant Cell 18(3):545-559.

Kerim T, Imin N, Weinman JJ, Rolfe BG. 2003. Proteome analysis of male gametophyte development in rice anthers. Proteomics 3(5):738-751.

Kerrebrock AW, Moore DP, Wu JS, Orr-Weaver TL. 1995. Mei-S332, a Drosophila protein required for sister-chromatid cohesion, can localize to meiotic centromere regions. Cell 83(2):247-256.

Kerzendorfer C, Vignard J, Pedrosa-Harand A, Siwiec T, Akimcheva S, Jolivet S, Sablowski R, Armstrong S, Schweizer D, Mercier R, Schlogelhofer P. 2006. The Arabidopsis thaliana MND1 homologue plays a key role in meiotic homologous pairing, synapsis and recombination. J Cell Sci 119(Pt 12):2486-2496.

Kimura S, Tahira Y, Ishibashi T, Mori Y, Mori T, Hashimoto J, Sakaguchi K. 2004.

DNA repair in higher plants; photoreactivation is the major DNA repair pathway in non-proliferating cells while excision repair (nucleotide excision repair and base excision repair) is active in proliferating cells 10.1093/nar/gkh591. Nucl Acids Res 32(9):2760-2767.

King J, Roberts LA, Kearsey MJ, Thomas HM, Jones RN, Huang L, Armstead IP, Morgan WG, King IP. 2002. A demonstration of a 1:1 correspondence between chiasma frequency and recombination using a Lolium perenne/Festuca pratensis substitution. Genetics 161(1):307-314.

Kirchhoff C, Willison K. 1990. Nucleotide and amino-acid sequence of human testis-derived TCP1. Nucleic Acids Res 18(14):4247.

Kitajima TS, Kawashima SA, Watanabe Y. 2004. The conserved kinetochore protein shugoshin protects centromeric cohesion during meiosis. Nature 427(6974):510-517.

Kitajima TS, Sakuno T, Ishiguro K, Iemura S, Natsume T, Kawashima SA, Watanabe Y. 2006. Shugoshin collaborates with protein phosphatase 2A to protect cohesin. Nature 441(7089):46-52.

Klimyuk VI, Jones JD. 1997. AtDMC1, the Arabidopsis homologue of the yeast DMC1 gene: characterization, transposon-induced allelic variation and meiosis-associated expression. Plant J 11(1):1-14.

Knoop V, Schuster W, Wissinger B, Brennicke A. 1991. Trans splicing integrates an exon of 22 nucleotides into the nad5 mRNA in higher plant mitochondria. Embo J 10(11):3483-3493.

Koncz C, Nemeth K, Redei GP, Schell J. 1992. T-DNA insertional mutagenesis in Arabidopsis. Plant Mol Biol 20(5):963-976.

Koornneef M. 1997. Plant development: timing when to flower. Curr Biol 7(10):R651-652.

Koren A, Ben-Aroya S, Kupiec M. 2002. Control of meiotic recombination initiation: a role for the environment? Curr Genet 42(3):129-139.

Korner CG, Wormington M, Muckenthaler M, Schneider S, Dehlin E, Wahle E. 1998. The deadenylating nuclease (DAN) is involved in poly(A) tail removal during the meiotic maturation of Xenopus oocytes. Embo J 17(18):5427-5437.

Koshiyama A, Hamada FN, Namekawa SH, Iwabata K, Sugawara H, Sakamoto A, Ishizaki T, Sakaguchi K. 2006. Sumoylation of a meiosis-specific RecA homolog, Lim15/Dmc1, via interaction with the small ubiquitin-related modifier (SUMO)-conjugating enzyme Ubc9. Febs J 273(17):4003-4012.

Kovalenko OV, Plug AW, Haaf T, Gonda DK, Ashley T, Ward DC, Radding CM, Golub EI. 1996. Mammalian ubiquitin-conjugating enzyme Ubc9 interacts with Rad51 recombination protein and localizes in synaptonemal complexes. Proc Natl Acad Sci U S A 93(7):2958-2963.

Kraft T, Sall T, Magnusson-Rading I, Nilsson NO, Hallden C. 1998. Positive correlation between recombination rates and levels of genetic variation in natural populations of sea beet (Beta vulgaris subsp. maritima). Genetics 150(3):1239-1244.

Krogh BO, Symington LS. 2004. Recombination proteins in yeast. Annu Rev Genet 38:233-271.

Kumar R, Bourbon HM, de Massy B. Functional conservation of Mei4 for meiotic DNA double-strand break formation from yeasts to mice. Genes Dev 24(12):1266-1280.

Kuromori T, Yamamoto M. 1994. Cloning of cDNAs from Arabidopsis thaliana that encode putative protein phosphatase 2C and a human Dr1-like protein by transformation of a fission yeast mutant. Nucleic Acids Res 22(24):5296-5301.

Lafarge S, Montane MH. 2003. Characterization of Arabidopsis thaliana ortholog of the

human breast cancer susceptibility gene 1: AtBRCA1, strongly induced by gamma rays. Nucleic Acids Res 31(4):1148-1155.

Lee H, Guo Y, Ohta M, Xiong L, Stevenson B, Zhu JK. 2002. LOS2, a genetic locus required for cold-responsive gene transcription encodes a bi-functional enolase. Embo J 21(11):2692-2702.

Lee JH, Paull TT. 2004. Direct activation of the ATM protein kinase by the Mre11/Rad50/Nbs1 complex. Science 304(5667):93-96.

Lee MW, Jelenska J, Greenberg JT. 2008. Arabidopsis proteins important for modulating defense responses to Pseudomonas syringae that secrete HopW1-1. Plant J 54(3):452-465.

Leonard JM, Bollmann SR, Hays JB. 2003. Reduction of stability of arabidopsis genomic and transgenic DNA-repeat sequences (microsatellites) by inactivation of AtMSH2 mismatch-repair function. Plant Physiol 133(1):328-338.

Lettier G, Feng Q, de Mayolo AA, Erdeniz N, Reid RJ, Lisby M, Mortensen UH, Rothstein R. 2006. The role of DNA double-strand breaks in spontaneous homologous recombination in S. cerevisiae. PLoS Genet 2(11):e194.

Lewis LK WJ, Resnick MA. 1999. Repair of endonuclease-induced double-strand breaks in Saccharomyces cerevisiae: essential role for genes associated with nonhomologous end-joining. Genetics 152(4):1513-1529.

Lhuissier FG, Offenberg HH, Wittich PE, Vischer NO, Heyting C. 2007. The mismatch repair protein MLH1 marks a subset of strongly interfering crossovers in tomato. Plant Cell 19(3):862-876.

Li GM. 2008. Mechanisms and functions of DNA mismatch repair. Cell Res 18(1):85-98.

Li J, Vaidya M, White C, Vainstein A, Citovsky V, Tzfira T. 2005. Involvement of KU80 in T-DNA integration in plant cells. Proc Natl Acad Sci U S A 102(52):19231-19236.

Li W, Chen, C., Markmann-Mulisch, U., Timofejeva, L., Schmelzer, E. , Ma, H. , Reiss, B. 2004. The Arabidopsis AtRAD51 gene is dispensable for vegetative development but required for meiosis. Proc Natl Acad Sci USA 101:10596–10601.

Lipkin SM, Moens PB, Wang V, Lenzi M, Shanmugarajah D, Gilgeous A, Thomas J, Cheng J, Touchman JW, Green ED, Schwartzberg P, Collins FS, Cohen PE. 2002. Meiotic arrest and aneuploidy in MLH3-deficient mice. Nat Genet 31(4):385-390.

Liu F, Ni W, Griffith ME, Huang Z, Chang C, Peng W, Ma H, Xie D. 2004. The ASK1 and ASK2 genes are essential for Arabidopsis early development. Plant Cell 16(1):5-20.

Liu XC, Dickinson, H.G. 1989. Cellular energy levels and their effect on male cell abortion in cytoplasmically male sterile lines of Petunia hybrida. Sex Plant Reprod 2:167–172.

Llorente B, Symington LS. 2004. The Mre11 nuclease is not required for 5' to 3' resection at multiple HO-induced double-strand breaks. Mol Cell Biol 24(21):9682-9694.

Lloyd A, Plaisier CL, Carroll D, Drews GN. 2005. Targeted mutagenesis using zinc-finger nucleases in Arabidopsis. Proc Natl Acad Sci U S A 102(6):2232-2237.

Loidl J. 1982. Further evidence for a heterochromatin-chiasma correlation in some Allium species. Genetica 60:31-35.

Luo G, Yao MS, Bender CF, Mills M, Bladl AR, Bradley A, Petrini JH. 1999. Disruption of mRad50 causes embryonic stem cell lethality, abnormal embryonic development, and sensitivity to ionizing radiation. Proc Natl Acad Sci U S A 96(13):7376-7381.

Lutziger I, Oliver DJ. 2000. Molecular evidence of a unique lipoamide dehydrogenase in

plastids: analysis of plastidic lipoamide dehydrogenase from Arabidopsis thaliana. FEBS Lett 484(1):12-16.

Lynn A, Soucek R, Borner GV. 2007. ZMM proteins during meiosis: crossover artists at work. Chromosome Res 15(5):591-605.

Ma H. 2005. Molecular Genetic Analyses of Microsporogenesis and Microgametogenesis in Flowering Plants. Annu Rev Plant Biol 56:393–434.

Mao Z, Bozzella M, Seluanov A, Gorbunova V. 2008. Comparison of nonhomologous end joining and homologous recombination in human cells. DNA Repair (Amst) 7(10):1765-1771.

Maratou K, Forster T, Costa Y, Taggart M, Speed RM, Ireland J, Teague P, Roy D, Cooke HJ. 2004. Expression profiling of the developing testis in wild-type and Dazl knockout mice. Mol Reprod Dev 67(1):26-54.

Markmann-Mulisch U, Wendeler E, Zobell O, Schween G, Steinbiss HH, Reiss B. 2007. Differential requirements for RAD51 in Physcomitrella patens and Arabidopsis thaliana development and DNA damage repair. Plant Cell 19(10):3080-3089.

Martini E, Diaz RL, Hunter N, Keeney S. 2006. Crossover homeostasis in yeast meiosis. Cell 126(2):285-295.

Masson JE, King PJ, Paszkowski J. 1997. Mutants of Arabidopsis thaliana hypersensitive to DNA-damaging treatments. Genetics 146(1):401-407.

Masson JE, Paszkowski J. 1997. Arabidopsis thaliana mutants altered in homologous recombination. Proc Natl Acad Sci U S A 94(21):11731-11735.

Mata J, Bahler J. 2003. Correlations between gene expression and gene conservation in fission yeast. Genome Res 13(12):2686-2690.

Mata J, Lyne R, Burns G, Bahler J. 2002. The transcriptional program of meiosis and sporulation in fission yeast. Nat Genet 32(1):143-147.

Mazina OM, Mazin AV, Nakagawa T, Kolodner RD, Kowalczykowski SC. 2004. Saccharomyces cerevisiae Mer3 helicase stimulates 3'-5' heteroduplex extension by Rad51; implications for crossover control in meiotic recombination. Cell 117(1):47-56.

McCormick S. 2004. Control of male gametophyte development. Plant Cell 16 Suppl:S142-153.

McGuinness BE, Hirota T, Kudo NR, Peters JM, Nasmyth K. 2005. Shugoshin prevents dissociation of cohesin from centromeres during mitosis in vertebrate cells. PLoS Biol 3(3):e86.

Meinke D, Muralla R, Sweeney C, Dickerman A. 2008. Identifying essential genes in Arabidopsis thaliana. Trends Plant Sci 13(9):483-491.

Melamed-Bessudo C, Yehuda E, Stuitje AR, Levy AA. 2005. A new seed-based assay for meiotic recombination in Arabidopsis thaliana. Plant J 43(3):458-466.

Mercier R, Grelon M. 2008. Meiosis in plants: ten years of gene discovery. Cytogenet Genome Res 120(3-4):281-290.

Mercier R, Jolivet S, Vezon D, Huppe E, Chelysheva L, Giovanni M, Nogue F, Doutriaux MP, Horlow C, Grelon M, Mezard C. 2005. Two meiotic crossover classes cohabit in Arabidopsis: one is dependent on MER3,whereas the other one is not. Curr Biol 15(8):692-701.

Mets DG, Meyer BJ. 2009. Condensins regulate meiotic DNA break distribution, thus crossover frequency, by controlling chromosome structure. Cell 139(1):73-86.

Mitchell AZ, Hanson MR, Skvirsky RC, Ausubel FM. 1980. Anther culture of Petunia: genotypes with high frequency of callus, root or plantlet formation. Z Pflanzenphysiol 100:131-146.

Miyawaki K, Matsumoto-Kitano M, Kakimoto T. 2004. Expression of cytokinin biosynthetic isopentenyltransferase genes in Arabidopsis: tissue specificity and regulation by auxin, cytokinin, and nitrate. Plant J 37(1):128-138.

Mizuno K HT, Ubukata T, Yamada T, Lehmann E, Kohli J, Watanabe Y, Iino Y, Yamamoto M, Fox ME, Smith GR, Murofushi H, Shibata T, Ohta K. 2001. Counteracting regulation of chromatin remodeling at a fission yeast cAMP response element-related recombination hotspot by stress-activated protein kinase, cAMP-dependent kinase and meiosis regulators. Genetics 159(4):1467-1478.

Moens PB. 1964. A new interpretation of meiotic prophase in Lycopersicum esculentum (tomato). Chromosoma 15:231-242.

Morita R, Hattori Y, Yokoi S, Takase H, Minami M, Hiratsuka K, Toriyama K. 2003. Assessment of utility of meiosis-associated promoters of lily for induction of germinal ds transposition in transgenic rice. Plant Cell Physiol 44(6):637-642.

Munn K, Steward R. 2000. The shut-down gene of Drosophila melanogaster encodes a novel FK506-binding protein essential for the formation of germline cysts during oogenesis. Genetics 156(1):245-256.

Nag DK WM, Petes TD. 1989. Palindromic sequences in heteroduplex DNA inhibit mismatch repair in yeast. Nature 340(6231):318-320.

Nakagawa T, Flores-Rozas H, Kolodner RD. 2001. The MER3 helicase involved in meiotic crossing over is stimulated by single-stranded DNA-binding proteins and unwinds DNA in the 3' to 5' direction. J Biol Chem 276(34):31487-31493.

Nicolas SD, Leflon M, Liu Z, Eber F, Chelysheva L, Coriton O, Chevre AM, Jenczewski E. 2008. Chromosome 'speed dating' during meiosis of polyploid Brassica hybrids and haploids. Cytogenet Genome Res 120(3-4):331-338.

Nilsson NO, Sall T, Bengtsson BO. 1993. Chiasma and recombination data in plants: are they compatible? Trends Genet 9(10):344-348.

Norbury CJ, Hickson ID. 2001. Cellular responses to DNA damage. Annu Rev Pharmacol Toxicol 41:367-401.

Osakabe K, Abe K, Yamanouchi H, Takyuu T, Yoshioka T, Ito Y, Kato T, Tabata S, Kurei S, Yoshioka Y, Machida Y, Seki M, Kobayashi M, Shinozaki K, Ichikawa H, Toki S. 2005. Arabidopsis Rad51B is important for double-strand DNA breaks repair in somatic cells. Plant Mol Biol 57(6):819-833.

Osakabe K, Abe K, Yamanouchi H, Takyuu T, Yoshioka T, Ito Y, Kato T, Tabata S, Kurei S, Yoshioka Y, Machida Y, Seki M, Kobayashi M, Shinozaki K, Ichikawa H, Toki S. 2005. Arabidopsis Rad51B is important for double-strand DNA breaks repair in somatic cells. Plant Mol Biol 57(6):819-833.

Osakabe K, Abe K, Yoshioka T, Osakabe Y, Todoriki S, Ichikawa H, Hohn B, Toki S. 2006. Isolation and characterization of the RAD54 gene from Arabidopsis thaliana. Plant J 48(6):827-842.

Osman K, Sanchez-Moran E, Higgins JD, Jones GH, Franklin FC. 2006. Chromosome synapsis in Arabidopsis: analysis of the transverse filament protein ZYP1 reveals novel functions for the synaptonemal complex. Chromosoma 115(3):212-219.

Palusa SG, Golovkin M, Shin SB, Richardson DN, Reddy AS. 2007. Organ-specific, developmental, hormonal and stress regulation of expression of putative pectate lyase genes in Arabidopsis. New Phytol 174(3):537-550.

Paques F, Haber JE. 1999. Multiple pathways of recombination induced by double-strand breaks in Saccharomyces cerevisiae. Microbiol Mol Biol Rev 63(2):349-404.

Pawlowski WP, Cande WZ. 2005. Coordinating the events of the meiotic prophase. Trends Cell Biol 15(12):674-681.

Pearson WR, Wood T, Zhang Z, Miller W. 1997. Comparison of DNA sequences with protein sequences. Genomics 46(1):24-36.

Pekker I, Alvarez JP, Eshed Y. 2005. Auxin response factors mediate Arabidopsis organ asymmetry via modulation of KANADI activity. Plant Cell 17(11):2899-2910.

Peloquin SJ, Boiteux LS, Carputo D. 1999. Meiotic mutants in potato. Valuable variants. Genetics 153(4):1493-1499.

Peters JL, Cnops G, Neyt P, Zethof J, Cornelis K, Van Lijsebettens M, Gerats T. 2004. An AFLP-based genome-wide mapping strategy. Theor Appl Genet 108(2):321-327.

Peters JL, Constandt H, Neyt P, Cnops G, Zethof J, Zabeau M, Gerats T. 2001. A physical amplified fragment-length polymorphism map of Arabidopsis. Plant Physiol 127(4):1579-1589.

Petukhova G, Van Komen S, Vergano S, Klein H, Sung P. 1999. Yeast Rad54 promotes Rad51-dependent homologous DNA pairing via ATP hydrolysis-driven change in DNA double helix conformation. J Biol Chem 274(41):29453-29462.

Pfeiffer TW. 1993. Recombination rates of soybean varieties from different periods of introduction and release. Theor Appl Genet 86:557-561.

Porceddu A, Reale L, Lanfaloni L, Moretti C, Sorbolini S, Tedeschini E, Ferranti F, Pezzotti M. 1999. Cloning and expression analysis of a Petunia hybrida flower specific mitotic-like cyclin. FEBS Lett 462(1-2):211-215.

Preuss D, Rhee SY, Davis RW. 1994. Tetrad analysis possible in Arabidopsis with mutation of the QUARTET (QRT) genes. Science 264(5164):1458-1460.

Primig M, Williams RM, Winzeler EA, Tevzadze GG, Conway AR, Hwang SY, Davis RW, Esposito RE. 2000. The core meiotic transcriptome in budding yeasts. Nat Genet 26(4):415-423.

Prinz S, Amon A. 1999. Dual control of mitotic exit. Nature 402(6758):133, 135.

Puchta H. 2005. The repair of double-strand breaks in plants: mechanisms and consequences for genome evolution. J Exp Bot 56(409):1-14.

Puchta H, Dujon B, Hohn B. 1996. Two different but related mechanisms are used in plants for the repair of genomic double-strand breaks by homologous recombination. Proc Natl Acad Sci U S A 93(10):5055-5060.

Puizina J, Siroky J, Mokros P, Schweizer D, Riha K. 2004. Mre11 deficiency in Arabidopsis is associated with chromosomal instability in somatic cells and Spo11-dependent genome fragmentation during meiosis. Plant Cell 16(8):1968-1978.

Qi LL, Friebe B, Gill BS. 2002. A strategy for enhancing recombination in proximal regions of chromosomes. Chromosome Res 10(8):645-654.

Rabitsch KP, Gregan J, Schleiffer A, Javerzat JP, Eisenhaber F, Nasmyth K. 2004. Two fission yeast homologs of Drosophila Mei-S332 are required for chromosome segregation during meiosis I and II. Curr Biol 14(4):287-301.

Rabitsch KP, Toth A, Galova M, Schleiffer A, Schaffner G, Aigner E, Rupp C, Penkner AM, Moreno-Borchart AC, Primig M, Esposito RE, Klein F, Knop M, Nasmyth K. 2001. A screen for genes required for meiosis and spore formation based on whole-genome expression. Curr Biol 11(13):1001-1009.

Ravi M, Marimuthu MP, Siddiqi I. 2008. Gamete formation without meiosis in Arabidopsis. Nature 451(7182):1121-1124.

Ray A, Langer M. 2002. Homologous recombination: ends as the means. Trends in Plant Science 7(10):435-440.

Reddy TV, Kaur J, Agashe B, Sundaresan V, Siddiqi I. 2003. The DUET gene is necessary for chromosome organization and progression during male meiosis in Arabidopsis and encodes a PHD finger protein. Development 130(24):5975-5987.

Reidt W, Wurz R, Wanieck K, Chu HH, Puchta H. 2006. A homologue of the breast cancer-associated gene BARD1 is involved in DNA repair in plants. Embo J 25(18):4326-4337.

Reiss B. 2003. Homologous recombination and gene targeting in plant cells. Int Rev

Cytol 228:85-139.
Reverdatto SV, Dutko JA, Chekanova JA, Hamilton DA, Belostotsky DA. 2004. mRNA deadenylation by PARN is essential for embryogenesis in higher plants. Rna 10(8):1200-1214.
Rhee SY, Somerville CR. 1998. Tetrad pollen formation in quartet mutants of Arabidopsis thaliana is associated with persistence of pectic polysaccharides of the pollen mother cell wall. Plant J 15(1):79-88.
Riggs CD. 1997. Meiotin-1: the meiosis readiness factor? Bioessays 19(10):925-931.
Ross KJ, Fransz P, Armstrong SJ, Vizir I, Mulligan B, Franklin FC, Jones GH. 1997. Cytological characterization of four meiotic mutants of Arabidopsis isolated from T-DNA-transformed lines. Chromosome Res 5(8):551-559.
Ross KJ, Fransz P, Jones GH. 1996. A light microscopic atlas of meiosis in Arabidopsis thaliana. Chromosome Res 4(7):507-516.
Salic A, Waters JC, Mitchison TJ. 2004. Vertebrate shugoshin links sister centromere cohesion and kinetochore microtubule stability in mitosis. Cell 118(5):567-578.
Salic A, Waters JC, Mitchison TJ. 2004. Vertebrate shugoshin links sister centromere cohesion and kinetochore microtubule stability in mitosis. Cell 118(5):567-578.
Sambrook J, Fritsch EJ, Maniatis T. 1989. Molecular Cloning: A Laboratory Manual, 2nd edn. Cold Spring Harbor, NY: Cold Spring Harbor Laboratory Press.
Sanchez Moran E, Armstrong SJ, Santos JL, Franklin FC, Jones GH. 2001. Chiasma formation in Arabidopsis thaliana accession Wassileskija and in two meiotic mutants. Chromosome Res 9(2):121-128.
Sanchez-Moran E, Jones GH, Franklin FC, Santos JL. 2004. A puromycin-sensitive aminopeptidase is essential for meiosis in Arabidopsis thaliana. Plant Cell 16(11):2895-2909.
Sanchez-Moran E, Mercier R, Higgins JD, Armstrong SJ, Jones GH, Franklin FC. 2005. A strategy to investigate the plant meiotic proteome. Cytogenet Genome Res 109(1-3):181-189.
Sanchez-Moran E, Mercier R, Higgins JD, Armstrong SJ, Jones GH, Franklin FC. 2005. A strategy to investigate the plant meiotic proteome. Cytogenet Genome Res 109(1-3):181-189.
Sanders PM, Lee PY, Biesgen C, Boone JD, Beals TP, Weiler EW, Goldberg RB. 2000. The arabidopsis DELAYED DEHISCENCE1 gene encodes an enzyme in the jasmonic acid synthesis pathway. Plant Cell 12(7):1041-1061.
Schaefer DG, Zryd JP. 1997. Efficient gene targeting in the moss Physcomitrella patens. Plant J 11(6):1195-1206.
Schewe MJ, Suzuki DT, Erasmus U. 1971. The genetic effects of mitomycin C in Drosophila melanogaster. II. Induced meiotic recombination. Mutat Res 12(3):269-279.
Schimenti J VL, Socolow D, Silver LM. 1987. An unstable family of large DNA elements in the center of the mouse t complex. J Mol Biol 194(4):583-594.
Schommer C, Beven A, Lawrenson T, Shaw P, Sablowski R. 2003. AHP2 is required for bivalent formation and for segregation of homologous chromosomes in Arabidopsis meiosis. Plant J 36(1):1-11.
Schroeder DF, Gahrtz M, Maxwell BB, Cook RK, Kan JM, Alonso JM, Ecker JR, Chory J. 2002. De-etiolated 1 and damaged DNA binding protein 1 interact to regulate Arabidopsis photomorphogenesis. Curr Biol 12(17):1462-1472.
Schultz N, Hamra FK, Garbers DL. 2003. A multitude of genes expressed solely in meiotic or postmeiotic spermatogenic cells offers a myriad of contraceptive targets. Proc Natl Acad Sci U S A 100(21):12201-12206.
Schwarzacher T. 2003. Meiosis, recombination and chromosomes: a review of gene isolation and fluorescent in situ hybridization data in plants. J Exp Bot

54(380):11-23.

Scott R, Dagless E, Hodge R, Paul W, Soufleri I, Draper J. 1991. Patterns of gene expression in developing anthers of Brassica napus. Plant Mol Biol 17(2):195-207.

Scott RJ, Spielman M, Dickinson HG. 2004. Stamen structure and function. Plant Cell 16 Suppl:S46-60.

Shaked H, Melamed-Bessudo C, Levy AA. 2005. High-frequency gene targeting in Arabidopsis plants expressing the yeast RAD54 gene. Proc Natl Acad Sci U S A 102(34):12265-12269.

Shechter D CV, Gautier J. 2004. Regulation of DNA replication by ATR: signaling in response to DNA intermediates. DNA Repair (Amst) 3(8-9):901-908.

Shen X, Mizuguchi G, Hamiche A, Wu C. 2000. A chromatin remodelling complex involved in transcription and DNA processing. Nature 406(6795):541-544.

Sherman JD, Stack SM. 1995. Two-dimensional spreads of synaptonemal complexes from solanaceous plants. VI. High-resolution recombination nodule map for tomato (Lycopersicon esculentum). Genetics 141(2):683-708.

Siaud N, Dray E, Gy I, Gerard E, Takvorian N, Doutriaux MP. 2004. Brca2 is involved in meiosis in Arabidopsis thaliana as suggested by its interaction with Dmc1. Embo J 23(6):1392-1401.

Silver LM, Olds-Clarke, P. 1984. Transmission ratio distortion of mouse t haplotypes is not a consequence of wild-type sperm degeneration. Dev Biol 105(1):250-252.

Smith TF, Waterman MS. 1981. Identification of common molecular subsequences. J Mol Biol 147(1):195-197.

Song B, Sung P. 2000. Functional interactions among yeast Rad51 recombinase, Rad52 mediator, and replication protein A in DNA strand exchange. J Biol Chem 275(21):15895-15904.

Sonoda E, Sasaki MS, Buerstedde JM, Bezzubova O, Shinohara A, Ogawa H, Takata M, Yamaguchi-Iwai Y, Takeda S. 1998. Rad51-deficient vertebrate cells accumulate chromosomal breaks prior to cell death. Embo J 17(2):598-608.

Specht S, Saeftel M, Arndt M, Endl E, Dubben B, Lee NA, Lee JJ, Hoerauf A. 2006. Lack of eosinophil peroxidase or major basic protein impairs defense against murine filarial infection. Infect Immun 74(9):5236-5243.

Stacey NJ, Kuromori T, Azumi Y, Roberts G, Breuer C, Wada T, Maxwell A, Roberts K, Sugimoto-Shirasu K. 2006. Arabidopsis SPO11-2 functions with SPO11-1 in meiotic recombination. Plant J 48(2):206-216.

Stack S, and L. K. Anderson. 1986. Two-dimensional spreads of synaptonemal complexes from solanaceous plants. III. Recombination nodules and crossing over in Lycopersicon esculentum. Chromosoma 94:253-258.

Stack SM, Anderson, L.K. 1986. Two-dimensional spreads of synaptonemal complexes from solanaceous plants. II. Synapsis in Lycopersicon esculentum. Am J Bot 73:264-281.

Strom L, Karlsson C, Lindroos HB, Wedahl S, Katou Y, Shirahige K, Sjogren C. 2007. Postreplicative formation of cohesion is required for repair and induced by a single DNA break. Science 317(5835):242-245.

Sugimoto-Shirasu K, Roberts GR, Stacey NJ, McCann MC, Maxwell A, Roberts K. 2005. RHL1 is an essential component of the plant DNA topoisomerase VI complex and is required for ploidy-dependent cell growth. Proc Natl Acad Sci U S A 102(51):18736-18741.

Sung P, Trujillo KM, Van Komen S. 2000. Recombination factors of Saccharomyces cerevisiae. Mutat Res 451(1-2):257-275.

Svetlanov A, Baudat F, Cohen PE, de Massy B. 2008. Distinct functions of MLH3 at recombination hot spots in the mouse. Genetics 178(4):1937-1945.

Sym M, Roeder GS. 1994. Crossover interference is abolished in the absence of a synaptonemal complex protein. Cell 79(2):283-292.

Szostak JW, Orr-Weaver TL, Rothstein RJ, Stahl FW. 1983. The double-strand-break repair model for recombination. Cell 33(1):25-35.

Takata M, Sasaki MS, Sonoda E, Morrison C, Hashimoto M, Utsumi H, Yamaguchi-Iwai Y, Shinohara A, Takeda S. 1998. Homologous recombination and non-homologous end-joining pathways of DNA double-strand break repair have overlapping roles in the maintenance of chromosomal integrity in vertebrate cells. Embo J 17(18):5497-5508.

Terasawa M, Ogawa H, Tsukamoto Y, Shinohara M, Shirahige K, Kleckner N, Ogawa T. 2007. Meiotic recombination-related DNA synthesis and its implications for cross-over and non-cross-over recombinant formation. Proc Natl Acad Sci U S A 104(14):5965-5970.

Thierry-Mieg D, Thierry-Mieg J. 2006. AceView: a comprehensive cDNA-supported gene and transcripts annotation. Genome Biol 7 Suppl 1:S12 11-14.

Toth A, Rabitsch KP, Galova M, Schleiffer A, Buonomo SB, Nasmyth K. 2000. Functional genomics identifies monopolin: a kinetochore protein required for segregation of homologs during meiosis i. Cell 103(7):1155-1168.

Twell D, Lalanne SKPaE. 1998. Asymmetric division and cell-fate determination in developing pollen. trends in plant science Vol. 3,(No. 8):305-310.

Uanschou C, Siwiec T, Pedrosa-Harand A, Kerzendorfer C, Sanchez-Moran E, Novatchkova M, Akimcheva S, Woglar A, Klein F, Schlogelhofer P. 2007. A novel plant gene essential for meiosis is related to the human CtIP and the yeast COM1/SAE2 gene. Embo J 26(24):5061-5070.

Ubeda F, Haig D. 2004. Sex-specific meiotic drive and selection at an imprinted locus. Genetics 167(4):2083-2095.

Urano K, Hobo T, Shinozaki K. 2005. Arabidopsis ADC genes involved in polyamine biosynthesis are essential for seed development. FEBS Lett 579(6):1557-1564.

Ursic D, Culbertson MR. 1991. The yeast homolog to mouse Tcp-1 affects microtubule-mediated processes. Mol Cell Biol 11(5):2629-2640.

Verweire D, Verleyen K, De Buck S, Claeys M, Angenon G. 2007. Marker-free transgenic plants through genetically programmed auto-excision. Plant Physiol 145(4):1220-1231.

Vittorioso P, Cowling R, Faure JD, Caboche M, Bellini C. 1998. Mutation in the Arabidopsis PASTICCINO1 gene, which encodes a new FK506-binding protein-like protein, has a dramatic effect on plant development. Mol Cell Biol 18(5):3034-3043.

von Wettstein D RS, Holm PB. 1984. The synaptonemal complex in genetic segregation. Annu Rev Genet 18:331-413.

Wang B-B, Brendel V. 2006. Molecular Characterization and Phylogeny of U2AF35 Homologs in Plants. Plant Physiol 140(2):624-636.

Wang TF, Kleckner N, Hunter N. 1999. Functional specificity of MutL homologs in yeast: evidence for three Mlh1-based heterocomplexes with distinct roles during meiosis in recombination and mismatch correction. Proc Natl Acad Sci U S A 96(24):13914-13919.

Wang Y, Yang M. 2006. The ARABIDOPSIS SKP1-LIKE1 (ASK1) protein acts predominately from leptotene to pachytene and represses homologous recombination in male meiosis. Planta 223(3):613-617.

Wang Z, Liang Y, Li C, Xu Y, Lan L, Zhao D, Chen C, Xu Z, Xue Y, Chong K. 2005. Microarray analysis of gene expression involved in anther development in rice (Oryza sativa L.). Plant Mol Biol 58(5):721-737.

Waterworth WM, Altun C, Armstrong SJ, Roberts N, Dean PJ, Young K, Weil CF, Bray

CM, West CE. 2007. NBS1 is involved in DNA repair and plays a synergistic role with ATM in mediating meiotic homologous recombination in plants. Plant J 52(1):41-52.

Watrin E, Peters JM. 2006. Cohesin and DNA damage repair. Exp Cell Res 312(14):2687-2693.

Watrin E, Peters JM. 2009. The cohesin complex is required for the DNA damage-induced G2/M checkpoint in mammalian cells. Embo J.

Wijeratne AJ, Chen C, Zhang W, Timofejeva L, Ma H. 2006. The Arabidopsis thaliana PARTING DANCERS gene encoding a novel protein is required for normal meiotic homologous recombination. Mol Biol Cell 17(3):1331-1343.

Wijnker E, de Jong H. 2008. Managing meiotic recombination in plant breeding. Trends Plant Sci 13(12):640-646.

Wilby AaP, JS. 1988. Recurrent patterns of chromosome variation in a species group. Heredity 61:55-62.

Xiao Y, Weaver DT. 1997. Conditional gene targeted deletion by Cre recombinase demonstrates the requirement for the double-strand break repair Mre11 protein in murine embryonic stem cells. Nucleic Acids Res 25(15):2985-2991.

Yamagishi Y, Sakuno T, Shimura M, Watanabe Y. 2008. Heterochromatin links to centromeric protection by recruiting shugoshin. Nature 455(7210):251-255.

Yamaguchi S, Decottignies A, Nurse P. 2003. Function of Cdc2p-dependent Bub1p phosphorylation and Bub1p kinase activity in the mitotic and meiotic spindle checkpoint. Embo J 22(5):1075-1087.

Yamaguchi-Iwai Y, Sonoda E, Sasaki MS, Morrison C, Haraguchi T, Hiraoka Y, Yamashita YM, Yagi T, Takata M, Price C, Kakazu N, Takeda S. 1999. Mre11 is essential for the maintenance of chromosomal DNA in vertebrate cells. Embo J 18(23):6619-6629.

Yang M, Hu Y, Lodhi M, McCombie WR, Ma H. 1999. The Arabidopsis SKP1-LIKE1 gene is essential for male meiosis and may control homologue separation. Proc Natl Acad Sci U S A 96(20):11416-11421.

Yang M, Ma H. 2001. Male meiotic spindle lengths in normal and mutant arabidopsis cells. Plant Physiol 126(2):622-630.

Yang X, Makaroff CA, Ma H. 2003. The Arabidopsis MALE MEIOCYTE DEATH1 gene encodes a PHD-finger protein that is required for male meiosis. Plant Cell 15(6):1281-1295.

Youds JL, Mets DG, McIlwraith MJ, Martin JS, Ward JD, NJ ON, Rose AM, West SC, Meyer BJ, Boulton SJ. RTEL-1 enforces meiotic crossover interference and homeostasis. Science 327(5970):1254-1258.

Yu Z, Guo R, Ge Y, Ma J, Guan J, Li S, Sun X, Xue S, Han D. 2003. Gene expression profiles in different stages of mouse spermatogenic cells during spermatogenesis. Biol Reprod 69(1):37-47.

Zheng Z, Xia Q, Dauk M, Shen W, Selvaraj G, Zou J. 2003. Arabidopsis AtGPAT1, a member of the membrane-bound glycerol-3-phosphate acyltransferase gene family, is essential for tapetum differentiation and male fertility. Plant Cell 15(8):1872-1887.

Zickler D, Kleckner N. 1998. The leptotene-zygotene transition of meiosis. Annu Rev Genet 32:619-697.

Zickler D, Kleckner N. 1999. Meiotic chromosomes: integrating structure and function. Annu Rev Genet 33:603-754.

Zou L, Elledge SJ. 2003. Sensing DNA damage through ATRIP recognition of RPA-ssDNA complexes. Science 300(5625):1542-1548.

**Appendix 1: Petunia partial cDNA sequences without a GenBank ID**

>**seq463**
TTANACCTNCGTTTGGGAACGANCNCAATATTTTTTGGGATTCGTTGTTTTGA
CCT

>**seq236**
ATTGGCCATGGGGGATAATGGGGAGCCCAAAAAAGGGAAATGNTTGGCATG
GATAGGGAACCTTCTGTAGGAACTTCAATCTTGTACATCT

>**seq43**
TCNTGCTGTACGTTGNTCTTCCCACAACGATTGGAAAGTAGCACAGCACCCC
TTTGTGTCT

>**seq76**
TTNCCCNNTTTNAACTGGGTCTTCACTGNACCCCTACTACNGAAGGAGATCA
ATACATCAAAGGACAGAATTTTGCACTACTATCTGGAACAAGCATGGCTACC
CCACACATTGCTGGAATTGCTGCTT

>**seq448**
GGGGGGTGGTCGGTAGNTACATATGCATNTCGAGGCTGTTTACATGTCTGNC
TGAGATCTTCNCACGTCTTCAAAGAAGGCTCNGAAAACTTGGTTAGACGGTC
CAGCACCCTCGT

>**seq27**
GCTGGCCAGTTGAATAAGCTTTTTTTGAACGTGAATCTGGTGT

>**seq335**
ATTCCTATAAAGTTGCTTACATCACAGTACCTGCTGGAGTTATTTAGCATAGT
AGAAGATGAGAGAAGTAGAAATCCAGACACACTAAACTCCAGAACTAATTA
TTTGTTGTCCGTAATGGCTGTTTTAGAAGGCCAGATTTTCTCAAGTGACATAA
CAGTCGCAGTGAACTGTTCCCTCTGTTTGTCTATGATTATCGGATGGCAAGAT
GCAGAAGCAGAAGCAGAAGTATCAGCTATGCAAAGGAACAACTGGTGTCGG
TTTATAGTAGAAGAGTTAGTGATGTCTTTGGGAACACCATCTTTGGCTACAAA
ATCTTTCGCGATCCATCACAAGCCTGCAA

>**seq53**
AGTTACTGTAGTGTTGACTATGTTTGAAATGAGGGAAATAGCCAGAGTTCAA
AGCCAATATATTGAACTCTATGCTCTTGTCTGTTATCCTGAACATTTCAAGGT
TGTTCAATCTAATCCGAT

>**mshseq32**
CNCNNNTTGAAAANCCNAGTGCTGCGTTCGTCTTTGTACTGCATTGAAAGCT
AACATTCTTGGAATCAACATTGATATTCCCATTGCACTAAGCTTGCTCAT

>**seq31**
CANAGCCTGTGTTGATAGAATTAGACTTGGAGAAAGGGNCCCCATTGAACCA
ATCAGTACTTATTTGTAAATCTAATTTCTTGCTCTTGCTTACTCAGGACTCATC
ATNGTAAACACCGAAAACGCACAGCACTCAAAAACTTCATATACTCAAATTT
CTTCACACTAGGTCTCACTTTATCACTCTTCATTTTCCTCT

>**seq71**
TTCNCTCCCCNNNNGTCTCACACATNCCTTCAGTGGAAGATGCTGCAGTAGT
NGGGCTGCCAGATGAAGGGGCAGGGGAGATACCAGCAGCATGGGTAGTCTT
GAACTCAACGGCAAAGGAAAGCAATGAGGACATAATCAACTACGTTCCATC
GACTGTAGCACAGTATAAACGAGTGAGAGTGGTGCAGTTTGTGGAAAAGATT
CCAAAATCTCCTTCTGGAAAAATAATGAGAAGAGTAATCAAGGAAAAGATG
TTAGAGATACTCAAGGGTGAACAAAGTGATGTTCCAAATACATTGTTGTAAT
AAACATCATTCTATCTTTCATGTTCTGTAAGGAAACAAGTATTCCACAATATC
TGCTCTTTTACATCTATAAAACTTGAACTTTAN

>**Pt40**
GAAGAAGGAGAATTACTTCTCTTGTGCAGTTGGCAGGACTCGTACAAATGCT
CGGTATCTGCTCAGTACCCCTGATGACATAGTTGCTTTTCTAAAGGAACTAGC
TGAAGCCTCTTC

>**seq399**
TTCCTANGANCNGATGNCNNCAGCAGCCCNACTCTATCTTTCCANCACAAGT
TGAGNAAGCACCAGNCCTGCANGAATAGGGGAGTTCGACTCCANCTTCCTCA
NNNGCATCGAGGATGTAAGTCTCACAAGGTGCATCAACCTCATGTTCTATAC
CATNTGGACAGACCAATTTGACCTTGTATACATTTGCCGATGCTCTAAAACCA
GAGTCAACTTTCAAGCCAAAGGATTTAGAGATGCTCCTTACAGAGCCCAGAG
AAGATGGGATTTTCACTAAGGCACTCTTTCTTTGGGTCTGCGATGCAGCTTTG
ANCATGCAGGTGGAAGGAAGTCTCACGGTCNACATGTTTACCTA

>**seq184**
CNTTTAAGNCCCNTTANATGCCTGCGNNGNATGCGGGAATAAGGTCCTCAGA
GGTGCGCATGAGTGGGAACAACACAAACAGGGCCGTGGCCATCGAAAACNA
ATTTGTCGACT

>**seq59**
TTAANNCCCTNTGAGCAGGGTCCTAATATTTTTCGACGACCATCAAAATGAA
CTGAAAAGACTAAAGCAAGCACTAAAAGCAGGATTCAGGCATCTTGTATTTG
AGGACAACTATGACACTGGTACTGGAGACCACTATTCTCTTACGCAGATGTG
CGATCAATTTTATATAAGAGGTGGGGGCCATAGTTGCTT

>**seq261**
GCCCGGAGGAATCACTGGATCAAAGAAGAAGCATTTNGGNAGGAGATTCTT
CATACGATCTANTGGCCGGTGAATCACTGTATCAAAGAGCGAGCAGGCGCCA
GGTT

>**seq66**
TGGTAACGANTTAGATTTTCGATGAAGCAGATTGATTGCACACATTCCAAAG
GTGGGCTCTGTGTAGATTCTGTCTCAATTACCCCAAGTGATCTCAAGAGGTGT
AGAAGAAAAGGGGT

>**seq60**
NTTNATTCNCCGCCNNGTGCCAACAGTATTTTCANGCAGCAATAAACAACGG
GCATTTTCATGTTACCTGATATTAGTCAGGTAAACGTTTCAGTGAACCGGTTC
ACAGCATTGGAAGTGGTGGAATTTACTGATAAAGGTACAGAACTTCCCAGTC
TTGATGTACATGGTAACCGTCTACGTGGTCACTTGCCCCTGAATT

>**pcr11**
CTTGAAGACCATTGGCGATCTGGACTATGCAGCAAAGACTAAGAACAGCACT
CAAGCACAGAAGTATTATGCAGAAACTGTATCTACC

>**pcr23**
TGTGTGTGAAGCCCCTATCATCTATGGTGATGTGAGCCGCCCAAACCCAATG
ACTGTCTTCTGGTCCTCAAAAGCTCAAAGCATGACAAAGAGGCCAATGAAGG
GAATGCTTACAGGCCCTGTCACCATTCTCAACTGGTCTTTTGTTAGAAATGAC
CAGCCAAGGTTTGAAACCTGCTACCAGATTGCTTTGGCCA

>**seq54**
CCATCAAAGTACTTTTATACGGATACTGNCAGGGAGATAGAGTCAAAATTGA
AGTACGTCCTTATGATTCAACCAAAGGGTGTAGAATTTATCGACTCCACAAC
AAAGATTTGAAGGAT

>**seq178**
ACATTNAAACCCCNNTTTANTTCCCGCANAGCCTAAANGGAAGGGCATCCGG
GGATTCATTTCAAGCTGCTTGCTGCCAACATGTGCTTGT

>**mshseq12**
TTANNACCCCNGNGGCNGATGAGTACAAGCATATGCTATGTGTAGACGGGA
GCAGCTATCGAGAAACCAATCACCT

>**seq85**
CNTCTCNCNTTTNNCANAACCNNAAAACTCGTAATAACNANNNCNTTNGCTA
CNCCCCTATNTATAAAGGGGCGTAAGTCACTTCACTCGCTAGGGGATGGGAT
TCATTCACTTGCATTCCTGCTAGCACTACAAAAAGCTCCGGACT

**Appendix 2: Genes closest to GFP and RFP marker integration site**

| Gene code | AGI co-ordinates (bp) | Associated marker | Marker insertion within gene | Gene name | Gene Annotation |
|---|---|---|---|---|---|
| At1G01580 | 209395 - 213041 | GCo73 | intron | AtFRO2 | ferric reductase; FRO2 transcript levels are undetectable under iron sufficient conditions; greatly induced iron-deficient medium (Connolly et al., 2003). |
| At1G19000 | 6560786 - 6562777 | RCo78 | exon 3 | - | myb family transcription factor; |
| At1G19290 | 6666717 - 6668954 | RCo32 | intron 2 | - | pentatricopeptide (PPR) repeat-containing protein; Putative DNA binding protein |
| AT3G01690 | 256544 - 258554 | GCo39 | 5 UTR | - | Esterase/lipase/thioesterase |
| AT3G15860 | 5361214 - 5361726 | RCo59 | 5 UTR intron | - | unknown protein |
| AT3G17190 | 5867398 - 5867954 | RCo90 | 5 UTR intron | - | unknown protein |
| AT3G23450 | 8410454 - 8412011 | RCo56 | incorrect annotation | - | unknown protein |
| AT3G43110 | 15102599 - 15103455 | Rco131 | intron 4 | - | unknown protein |
| AT3G60980 | 22576284 - 22577720 | GCo76 | 5 UTR | - | pentatricopeptide (PPR) repeat-containing protein; similar to GRP23 |
| AT5G13000 | 4110298 - 4121430 | RCo118 | | AtGSL12 | 1,3-beta-glucan synthase activity |
| AT5G25560 | 8897904 - 8901707 | GCo61 | 5 UTR | - | zinc finger (C3HC4-type RING finger) family protein; |
| AT4G15180 | 8651406 - 8662587 | RCo5 | exon | - | SET domain-containing protein; similar to EFS (EARLY FLOWERING IN SHORT DAYS) |

**Appendix 3: Overview of recombination rates between all GFP and RFP intervals analyzed**

| Genotype | Chr. | RFP | GFP | Both | None | Total | %RF |
|---|---|---|---|---|---|---|---|
| MSH5-2 +/+ :: 1C-D +/- | 1 | 132 | 96 | 304 | 277 | 809 | 28 |
| msh5-2 -/- :: 1C-D +/- | 1 | 22 | 23 | 206 | 250 | 501 | 9 |
| MSH5-2 +/+ :: 5A-A +/- | 5 | 50 | 55 | 228 | 226 | 559 | 19 |
| msh5-2 -/- :: 5A-A +/- | 5 | 4 | 6 | 155 | 132 | 297 | 3 |
| At2G28620 +/+ :: Col3_4/20 +/- | 3 | 140 | 112 | 327 | 348 | 927 | 27 |
| At2G28620 -/- :: Col3_4/20 +/- | 3 | 102 | 92 | 225 | 232 | 651 | 30 |
| At2G28620 +/+ :: 5A-A +/- | 5 | 69 | 68 | 244 | 268 | 649 | 21 |
| At2G28620 -/- :: 5A-A +/- | 5 | 20 | 21 | 62 | 77 | 180 | 23 |
| At3g55520 +/+:: 5A-A +/- | 5 | 82 | 55 | 142 | 133 | 412 | 33 |
| At3g55520 -/-:: 5A-A +/- | 5 | 108 | 88 | 245 | 241 | 682 | 29 |
| At3g55520 +/+ :: 1C-D +/- | 1 | 37 | 48 | 189 | 221 | 495 | 17 |
| At3g55520 -/- :: 1C-D +/- | 1 | 61 | 70 | 293 | 287 | 711 | 18 |
| RuvX OE :: Col3_4/20 +/- | 3 | 155 | 173 | 489 | 466 | 1283 | 26 |
| recQL4A -/- :: Col3_4/20 +/- | 3 | 164 | 179 | 494 | 550 | 1387 | 25 |
| WT +/+ :: Col3_4/20 +/- | 3 | 242 | 256 | 731 | 725 | 1995 | 25 |

# Abbreviations

| | |
|---|---|
| HR | homologous recombination |
| DSBs | double stranded breaks |
| CO | crossover |
| NHEJ | Non-Homologous End Joining |
| BIR | Break-Induced-Replication |
| SDSA | Synthesis Dependant Strand Annealing |
| GC | gene conversion |
| DSBR | Double Strand Break Repair |
| SC | synaptonemal complex |
| RNs | recombination nodules |
| NCO | non-crossover |
| SEI | Single end invasion |
| D-loop | displacement loop |
| dHJs | double Holliday junctions |
| NCO | non-crossover |
| MRN/X | MRE11-RAD50-NBS/XRS1 |
| SSA | single strand annealing |
| MMR | mismatch repair |
| ZFN | Zinc finger nucleases |
| GT | Gene targeting |
| PTLPDs | lipoamide dehydrogenases |
| ATM | *Arabidopsis thaliana Ataxia telangiectasia mutated* |
| ATR | *Arabidopsis thaliana Ataxia telangiectasia and RAD3 related* |
| *DDE1* | *delayed dehiscence1* |
| *AtSKI8* | *Arabidopsis thaliana Super Killer 8* |
| *AtMRE11* | *Arabidopsis thaliana Meiotic Recombination 11* |
| *AtSPO11* | *Arabidopsis thaliana Sporulation Protein 11* |
| *AtPRD1* | *Arabidopsis thaliana Putative Recombination Initiation Defect 1* |
| *AtPRD2* | *Arabidopsis thaliana Putative Recombination Initiation Defect 2* |
| *AtPRD3* | *Arabidopsis thaliana Putative Recombination Initiation Defect 3* |
| *AtBRCA1* | *Arabidopsis thaliana Breast Cancer Susceptibility 1* |
| *AtBRCA2* | *Arabidopsis thaliana Breast Cancer Susceptibility2* |
| *AtRPA2* | *Arabidopsis thaliana Replicon Protein A 2* |
| *AHP2* | *Arabidopsis Homologous Pairing 2* |
| *AtSDS1* | *Arabidopsis thaliana Solo Dancers 1* |
| *AtTOP3a* | *Arabidopsis thaliana topoisomerase (DNA) III alpha* |
| *RMI1* | *Arabidopsis thaliana RecQ mediated genome instability 1* |
| *ATK1* | *Arabidopsis thaliana kinesin 1* |

| | |
|---|---|
| *AtMMD1* | *Arabidopsis thaliana Male Meiocyte Death 1* |
| *ATM* | *Ataxia telangiectasia mutated* |
| *ATR* | *Ataxia telangiectasia and RAD3 related* |
| *AtRAD9* | *Arabidopsis thaliana Radiation 9* |
| *AtRAD17* | *Arabidopsis thaliana Radiation 17* |
| *AtRAD50* | *Arabidopsis thaliana Radiation 50* |
| *AtMRE11* | *Arabidopsis thaliana Meiotic Recombination 11* |
| *AtNBS1* | *Arabidopsis thaliana Nijmegen Breakage Syndrome 1* |
| *AtCOM1* | *Arabidopsis thaliana Completion Of Meiotic recombination* |
| *AtRAD51* | *Arabidopsis thaliana Radiation 51* |
| *AtXRCC2* | *Arabidopsis thaliana X-ray repair cross-complementing 2* |
| *AtDMC1* | *Arabidopsis thaliana Disruption of Meiotic Control 1* |
| *AtRAD54* | *Arabidopsis thaliana Radiation 54* |
| *RECQL4A* | *Arabidopsis thaliana RecQ -like 4A* |
| *AtPTD1* | *Arabidopsis thaliana Parting Dancers 1* |
| *AtMUS81* | *Arabidopsis thaliana methyl methansulfonate UV sensitive 81* |
| *AtEME1A* | *Arabidopsis thaliana Essential Meiotic Endonuclease 1A* |
| *AtEME1B* | *Arabidopsis thaliana Essential Meiotic Endonuclease 1B* |
| *SHOC1* | *Shortage in Chiasmata 1* |
| *AtMPA1* | *Arabidopsis thaliana meiotic prophase aminopeptidase 1* |
| *AtMER3* | *Arabidopsis thaliana ATP-dependent helicase/ DNA helicase* |
| *AtMSH2* | *Arabidopsis thaliana MutS homolog 2* |
| *AtMSH4* | *Arabidopsis thaliana MutS homolog 4* |
| *AtMSH5* | *Arabidopsis thaliana MutS homolog 5* |
| *AtMLH1* | *Arabidopsis thaliana MutL homolog 1* |
| *AtMLH3* | *Arabidopsis thaliana MutL homolog 3* |
| *AtPMS1* | *Arabidopsis thaliana post-meiotic segregation 1* |

## *Acknowledgements*

I would like to thank all those who have helped me accomplish my Ph.D. research during 2004-2008.

Firstly, thanks to Tom, my promoter, who has been very positive in his outlook, given me advice, been sensitive and facilitated my progress. Tom, I will remember the trips we made between the Nijmegen and Wageningen labs discussing work in the car and your quote before leaving for the day "Remember, there is always another day".

My heart-felt gratitude extends to my supervisor and co-promoter Janny in whom I have found a good friend and guide. Janny, I am grateful to you for providing me with this opportunity to work with you. I have benefitted from your critical thinking, organization skills and clarity of thought in scientific analysis. I always appreciated your critical feedback.

Hans, my promoter, I thank you for your valuable inputs to the cytology work as well as your help with image analysis and scientific writing. Interactions that you facilitated with Paul Franz and Song Bin Chen to learn techniques like chromosomal spreads and FISH analysis that were important for my work. I will cherish the lighter moments that you, Dora and I shared together and the wonderful dinner that you cooked for us at your home. The lab meetings and interactions with members of your group- Dora, Janny, Penka, Radim, Eric, Lak and Marijke were inspiring.

I had a good time with the Plant Genetics labmates Filip, Stefan, Anneke, Jan, Partha, Andrea, Sandra, Michael, Annelies, Antoine and members of Plant Cell Biology lab Titi, Richard, Peter, Jan, Marian, Lisette, Tomek, Sisi, Manoko, Maaike, Wim, Anna, Klaas, and Meena for their cooperation and help in the lab. I cannot thank my senior Filip enough for being so helpful with the data transition and his kindness. Else, thank you for helping me throughout with administrative work. I am grateful to Marian who has helped me at very critical moments in my experiments especially while I was away. My special thanks to Annemiek, Simone Camps, Jan Zethof, Geert-Jan, and Mieke Wolters for experimental work and technical support; Liesbeth Pierson for help with microscopy and image analysis. Thanks to short-term students Bas, Mihoko, Melissa, Roxanne and Marc for their good work. Thanks to Gerard, Walter, Evet and Harry for facilitating my work at the greenhouse and their warm smiles.

In my second year, I spent an invaluable six-month period in Dr. Mathilde Grelon's lab in INRA, France. I thoroughly enjoyed work and the company of Mathilde Grelon, Christine Mezard, Raphael Mercier and all members of the INRA meiosis group -Gislane, Jan, Julian, Silvia, Christine

Harlow, Daniel, Nicole, Arnaud and Fabien. Mathilde, largely facilitated my stay, the screening work and was very kind to make arrangements for my family when they were visiting me. I appreciate the help of Liudmila Chelysheva who taught me immunocytology and for the great day out in Paris. I appreciate the hospitality extended by Liudmila, Christine and Ghislaine who organized home parties.

My interaction with our collaborators at KeyGene was stimulating. Many thanks to Daphne Rainey for bioinformatic analysis, Ellen van Enckevort for contributing to the recombination work and Frank Lhussier for help with automation of seed counts. We are greatful to Jean E. Masson who has kindly provided us seeds of *xrs4*.

I have been very lucky to stay with Wim and Ricky Miltenburg who took wonderful care of me and made my stay comfortable. I have found extended family in them. The food, movies and company of my lovely neighbor Willemien and Indian friends Chandrakala, Deepak, Gowri, Rajagopal, Partha, Suresh, Ram, Tripti at Nijmegen and my dear friend Aarati at Wageningen were memorable. The women's cricket team at Quick, Nijmegen including Anja, Lotte, Maricelle, and Nicole were great fun to train with and play cricket on weekends.

Director of Kreedaranga Sujaya Bhagwan, associate Nalini and the whole group at Kreedaranga have been wonderful in helping us take care of our son Anikait. Above all, this endeavor has been possible only due to the cooperation and unconditional support and love of my husband Jayaprakash, son Anikait, my parents and the rest of my family.

With warm wishes,
Veena

# *Curriculum vitae*

Veena Hedatale was born in Bangalore, India on 03 June, 1972. She completed her Bachelor of Science (BSc.) in 1993 from Vishveshwarapuram College of Science, Bangalore. In 1996, she completed her Master of Science (MSc.) degree in Microbiology from Bangalore University Bangalore, India. Her first project was as a research assistant with Dr. Susan. R. McCouch to contribute to the development of microsatellite markers and a high density linkage map in rice in the Department of Plant Breeding at Cornell University, USA (1996 – 1999). She then worked for the agricultural biotechnology company Monsanto Research Center, India in the Genome Knowledge Enhancement Programme as a scientist between 1999 and 2004. In 2004, she started to pursue a Ph.D. with Prof. Dr. Tom Gerats in Plant Genetics, Radboud University, The Netherlands. In 2006, she visited the lab of Dr. Mathilde Grelon, INRA, Versailles, France, for six months under the Marie Curie Early Stage Training Fellowship to study meiosis and recombination. Her thesis work presented here is the outcome of her Ph.D. research concerning meiotic recombination in *Arabidopsis* and *Petunia hybrida*. She returned to India in 2008 and is currently a senior scientist for Strand Life Sciences in Bangalore.

**Publications**

Hedatale V, Cnudde F, de Jong H, Pierson ES, Rainey DY, Zabeau M, Weterings K, Gerats T, Peters JL. Changes in gene expression during male meiosis in Petunia hybrida. Chromosome Res. 2006; 14(8):919-32.

Hedetale V, Blair MW, McCouch SR. Fluorescent-labeled microsatellite panels useful for detecting allelic diversity in cultivated rice (Oryza sativa L). Theor Appl Genet. 2002 Aug; 105(2-3):449-457.